ON THE CRANIAL OSTEOLOGY OF CHIROPTERA. I. *PTEROPUS* (MEGACHIROPTERA: PTEROPODIDAE)

NORBERTO P. GIANNINI

Division of Vertebrate Zoology (Mammalogy), American Museum of Natural History (norberto@amnh.org)

JOHN R. WIBLE

Section of Mammals, Carnegie Museum of Natural History, 5800 Baum Boulevard, Pittsburgh, PA 15206 (WibleJ@CarnegieMNH.Org)

NANCY B. SIMMONS

Division of Vertebrate Zoology (Mammalogy), American Museum of Natural History (simmons@amnh.org)

BULLETIN OF THE AMERICAN MUSEUM OF NATURAL HISTORY
CENTRAL PARK WEST AT 79TH STREET, NEW YORK, NY 10024
Number 295, 134 pp., 50 figures
Issued January 12, 2006

 ISSN 0003-0090

CONTENTS

ABSTRACT

Although detailed anatomical descriptions of skull morphology are available for representatives of many mammalian orders, no such descriptive work exists for bats, a group that comprises over 20% of extant mammalian species. In this paper, we provide a detailed description of the skull of *Pteropus* (Mammalia: Chiroptera: Megachiroptera: Pteropodidae) and establish a system of cranial nomenclature following the Nomina Anatomica Veterinaria. Based on a series of specimens of *Pteropus lylei*, we describe the skull as a whole and the morphology of external surfaces of 24 bones (7 rostral, 16 cranial, plus the mandible) and 17 teeth. We describe internal surfaces and additional bones of disarticulated skulls of *Pteropus livingstonii* and use material from the same species to describe the middle ear ossicles and the petrosal bone. We include a description of the hyoid apparatus and larynx based on *Pteropus tonganus* and a description of the deciduous dentition based on *Pteropus hypomelanus*. Using a sectioned fetus, we determine the content and homology of all cranial foramina present in the skull of *Pteropus*. We outline the ontogenetic changes from newborn pups to adults, considering changes in skull shape and the sequence of bone fusion and tooth eruption. Based on selected comparisons to other megabats, we discuss broad patterns of variation in general cranial shape, and interspecific variation in sutures, foramina, processes, and dentition. Overall, this work establishes a descriptive and nomenclatorial benchmark for chiropteran skull anatomy in line with similar works in other mammalian orders, with the aim of creating common ground for comparative, phylogenetic, and functional studies of the bat skull, including comparisons with other mammals.

INTRODUCTION

Detailed studies of skull morphology of selected fossil and living mammals have generated a solid basis of description and nomenclature for comparative functional analyses, systematic studies, and phylogenetic analyses of a number of mammalian clades. Examples include early Tertiary leptictid insectivorans (Novacek, 1986), the Paleocene metatherian *Pucadelphys* (Marshall and Muizon, 1995), the Late Cretaceous multituberculate *Kryptobaatar* (Wible and Rougier, 2000), the Late Cretaceous eutherian *Zalambdalestes* (Wible et al., 2004), the extant short-tailed opossum *Monodelphis* (Wible, 2003), and the extant yellow armadillo *Euphractus* (Wible and Gaudin, 2004). Although bats comprise over 20% of extant mammalian species (Simmons, 2005), no such detailed anatomical study of a bat skull has been completed to date. Some studies have investigated a portion of the bat skull in detail—such as works on the ear region (Henson, 1961, 1970; Novacek,1985a, 1985b, 1987, 1991; Wible and Davis, 2000), the ethmoid region (Bhatnagar and Kallen, 1974; Kämper and Schmidt, 1977), and the hyoid apparatus (Sprague, 1943)—but the skull as a whole has never been subject to a comprehensive anatomical treatment. Because alpha-level systematics and morphology-based phylogenetics of mammals tend to rely heavily on craniodental characters, lack of a standardized reference for bats has made communication about bat skull morphology difficult and has impeded comparative studies with other mammals. Several new bat species are described every year (Simmons, 2005), some of which are new megachiropterans (e.g., Maryanto and Yani, 2003), and it is important that the details of their morphology be adequately communicated to the scientific community. Molecular studies are increasingly identifying cryptic species that are difficult to distinguish morphologically (e.g., Ruedi and Mayer, 2001; Mayer and von Helversen, 2001; Campbell et al., 2004), making precision in anatomical terminology all the more important. Increasingly sophisticated functional studies of feeding behavior (e.g., Dumont, 1999, 2003; Nicolay and Dumont, 2000) and evolutionary relationships (e.g., Simmons and Geisler, 1998, 2002; Gunnell and Simmons, in press) similarly require more detailed information on skull morphology and element homology. As the diversity of bats continues to be unveiled, the need for standardized frames of reference for describing and analyzing bat cranial morphology will only increase.

The aim of our work is to provide a detailed description of the skull of a representative of Chiroptera, in this case a megachiropteran, that will help fill the vacuum of anatomical description for bats. This represents a special challenge because adult bats are characterized by relatively complete fusion of cranial bones. Thus, ontogenetic considerations are fundamental to understanding the structure of individual bones, relationships among different bones, locations of contacts between elements, and the exact placement of structures such as foramina and processes. We chose to focus our study on the megachiroptean bat *Pteropus* because these animals are relatively large, are well represented in museum collections, and are commonly cited in the comparative literature on bats. The foundation of our understanding of megachiropteran systematics was provided by Andersen (1912), who used many cranial features in his characterizations of subfamilies, genera, and species in the family Pteropodidae. Much of the terminology subsequently applied to pteropodid crania (e.g., by Bergmans, 1976, 1977, 1980, 1988, 1989, 1990, 1994, 1997, 2001; Bergmans and Rozendaal, 1988; Koopman, 1989, 1994; and others) was derived from Andersen's (1912) work. However, neither he nor any subsequent author provided a detailed description of the megachiropteran skull, and terminology has not been uniformly applied, even within this relatively restricted family. Here we provide a detailed anatomical description of the skull of *Pteropus*. This description includes the skull as a whole, the external surfaces of each bone as they appear in intact skulls, the internal surfaces of bones as they appear in disarticulated skulls, the dentition, and the contents of all cranial foramina. We provide a terminology consistent with the Nomina Anatomica Veterinaria (NAV), as well as pertinent synonyms from the bat literature and extensions to cases not covered by the NAV.

MATERIAL AND METHODS

TAXONOMIC SAMPLE: *Pteropus* is one of the most speciose genera of bats, including 67 currently recognized species representing 18 species groups (Simmons, 2005). Andersen (1912) described three skull types in *Pteropus* using *P. hypomelanus*, *P. anetianus*, and *P. scapulatus* as models. Andersen (1912) considered *P. hypomelanus* as representative of the genus because it lacks obvious specializations such as a short rostrum associated with heavy teeth (characteristic of the *anetianus* type) or an excessively weak cheek tooth dentition (*scapulatus* type). Andersen (1912) viewed these specialized forms as occupying the ends of a gradient; most *Pteropus* species fit in between, associated with the relatively unmodified *hypomelanus* type near the middle of the gradient. Our studies focused on comparatively unspecialized *Pteropus* species with *hypomelanus*-type skulls sensu Andersen (1912).

We chose *Pteropus lylei* K. Andersen, 1908 (*vampyrus* species group) as the principal subject of our descriptions on the basis of the availability of a beautifully preserved series of young adults housed at the Carnegie Museum of Natural History (CM), complemented by a collection at the American Museum of Natural History (AMNH, see below). We also examined comparative material from other megachiropteran species housed at those museums and at the Museum of Natural History, London (BMNH), the Field Museum of Natural History, Chicago (FMNH), the Royal Ontario Museum, Toronto (ROM), and the United States National Museum of Natural History, Smithsonian Institution, Washington, DC (USNM). We include descriptions of *Pteropus capistratus* (*personatus* species group), *Pteropus livingstonii* (*livingstonii* species group), and *Pteropus hypomelanus* (*subniger* species group) in order to treat aspects of the skull anatomy that were not accessible to examination in our specimens of *P. lylei*. Again, the selection was based on the suitability of specimens for the descriptive tasks. In particular, features of the auditory region were studied in further detail in *P. livingstonii*, whereas aspects of skull growth and bone fusion were studied in *P. lylei* and *P. capistratus*. Newborn *P. hypomelanus* were used to describe the deciduous dentition. Specimens of *Pteropus neohibernicus* (*neohibernicus* species group) and *Pteropus vampyrus* (*vampyrus* species group) were also used for comparative purposes.

ANATOMICAL SPECIMENS: Our descriptions are based primarily on CM 87972, a subadult male of *Pteropus lylei* from Thailand (Chon Buri Province). This specimen has M2 and m3 only partially erupted and most skull bones unfused (sutures clearly visible). The condylobasal length of CM 87972 is 50.7 mm. Comparisons were frequently made with CM 87973, another subadult of the same series. Other specimens examined included AMNH 30217, 217045, 237593, 237594, 237595, 237596, 237598, 237599, 240005, and 240006. Of these, two specimens (AMNH 30217 and 217045) are old individuals with extreme tooth wear (see Dentition) and almost complete bone fusion, whereas two (AMNH 240005 and 240006) are much younger, at an age stage only slightly older than the Carnegie specimens. The remainder of the AMNH sample consisted of adults with fully erupted permanent teeth and varying levels of tooth wear and bone fusion. The specimen of *Pteropus capistratus* (AMNH 194276) is a newborn pup with most deciduous teeth and no permanent teeth erupted. The specimens of *Pteropus livingstonii* used for the additional descriptions of the auditory region and internal surfaces of the skull were AMNH 274466, 274477, and 274515. Additional specimens used occasionally for comparative purposes included *Pteropus neohibernicus* AMNH 152402 and *Pteropus vampyrus* AMNH 198691.

THE HISTOLOGICAL SPECIMEN: Our histological observations are based on a 93.5-mm crown–rump length fetus of *Pteropus* sp. cataloged as No. 831 in the Duke University Comparative Embryological Collection, Durham, NC. The head was serially sectioned in a frontal plane, with section thicknesses of 16 μm, and stained with Mallory's trichrome. The basicranial vasculature and anatomy of this specimen were described by Wible (1992). For detailed descriptions of the chondrocrania of pteropodids, the reader is referred to Starck (1943) and Jurgens (1963). The former describes a younger stage fetus of *Pteropus seminudus* (= *Rousettus leschenaultii* following Koopman, 1993), and the latter describes a later stage fetus of *Rousettus aegyptiacus*.

DESCRIPTIONS AND TERMINOLOGY: Based on CM 87972, we describe the external skull osteology in two main sections. The section on the skull as a whole includes an overview of the skull regions, along with more detailed descriptions of the rostral, dorsal, lateral, ventral, and occipital views. The bones of the skull are subsequently described one by one in more detail in the following section. Names of general structures of the skull are given in the first section in English with their equivalent Latin terminology from the fourth edition of the Nomina Anatomica Veterinaria (NAV, 1994) italicized and in parentheses: for instance, the glenoid fossa (*fossa mandibularis*). The Latin name is given at the most relevant (usually the first) mention. When the English name corresponds with the Latin name, we italicize it once, at first use: for instance, the *foramen magnum*.

In the section on the skull as a whole, we describe overall external aspects of bony structures; descriptions in this section are not intended to be exhaustive, and only the most conspicuous traits are treated. In the bone-by-bone section, we greatly increase the detail of descriptions, also introducing some level of redundancy. Here we incorporate all specific terminology directly related to each bone (e.g., foramina, processes, borders, shapes, surfaces, and relationships with other bones) with the same English (*Latin*) convention. We also include the NAV arthrological nomenclature, defining the articulation at first use and naming it in English (and *Latin*). For instance, the articulation between the nasal and the frontal will be defined once as the frontonasal suture (*sutura frontonasalis*) and described in the treatment of the nasal (later mentions of this suture are in English). Often, reference is made to terminology used in cranial anatomy of the dog based on Evans (1993), because the dog skull has been described and illustrated in great detail.

We deal mainly with external surfaces and other structures that are externally visible in intact skulls. All bones are described in detail except for the ethmoid complex (mostly hidden from view in intact skulls) and, partially, the vomer (whose only visible parts are the incisive incisure rostrally and the

sphenoid incisure caudally) and the ventral nasal concha. We also describe the *pars cochlearis* of the petrosal and the middle ear ossicles, which is included in the NAV in the *organum vestibulocochlearis* (*organa sensuum*). To that, we add internal or medial views of elements of the auditory region, namely the middle ear ossicles and the petrosal. For this description, we used petrosals and middle ear ossicles of *Pteropus livingstonii*, which were available detached from the skull.

Using the partially disarticulated skulls of *Pteropus livingstonii* AMNH 274466 and 274477, we describe the internal surfaces of the skull. Ten such surfaces are available for examination as separate units, each including one to several bones, depending on the stage of bone fusion in different parts of the skull. These internal surfaces are the nasal, premaxillary, maxillary (including the maxilla and the ventral nasal concha), palatine, fronto-ethmoid complex (including also the vomer), presphenoid (including presphenoid and orbitosphenoid), basisphenoid (including the regions corresponding to the basisphenoid and alisphenoid), parietal (including parietal and interparietal), squamosal, and occipital (including the four occipital bones). In addition, we describe the shape of sutures that become visible only with disarticulation of the skull elements. The internal surfaces of the petrosal and ectotympanic are treated in the corresponding treatments of those bones.

For the sake of completeness, we also describe in detail the hyoid apparatus and the larynx, i.e., the posterior part of the visceral or branchial skeleton, which is frequently preserved together with macerated osteological material and is a potential source of characters in comparative anatomy, especially in Megachiroptera. We used the subadult female *Pteropus tonganus* USNM 566608 as the subject of our description; other specimens (detailed below) were used to draw some basic comparisons within *Pteropus*. In our centerpiece specimen, the hyoid apparatus is intact and detached from both the skull and the laryngeal elements. For comparisons and further illustration, we direct the reader to Sprague (1943), who studied the hyoid and larynx of members of each bat family recognized at the time, including megachiropterans sampled from main taxonomic groupings based on Andersen (1912).

We used the entire sample of *Pteropus lylei* to describe the permanent dentition in an exhaustive way. This includes dental formula, pattern of occlusion and tooth wear, and a detailed description of the structure of each tooth. The convention used for tooth abbreviation is initial letter for each tooth type (i.e., incisors, canines, premolars, and molars), in upper case for upper teeth and in lower case for lower teeth, followed by a number indicating the individual tooth. For instance, I2 denotes the second upper incisor, C denotes the upper canine, P4 denotes the fourth upper premolar, and m3 denotes the third lower molar. In dental formulae, we give the number of teeth arranged by tooth type, using upper case. The dental formula of *P. lylei* is I2/2, C1/1, P3/3, M2/3, indicating that the species possesses 2 upper/2 lower incisors, 1 upper/1 lower canine, 3 upper/3 lower premolars, and 2 upper/3 lower molars. Premolars are designated P1, P3, P4, p1, p3, and p4; that is, P2 and p2 are assumed to be missing in bats in general. The dental formula for the deciduous dentition is dI2/2, dC1/1, dP2/2.

The sectioned *Pteropus* fetus was used to reconstruct associations between soft tissues and osteological structures. The contents of foramina are described in a separate section. Other observations (e.g., muscle attachments) are included in sections that deal with the appropriate bones. For the soft-tissue structures, we use English versions of NAV terms, unless noted.

Comparisons were made between young and adult individuals in order to describe ontogenetic changes that affect cranial osteology. Other comparisons were made with other megachiropterans so as to evaluate the level of generality of descriptions of particular bones or structures. Comparisons of this kind were primarily made with other pteropodine megachiropterans, a group that, according to Bergmans (1997), includes *Pteropus* (67 species; Simmons, 2005), *Pteralopex* (5 or 6 species), *Acerodon* (6 species), *Neopteryx* (1 species), and *Styloctenium* (1 species). *Eidolon* (2 species) may join this group as well (Giannini and Simmons, 2005). For selected comparisons (e.g., variation in

foramina), a wider sample of megachiropterans was considered.

Usage of directional terms varies; in general, we follow Evans (1993) and the NAV. In most skull structures, we use rostral (or anterior) and caudal (or posterior), dorsal, and ventral. In oral and dental structures, we use lingual (or medial), buccal (or lateral, or vestibular), occlusal, rostral (or mental), caudal, upper, and lower. In the hyoid apparatus, we use cranial, caudal, lateral, medial, proximal, and distal. Finally, following Evans (1993), nomenclature of joints includes the joint types synovium, synchondrosis, and suture, the latter falling into four categories: plane, squamous, foliate, and serrate. Specific joints are referred to by either their English or Latin names, except the *sutura squamosa* (between the squamosal and parietal bones), which is always referred to in Latin to avoid confusion with the suture type of the same English name that occurs widely in the skull.

THE SKULL AS A WHOLE

Regions of the Skull

The *rostrum* is formed by the paired nasal, premaxilla, maxilla, ventral nasal concha, palatine, lacrimal, jugal, and mandible (*ossa faciei*). In *Pteropus lylei* CM 87972, the rostrum, as measured from the rostralmost edge of the premaxilla to the caudalmost tip that the palatine contributes to the ectopterygoid process, is slightly longer than half the length of the entire skull. The *cranium* is formed by the paired frontal, parietal, pterygoid, orbitosphenoid, alisphenoid, squamosal, petrosal, entotympanic, ectotympanic, and exoccipital (plus the middle ear ossicles in the *auris*), and the unpaired interparietal, vomer, ethmoid, presphenoid, basisphenoid, basioccipital, and supraoccipital (*ossa cranii*). We have examined the skull of *P. lylei* CM 87972 and its structures in dorsal (fig. 1), lateral (fig. 2), ventral (fig. 3), rostral (fig. 4), and oblique occipital (fig. 5) views, as well as the mandible in lateral (fig. 6), occlusal (fig. 7), and mental (fig. 8) views.

The apex (*regio naris*) is formed by the premaxillae ventrolaterally and the nasals dorsally, which enclose the osseous nasal opening (*apertura nasi ossea*) or external nasal aperture. The dorsal surface of the rostrum (*regio dorsalis nasi*) is formed chiefly by the nasals, which are edged by the dorsalmost extension of the maxillae laterally (fig. 1). The lateral wall of the rostrum (*regio maxillaris*) is formed almost in its entirety by the rostral process of the maxilla (fig. 2). The hard palate (*palatum osseum*) is composed of the palatine process of the maxilla rostrolaterally and the transverse process of the palatine caudally (figs. 3, 9). The premaxilla does not contribute to the hard palate because its palatine process is not ossified. The zygomatic arch (*arcus zygomaticus*, *regio zygomatica*) or zygoma is formed by the zygomatic process of the maxilla and the small jugal bone, which articulate caudally with the zygomatic process of the squamosal in the temporal region (see fig. 2 and below). The orbital region (*regio orbitalis*), in the middle of the skull laterally, is a large depression containing the fossa for the eyeball (*bulbus oculi*) or orbit (*orbita*). Ventral to the orbit is the pterygopalatine fossa (*fossa pterygopalatina*). Dorsal to the orbit is the forehead (*frons*) of the frontal region (*sinciput*, *regio frontalis*), which is formed exclusively by the frontal bone (fig. 1). Caudal to the orbital region is the rostral aspect of the braincase, with the *fossa temporalis* and *fossa infratemporalis* dorsally and ventrally, respectively. In the temporal region (*regio temporalis*), the squamosal projects rostrolaterally its zygomatic process, which comprises the posterior third of the zygomatic arch. The root of the zygomatic process (figs. 3, 5) overlies the glenoid fossa (*fossa mandibularis*), the cranial component of the temporomandibular joint (*articulatio temporomandibularis*, a synovial joint). Another component of the temporal region is the auditory region (*auris*), including the petrosal bone, ectotympanic, entotympanic, and the middle ear ossicles, located ventromedial to the squamosal and lateral to the basioccipital (see figs. 3, 5, and below). The dorsolateral aspect of the parietal region (*regio parietalis*, formed by the parietals and interparietal) is the *planum parietale*, the largest exposure of the braincase. The temporal and parietal regions provide both protection to the brain and origin to the *m. temporalis*.

In the ventral side, caudal to the hard palate (fig. 10), the *choanae* open anteriorly into the paired nasopharyngeal meatus (*meatus nasopharyngeus*). The basicranium (*basis cranii externa*) forms, in tandem with the ventral component of the occipital complex (see below), the floor of the braincase (fig. 3). It extends from the dorsolateral orbitosphenoid and alisphenoid bones (*alae temporales et orbitales*), which provide osseous basement to the caudal orbit and the infratemporal fossa, to the medial (pre- and basi-) sphenoid bones, which roof the nasopharyngeal meatus. Four ossifications—the unpaired supraoccipital and basioccipital (dorsal and ventral) and the paired exoccipitals (lateral)—as well as a small exposure of the petrosal, form the *occiput*, surrounding the large *foramen magnum* for the passage of the spinal cord and associated vessels (fig. 5).

The paired mandible consists of a tooth-bearing body connected anteriorly with its bilateral counterpart through the mandibular symphysis, and a *ramus* posteriorly (figs. 6, 7). The latter has a coronoid process and a mandibular condyle that articulates with the squamosal, forming the mandibular component of the temporomandibular joint.

Rostral View of the Skull

The apex of the rostrum consists of a large, almost heart-shaped external nasal aperture bordered ventrolaterally by the dorsally divergent premaxillae and dorsally by the nasals. Visible through the external nasal aperture inside the nasal cavity (*cavum nasi*) are the paired ventral nasal concha (*concha nasalis ventralis*) or maxilloturbinate, the incisive incisure of the *vomer* (also visible through the incisive fissure ventrally), the nasal septum (*septum nasi osseum*), and the very tip of the ethmoturbinals (*ethmoturbinalia*). Four incisors are attached to the premaxillae (see Dentition below).

Dorsal Surface of the Skull

The principal components of the rostrum are the dorsal surface of the nasals medially and the rostral process of the maxillae laterally, with a limited contribution of the premaxillae in the rostrolateral angles. The breadth of the rostrum increases abruptly at the level of the canines to accommodate the canine roots and the correspondingly prominent juga. There is only a modest widening of the rostrum caudal to the canines. The lacrimal is visible laterally in dorsal view (fig. 1). On the ventrocaudal angle of the rostrum, the large root of the zygomatic arch, in association with the alveolar process of the maxilla, forms a roughly triangular plate. The rostrolateral edge of the zygomatic root is a bridge of bone perforated by the infraorbital canal (*canalis infraorbitalis*). The horizontal plate of the root, widely visible in dorsal view, represents the maxillary tuberosity. The open roots of M1 and M2 protrude in that surface—which is also the floor of the pterygopalatine fossa, a space that funnels rostrally into the infraorbital canal. The caudal edge of the zygomatic root is deeply concave (fig. 3); it converges caudolaterally with the rostrolateral edge of the root, leading to the laterally compressed arches themselves. Shortly after, the maxillary part of the arch meets the small jugal, which constitutes the middle portion of the arch. The posterior zygomatic root, dorsoventrally compressed, is contributed by the zygomatic process of the squamosal, which joins the braincase laterally. The posterior zygomatic root projects rostrolaterally from the braincase and widely overlaps the jugal dorsally.

The frontal forms the central portion of the dorsal surface of the skull (fig. 1). The dorsal aspect of the frontal may be divided into a short, preorbital area, a laterally biconcave interorbital area rostrally, bounded by the supraorbital margin (*margo supraorbitalis*), and an approximately rectangular postorbital plate caudally. The prominent postorbital processes (*processus zygomaticus*) arise between the two posterior areas. The large postorbital foramen pierces the root of each postorbital process.

The braincase is large and bulbous, with a roughly piriform shape. CM 87872 shows a smooth cranial surface with no temporal lines. The rounded surface of each parietal (*planum parietale*) and the interparietal caudomedially are visible in dorsal view, whereas the lateral contribution from the squamosal to the braincase (the *squama*) is hidden in this view.

Fig. 1. Dorsal view of the skull of *Pteropus lylei* CM 82972, with accompanying line drawing. Scale = 5 mm. Abbreviations: **C** upper canine; **fr** frontal; **ip** interparietal; **ju** jugal; **lac** lacrimal; **mx** maxilla; **na**

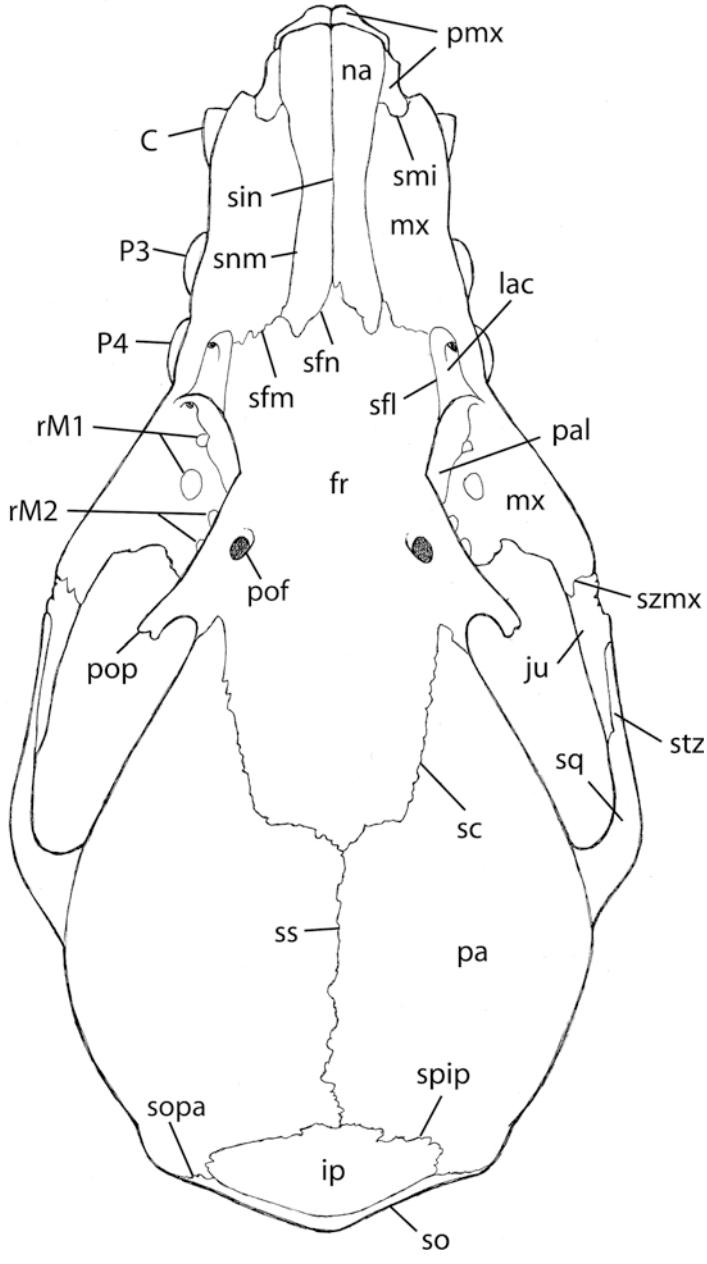

Fig. 1. Continued.

nasal; **P3** third upper premolar; **P4** fourth upper premolar; **pa** parietal; **pal** palatine; **pmx** premaxilla; **pof** postorbital foramen; **pop** postorbital process; **rM1** roots of first upper molar; **rM2** roots of second upper molar; **sc** sutura coronalis; **sfl** sutura frontolacrimalis; **sfm** sutura frontomaxillaris; **sfn** sutura frontonasalis; **sin** sutura internasalis; **smi** sutura maxilloincisiva; **snm** sutura nasomaxillaris; **so** supraoccipital; **sopa** sutura occipitoparietalis; **spip** sutura parietointerparietalis; **sq** squamosal; **ss** sutura sagittalis; **stz** sutura temporozygomatica; **szmx** sutura zygomaticomaxillaris.

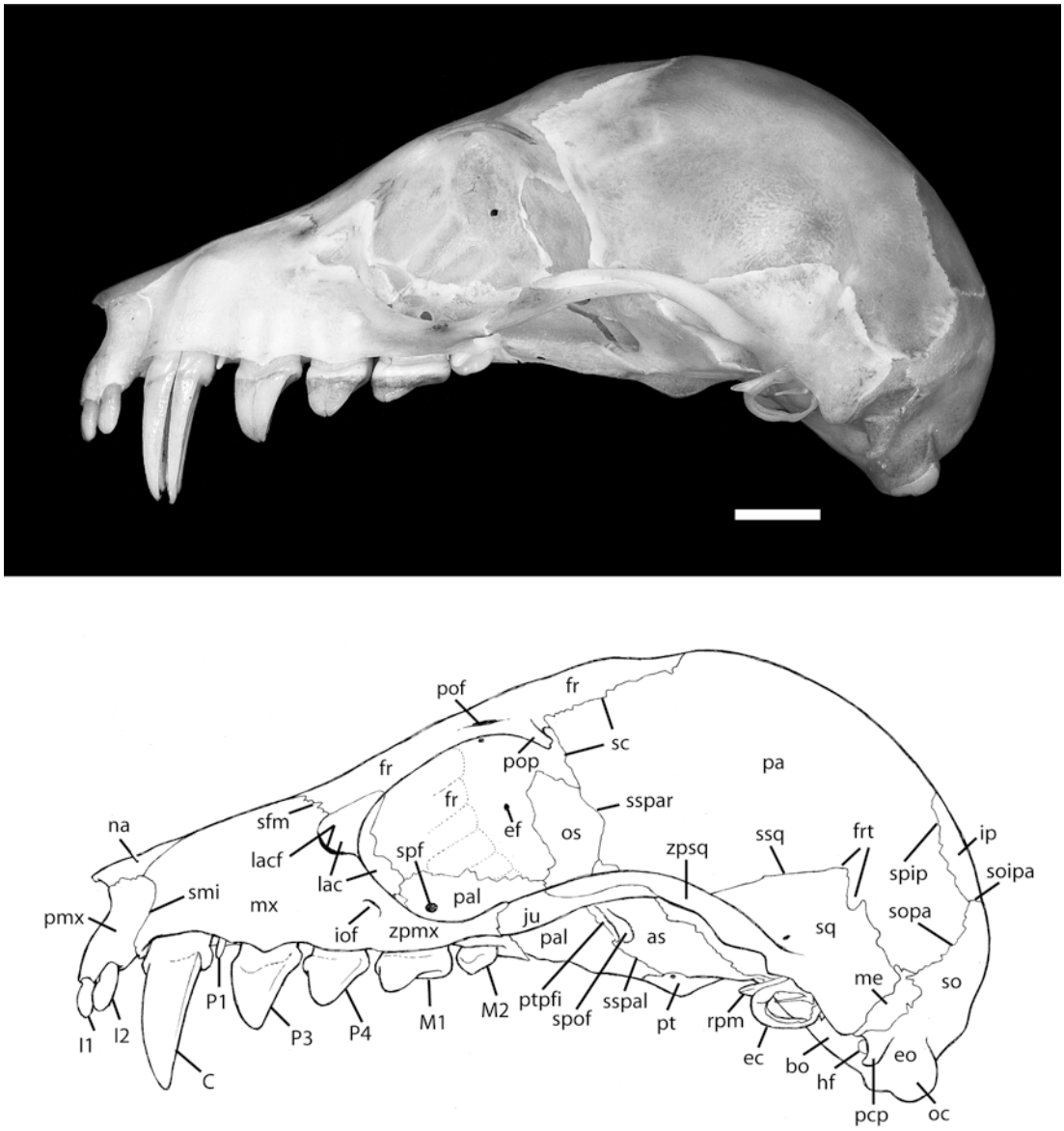

Fig. 2. Lateral view of the skull of *Pteropus lylei* CM 82972, with accompanying line drawing. Scale = 5 mm. Abbreviations: **as** alisphenoid; **bo** basioccipital; **C** upper canine; **ec** ectotympanic; **ef** ethmoidal foramen; **eo** exoccipital; **fr** frontal; **frt** foramina for rami temporales; **hf** hypoglossal foramen; **I1** first upper incisor; **I2** second upper incisor; **iof** infraorbital foramen; **ip** interparietal; **ju** jugal; **lac** lacrimal; **lacf** lacrimal foramen; **M1** first upper molar; **M2** second upper molar; **me** mastoid exposure of petrosal; **mx** maxilla; **na** nasal; **oc** occipital condyle; **os** orbitosphenoid; **P1** first upper premolar; **P3** third upper premolar; **P4** fourth upper premolar; **pa** parietal; **pal** palatine; **pcp** paracondylar process; **pmx** premaxilla; **pof** postorbital foramen; **pop** postorbital process; **pt** pterygoid; **ptpfi** pterygopalatine fissure; **rpm** rostral process of malleus; **sc** sutura coronalis; **sfm** sutura frontomaxillaris; **smi** sutura maxilloincisiva; **so** supraoccipital; **soipa** sutura occipitointerparietalis; **sopa** sutura occipitoparietalis; **soipa** sutura occipitointerparietalis; **spf** sphenopalatine foramen; **spip** sutura parietointerparietalis; **spof** sphenorbital fissure; **sq** squamosal; **sspal** sutura sphenopalatina; **sspar** sutura sphenoparietalis; **ssq** sutura squamosa; **zpmx** zygomatic process of maxilla; **zpsq** zygomatic process of squamosal.

Lateral Surface of the Skull

The rostrum is formed chiefly by the maxilla in lateral view (fig. 2), and its gently convex lateral surface is marked anteriorly by the alveolar juga of the canines. Rostrally, the procumbent premaxilla projects anteriorly beyond the rostral end of the nasal; ventrally, it extends below the level of the alveolar line. The alveolar line is sinuous, with rounded valleys and peaks corresponding to the locations of individual teeth and spaces between them. The upper tooth row consists of two incisors followed by a large canine, a minute P1 and four well-developed cheek teeth (two premolars and two molars; see Maxilla and Dentition). Dorsally, the rostrum gently ascends to meet the frontal, which in turn continues rising to the coronal (= frontoparietal) suture (seen in dorsal view). Posteriorly, the thin, elongated anterior zygomatic root projects caudolaterally from the maxilla. The anterior zygomatic root is pierced by a large infraorbital canal. The anterior zygomatic root meets the jugal well away from the contact with the alveolar process of the maxilla. The jugal occupies the middle portion of the dorsoventrally thin, gently arched, mediolaterally compressed zygomatic arch, and it is widely overlaid by the zygomatic process of the squamosal.

The orbit is large, placed slightly off center in the middle portion of the skull (fig. 2). The rounded orbital outline is delimited rostroventrally by the small, triangular lacrimal and the anterior root of the zygomatic arch, and dorsally by the frontal and its postorbital process. The orbit is not bounded caudally by bone as in individuals of some large-sized species of *Pteropus* and allies (*Acerodon*, *Pteralopex*), in which the orbital ligament (*lig. orbitale*) ossifies to produce a complete osseous bar connecting the postorbital process and zygomatic arch (this bar is sometimes called the jugal spine). The orbital fossa is gently concave and is continuous caudally with the temporal fossa.

Ventral to the orbit is the pterygopalatine fossa, which is formed mainly by the oblique, mediodorsally oriented plane of the perpendicular process of the palatine. There is only a faint infratemporal crest on the alisphenoid delimiting the temporal fossa from the infratemporal fossa in CM 87972. In our sample, some specimens (e.g., AMNH 237593) show a slightly more robust infratemporal crest. In the ventrocaudal conjunction of the orbit and pterygopalatine fossa are the openings of the optic canal and sphenorbital fissure, as well as the transverse cleft that separates the palatine and the pterygoid, the pterygopalatine fissure (fig. 2). Caudal to the sphenorbital fissure, the convex alisphenoid forms the rostroventral border of the braincase. Caudal to that area is the glenoid fossa, barely visible in lateral view, underlying the posterior zygomatic root. Immediately caudal to the glenoid fossa, the external acoustic meatus (*meatus acusticus externus*) opens laterally, showing an arched dorsal margin that is the attachment area of the small, oval ectotympanic. The manubrium of the malleus is visible inside the ectotympanic. Where the temporal area merges with the occipital region, three successively larger protuberances appear caudally: the posttympanic process of the squamosal, the paracondylar process of the exoccipital, and the occipital condyle.

In lateral view (fig. 2), the braincase as a whole is oval in shape, with the most convex point approximately at the center of the parietal. The braincase shows two distinctive traits. First, the ventral deflection of the basicranial axis with respect to the rostral axis is extraordinarily pronounced, which is all the more noticeable if the rostral axis is held horizontally. If an imaginary line is projected caudally at the level of the alveolar line, it intersects a point on the cranium at the level of the external occipital protuberance of the supraoccipital. Second, the occipital region protrudes caudally, forming the so-called "tubular occiput" (Miller, 1907; Andersen, 1912) typical of adult pteropodine megachiropterans (especially *Pteropus*). In his description of the skull, Andersen (1912: 61) stated that the "occiput [is] produced backward and downward, as a short tube". This trait is more easily observed if the skull is held with the basicranial axis aligned horizontally. In that position, the occipital condyles project caudally beyond an imaginary vertical line at the level of the incipient nuchal crest.

Fig. 3. Ventral view of the skull of *Pteropus lylei* CM 82972, with accompanying line drawing. Scale = 5 mm. Abbreviations: **apf** accessory palatine foramen; **as** alisphenoid; **bcc** posterior basicochlear commissure; **bcf** basicochlear fissure; **bo** basioccipital; **bs** basisphenoid; **C** upper canine; **cf** carotid foramen; **ec** ectotympanic; **ecptp** ectopterygoid process; **en** rostral entotympanic; **eo** exoccipital; **fc** fenestra cochleae; **if** incisive fissure; **fm** foramen magnum; **fo** foramen ovale; **fr** frontal; **gf** glenoid fossa; **ham** hamulus pterygoideus; **hf** hypoglossal foramen; **I1** first upper incisor; **I2** second upper incisor; **jf** jugular foramen; **ju** jugal; **M1** first upper molar; **M2** second upper molar; **mapf** major palatine foramen; **me**

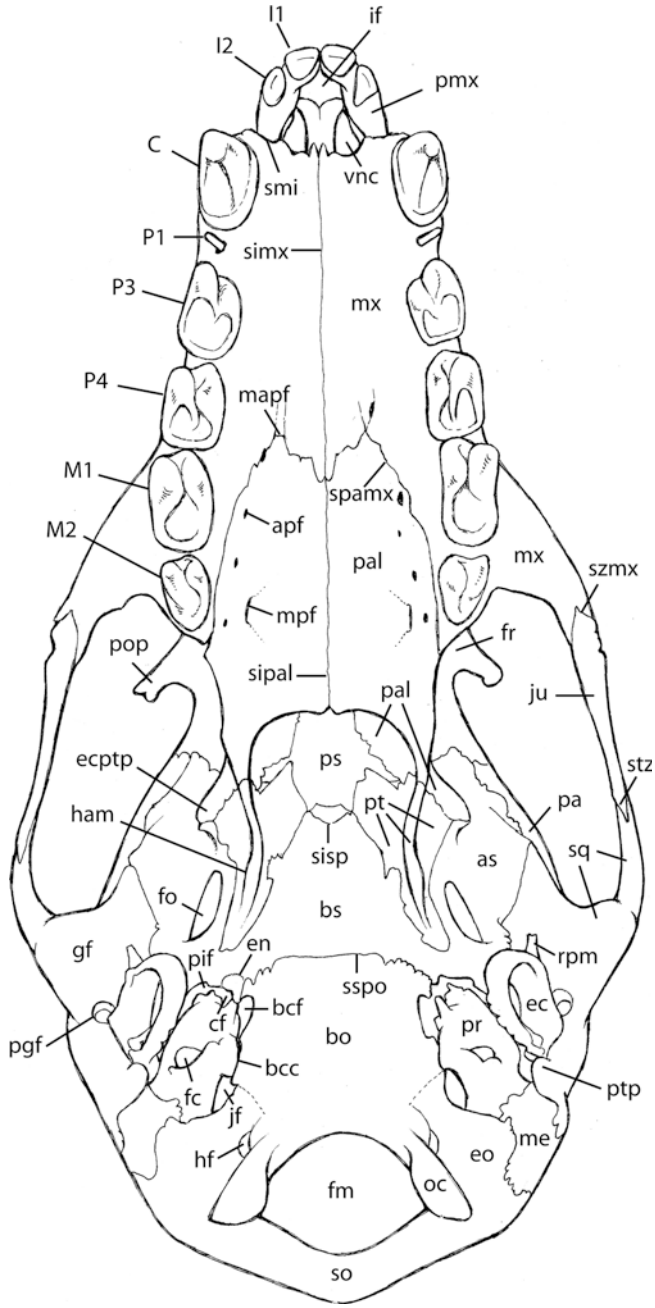

Fig. 3. Continued.

mastoid exposure of petrosal; **mpf** minor palatine foramen; **mx** maxilla; **oc** occipital condyle; **P1** first upper premolar; **P3** third upper premolar; **P4** fourth upper premolar; **pa** parietal; **pal** palatine; **pgf** postglenoid foramen; **pif** piriform fenestra; **pmx** premaxilla; **pop** postorbital process; **pr** promontorium of petrosal; **ps** presphenoid; **pt** pterygoid; **ptp** posttympanic process; **rpm** rostral process of malleus; **simx** sutura intermaxillaris; **sipal** sutura interpalatina; **sisp** synchondrosis intersphenoidalis; **smi** sutura maxilloincisiva; **so** supraoccipital; **spamx** sutura palatomaxillaris; **sq** squamosal; **sspo** synchondrosis sphenoccipitalis; **stz** sutura temporozygomatica; **szmx** sutura zygomaticomaxillaris; **vnc** ventral nasal concha or maxilloturbinal.

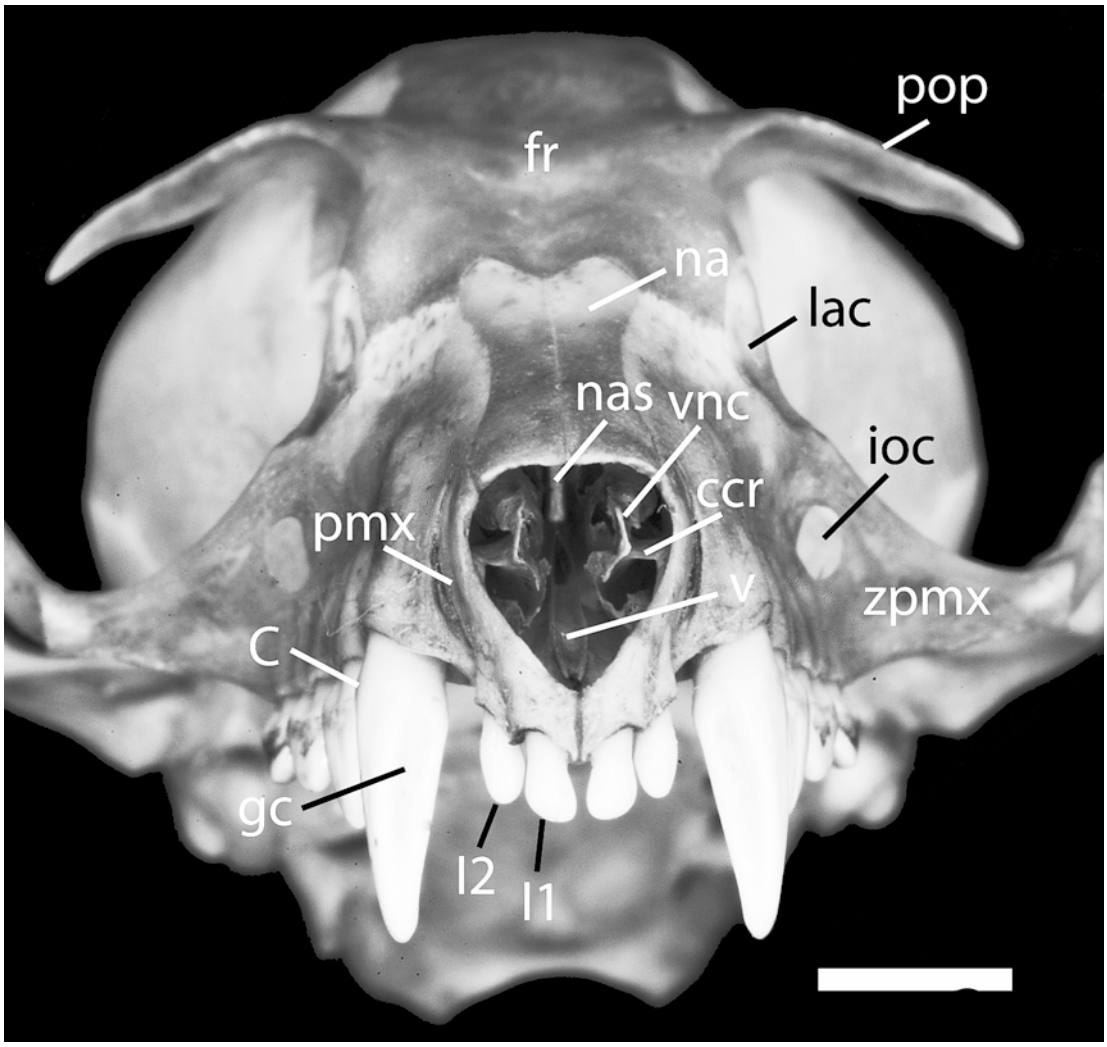

Fig. 4. *Pteropus lylei* AMNH 237595, rostral view of the skull. Scale = 5 mm. Abbreviations: **C** upper canine; **ccr** conchal crest; **fr** frontal; **gc** groove of upper canine; **I1** first upper incisor; **I2** second upper incisor; **ioc** infraorbital canal; **lac** lacrimal; **na** nasal; **nas** nasal septum; **pmx** premaxilla; **pop** postorbital process; **v** vomer; **vnc** ventral nasal concha; **zpmx** zygomatic process of maxilla.

Ventral Surface of the Skull

The ventral surface of the skull shows the hard palate (figs. 3, 9), the basipharyngeal canal or choanal region (figs. 3, 10), the basicranium, the auditory region, and the ventral side of the zygomatic arches (fig. 3). The premaxillae project beyond the rostral edge of the canines. A wide I2–C diastema is present. The C–C distance is markedly wider than the maximum premaxillary width. The bulk of the rostrum ends abruptly in front of the canines. Rostral to the C–C line is the large incisive fissure surrounded rostrolaterally by the left and right premaxillae, which project and converge to each other rostromedially. The length of the hard palate (23.8 mm, measured from the rostralmost end of the palatine process of the maxilla to the caudalmost extension of the palatine in the midsagittal line) is considerably greater than its width (15.2 mm, measured as the distance between the lateralmost points of the left and right M1). The upper tooth row is

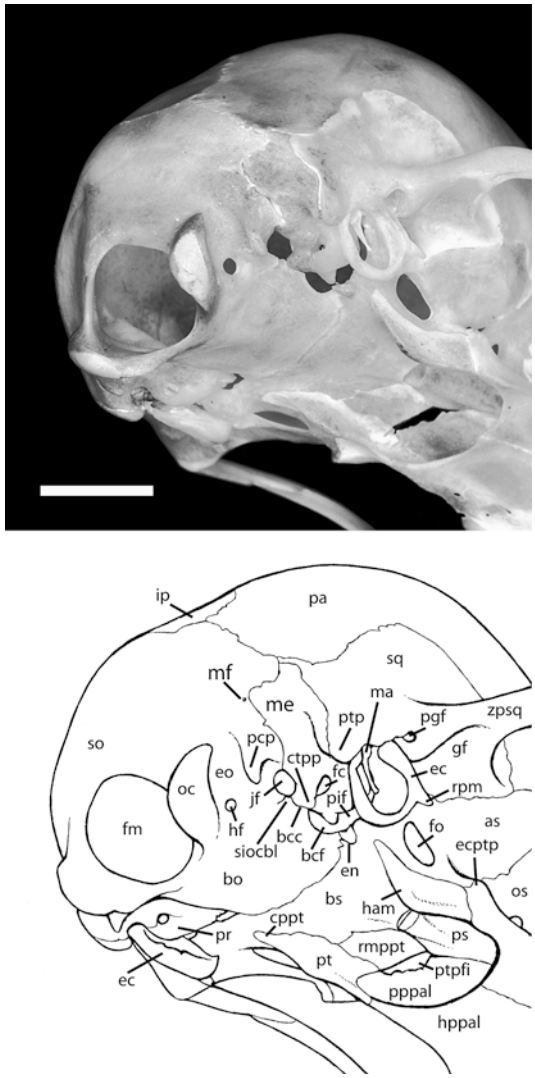

Fig. 5. *Pteropus lylei* CM 82972, oblique occipital view. Scale = 5 mm. Abbreviations: **as** alisphenoid; **bcc** posterior basicochlear commissure; **bcf** basicochlear fissure; **bo** basioccipital; **bs** basisphenoid; **cppt** caudal process of pterygoid; **ctpp** caudal tympanic process of petrosal; **ec** ectotympanic; **ecptp** ectopterygoid process; **en** rostral entotympanic; **eo** exoccipital; **fc** fenestra cochleae; **fm** foramen magnum; **fo** foramen ovale; **gf** glenoid fossa; **ham** hamulus pterygoideus; **hf** hypoglossal foramen; **hppal** horizontal process of palatine; **ip** interparietal; **jf** jugular foramen; **ma** malleus; **me** mastoid exposure of petrosal; **mf** mastoid foramen; **oc** occipital condyle; **os** orbitosphenoid; **pa** parietal; **pcp** paracondylar process; **pgf** postglenoid foramen; **pif** piriform fenestra; **pppal** perpendicular process of palatine; **pr** promontorium of petrosal; **ps** presphenoid; **pt** pterygoid; **ptp** posttympanic process; **ptpfi** pterygopalatine fissure; **rmppt** rostromedial process of pterygoid; **rpm** rostral process of malleus; **siocbl** synchondrosis intraoccipitalis basilateralis; **so** supraoccipital; **sq** squamosal; **zpsq** zygomatic process of squamosal.

only slightly divergent from the canine root to M2. The interdental palate is a smooth, gently concave surface perforated laterally by foramina of the palatine nerve and vessels complex (see Maxilla, Palatine, and Foramina Contents and Homology). There is a large, caudally projecting postdental palate. Laterally, the postdental palate is roughly straight, converging only slightly medially until it reaches the pterygoid, where the palate contributes to the large ectopterygoid process. Medially, the postdental palate takes the shape of a wide ∩, ending in the midpoint between the caudal border of M2 and the ectopterygoid process. This caudal edge is slightly deflected ventrally, increasing the concavity of the postdental palate. Immediately caudal is the ventrally open basipharyngeal canal, which is roofed by the presphenoid and basisphenoid and framed laterally by the pterygoids (fig. 10). In this area, the nasopharyngeal duct is wide and relatively shallow. Lateral to the pterygoid is the convex surface of the alisphenoid, which is pierced by the large foramen ovale. Lateral to the foramen ovale is the large glenoid fossa and the posterior root of the zygomatic arch.

The basioccipital presents a wide, slightly convex surface that leads caudally to the large opening of the foramen magnum and the projecting occipital condyles. Laterally, the basioccipital has a relatively narrow contact with the petrosal in the posterior basicochlear commissure. Rostral to this commissure is the basicochlear fissure, which on the left side of CM 87972 is confluent with the piriform fenestra, whereas on the right side it is separated from the latter by the small entotympanic (see details in Basioccipital). The entotympanic element is a short, peglike rostral entotympanic, preserved only on the right side in CM 87972 and variously attached to the basicranium in other specimens (see Entotympanic). Caudal to the

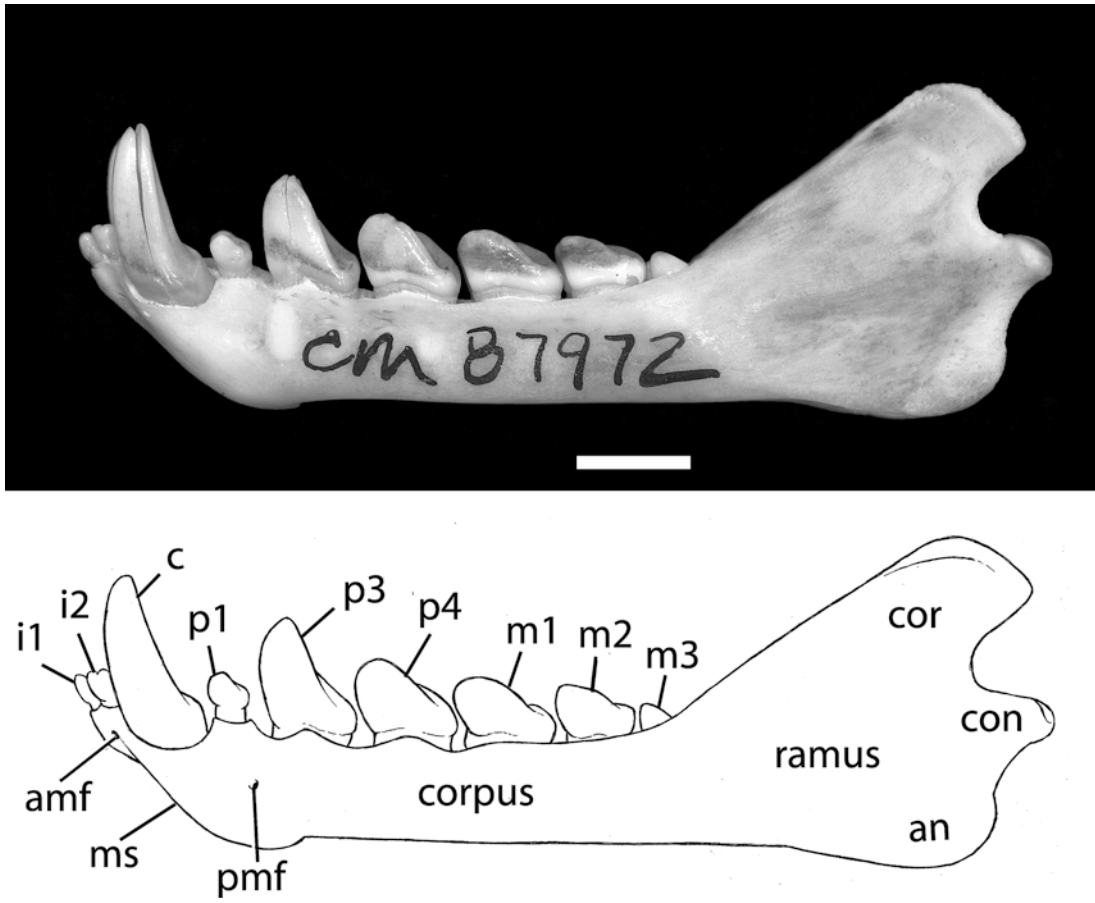

Fig. 6. *Pteropus lylei* CM 82972, lateral view of the left mandible, with accompanying line drawing. Scale = 5 mm. Abbreviations: **amf** anterior mental foramen; **an** angle of mandible; **c** lower canine; **con** mandibular condyle; **cor** coronoid process of mandible; **i1** first lower incisor; **i2** second lower incisor; **m1** first lower molar; **m2** second lower molar; **m3** third lower molar; **ms** mental surface; **p1** first lower premolar; **p3** third lower premolar; **p4** fourth lower premolar; **pmf** posterior mental foramen.

posterior basicochlear commissure is the large jugular foramen. Caudal to this foramen is the paracondylar process of the exoccipital.

The petrosal lies lateral to the basioccipital. It has a rounded promontorium with a large, caudoventrally directed round window, a large fossa for the *m. stapedius* caudolaterally, and a large, rather featureless mastoid exposure caudally. The ectotympanic attaches to the border of the external acoustic meatus (of which the posttympanic process is visible ventrally). The ectotympanic is inclined ventromedially. The anterior or rostral process of the malleus is visible on the anterior surface of the ectotympanic ring, with the glenoid fossa in the background. The large postglenoid foramen appears between the glenoid fossa and the external acoustic meatus.

Caudal Surface of the Skull

The occiput (fig. 5) is dominated by the very large foramen magnum. The occipital condyles, the cranial counterparts of the atlanto-occipital joint (*articulatio atlanto-occipitalis*), are obliquely placed on the lateral (and slightly ventral) margin of the foramen. Flanking the condyles are the small, ventrally oriented paracondylar

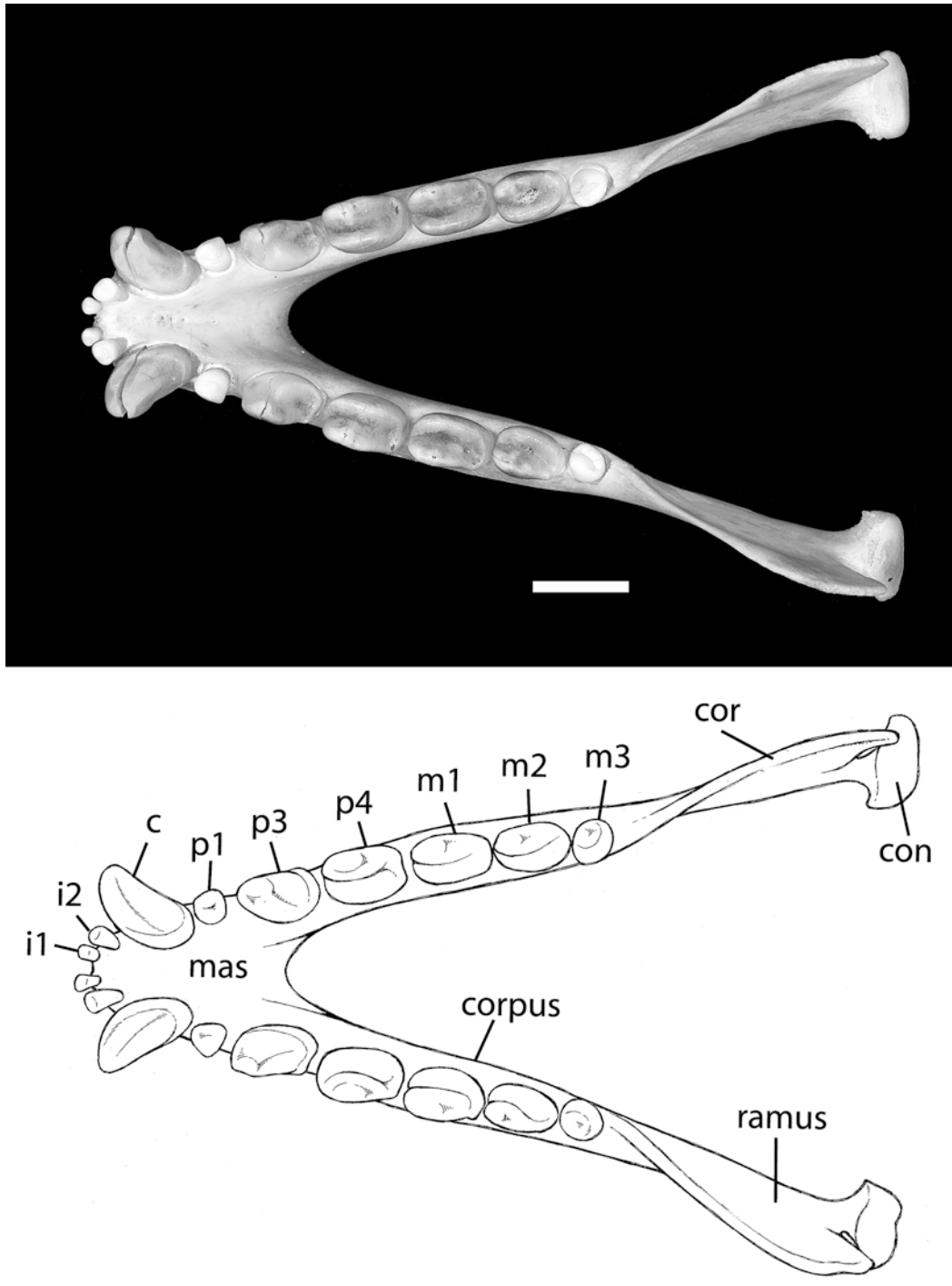

Fig. 7. *Pteropus lylei* CM 82972, occlusal view of the mandible, with accompanying line drawing. Scale = 5 mm. Abbreviations: **c** lower canine; **con** mandibular condyle; **cor** coronoid process of mandible; **i1** first lower incisor; **i2** second lower incisor; **m1** first lower molar; **m2** second lower molar; **m3** third lower molar; **mas** mandibular symphysis; **p1** first lower premolar; **p3** third lower premolar; **p4** fourth lower premolar.

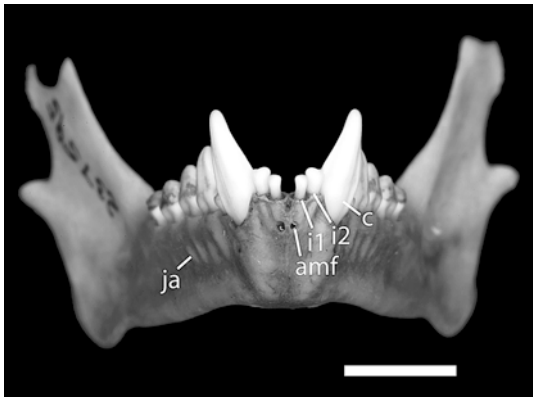

Fig. 8. *Pteropus lylei* AMNH 237595, rostral view of the mandible. Scale = 5 mm. Abbreviations: **amf** anterior mental foramen; **c** canine; **ja** dental juga; **i1** first upper incisor; **i2** second upper incisor.

processes of the exoccipital and, lateral to them, the flat mastoid exposure of the petrosal. The tubular structure of the occiput is evinced, in this view, by the pronounced slope of the supraoccipital area. In adult *Pteropus lylei* (e.g., AMNH 237593), a strong nuchal crest (*crista nuchalis*) is present (see Occipital Complex and Comparisons).

THE SKULL BONES

ROSTRAL BONES (*OSSA FACIEI*)

NASAL

The nasal (*os nasale*) is a paired bone that covers the dorsum of the rostrum from its apex to the level of P4 (fig. 1). The nasals have their rostral margin free (fig. 2), and articulate with each other in the median plane, forming the straight internasal suture (*sutura internasalis*; fig. 1). In turn, each nasal contacts the premaxilla anteroventrally, forming the nasoincisive suture (*sutura nasoincisiva*), the maxilla lateroventrally, forming the nasomaxillary suture (*sutura nasomaxillaris*), and the frontal caudally, forming the frontonasal suture (*sutura frontonasalis*). The dorsal surface of the nasals is roughly flat, with the rostrolateral angle slightly deflected downward (figs. 1, 2). The rostral edge is roughly square and forms the dorsal edge of the external nasal aperture, with little nasal overhang of that aperture. The nasomaxillary suture is gently bowed inward and runs along most of the length of the nasals. The frontonasal suture is W-shaped due to the roughly triangular posterolateral frontal process (*processus frontalis*) of each nasal penetrating the frontal as a wedge (fig. 1). Laterally, only the anterior tip of the nasals is visible (fig. 2). There are no foramina in the nasals.

PREMAXILLA

The premaxilla (*os incisivum*) is a paired bone located in the apex of the skull, forming the ventrolateral rim of the external nasal aperture (figs. 1–4). In the Pteropodidae, the premaxilla is composed of a lateromedially oriented body (*corpus ossis incisivi*), sometimes called the alveolar process of the premaxilla, and the dorsoventrally oriented nasal process (*processus nasalis*), whereas the palatine process (*processus palatinus*) is not ossified. The left and right bodies articulate by a plane suture, the short interincisive suture (*sutura interincisiva*). Each body bears the alveoli for two incisors (in general, *alveoli dentales*). The depth of the body increases from the alveolus of I1 to I2, and the alveolar line (*margo alveolaris* of the premaxilla) gently arches above each tooth.

The nasal process is a laterally compressed lamina that reaches the nasal dorsally, forming the nasoincisive suture, and contacts the rostral process of the maxilla caudally, forming the foliate maxilloincisive suture (*sutura maxilloincisiva*; equivalent to *sutura incisivomaxillaris* of the dog). In lateral view, the nasal process shows as a bar of bone directed dorsocaudally, maintaining a roughly constant width throughout its length. In rostral view, the two nasal processes diverge

→

Fig. 9. *Pteropus lylei* CM 82972, ventral view of hard palate. Scale = 5 mm. Abbreviations: **apf** accessory palatine foramina; **bs** basisphenoid; **C** upper canine; **ecptp** ectopterygoid process; **hppal** horizontal process of palatine; **I1** first upper incisor; **I2** second upper incisor; **if** incisive fissure; **iiv** incisura

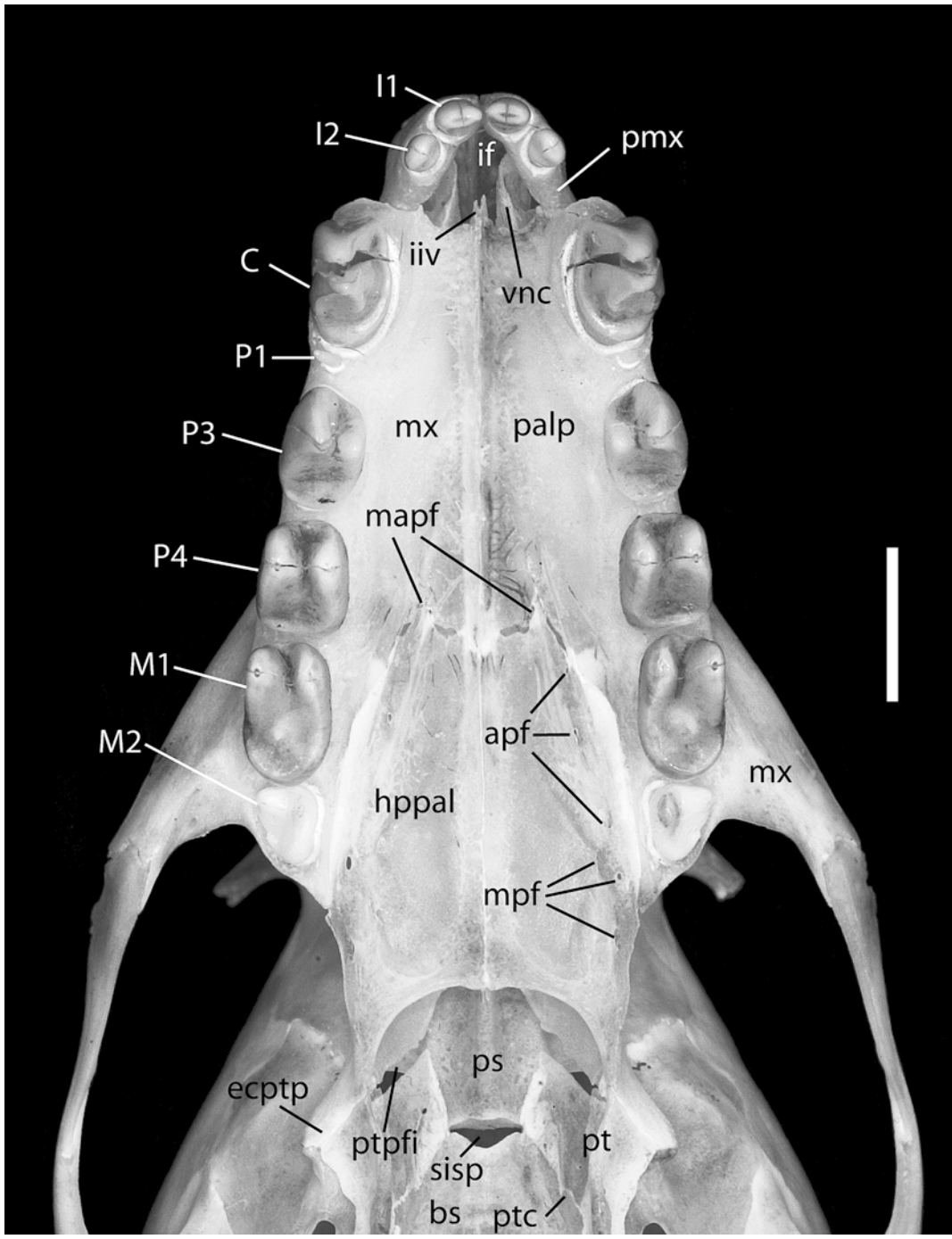

incisiva of vomer; **M1** first upper molar; **M2** second upper molar; **mapf** major palatine foramina; **mpf** minor palatine foramina; **mx** maxilla; **P1** first upper premolar; **P3** third upper premolar; **P4** fourth upper premolar; **palp** palatine process of maxilla; **pmx** premaxilla; **ps** presphenoid; **pt** pterygoid; **ptc** opening of pterygoid canal; **ptpfi** pterygopalatine fissure; **sisp** synchondrosis intersphenoidalis; **vnc** ventral nasal concha.

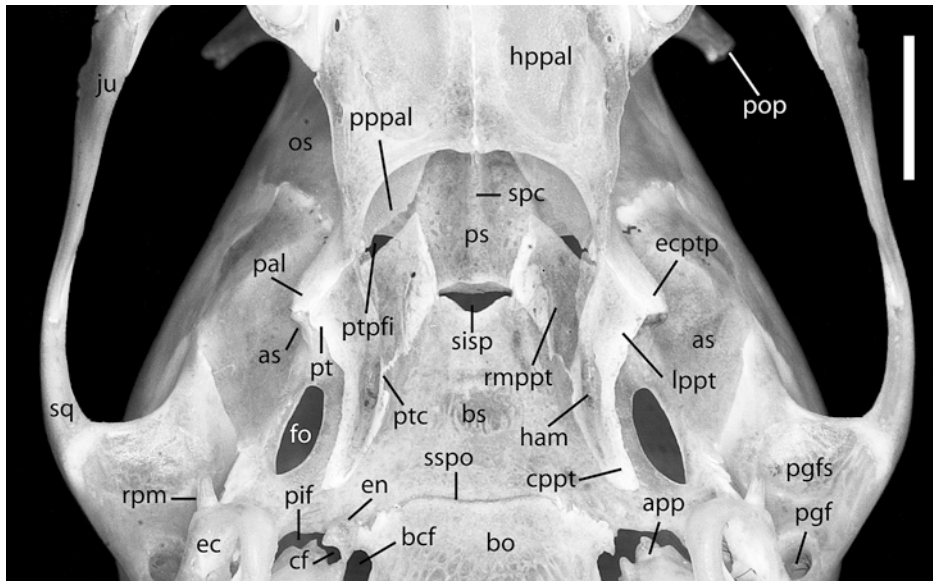

Fig. 10. *Pteropus lylei* CM 82972, ventral view of the nasopharyngeal region. Scale = 5 mm. Indicated on the right ectopterygoid process are the contributions of its three component bones: the palatine (**pal**), alisphenoid (**as**), and pterygoid (**pt**). Abbreviations: **app** apex parties petrosa; **as** alisphenoid (contribution of the alisphenoid to the ectopterygoid process); **bcf** basicochlear fissure; **bo** basioccipital; **bs** basisphenoid; **cf** carotid foramen; **cppt** caudal process of pterygoid; **ec** ectotympanic; **ecptp** ectopterygoid process; **en** rostral entotympanic; **fo** foramen ovale; **gf** glenoid fossa; **ham** hamulus pterygoideus; **hppal** horizontal process of palatine; **isv** incisura sphenoidalis of vomer; **ju** jugal; **lppt** lateral process of pterygoid; **os** orbitosphenoid; **pal** palatine (contribution of the palatine to the ectopterygoid process); **pgf** postglenoid foramen; **pif** piriform fenestra; **pop** postorbital process; **pppal** perpendicular process of palatine; **ps** presphenoid; **pt** pterygoid (contribution of the pterygoid to the ectopterygoid process); **ptc** pterygoid canal; **ptpfi** pterygopalatine fissure; **rmppt** rostromedial process of pterygoid; **rpm** rostral process of malleus; **sisp** synchondrosis intersphenoidalis; **spc** sphenoidal crest; **sq** squamosal; **sspo** spheno-occipital synchondrosis.

dorsally, forming a V-shaped structure, with the nasals dorsally bridging the gap between the two arms of the V, thereby closing the perimeter of the external nasal aperture. The nasoincisive suture is plane and gently convex. The maxilloincisive suture is incomplete dorsoventrally, so there is a notch separating the ventral half of the premaxilla and the maxilla. As a consequence of this notch, the premaxillary bodies do not articulate with the maxilla, creating a wide diastema between I2 and C.

In ventral view (figs. 3, 9), the left and right premaxillae surround a single large median opening between themselves and the anterior edge of the palatine process of the maxilla. This opening, the incisive fissure (the double *fissura palatina* of the dog), is formed by the coalescence of the paired incisive foramina (see Foramina below). There are no other foramina in the external surface of the premaxillae.

Maxilla

The maxilla (*os maxillare*) is paired and is the major component of the rostrum, together with the premaxilla forming the upper jaw. Each maxilla consists of a body with a large external surface or rostral process (*facies facialis*), which constitutes the bulk of the lateral wall of the rostrum, and a palatine process (*processus palatinus*), which forms the anterior portion of the hard palate (*palatum osseum*). At the intersection of these two processes is the alveolar surface (*processus alveolaris*), which bears the alveoli for six teeth and contributes to the anterior floor of the orbit caudally (figs. 2, 3, 9). The two maxillae articulate with each other along the

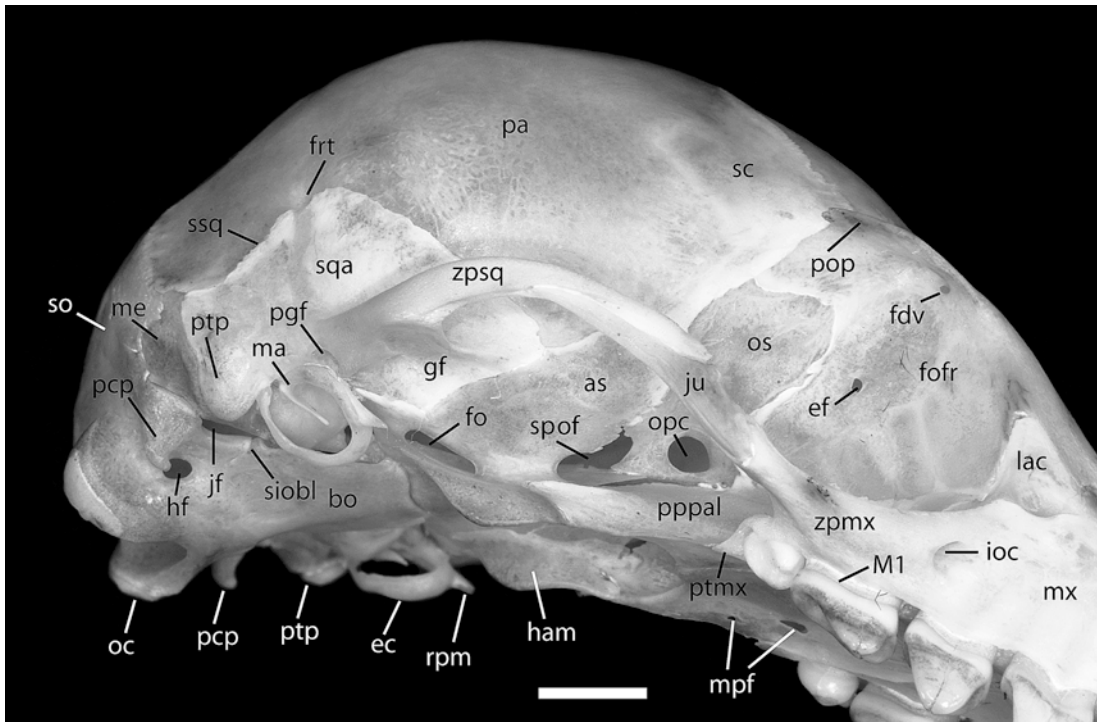

Fig. 11. *Pteropus lylei* CM 87972, ventrolateral view of the right orbital region. Scale = 5 mm. Abbreviations: **as** alisphenoid; **bo** basioccipital; **ec** ectotympanic; **ef** ethmoidal foramen; **fdv** foramen for frontal diploic vein; **fo** foramen ovale; **fofr** facies orbitalis of frontal; **frt** foramen for ramus temporalis; **gf** glenoid fossa; **ham** hamulus pterygoideus; **hf** hypoglossal foramen; **ioc** infraorbital canal; **jf** jugular foramen; **ju** jugal; **lac** lacrimal; **M1** first upper molar; **ma** malleus; **me** mastoid exposure; **mpf** minor palatine foramen; **mx** maxilla; **oc** occipital condyle; **opc** optic canal; **os** orbitosphenoid; **pa** parietal; **pcp** paracondylar process; **pgf** postglenoid foramen; **pop** postorbital process; **pppal** perpendicular process of palatine; **ptmx** pterygoid process of maxilla; **ptp** posttympanic process; **rpm** rostral process of malleus; **sc** sutura coronalis; **siobl** synchondrosis intraoccipitalis basilateralis; **so** supraoccipital; **spof** sphenorbital fissure; **sqa** squama of squamosal; **ssq** sutura squamosa; **zpmx** zygomatic process of maxilla; **zpsq** zygomatic process of squamosal.

midsagittal line in the anterior hard palate, forming the intermaxillary suture (*sutura intermaxillaris*, part of *sutura palatina mediana* in the NAV).

The rostral process of the maxilla contacts the premaxilla anteriorly, the nasal dorsally (sutures described above), the frontal posterodorsally, forming the frontomaxillary suture (*sutura frontomaxillaris*), the lacrimal posteriorly in the orbital margin (*margo orbitalis*), forming the lacrimomaxillary suture (*sutura lacrimomaxillaris*), and the jugal posteroventrally, forming the zygomaticomaxillary suture (*sutura zygomaticomaxillaris*). Inside the pterygopalatine fossa (*fossa pterygopalatina*) ventral to the orbit, the maxilla contacts the lacrimal dorsally and the perpendicular lamina of the palatine posteriorly, the latter forming the palatomaxillary suture (*sutura palatomaxillaris* in Evans, 1993; *sutura palatina transversa* in the NAV). Finally, the ventral limit of the rostral process in lateral view is the sinuous alveolar line (*margo alveolaris* of the maxilla).

The surfaces of the rostral processes are altered by the prominent juga of the canines, whose roots are located high on the side of the nasomaxillary suture. The roots of the postcanine teeth are clearly visible through the bone but do not significantly modify the rostral surface (i.e., the tooth roots do not alter the surface to form alveolar juga).

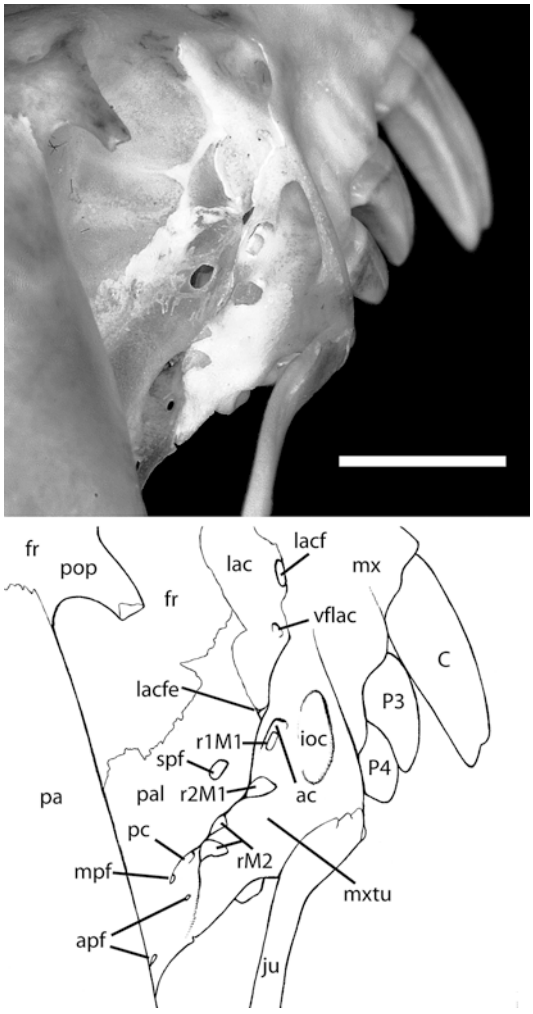

Fig. 12. *Pteropus lylei* CM 82972, caudolateral view of the right orbital region. Scale = 5 mm. Abbreviations: **ac** alveolar canal; **apf** accessory palatine foramina; **C** upper canine; **fr** frontal; **ioc** infraorbital canal; **ju** jugal; **lac** lacrimal; **lacf** lacrimal foramen; **lacfe** lacrimal fenestra; **mpf** minor palatine foramen; **mx** maxilla; **mxtu** maxillary tuberosity; **P3** third upper premolar; **P4** fourth upper premolar; **pa** parietal; **pal** palatine; **pc** palatine canal; **pop** postorbital process; **r1M1** anterior root of first upper molar; **r2M1** posterior root of first upper molar; **rM2** roots of second upper molar; **spf** sphenopalatine foramen; **vflac** vascular foramen of lacrimal.

Dorsal to the P4–M1 embrasure (in general, *septa interalveolaria*) and between the posterior root of P4 and the orbital rim, the rostral process is pierced by the infraorbital foramen (*foramen infraorbitale*), the anterior opening of the infraorbital canal. This foramen is elliptical in shape with its major axis oriented at ca. 45 degrees to the alveolar line. Inside the left infraorbital canal, a foramen in the floor represents the alveolar canal (*canalis alveolaris*) for the rostral and middle superior alveolar nerves. Apparently, the same foramen is also present on the right side but is displaced slightly posteriorly into the orbit right behind the ventral margin of the maxillary foramen (*foramen maxillare*), the caudal opening of the infraorbital canal (fig. 12). No other foramina are present in the rostral process, but traces of a few nutrient foramina (now obliterated) are irregularly distributed on the rostral surface.

The posterior edge of the rostral process describes an oblique line that successively contacts the frontal and the lacrimal, forms the ventral portion of the orbital rim, and continues in the zygomatic arch posteriorly (fig. 2). The frontomaxillary suture is roughly straight and is minutely serrated, running posterolaterally from the external-most point of nasal–frontal contact to the lacrimal (this area is the frontal process of the maxilla or *processus frontalis* of the dog). The lacrimomaxillary suture is concave. Ventral to this, the maxilla forms the infraorbital margin (*margo infraorbitalis*). Posteroventrally, a flat lamina of bone bridges over the short infraorbital canal and continues backward to form the elongated zygomatic process of the maxilla (*processus zygomaticus*), which contacts the jugal at approximately the midpoint of the ventral orbital semicircumference. Therefore, the anterior zygomatic root lies entirely in the maxilla.

The zygomatic process is slender, with an inconspicuous ventral crest in the masseteric margin (*margo massetericus* of the maxilla) extending from the alveolar line (at the level of the anterior half of M1) to the contact with the jugal. This crest is for the origin of the *m. masseter.* The foliate zygomaticomaxillary suture is very irregular, concave laterally, and sinuous medially. Laterally, the zygomatic process rises slightly posteriorly, so the articulation with the jugal is above (ca. 1 mm) the alveolar line. The root of the

zygomatic process is horizontally expanded as a flat, roughly triangular plate and joins the rear of the alveolar surface medially in the anterior orbital floor (figs. 1, 3).

The alveolar surface is in the ventrolateral portion of the maxilla. It contains the alveoli for the canine and five postcanine teeth: three premolars (P1, P3, and P4) and two molars (M1 and M2). The caudal portion of the alveolar surface of the maxilla contributes to the anterior orbital floor. In lateral view, the alveolar border (*margo alveolaris*) describes a low, gentle sinusoid with small rounded peaks in the P1–P3, P3–P4, and (shallower) P4–M1 embrasures, and small rounded valleys in P3 and P4 between the two roots of each tooth. Behind the P4–M1 embrasure, the alveolar border is relatively smooth and straight. The alveolus for the canine is the largest one, oval in shape, with its edge thin and sharply defined laterally and less so medially. Posteriorly, the canine alveolus is partially coalesced with the extremely small alveolus of the minute P1. There are no marked diastemata. The alveoli of P3 and P4 are similar in size and shape; the M1 alveolus is slightly longer than the P3 or P4 alveoli; the alveolus of M2 is half the length of the M1 alveolus but approximately the same width anteriorly, decreasing slightly posteriorly. Ventrally, the posterior edge of the alveolar area follows the outline of M2 and tapers to a small point. This is the pterygoid process of the maxilla (*processus pterygoideus*; fig. 11), which is a free projection in the dog. In *Pteropus*, the pterygoid process abuts medially the lateral edge of the palatine bone, and there is no free-standing portion. Within the pterygopalatine fossa, the surface of the posteriorly directed alveolar process is swollen between the shelf of the zygomatic root and the sphenoidal process of the palatine, forming the maxillary tuberosity (*tuber maxillae*; fig. 12). The two open roots of M1 are visible anteriorly in the orbital floor through their respective alveolar foramina (*foramina alveolaria*), the anterior one partially concealed by bone, as well as the two smaller (also open) roots of M2 posteriorly. On both sides, the M2 roots are displaced medially from the line of the M1 roots, the latter seemingly in line with the roots of the other cheek teeth. The rostrally directed alveolar canal, which has an intramaxillary course (see below), opens immediately dorsal and rostral to the anterior root of M1. Lateral to the M1 roots lies a large, posteriorly directed, oval opening, the maxillary foramen. The surface of the small portion of maxillary bone immediately dorsal to the anterior root of M1 and the maxillary foramen (i.e., the maxillary portion that contacts the lacrimal in the orbital surface) is porous and shows many minute foramina distributed irregularly, in addition to one slightly larger and distinct foramen present on both sides. At the juncture of the lacrimal, palatine, and maxilla, there is a small vacuity of comparable size and shape on both sides (also present bilaterally in CM 87973), the lacrimal fenestra (fig. 12).

The palatine processes form a transverse shelf of bone that occupies the anterior two-thirds of the hard palate. The free, anterior edge of the maxillary halves is biconcave, each side with a small median point that underlies the vomer's incisive incisure. The intermaxillary suture is slightly raised, forming a low crest that extends from the anterior edge of the canine to the P4–M1 embrasure. Posteriorly, the palatine processes articulate with the paired palatine bones, forming the palatal portion of the palatomaxillary suture (*sutura palatomaxillaris*). This suture of both maxillary halves with their respective palatine halves has the shape of a high arch or parabola whose vertex is in the midsagittal line at the level of the P4–M1 embrasure. However, the area of the vertex is very irregular and slightly convex. The palatomaxillary suture terminates immediately behind M2. The surface of the palatine process is slightly vaulted toward the midline; this feature increases gently posteriorly and continues smoothly onto the palatine bones. The major palatine foramen (*foramen palatinus major*) is located on the suture between the maxilla and the palatine (right side) or immediately anterior to that suture (left side). On both sides, a palatine sulcus (*sulcus palatinus*) extends forward from the major palatine foramen, converging near the midsagittal line and waning until it disappears at the level of P3. There are no other foramina in the palatine process of the maxilla.

Ventral Nasal Concha

The ventral nasal concha (*concha nasalis ventralis*), or maxilloturbinate, is a paired bone of the nasal cavity (see Internal Surfaces of the Skull). Only its rostral end is visible externally, through the external nasal aperture (figs. 3, 4, 9). In rostral view, the right ventral nasal concha of CM 87972 has a laterally compressed S-shape, with the concavity of a dorsal scroll facing medially, the concavity of a ventral scroll facing laterally, and a barely visible basal lamina that attaches laterally to the conchal crest of the internal surface (*facies nasalis*) of the maxilla. In CM 87972 the left side is similar to the right side, but the dorsal concavity is slightly smaller. In rostral oblique view, the rostral end is somewhat wedge-shaped. The spaces in the nasal cavity include the relatively wide common nasal meatus (*meatus nasi communis*) between the two ventral nasal conchae in front of the nasal septum, the middle dorsal meatus (*meatus nasi medius*) between the dorsal aspect of the conchae and the nasals, and the ventral nasal meatus (*meatus nasi ventralis*) between the ventral aspect of the conchae and the nasal surface of the maxilla. The rostral end of the ethmoturbinals (*ethmoturbinalia*) and the nasal septum are also visible through the external nasal aperture (fig. 4), but the surfaces available for external examination are extremely small (see Internal Surfaces of the Skull).

Palatine

The palatine bone (*os palatinum*) is paired and forms the caudal part of the hard palate, the lateroventral wall of the nasopharyngeal meatus, and its external counterpart, the medial wall of the pterygopalatine fossa (figs. 9–12). Each palatine has two thin laminae: the horizontal process (*lamina horizontalis*) and the perpendicular process (*lamina perpendicularis*). The left and right horizontal processes articulate along the midsagittal line in the posterior hard palate, forming the interpalatine suture (part of *sutura palatina mediana* in the NAV), which is continuous with the intermaxillary suture.

The horizontal process of the palatine rostrally contacts the palatine process of the maxilla (suture described above) and dorsally contacts the sphenoidal incisure of the vomer, forming the vomeropalatine suture (*sutura vomeropalatina dorsalis*). The anterior margin of the two palatines (at the transverse suture) is very irregularly concave. The lateral edge is bowed outward. The caudal edge is free and deeply concave, forming a wide ∩-shaped margin. The lateral margins of the postdental palate are slightly bowed inward and converge slightly toward the midsagittal line; in some specimens, a shallow notch is present in the midpoint alongside this margin (e.g., CM 87973). The lateral and caudal edges meet at a caudal point that contacts the pterygoid (see below). The ventral surface is arched, continuing smoothly and accentuating the trend seen in the palatine process of the maxilla. The interpalatine suture is straight and plane. The bone density of the palatine surface (*facies palatina*) varies in relation to the proximity of the interpalatine suture and caudal palatine margin, where the bone is noticeably thicker. In the remainder of the palatine surface, the bone is translucently thin. A series of five small lateral foramina, aligned with the lateral margin of the palatine, are found near the lateral margin of the palatine surface. The homologies of these foramina are discussed at length below on the basis of the sectioned fetus (see Foramina Contents and Homology). Based on the fetus, the rostral three of the lateral foramina are dependents of the overlying palatine canal (*canalis palatinus*) for the major palatine nerve and artery, which exit rostrally via the major palatine foramen; these three lateral foramina are identified here as accessory palatine foramina (fig. 9). The caudal two foramina are dependents of another, larger foramen that opens medially on the ventral surface of the palate between the level of the third and fourth lateral foramina, identified as the minor palatine foramen (*foramen palatinum caudale*). The bilateral discrepancy includes an extra medial foramen on the right side, the double-opening condition of the left fifth lateral foramen, and the location of the first accessory foramen (on the palatomaxillary suture on the right side, on the palatine

surface on the left side). There is also a minute nutrient foramen on each side of the interpalatine suture, located in slightly different positions (left side foramen is more caudal; both foramina are placed at the level of the caudal edge of M2). The palatine surface is impressed by a wide sulcus of conical shape that expands medially and whose vertex is at the minor palatine foramen.

The dorsal surface of the palate (*facies nasalis*) is flat with a bilateral low ridge, the nasal crest (*crista nasalis*), alongside the interpalatine suture. The sphenoidal incisure of the vomer (see below) articulates with this crest in the vomeropalatine suture.

The perpendicular process of the palatine externally forms the side of the pterygopalatine fossa (fig. 11) and internally forms the lateral wall of the nasopharyngeal meatus (fig. 10). It is oriented dorsomedially at ca. 45 degrees, with a slightly arched surface. It contacts the maxilla rostrally (sutures described above), the frontal dorsally, forming the frontopalatine suture (*sutura frontopalatina*), the lacrimal anterodorsally, forming the palatolacrimal suture (*sutura palatolacrimalis*), the presphenoid dorsomedially, forming the sphenopalatine suture (*sutura sphenopalatina*), and the pterygoid caudally, forming the pterygopalatine suture (*sutura pterygopalatina*). A vacuity separates the caudomedial edge of the palatine from the rostromedial edge of the pterygoid, termed here the pterygopalatine fissure (fig. 9). The frontopalatine suture is squamous, nearly horizontal, and somewhat irregular. The palatolacrimal suture is a short (ca. 1 mm), oblique contact on the left side, and a point contact on the right side. The elliptical sphenopalatine foramen (*foramen sphenopalatinum*) is located anteriorly within the palatine at the level of the posterior root of M1 (fig. 12) and is a single round opening on each side (double bilaterally in CM 87973). Caudally, the pterygopalatine fissure is visible on the lateral surface. The dorsal openings of the palatine foramina complex are visible, corresponding to the fourth and fifth lateral palatine foramina described above, which are included in the sulcus that leads to the caudal opening of the palatine canal rostrally. A sphenoidal process (*processus sphenoidalis*) projects caudoventrally from the external surface of the perpendicular palatine lamina, contributing to the rostral portion of the tripartite ectopterygoid process (the pterygoid and the alisphenoid contribute correspondent parts). The shape of the internal surface of the perpendicular lamina is given by the roughly elliptical perimeter of the choanae in the basipharyngeal canal. This shape is distorted by the nasal crest of the palatine ventrally and by the sphenoid crest dorsally, which together split the nasopharyngeal meatus into paired openings rostrally. The two perpendicular laminae approach the presphenoid dorsally but contact it only rostrally, leaving an oblique cleft that is continuous with the pterygopalatine fissure between the caudomedial end of the palatine and the pterygoid. Another small vacuity is present in the tripartite space between the palatine, the rostral end of the presphenoid, and the caudal edge of the wing of the vomer. The vomerine wing is overlapped slightly by the palatine, but this suture is barely visible externally.

Lacrimal

The lacrimal (*os lacrimale*) is a paired, roughly pyramidal bone with an external triangular outline, located in the rostral margin of the orbit (figs. 2, 12). The lacrimal has two surfaces, orbital (*facies orbitalis*) and facial (*facies facialis*), separated by the orbital crest (*crista orbitalis*). The lacrimal contacts the palatine caudally, the maxilla rostrally and ventrally (sutures described above), and the frontal dorsally and caudally, forming the frontolacrimal suture (*sutura frontolacrimalis*). The last one is squamous, roughly straight on the rostral exposure, and crescentic (concave) and somewhat irregular in the orbit. The orbital rim crosses through the lacrimal, forming the orbital crest, a consequence of the two surfaces, facial and orbital, meeting at different inclinations. The facial surface is level with the surface of the rostrum, and the orbital surface lies inside the orbit.

The major feature of the large facial exposure of the lacrimal is the lacrimal foramen (*foramen lacrimale*), the opening of the lacrimal canal (*canalis lacrimalis*) that expands in the fossa for the lacrimal sac

(*fossa sacci lacrimalis*). It is located anterior to the orbital rim, immediately dorsal to the suture with the maxilla, which participates in the ventral margin of the foramen (fig. 12) but does not contribute to the lacrimal canal, which lies entirely within the lacrimal. The dorsal margin of the lacrimal foramen is poorly defined. Inside the orbit, there is a small, unnamed foramen that is connected with the major lacrimal foramen via an oblique, anterodorsally directed canal (fig. 12). On the basis of its content (see Foramina Contents and Homology), we term it here the vascular foramen of the lacrimal. The ventral margin of this foramen is contributed by the maxilla on the left side. The orbital surface of the lacrimal is porous, with several minute foramina of irregular distribution, whereas the facial surface is smooth. In CM 87973, there is a small, oval opening in the suture between the right orbital processes of the lacrimal and frontal, slightly below the level of the lacrimal foramen. Most specimens exhibit similar openings, but a shallow pit (with no patent foramina) is present in this position on the left side in CM 87973 and on both sides in CM 87972. Based on the study of the *Pteropus* fetus, this opening transmits the *m. obliquus ventralis* and, therefore, is a lacrimal fenestra (Fig. 12; Wible and Gaudin, 2004).

JUGAL

The jugal bone (*os zygomaticum*) is a paired, small, laterally compressed element located at the center of the zygomatic arch between the anterior root of the arch (contributed entirely by the zygomatic process of the maxilla) and the posterior root (contributed entirely by the zygomatic process of the squamosal; figs. 2, 11). The jugal has two surfaces, lateral (*facies lateralis*) and orbital (*facies orbitalis*), and two margins, the dorsal infraorbital margin (*margo infraorbitalis*) and the ventral masseteric margin (*margo massetericus*). The zygomaticomaxillary suture is described above. The jugal has a long, posteriorly directed process (*processus temporalis*) that articulates with the squamosal via the foliate temporozygomatic suture (*sutura temporozygomatica*). The lateral suture with the squamosal starts dorsally at approximately one-third the length of the jugal, continuing diagonally down until the end of the jugal ventrally (at about the midpoint of the zygomatic process of the squamosal). Medially, the jugal contributes a larger portion to the middle arch, but the shape of the suture with the squamosal is still similar to the suture on the lateral surface, only slightly bowed dorsally. The dorsal free margin of the jugal is short and extremely irregular. Immediately dorsal to the masseteric margin on the lateral surface is a noticeable longitudinal striation that runs the length of the jugal, accompanied by another shorter striation that is dorsal and anterior to the major striation. In that area, the bone shows short, irregular incisive marks and small nutrient foramina. Based on the fetus, the *m. masseter, pars profunda* arises from the medial side of the zygoma and the superficial masseter from the masseteric margin (and a very small part of the ventrolateral surface). The bulk of the lateral surface of the zygoma in the fetus is free of muscle (see fig. 32), suggesting that all muscle attachment probably lies ventral to the longitudinal striation in the adult. On the right side of CM 87972, there is a single nutrient foramen near the dorsal free edge of the jugal. The fetus also has one foramen that transmits a vein.

CRANIAL BONES (*OSSA CRANII*)

FRONTAL

The frontal bone (*os frontale*) is paired and forms the forehead of the skull (fig. 1) and the bulk of the orbital wall (*pars orbitalis* of the frontal; fig. 2). In CM 87972, the frontals are solidly fused with no trace of the interfrontal suture (*sutura interfrontalis*, by which the left and right frontals articulate along their midsagittal contact). The most prominent feature of the frontal is the large postorbital process (supraorbital or zygomatic process of the dog, *processus zygomaticus*).

In dorsal view (fig. 1), the frontal is a long, roughly rectangular plate (*squama frontalis*) with preorbital (*pars nasalis*), interorbital, and postorbital areas. Paired postorbital processes project from the lateral border just caudal to the midpoint of the dorsal length of the frontal. In the short preorbital area, the

frontal contacts the nasal, the maxilla, and the lacrimal (sutures described above). In dorsal view, the interorbital area shows a slight but noticeable constriction. The circular orbital rim (*margo orbitalis*) continues caudally in the caudoventrolaterally directed postorbital process. The postorbital process has a wide base that tapers caudally to a blunt, squared-off tip (slightly bifid on the right side). The free process overhangs the orbit by 2.3 mm in CM 87972, forming a small triangular roof over the posterior half of the orbital concavity. The rostral margin of the postorbital process is almost straight in dorsal view, whereas the caudal margin is deeply concave. In the rostral margin on the left side is a minute, oblique notch, accompanied by a sulcus, which suggests the passage of a nerve and/or vessel. Based on the *Pteropus* fetus, this notch and sulcus may accommodate the frontal nerve and vessels (see fig. 31).

Caudal to the postorbital process, the dorsolateral exposure of the frontal is broadly overlapped by a wedge-shaped rostral process of the parietal in the coronal suture (*sutura coronalis*, equivalent to the *sutura frontoparietalis* of the dog). This suture is therefore squamous. The suture lines from each side converge slightly until they abruptly turn inward in a roughly right angle to meet each other in the midsagittal line. This point is located approximately midway between the root of the postorbital process and the interparietal.

The dorsal surface of the frontal shows two prominent features: the postorbital foramen and the frontal sinus. In the midpoint of the frontal length, on the rostral half of the root of the postorbital process, the frontal is pierced by the large postorbital foramen. Each foramen is a slightly oval opening that communicates the orbit with the skull roof. In close relationship with the postorbital foramen, there are three (right side of CM 87972) or four (left side) minute foramina associated with the frontal diploic vein. The extra foramen on the left side opens on the dorsal surface of the frontal, close to the inner edge of the postorbital foramen. The frontal sinus (*sinus frontalis*) can be studied because of the thinness of the frontal bone. Each of the paired sinuses is divided into a medial and a lateral part. The latter is the larger; it follows the orbital rim from the lacrimal to the postorbital foramen and shows a modestly swollen surface. As a consequence, the medial aspect of the interorbital surface is a slightly depressed passage connecting the preorbital and postorbital regions of the frontal. The medial part is not swollen, but its extension can be seen because of the transparency of the bone; it is short and placed medial to the anterior half of the lateral part. Its anterior edge is defined by the sutures with the lacrimal, maxilla, and nasal; the posterior edge of each side converges in the midsagittal line. Posterior to the postorbital processes, the surface of the frontal is smooth and slightly domed.

The frontal occupies most of the orbital wall, where it contacts the lacrimal rostrally, the palatine ventrally (sutures described above), and the orbitosphenoid caudally, forming the sphenofrontal suture (*sutura sphenofrontalis*). The frontal also contacts the parietal posterodorsally, continuing the frontoparietal suture into the orbit (fig. 2). The sphenofrontal suture is squamous ventrally, and it turns gradually plane dorsally. The shape of this suture resembles one side of a lyre: it is convex caudoventrally, concave caudodorsally, and gently rounded dorsally as it curves posteroventrally to meet the parietal. The thinness of the bone in the orbital surface permits observation of structures of the medial side of the orbital wall. There is a rostrally convex line running from the postorbital foramen to the point of triple articulation between the frontal, the palatine, and the orbitosphenoid. This line marks the placement of the cribriform plate of the ethmoid (*lamina cribrosa*; see below). Four oblique lines (the dorsalmost line is incomplete) run between the line of the cribriform plate and the rostroventral limit of the frontal. These are lines of internal attachment of the ethmoturbinates (*ethmoturbinalia*), whose delicate laminae scroll inside the five interlinear spaces. The surface between the line of the cribriform plate and the anterior orbital rim corresponds to a wide squamous suture by which the frontal completely overlaps the ethmoid bone laterally, the frontoethmoidal suture (*sutura frontoethmoidalis*). The surface between the line of the

cribriform plate and the suture with the orbitosphenoid is smooth; its translucence reveals that it is devoid of bony structures medially. In the center of this area is the small, round, ventrally directed ethmoidal foramen (*foramen ethmoidale*). The ethmoidal foramen is very large in CM 87973 (larger than the optic foramen; see Foramina) and opens between the frontal and orbitosphenoid.

Parietal

The parietal bone (*os parietale*) is the major element forming the skull roof (figs. 1, 2). The braincase owes its bulbous shape (described above) chiefly to the curvature of the paired parietals. These protect the dorsolateral surface of the brain and provide most of the attachment area of the m. temporalis. In CM 87972, the surface of the bone is entirely smooth, so the limits of the temporal fossa are not evident. In adult *Pteropus lylei* (e.g., AMNH 237593) and most *Pteropus* species, however, the temporal fossa is delimited by the sagittal crest on the parietal (plus the infratemporal crest of the alisphenoid and the nuchal crest of the supraoccipital; see also Development).

The parietal has four borders: rostral or frontal (*margo frontalis*), dorsal or sagittal (*margo sagittalis*), ventral or squamous (*margo squamosus*), and caudal or occipital (*margo occipitalis*). The parietals contact each other in the corresponding sagittal border through the sagittal suture (*sutura sagittalis*), and in turn each parietal contacts the frontal rostrodorsally (suture described above), the orbitosphenoid rostrolaterally, forming the sphenoparietal suture (*sutura sphenoparietalis*), the alisphenoid anteroventrally (the continuation of the *sutura sphenoparietalis*), the squamosal ventrally, forming the *sutura squamosa*, the interparietal mediocaudally (*sutura parietointerparietalis*), and the supraoccipital laterocaudally, forming the occipitoparietal suture (*sutura occipitoparietalis* in Evans, 1993; part of lambdoid suture, *sutura lambdoidea* in the NAV). There is also a short contact with the mastoid exposure of the petrosal.

The sagittal suture is plane, slightly irregular, and follows the midsagittal line with little deviation. The frontoparietal suture is described above. The rostral border is an oblique suture directed caudoventrally; the suture is squamous, with the parietal slightly overlapping the frontal and the orbitosphenoid. The suture turns rostrally in its ventral quarter to meet the tripartite articulation of the orbitosphenoid, alisphenoid, and parietal. There the ventral border of the parietal begins, as a sinusoidally shaped squamous suture with the alisphenoid. The parietal is overlapped by a rounded, dorsal process of the alisphenoid. The chief suture of the ventral border is with the squamosal, whose dorsal lamina widely overlaps the parietal. The sutura squamosa is broadly wedge-shaped, with a straight anterior border directed dorsocaudally and a subtly convex posterior border directed ventrocaudally. Near the dorsal vertex of this triangle-shaped suture lies the foramen for ramus temporalis, which is dorsally directed with two small openings in the left side and a single, larger opening in the right side. The foramina are between the squamosal and the parietal, with a short sulcus present in the parietal surface leading from the foramen. The suture with the petrosal is < 2 mm in length. Next is the dorsomedially directed occipitoparietal suture. This is a squamous suture (with serrated border) where the supraoccipital is slightly overlapped by the parietal. The parietointerparietal suture shows the same structure; its caudalmost extreme is at the tripartite articulation of the parietal, supraoccipital, and interparietal. From this point, the suture runs rostrodorsally, converging with its bilateral counterpart in the midsagittal line. The curvature of the suture, which describes an arch when both sides are taken together, is somewhat interrupted by a small ingression of the parietal into the interparietal surface near the midsagittal line. This shows as a notch in the interparietal. In this small region are the first signs of fusion between the interparietal and parietal on the left side.

Our study of the *Pteropus* fetus revealed another part of the parietal that was not readily apparent to us in our study of the intact adult skull (but see Internal Surfaces of the Skull). In the fetus, the parietal con-

tributes an epitympanic wing (sensu MacPhee, 1981): an exposure in the tympanic roof interposed between the sphenoid anteriorly (the basisphenoid and alisphenoids are represented by a single ossification), the squamosal laterally, and the tegmen tympani of the petrosal posteriorly (see figs. 34, 35). This parietal epitympanic wing has a foramen and a sulcus associated with the ramus superior of the stapedial artery (fig. 34). After this discovery, we subsequently identified the parietal epitympanic wing on the left side of CM 87973. It is a small, lobster claw–shaped exposure in the tympanic roof, with the open end of the claw directed anteromedially, positioned lateral to the posterolateral margin of the piriform fenestra. It contacts the alisphenoid anteriorly and medially, the petrosal posteriorly, and is underlain laterally by the squamosal. In the gap between the parietal epitympanic wing and the squamosal is the opening into a small vascular canal directed posterodorsolaterally.

Interparietal

The interparietal (*os interparietale*) is an unpaired bone that forms the mediocaudal portion of the skull roof between the parietals and the supraoccipital (fig. 1). The parietointerparietal suture is described above. The suture with the supraoccipital (unnamed in the dog, because the interparietal is fused with the supraoccipital prenatally; Evans, 1993) is termed here the occipitointerparietal suture (*sutura occipitointerparietalis*), part of the lambdoid suture (*sutura lambdoidea*) in the NAV, which has three sections: two bilateral portions that run from the tripartite point of articulation of the parietal, interparietal, and supraoccipital on each side, converging medially and slightly posteriorly to meet a central portion that is essentially perpendicular to the sagittal axis and slightly concave. This suture is minutely serrated, and there is no significant overlap between the two contacting bones. The surface of the interparietal is smooth and somewhat domed over the central portion of the occipitointerparietal suture, a feature accentuated in the adjacent area of the supraoccipital (see below). No foramina are found in the interparietal.

Pterygoid

The pterygoid bone (*os pterygoideum*) is a small, paired element located caudal to the palatine in the basipharyngeal canal, ventral to the sphenoidal complex (figs. 3, 5, 10). The pterygoid contacts the perpendicular process of the palatine rostrolaterally (suture described above), the presphenoid rostromedially, and the basi-alisphenoid complex dorsocaudally, forming the pterygosphenoid suture (*sutura pterygosphenoidalis*). The pterygoid has two surfaces: a nasopharyngeal surface (*facies nasopharyngea*, medial and facing the nasopharyngeal meatus) and a pterygopalatine surface (*facies pterygopalatina*, lateral and facing the pterygopalatine fossa). It has a caudoventral angle or hamulus (*hamulus pterygoideus*; fig. 11), and three processes seen in ventral view (fig. 10): rostromedial, lateral (ectopterygoid), and caudal (all unnamed in the NAV).

The pterygopalatine surface of the pterygoid is concave. Its rostral end projects laterally and joins the respective processes of the palatine and alisphenoid that together form the ectopterygoid process. Caudal to the ectopterygoid process, the lateral margin of the pterygoid runs beneath the sphenoid and describes a crescentic (concave) line that ends at the level of the caudal margin of the foramen ovale (see Alisphenoid and Foramina below). The pterygopalatine surface has a small, round foramen in its center on the left side and two smaller foramina in the same place on the right side in CM 87972; based on the sectioned fetus, these foramina transmit veins.

The medial surface of the pterygoid has a rectangular rostromedial projection that contacts the presphenoid and the basisphenoid. The medial surface is separated from the palatine rostrally by the pterygopalatine fissure. On both sides, there is a posteriorly directed aperture in the midlateral part of the suture with the basisphenoid. Extending anteriorly from this aperture is a faint sulcus on the dorsal surface of the pterygoid open within the cranial cavity. The faint impression of this sulcus is visible ventrally. This aperture represents the pterygoid canal (*canalis pterygoideus*), which connects the basipharyngeal canal to the *cavum epiptericum*

(sensu Gaupp, 1902, 1905), the extradural space within the cranial cavity housing the trigeminal ganglion. The rostromedial process has a small foramen of uncertain function on its surface near the contact with the presphenoid, almost obliterated on the left side.

The hamulus of the pterygoid is a low and rounded process, laterally concave and slightly divergent caudally, that reaches its maximum depth at its longitudinal midpoint and ascends gently to the level of the basisphenoid as it continues posteriorly (figs. 10, 11). The ventral margin is slightly thickened, forming an inconspicuous lip.

Vomer

The *vomer* is an unpaired bone of the nasal cavity. It consists of a sagittal part and a horizontal part (Evans, 1993). The former is formed by two low, parallel laminae (*laminae lateralis*) that rest over the intermaxillary suture, with deeply forked rostral and caudal ends, the incisive and sphenoidal incisures (*incisura incisiva et sphenoidalis*, respectively), and a ventral crest (*crista vomeris*). The dorsally opened structure formed by the laminae, the *sulcus septi nasi* of the dog or *sulcus vomeris* (*septalis*) of the NAV, receives the septal cartilage (*septum nasi*, its cartilaginous rostral part removed in CM 87972), which can be fully ossified in old adults (e.g., AMNH 217045). The horizontal part is formed by bilateral wings (*alae vomeris*). Only the rostral and caudal ends are accessible for examination through the external nasal aperture (fig. 4) and the choanae, respectively. The incisive incisure is also visible through the incisive fenestra in ventral view (figs. 3, 9). The ventral surface was examined in a disarticulated skull of *Pteropus livingstonii* (see fig. 24 and Internal Surfaces of the Skull).

Posteriorly, the caudal part of the vomerine wings has a dorsal point contact with the presphenoid (*sutura vomerosphenoidalis*) only on the right side. The contact of the caudal edge of the vomerine wings with the facies nasopharyngea of the perpendicular process of the palatine (*sutura vomeropalatina dorsalis*) is barely visible inside the nasopharyngeal meatus. No foramina are present in the vomer.

Sphenoid Complex

The sphenoid complex comprises the unpaired presphenoid (*os presphenoidale*) and basisphenoid (*os basisphenoidale*), and the paired orbitosphenoids (*ossa orbitosphenoidales*) and alisphenoids (*ossa alisphenoidales*). Together, these bones constitute the rostral two-thirds of the basicranium. The presphenoid is in the midline roof of the basipharyngeal canal (fig. 10); if fused to the orbitosphenoids, as in CM 87972, it is called the *corpus* of the *os presphenoidale*. The basisphenoid is in the midline of the basicranium between the presphenoid and the basioccipital; if fused to the alisphenoid, as in CM 87972, it is called the *corpus* of the *os basisphenoidale*. The orbitosphenoids are located dorsolateral to the presphenoid, projecting into the orbital wall; if fused to the presphenoid, they are called the orbital (or lesser) wings of the (pre)sphenoid (*alae orbitales* of the dog). The alisphenoids are located dorsolateral to the basisphenoid, forming the anteroventral side of the braincase; if fused to the basisphenoid, they are called the temporal (or greater) wings of the (basi)sphenoid (*alae temporales* of the dog). The adjectives "lesser" and "greater" are of little value in megachiropterans because the orbitophenoids are unusually large bones that greatly exceed the alisphenoids in dorsal extension (figs. 2, 11). In CM 87972, conspicuous sutures and gaps distinguish the presphenoid + orbitosphenoid from the basisphenoid + alisphenoid, but there is no evidence of a division between the basisphenoid and alisphenoid, or between the presphenoid and orbitosphenoid (nor are divisions evident in the fetus examined; see fig. 32 and Skull Development). However, each of the four bones will be given a separate treatment for descriptive purposes.

Presphenoid: The presphenoid is an element whose nasopharyngeal exposure (the chief part visible externally) has a rhomboidal shape with the rostral and caudal ends truncated (fig. 10). The presphenoid has a point contact with the sphenoidal incisure of the vomer rostroventrally; it contacts the palatine anterolaterally and the pterygoid posterolaterally (sutures described above). The rhomboidal shape of the ventral surface

of the presphenoid is due to the oblique contacts of the palatines and pterygoids (fig. 10). The truncated anterior and posterior surfaces are perpendicular to the ventral surface and are subcircular in shape. These surfaces do not contact any bone rostrally or caudally. The caudal surface matches a similarly truncated rostral end of the basisphenoid, which reflects the loss of an interlocking cartilage in the macerated skull of CM 87972 (the intersphenoidal synchondrosis). The ventral surface of the presphenoid is ridged in the midsagittal line by the marked sphenoidal crest (*crista sphenoidalis*). Dorsolaterally, the presphenoid is fused to the orbitosphenoids, but the relationship of these bones is best seen in orbital view (see below). No foramina are present in the presphenoid, although the optic canal lies between it and the orbitosphenoid (see below).

ORBITOSPHENOID: The paired orbitosphenoids form the caudal portion of the orbital wall, rising obliquely in the dorsolateral direction from their fused juncture with the presphenoid to extend up to three-quarters of the orbital height (figs. 2, 11). The surface of the orbitosphenoid lies at an obtuse angle with the frontal in the orbital wall. The orbitosphenoid contacts the frontal rostrally and dorsally, the parietal dorsocaudally (sutures described above), and the alisphenoid ventrocaudally, and it is fused to the presphenoid ventrally. The orbitosphenoid is overlapped by the parietal. The caudal margin of the orbitosphenoid then contacts the alisphenoid and is again fairly widely overlapped by this bone in a straight (right side) or irregularly and slightly concave (left side) suture. Ventrally, the orbitosphenoid fuses with the presphenoid rostral to the large sphenorbital fissure (see below).

The major feature of the orbitosphenoid is the large, round optic canal (*canalis opticus*), which opens in the base of the bone. In the *Pteropus* fetus, the presphenoid forms the floor of the optic canal, the orbitosphenoid forms the roof; the anterior and posterior walls are cartilaginous. We are unsure exactly how this translates to the adult. In CM 87972, there is a longitudinal ridge that extends forward from the anteroventral margin of the optic canal. In the fetus, this ridge, the cartilaginous *ala hypochiasmatica*, provides attachment for extraocular muscles, and its base is formed by the presphenoid. It seems likely that the presphenoid-orbitosphenoid juncture in the adult is near this ridge. In CM 87972, the rostral edge of the optic canal is deflected inward, and its rostroventral edge becomes more prominent in lateral view. Caudal to the optic canal is the rostral edge of the sphenorbital fissure, a large opening shared with the alisphenoid caudally and floored by the rostromedial process of the pterygoid. The contour of the rostral edge of the sphenorbital fissure is more acutely concave in its dorsal portion. In the sphenorbital fissure coalesce the following foramina of the dog: the rostral alar foramen (*foramen alare rostrale*), the *foramen rotundum*, and the variably present foramen for the zygomatic nerve.

BASISPHENOID: This bone forms the floor of the braincase between the presphenoid and the basioccipital, as well as the roof of the posterior part of the nasopharyngeal meatus (figs. 3, 10). The basisphenoid has an approximately triangular shape defined by the oblique suture with the rostromedial process of the pterygoid laterally (described above) and the perpendicular suture with the basioccipital caudally. The bone is truncated in its salient anterior end in the area where a missing cartilage of the spheno-occipital joint (*synchondrosis spheno-occipitalis*) was placed (see Presphenoid). This truncation is deeply concave in ventral view; it presents a disklike surface in rostral view that matches the caudal end of the presphenoid. In the caudal margin of the basisphenoid, the spheno-occipital synchondrosis is largely plane, although the basisphenoid is slightly overlapped by the basioccipital on the lateral side of that perpendicular suture. This suture is straight medially and is directed caudally toward its lateral end, where it becomes interdigitated. The ventral surface of the basisphenoid is essentially flat medially; laterally, the basisphenoid is gently depressed alongside the oblique suture with the pterygoid, and then it steadily descends behind the closely adpressed pterygoid until reaching its ventralmost point at the level of the large foramen ovale in the area of the alisphenoid.

Laterally, the basisphenoid is fused with the alisphenoid; there is no trace of a suture

in the likely contact zone dorsal to the pterygoid and immediately caudal to its posterior process. The rostral edge of the large piriform fenestra occurs in the posterior portion of the basisphenoid-alisphenoid contact zone. The basisphenoid contacts the entotympanic (preserved only in the right side in CM 87972) at the occipitosphenoid suture (see Entotympanic). The only foramen present in the bony area attributed to the basisphenoid is the carotid foramen (described with the Petrosal below).

ALISPHENOID: The alisphenoid is fused seamlessly to the basisphenoid, and therefore may be treated as a process of the basisphenoid (the above mentioned *ala temporalis*) for practical purposes. It contacts the orbitosphenoid rostrally, the parietal dorsally, the pterygoid rostroventrally (all sutures described above), and the squamosal caudoventrally, forming the sphenosquamosal suture (*sutura sphenosquamosa*), and it is fused to the basisphenoid medially (fig. 10). The bulk of the alisphenoid is in the infratemporal fossa, whose limit with the temporal fossa above is obscurely marked by an incipient, roughly horizontal infratemporal crest (*crista infratemporalis*) that divides the dorsal third from the ventral two-thirds of the alisphenoid (fig. 11). Except for this crest, the surface of the alisphenoid is entirely smooth. As the alisphenoid extends rostrodorsally, it bends following the curvature of the braincase; the infratemporal crest marks a sort of inflection point in the upward course of the alisphenoid curvature. The alisphenoid is widely overlapped by the squamosal. The sphenosquamosal suture is roughly straight, caudoventrally directed, then horizontal from approximately the level of the posterior edge of the foramen ovale (see below).

On the right side of CM 87972 and bilaterally in CM 87973, the alisphenoid has a distinct process that partially divides the sphenorbital fissure into superior and inferior halves. This partial division reflects the situation in the fetus, with its contents divided into distinct superior and inferior bundles (see Foramina Contents and Homology).

The alisphenoid contributes to the rostral margin of the piriform fenestra, which lies in the juncture area of the basisphenoid and the alisphenoid (figs. 3, 10). The posterior margin of the piriform fenestra is formed by the petrosal. A shelf of bone from the alisphenoid is directed caudolaterally into the tympanic roof between the piriform fenestra and the ventral postglenoid area of the squamosal. Based on CM 87973, this epitympanic wing of the alisphenoid has a point contact with the petrosal and a broader contact with the epitympanic wing of the parietal.

Two salient features are present in the alisphenoid. First, there is a large, elliptical opening, the *foramen ovale* (figs. 3, 5, 10, 11). This is a composite foramen, transmitting the contents of the coalesced foramen ovale and alisphenoid canal (caudal alar foramen of the dog, *foramen alare caudale*; see Foramina Contents and Homology). Second, immediately anterior to the rostral margin of the foramen, there is an anterolateroventrally directed projection that contributes to the tripartite ectopterygoid process, formed by contributions from the palatine, the pterygoid, and the alisphenoid (figs. 3, 5, 10). The alar canal of the dog runs right above this process but outside the braincase, connecting the foramen ovale with the sphenorbital fissure (*fissura orbitalis*).

SQUAMOSAL

The squamosal (*os temporale*, *pars squamosa*) is a paired bone located laterally in the braincase—the flattened squama—bearing a prominent process that arches rostrolaterally, forming the posterior half of the zygoma—the zygomatic process (*processus zygomaticus* of the squamosal; figs. 2, 5, 11). Ventral to the root of the zygomatic process is the glenoid fossa (figs. 3, 5). The squamosal also contacts the ectotympanic (*annulus tympanicus*) in the opening of the external acoustic meatus.

The squama is a lamina that widely overlaps the parietal dorsally, the alisphenoid rostroventrally (sutures described above), and the pars canalicularis of the petrosal laterally and caudally, forming the squamosomastoid suture (*sutura squamosomastoidea*). The shape of the squama is triangular in its dorsal portion, with a vertex pointing directly dorsally at or near the foramen for

ramus temporalis in the sutura squamosa (see above). Caudally, the squama almost reaches the incipient nuchal crest, overlapping the pars canalicularis and thus concealing the lateral exposure of the petrosal.

Projecting laterally from the squama is the zygomatic process. The process has a wide, roughly triangular root placed horizontally just rostral to the external acoustic meatus. The dorsal surface of the root is a depression that provides attachment for the m. temporalis. A small, rostrally directed foramen is present on both sides at the posteromedial base of the zygomatic root (only on the right side in CM 87973), and it communicates with the postglenoid foramen (*foramen retroarticulare*; see below). The sectioned fetus does not have a comparable foramen. In the ventral surface of the zygomatic root is the glenoid fossa, formed entirely within the squamosal; it is elliptical in shape, wider than long, and is limited anteriorly by the concave rostral margin of the zygomatic root, and posteriorly by the gradually sloping, blunt postglenoid process (*processus retroarticularis*; see fig. 43). Immediately posterior to the postglenoid process is the postglenoid foramen, a large, round, ventrally directed opening (figs. 3, 5, 10). Medial to the glenoid fossa, the squama shows a triangular lamina that overlaps the alisphenoid (suture described above). From the root, the zygomatic process arises as a thin bar of bone directed first laterally, then rostrodorsally. The process describes a low arch as it reaches the orbit, where it contacts the jugal. The jugal underlies the anterior half of the zygomatic process (suture described above). As is the case with the rest of the arch, the zygomatic process of the squamosal is laterally compressed and shows two surfaces: medial (*facies medialis*) and lateral (*facies lateralis*). Both surfaces are smooth. The dorsal margin of the process is thin, whereas the ventral margin has a longitudinal concavity for the attachment of the *m. massetericus*.

The squamosal contributes the arched dorsal margin of the external acoustic meatus. The meatus begins rostrally immediately ventral to the postglenoid foramen, where the anterior leg or crus of the ectoympanic attaches through ligaments (see below). It ends in the blunt posttympanic process (*processus retrotympanicus*), located below the level of the opening of the postglenoid foramen, receiving ventrally the posterior leg of the ectotympanic. The posttympanic process is buttressed medially by the posterior continuation of the crista parotica of the petrosal.

Petrosal

The petrosal (*os temporale*, *pars petrosa*) is the paired bone in the cranial base that houses the organs of hearing and equilibration. Two divisions of the petrosal are generally recognized: the more anteroventromedial *pars cochlearis*, enclosing the cochlear duct and the saccule of the inner ear, and the more posterodorsolateral *pars canalicularis*, enclosing the utricle and the semicircular canals.

In CM 87972, the petrosal has three surfaces largely uncovered by other bones: the tympanic surface within the middle ear (*facies tympanica* of the dog), the cerebral and cerebellar surface within the cranial cavity (*facies encephalica* of the dog), and the mastoid exposure on the occiput (*processus mastoideus* of the dog). The pars cochlearis has about a 2-mm-long, plane contact with the basioccipital medially, point contacts with the basisphenoid anteromedially on either side of the carotid foramen, and a point contact with the alisphenoid anterolaterally at the posterolateral corner of the piriform fenestra. The pars canalicularis (via its concave, triangular *facies occipitalis*) contacts the exoccipital and supraoccipital posteromedially, forming the occipitomastoid suture (*sutura occipitomastoidea*), a foliate suture. Most of the lateral surface of the pars canalicularis, roughly trapezoidal in shape, is overlaid by the squamosal, forming the squamosomastoid suture, a squamous suture, at the junction of the occiput and the sidewall of the braincase, where the lateral aspect of the mastoid exposure abuts the posterior aspect of the squamosal. Between its contacts with the squamosal and the supraoccipital, the pars canalicularis has a short plane suture with the parietal. It also has about a 1-mm plane contact with the epitympanic wing of the parietal anterolaterally. Finally, the petrosal has contacts with

the entotympanic, ectotympanic, incus, and stapes (see below). In CM 87972, four apertures are found in the anterior and lateral borders of the petrosal. From anterolateral to posteromedial, these are the piriform fenestra between the petrosal, basisphenoid, and alisphenoid; the carotid foramen (*foramen caroticum internum* of the dog) between the petrosal, basisphenoid, and entotympanic; the basicochlear fissure (*fissura petrooccipitalis*) between the petrosal and basioccipital; and the jugular foramen (*foramen jugulare*) between the petrosal, exoccipital, and basioccipital (right side only).

Because much of the petrosal in the intact skull is not readily accessible for study, we use as the centerpiece of our descriptions isolated petrosals of *Pteropus livingstonii* AMNH 274477, with differences from the CM *P. lylei* noted (figs. 13–15). The therian petrosal is roughly the shape of a tetrahedron with the following four surfaces: tympanic or ventral, encephalic or dorsal, squamosal or lateral, and mastoid or lambdoid (MacIntyre, 1972; Wible, 1990). We treat each of these four sides of AMNH 274477 separately below.

In tympanic view, the most prominent feature is the dome-shaped *promontorium*, the main part of the pars cochlearis (fig. 13). The promontorium is not a symmetrical dome; its lateral aspect is flatter than its medial, and it is longer than wide. The shape of the promontorium is reflective of the enclosed cochlear duct, which Gray (1907) reported to be two coils in *Pteropus medius* (= *P. giganteus*), although he did not specify how the measurements were made. Two apertures are found in the posterior and posterolateral aspects of the promontorium: the round window (*fenestra cochleae*) and oval window (*fenestra vestibuli*), respectively. The fenestra cochleae is oval, wider than high, and directed posteriorly and slightly ventrally. It is closed in life by the secondary tympanic membrane (*membrana tympani secundaria*). The dorsal margin of the fenestra cochleae is recessed within a shallow cochlear fossula (sensu MacPhee, 1981), the posteroventral margin of which is formed by the medial section of the caudal tympanic process (see below). The cochlear fossula is broader in the CM *Pteropus lylei* than in AMNH 274477. The fenestra vestibuli, which accommodates the footplate of the stapes, is also oval, with a stapedial ratio of 1.81 (length/width, according to Segall, 1970). The fenestra vestibuli is directed laterally and slightly ventrally and sits within a shallow vestibular fossula (sensu MacPhee, 1981). The rim of the vestibular fossula has the same shape as the oval window except for its ventral margin, which is convex rather than concave. As a consequence of its position and orientation, the oval window is largely hidden in direct ventral view. At the anteromedial corner of the promontorium is a small, triangular process that is directed anteroventrally (*apex parties petrosa*). Based on CM 87973, this process is underlain by the basisphenoid, and together these form the lateral margin of the carotid foramen. The anterolateral surface of the promontorium has a very shallow depression; based on the *Pteropus* fetus (fig. 34), this is the fossa for the *m. tensor tympani* (*fossa m. tensor tympani* of the dog).

The ventral surface of the pars cochlearis in CM 87972 has an additional process wholly lacking from AMNH 274477. This process is a narrow, rounded shelf that is directed ventromedially from the medial aspect of the promontorium. The anterior end of this shelf is underlain by the entotympanic. There is a shallow, longitudinal concavity where this shelf meets the anteromedial promontorial surface that is directed at the carotid foramen and represents a carotid sulcus. In CM 87973, this shelf is hypertrophied, being both wider and longer, and contacts the basisphenoid to contribute to the medial margin of the carotid foramen.

The bulk of the pars canalicularis in tympanic view is represented by a broad shelf lateral to the promontorium. Near the lateral margin of this shelf is a sinuous ridge of varying height that extends the length of the shelf. The most prominent point on this ridge is posteriorly, where there is a short process that is directed toward, but falls short of, the back of the promontorium. This process is the tympanohyoid or tympanohyal (*tympanohyoideum*), the ossified proximal segment of Reichert's (hyoid) cartilage; the ridge to which the tympanohyoid is fused is the crista

parotica. The segment of the tympanohyoid proximal to the crista parotica is rod-shaped posteriorly, with a narrow anterior shelf. Distally, the rod-shaped part bifurcates into a short anterior leg forming the medial edge of the anterior shelf and a longer posterior leg that tapers to a point. Based on CM 87972, the posterior crus of the ectotympanic abuts the ventral surface of the proximal tympanohyoid. The crista parotica extends both anteriorly and posteriorly from the tympanohyoid. The sharp posterior continuation curves dorsally onto the mastoid exposure and is covered anterolaterally by the posttympanic process of the squamosal. At the junction of the tympanohyoid and the posterior continuation of the crista parotica is the exit of the facial nerve from the middle ear, the stylomastoid notch (*foramen stylomastoideum* in the dog). The more rounded anterior continuation of the crista parotica decreases in height anteriorly and, opposite the oval window, leads to a crescentic depression: the fossa incudis for the crus breve of the incus. The fossa incudis is not flat, but is angled such that its lateral aspect is dorsal to its medial aspect. Based on CM 87972, the squamosal forms the stout lateral wall of the fossa incudis. The lower medial wall of the fossa incudis is formed by a sharp ridge that is continuous with the crista parotica. This ridge increases in height anteriorly, levels off to a flat area, and then decreases in height to the anterolateral margin of the petrosal. This ridge is the ventral edge of the *tegmen tympani*, which is unusual in bats in that it has a near vertical component rather than merely forming a horizontal roof over the middle ear (Wible and Novacek, 1988; Wible, 1992; Wible and Martin, 1993). As noted in other bats previously (Wible and Novacek, 1988), in the *Pteropus* fetus, the tendon of the m. tensor tympani wraps around the back of the ventral edge of the tegmen tympani (fig. 35), an arrangement that likely influences the direction of muscle action.

Medial to the crista parotica and the ventral edge of the tegmen tympani is a broad trough that curves around the lateral margin of the promontorium (fig. 13). This trough extends nearly the length of the pars canalicularis, but falls short of the anterolateral border. Just behind that border, this trough begins at a round, posteriorly directed foramen. This is the secondary facial foramen, by which the facial nerve enters the middle ear from the *cavum supracochleare* (Voit, 1909; *geniculum canalis facialis*). Forming the floor of the secondary facial foramen is a horizontal part of the tegmen tympani that connects to the promontorium. The trough from the secondary facial foramen to the stylomastoid notch is occupied by the facial nerve and, therefore, is the facial sulcus. However, in the narrow interval between the stylomastoid notch and the posterolateral margin of the petrosal, the trough is occupied by the m. stapedius and, so, is the fossa for the m. stapedius (*fossa m. stapedius* of the dog).

The pars canalicularis in tympanic view is also represented by a narrow shelf of bone posterior to the promontorium. The ventral margin of this shelf is the medial section of the caudal tympanic process of the petrosal, or CTPP (sensu MacPhee, 1981), which contributes to the dorsal margin of the cochlear fossula. The medial section of the CTPP is concave and, in direct posterior view, nearly completely shields the round window from view. The CM *Pteropus lylei* differ from AMNH 274477 in their inflation of this region. The medial section of the CTPP is more bulbous, extending the posterior margin of the petrosal, and more prominent, fully shielding the round window in direct posterior view. Whereas the CTPP is a simple, concave ridge in AMNH 274477, in the CM *P. lylei* the central portion of this concave ridge is raised, delimited by sharp edges, and resembles an anvil.

The encephalic view (fig. 14) is dominated by two large depressions, the smaller internal acoustic meatus (*meatus acusticus internus*) anteroventromedially and the larger subarcuate fossa (*fossa subarcuata*) posterodorsolaterally. The former lies in the pars cochlearis and the latter in the pars canalicularis. An oblong aperture (*porus acusticus internus*) leads into the internal acoustic meatus, which is divided into superior and inferior fossae by a low transverse crest (*crista transversa*). The smaller superior fossa (*foramen acusticum superius*) includes the facial nerve area (*area nervus facialis*) anterolaterally and the dorsal vestib-

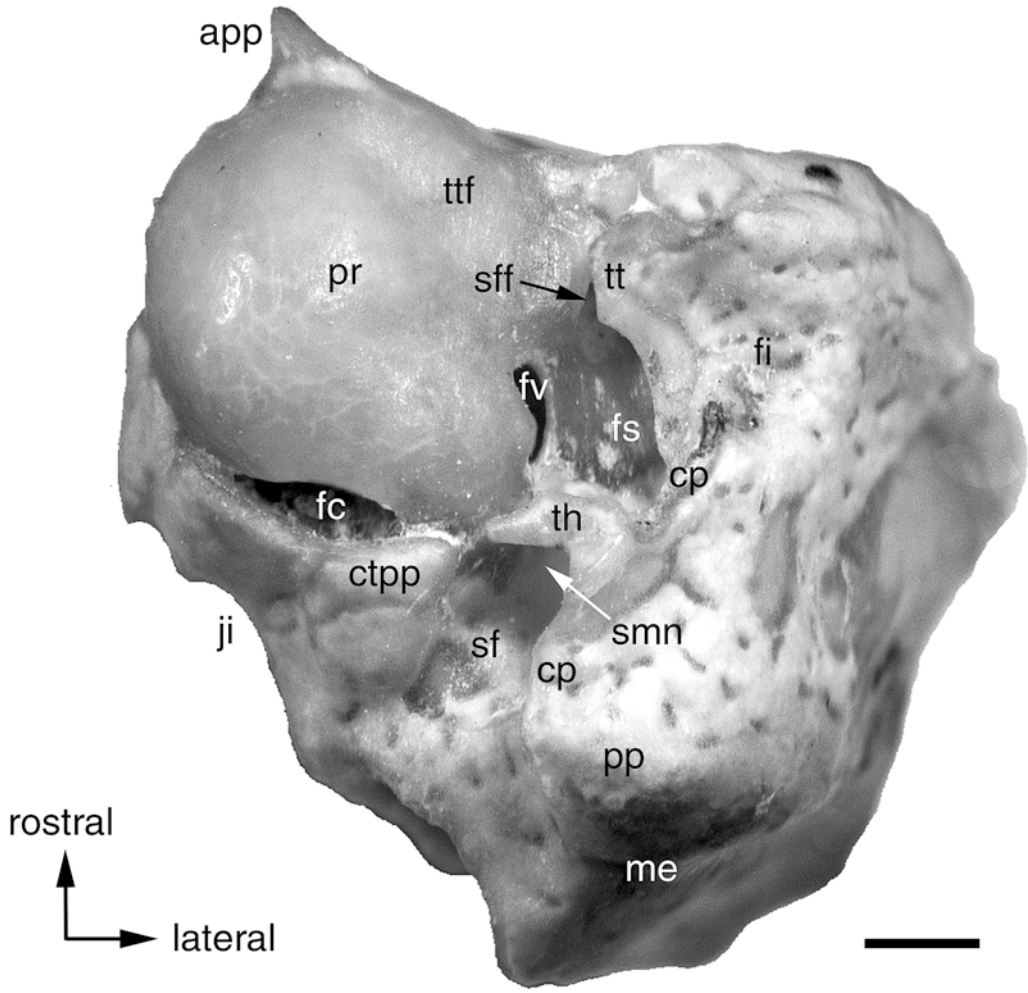

Fig. 13. *Pteropus livingstonii* AMNH 274477, left petrosal bone in oblique ventral view (tympanic surface). Scale = 1 mm. Abbreviations: **app** apex parties petrosa; **cp** crista parotica; **ctpp** caudal tympanic process of petrosal; **fc** fenestra cochleae; **fi** fossa incudis (medial wall); **fs** facial sulcus; **fv** fenestra vestibuli; **ji** jugular incisure; **me** mastoid exposure of petrosal; **pp** paroccipital process of petrosal; **pr** promontorium of petrosal; **sf** stapedius fossa; **sff** secondary facial foramen; **smn** stylomastoid notch; **th** tympanohyoid; **tt** tegmen tympani; **ttf** tensor tympani fossa.

ular area (*area vestibularis superior*) posteromedially, for passage of the facial nerve and part of the vestibular nerve, respectively. The inferior fossa (*foramen acusticum inferius*) includes the large, kidney-shaped cochlear area (*area cochleae*) and the small, round ventral vestibular area (*area vestibularis inferior*), for the cochlear nerve and the remainder of the vestibular nerve, respectively. Within the cochlear area is the spiral tract of minute foramina (*tractus spiralis foraminosus*) for the fascicles of the cochlear nerve. The subarcuate fossa, which houses the paraflocculus of the cerebellum, is a deep, wide depression that occupies a considerable portion of the pars canalicularis. Leading into the subarcuate fossa is a kidney-shaped aperture that is narrower than the subarcuate fossa proper. Because of the thinness of the bone, the posterior semicircular canal (*canalis semicircularis posterior*) and the crus commune (*crus osseum commune*), which lie in the

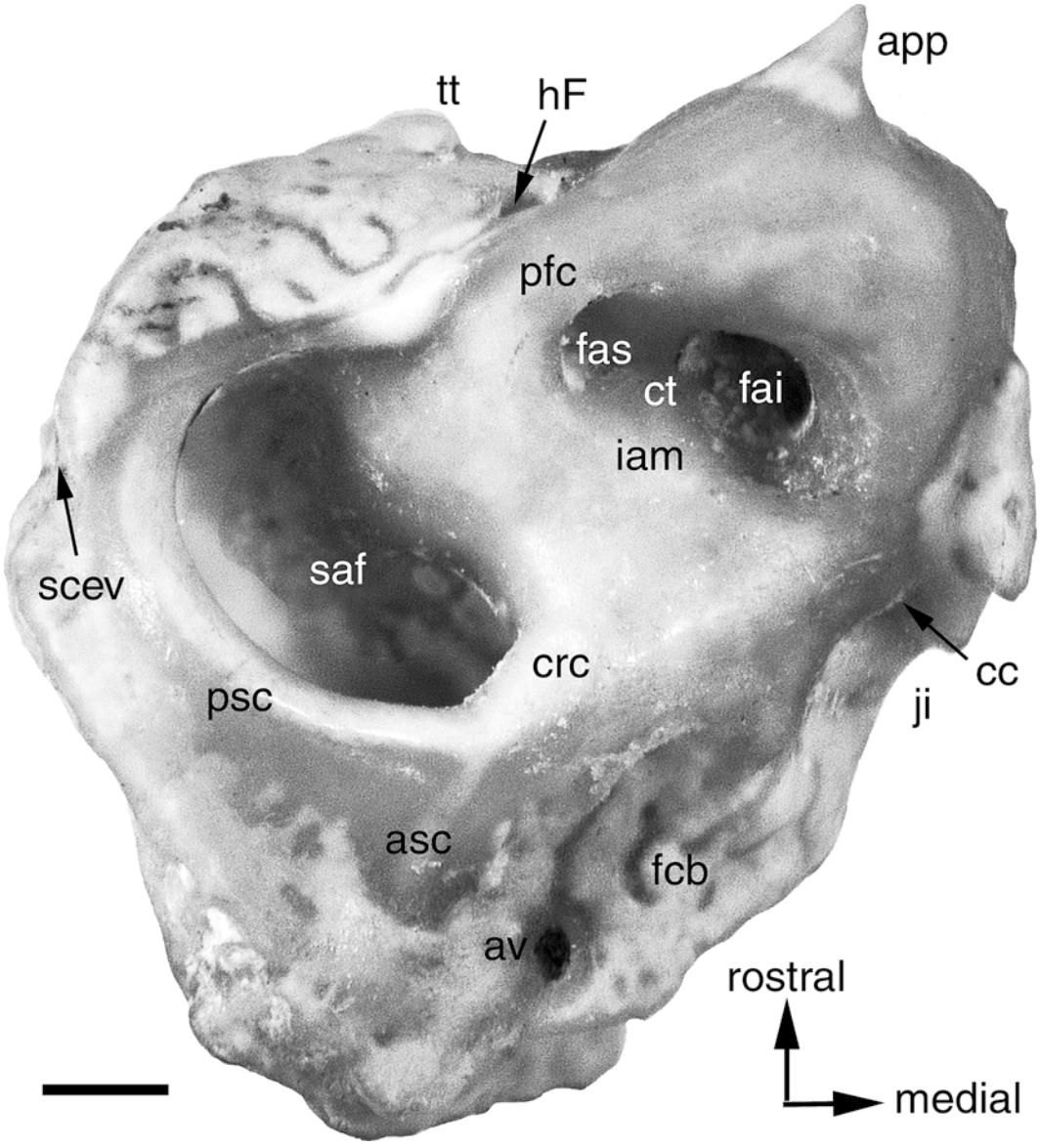

Fig. 14. *Pteropus livingstonii* AMNH 274477, left petrosal bone in dorsal view (encephalic surface). Scale = 1 mm. Abbreviations: **app** apex parties petrosa; **asc** anterior semicircular canal; **av** aqueductus vestibuli; **cc** cochlear canaliculus; **crc** crus commune; **ct** crista transversa of petrosal; **fai** foramen acusticum inferius; **fas** foramen acusticum superius; **fcb** fossa cerebellaris; **hF** hiatus Fallopii; **iam** internal acoustic meatus; **ji** jugular incisure; **pfc** prefacial commissure; **psc** posterior semicircular canal; **saf** subarcuate fossa; **scev** sulcus for capsuloparietal emissary vein; **tt** tegmen tympani.

rim of the subarcuate fossa, are visible. Also visible is the part of the anterior semicircular canal (*canalis semicircularis anterior*) proximal to the crus commune.

Three additional apertures are visible on the encephalic surface (fig. 14). The largest of these is on a narrow shelf of bone anterolateral to (and sloping away from) the

foramen acusticum superius and is partially hidden in direct dorsal view by the bar of bone (prefacial commissure) forming the lateral margin of the internal acoustic meatus. This anteriorly directed, oval aperture is the hiatus Fallopii, the anterior opening of the cavum supracochleare. Based on CM 87971, part of the shelf of bone posterolateral to the hiatus Fallopii is covered by the parietal (see below). The second aperture is on a narrow shelf of bone posteromedial to the foramen acusticum inferius the jugular incisure (*incisura jugularis*). This foramen is also partially hidden in direct dorsal view as it faces posteromedially into the jugular foramen. This is the opening by which the perilymphatic duct (*ductus perilymphaticus*) enters the petrosal, the cochlear canaliculus (*apertura externa canaliculus cochleae*). The third aperture is on a narrow shelf medial to the subarcuate fossa. This shelf has a faint depression, the *fossa cerebellaris*, and in the posterior part of this fossa is the oval, posteriorly directed opening by which the endolymphatic duct (*ductus endolymphaticus*) enters the petrosal, the vestibular aqueduct (*apertura externa aqueductus vestibuli*). A shallow sulcus leads into the vestibular aqueduct from behind. Lastly, posterodorsal to the subarcuate fossa (and running parallel to it) is a short, very shallow sulcus for the capsuloparietal emissary vein (*sinus temporalis*).

The most dominant feature in squamosal view (fig. 15) is the trapezoidal surface covered by the squamosal in the intact skull. The irregular ventral margin of this surface is formed by the crista parotica posteriorly and the tegmen tympani anteriorly. The posteroventral aspect of this surface has a noticeable bulge, which in the intact skull is covered by the posttympanic process of the squamosal. This bulge corresponds in position to the mastoid process (*processus mastoideus* in Schaller, 1992). As noted by MacPhee (1981), that term has been used for a variety of probably non-homologous bumps on the petrosal. Following Wible and Gaudin (2004), we prefer the term paroccipital process for this bulge. The anterodorsal aspect of the trapezoidal surface has a very shallow sulcus for the capsuloparietal emissary vein that is continuous with the sulcus reported on the encephalic surface. Anterior to the trapezoidal squamosal surface is a roughly triangular surface whose vertex is the ventral edge of the tegmen tympani. The ventral half of this shelf is covered by the parietal, based on CM 87971.

The mastoid exposure of the petrosal (figs. 5, 13, 15) is roughly rectangular, taller than wide. Dorsally, it contacts the parietal laterally and the supraoccipital medially. The contact with the parietal is shorter (ca. 2 mm) and straight; that with the supraoccipital (ca. 3 mm) is sinuous, with a degree of interdigitation. Medially, the mastoid exposure contacts the exoccipital at a slightly concave suture; this joint shows some interdigitation in the dorsal part. Laterally, it contacts the squamosal at a convex suture. The free ventral margin is concave, with a sharp prominence in the ventrolateral corner, the posterior continuation of the crista parotica. In CM 87973, a distinct ridge curves dorsomedially from the ventral end of the posterior continuation of the crista parotica and continues onto the paracondylar process of the exoccipital; this ridge is very faint in AMNH 274477. Based on the fetus, the *m. sternomastoideus* (Evans, 1993; *musculus sternocephalicus, pars mastoidea* in the NAV) attaches to this ridge, the posttympanic process of the squamosal, and the paracondylar process of the exoccipital. At the dorsomedial corner of the mastoid exposure in CM 87972 is a small mastoid foramen (*foramen mastoideum*), which is 0.4 mm on the left and smaller on the right. The petrosal only contributes to the border of the left mastoid foramen. Based on *Pteropus capistratus* AMNH 194276, the mastoid foramen is at the junction of the exoccipital and supraoccipital with the mastoid exposure.

Entotympanic

A rostral entotympanic (*rostrales entotympanicum* of Klaauw, 1922) is present in *Pteropus*, including the species described here. Novacek (1980, 1991) figured the rostral entotympanic in *P. poliocephalus*. This tiny, peglike element is located in the basicranium ventral to the juncture of the basisphenoid and basioccipital, at the basico-

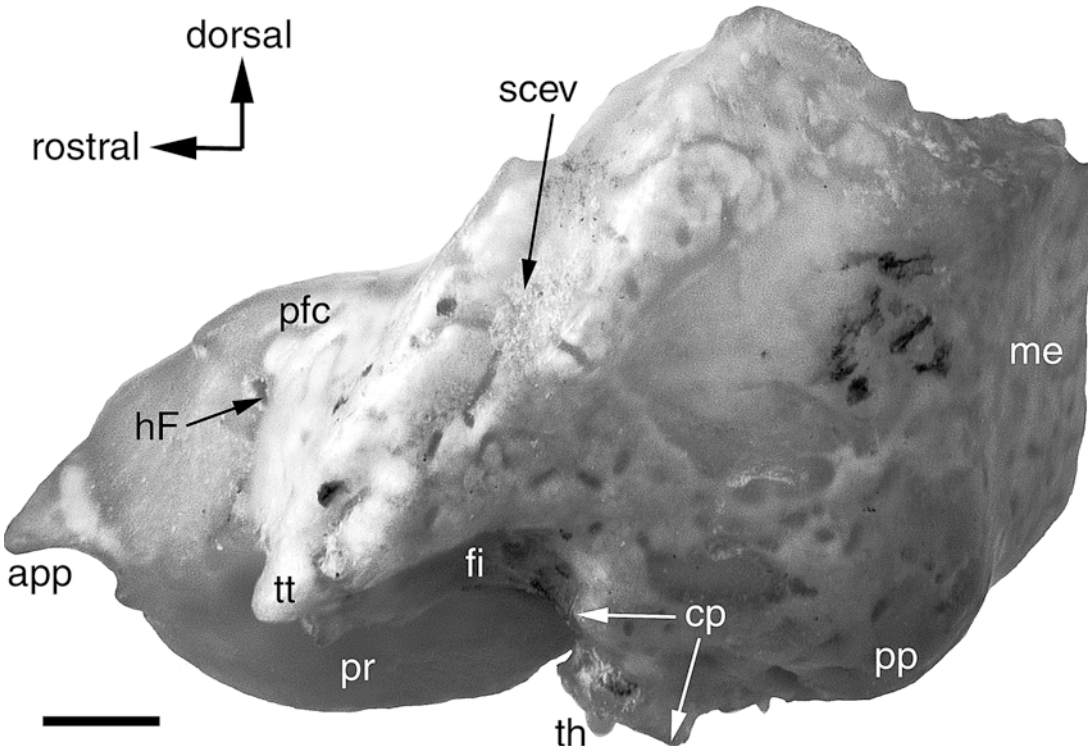

Fig. 15. *Pteropus livingstonii* AMNH 274477, left petrosal bone in lateral view (squamosal surface). Scale = 1 mm. Abbreviations: **app** apex parties petrosa; **cp** crista parotica; **fi** fossa incudis; **hF** hiatus Fallopii; **me** mastoid exposure of petrosal; **pfc** prefacial commissure; **pp** paroccipital process of petrosal; **pr** promontorium of petrosal; **scev** sulcus for capsuloparietal emissary vein; **th** tympanohyoid; **tt** tegmen tympani.

chlear fissure (it is lost from the left side of the macerated skull of CM 87972). The bone presents a roughly tetragonal shape (figs. 3, 5, 10). The medial, roughly triangular surface has a concave caudal margin and a rostrodorsal vertex. The base of the entotympanic underlies the occipitosphenoid suture; the lateral and caudal sides are partially hidden. The shape is far more irregular in other specimens, and in AMNH 237596 the right entotympanic is divided in two parts. In adult specimens, when it is preserved, the entotympanic may be caudally displaced, reaching the petrosal and even fusing to it, while losing contact with the basisphenoid and exoccipital (e.g., in AMNH 237593). In the *Pteropus* fetus, the cartilaginous rostral entotympanic is an irregular U-shaped structure that sits beneath the anterior pole of the promontorium (see reconstruction in Wible and Martin, 1993: fig. 6). The main body of the rostral entotympanic lies anteriorly (below the carotid foramen in fig. 33) and has two posteriorly directed curved arms, one ventromedial and the other dorsolateral (the posterior end of which is seen in fig. 34).

In addition to a rostral entotympanic, the *Pteropus* fetus has a flat cartilaginous caudal entotympanic (*caudales entotympanicum* of Klaauw, 1922), longer than wide, which abuts the medial aspect of the posterior crus of the ectotympanic and fills in the space between that bone, the promontorium, and the rostral entotympanic (figs. 33–35; see reconstruction in Wible and Martin, 1993: fig. 6). There is no trace of this element in the osteological specimens, which suggests that, unlike the rostral entotympanic, the caudal entotympanic does not ossify in the adult.

Ectotympanic

The ectotympanic (*annulus tympanicus*) is a small, ring-shaped bone located ventral to the concave margin of the squamosal between the postglenoid and posttympanic processes, in the dorsal border of the external acoustic meatus (joint unnamed in the NAV; figs. 2, 3, 5). The ectotympanic is elliptical in shape (fig. 16A, B) and conspicuously inclined ventromedially (figs. 3, 16C, 43). In ventral view, the annulus steadily increases in width rostrodorsally (fig. 3). Its irregular medial margin has a small lamina flaring medially (fig. 3; the styliform process of Henson, 1970). The annulus is horseshoe-shaped and has two arching branches (*crura*), anterior and posterior, that are continuous ventromedially (fig. 16). The *crus anterior* abuts the medial margin of the squamosal and extends its contact from the level of the rostral edge of the postglenoid foramen to beyond the midpoint of the arch of the external acoustic meatus (fig. 2). The lateral margin of the anterior crus is thickened. The *crus posterior* is noticeably thinner, and it has a restricted area of contact with the tympanohyoid (see Petrosal). The crura do not contact each other dorsolaterally, being separated by a space of ca. 1 mm. The annulus has a deep medial sulcus (*sulcus tympanicus*) that is roughly constant in width throughout (fig. 16C). The tympanic membrane (*membrana tympani*) attaches to the medial border of the sulcus. The ectotympanic and tympanic membrane form the lateral limit of the tympanic (or middle ear) cavity (*cavum tympani*).

In CM 87972, both ectotympanics are in place, precluding a full view of the medial aspect of the bones. Examination is possible in *Pteropus livingstonii* AMNH 217044, whose ectotympanics are detached from the skull base. In this specimen, the ectotympanic shows a slightly expanded medial border with the small flange described above projecting directly medially. Dorsally, the rostral process of the malleus (see below) overhangs the anterior crus. The rostral process is fused ventrally to the anterodorsal surface of the anterior crus medial to the raised lateral border of the crus. Seams are clearly visible in the contact of the rostral process and the anterior crus.

Middle Ear Ossicles

The three middle ear ossicles (*ossicula auditus*)—the *malleus*, the *incus* and the *stapes*—lie in the tympanic or middle ear cavity (*cavum tympani* in the *auris media*). As in mammals in general, the malleus is formed embryologically by two components from the fetal lower jaw (Klaauw, 1922; Jurgens, 1963). The malleus per se is derived from the articular. The second element is the rostral or anterior process, which is continuous with the malleus (hence the term outer lamella of processus gracilis in Jurgens, 1963) and homologous to the gonial bone (= prearticular). The incus (derived from the quadrate) and the stapes successively transmit sound to the inner ear through the fenestra vestibuli of the petrosal. Doran (1878) gave a rather superficial description of the malleus, incus, and stapes of *Pteropus*, based on *P. hypomelanus* and *P. edulis* (most likely a synonym of *P. vampyrus*), and Wassif (1948) provided a detailed description of the ossicles in *Rousettus aegyptiacus*. A description of the three bones, based on *P. lylei* and *P. livingstonii*, follows.

Malleus: The malleus (fig. 16A–C), the first bone in the ossicular chain, articulates with the incus, forming the incudomalleolar joint (*articulatio incudomallearis*), reported to be a synovial joint in *Pteropus giganteus* (Hinchcliffe and Pye, 1969). The malleus has a head (*caput mallei*) with a large articular facet for the incus, an osseous lamina whose caudal margin is the neck (*collum mallei*), a rostral or anterior process (*processus rostralis*), a manubrium (*manubrium mallei*), a lateral process (*processus lateralis*), and an orbicular apophysis.

The dorsalmost part of the malleus is the head—a roughly conical process with the apex directed rostroventrally. The head is hollowed ventrally, resulting in a hoodlike appearance, where the head receives the lateral ridge of the rostral process in its ventral cavity (see below). Caudal to the head is the concave facet for the incus, which has two surfaces—a wide, oblique caudodorsal surface and a narrow caudoventral portion—

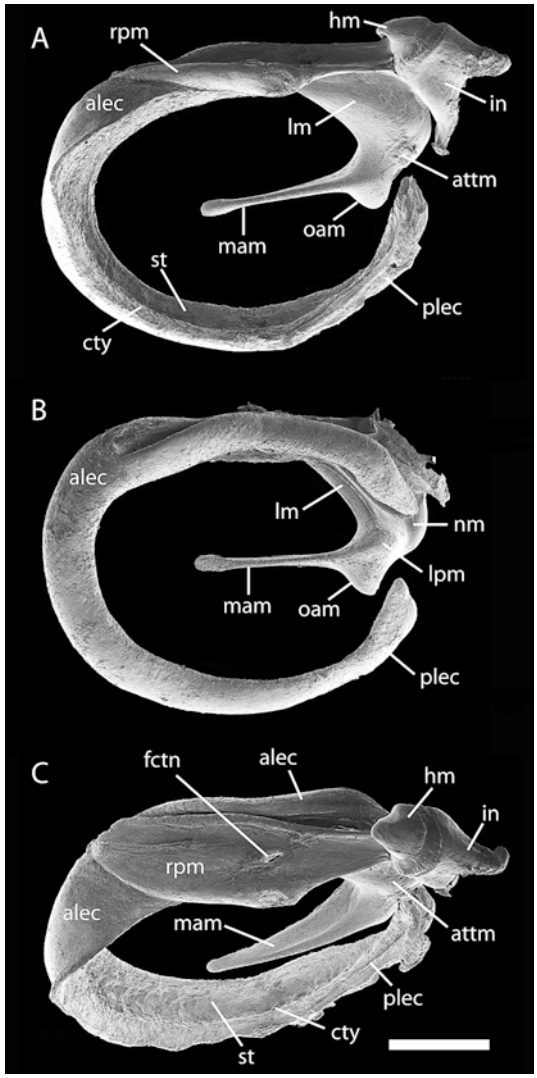

Fig. 16. *Pteropus livingstonii* AMNH 274466, medial (**A**), lateral (**B**), and oblique dorsal (**C**) views of the right (**A** and **C**) and left (**B**) ectotympanic and articulated malleus and incus (broken). Scale = 1 mm. Abbreviations: **alec** anterior leg of ectotympanic; **attm** attachment of tensor tympani muscle; **cty** crista tympanica; **fctn** foramen for the chorda tympani nerve; **hm** head of malleus; **in** incus; **lm** lamina of malleus; **lpm** lateral process of malleus; **mam** manubrium of malleus; **nm** neck of malleus; **oam** orbicular apophysis of malleus; **plec** posterior leg of ectotympanic; **rpm** rostral process of malleus; **st** sulcus tympanicus.

meeting at a roughly 90 degree angle. Ventral to the head is the osseous lamina of the malleus; it is a deep and thin plate of bone that buttresses the rostral process rostroventrally and joins the manubrium ventrally. Laterally, the osseous lamina is framed by two thick borders: one in the ventral margin of the lamina, and the other, deeply convex caudally, in the caudal margin reaching the head of the malleus (the neck). Medially, the osseous lamina shows a smooth and slightly convex surface. The m. tensor tympani attaches in the caudal area of the medial surface; there is only a faint scar that indicates the site of attachment (i.e., a conspicuous *processus muscularis* is absent). At the ventralmost point of the osseous lamina, three heterogeneous processes arise in different directions: laterally, the lateral process; caudally, the orbicular apophysis; and ventrocaudally, the manubrium. The lateral process is a short, somewhat elliptical eminence oriented dorsoventrally that is continuous with the lateral margin of the manubrium. The slightly larger orbicular apophysis also has an elliptical base, lateromedially oriented, whose domed top faces caudally. The orbicular apophysis shows an irregular depression in its caudal side. In turn, the lateral process hides a deep fossa in its medial contact with the osseous lamina. The long, swordlike manubrium is a rostrocaudally flat process with a small spatulate end that attaches to the tympanic membrane. In caudal view, the manubrium is wide at the level of the orbicular apophysis. The lateral margin of the manubrium is almost straight, whereas the medial margin is dorsally convex and becomes almost straight ventrally as it reaches the end of the process.

The rostral process of the malleus consists of a horizontal inner lamella, corresponding to the rostral process of the malleus per se, and a partly vertical outer lamella, corresponding to the gonial (Jurgens, 1963). The limits of the two areas cannot be established precisely in our specimens. The rostral process as a whole is a large, dorsally concave lamina with a curving lateral border that accompanies the lateral border of the ectotympanic, and a low and wide medial portion. From the rostral end, the lateral

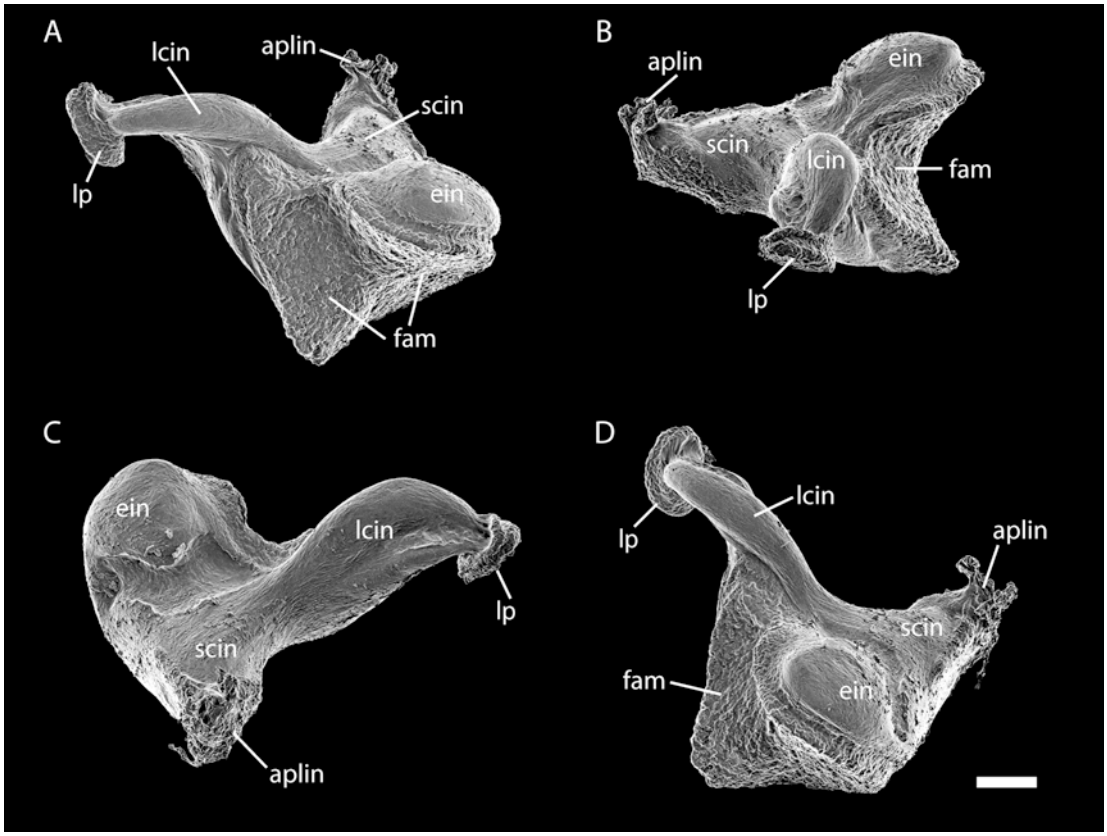

Fig. 17. *Pteropus livingstonii* AMNH 274466, diverse views (**A** to **D**) of the isolated left incus. When articulated, the long crus (**lcin**) points medially and the short crus (**scin**) points dorsally. Scale = 0.2 mm. Abbreviations: **aplin** attachment of posterior ligament of incus; **ein** unnamed round eminence of incus; **fam** incudal facet for head of malleus; **lcin** long crus of incus; **lp** lenticular process of incus; **scin** short crus of incus.

border rises caudally as a roughly vertical ridge that remains level throughout until it is slightly upturned immediately ventral to the head of the malleus. The ridge is thin, with its dorsal margin strengthened by a longitudinal thickening of the bone. Medially, the lamina descends into a shallow basin with its widest portion roughly at the caudal two-thirds of its length. At this point, in the medial border, the lamina has a shallow depression and a small rounded prominence. From that point caudally, the lamina conspicuously decreases in breadth to meet the outer lamella ventral to the head. Rostrally, the lamina develops a shallow sulcus that ends at its apex. Based on *Rousettus* (Jurgens, 1963: fig. 11), this sulcus held Meckel's cartilage in the fetus, and based on the *Pteropus* fetus it also held the chorda tympani nerve. The medial border of the lamina is convex, growing thicker to form a torus medially. The rostral process is pierced by the foramen for the chorda tympani nerve, a small oval opening in the substance of the lamina (figs. 16C, 35). This opening is slightly rostrodorsally oriented. Ventrally, the rostral process is ankylosed to the dorsal surface of the anterior crus of the ectotympanic.

INCUS: The incus (fig. 17A–D), the second bone in the ossicular chain, articulates with the stapes, forming the incudostapedial joint (*articulatio incudostapedia*), reported not to be a synovial joint in *Pteropus*

giganteus (Hinchcliffe and Pye, 1969). The incus of AMNH 240006 was examined in situ, whereas the incus of AMNH 237596 was observed isolated. The incus has two stout legs, short (*crus breve*) and long (*crus longum*), connected by an incudal body (*corpus incudis*) that contains the facet for the malleus. The two crura diverge from one another nearly at right angles. The short crus points dorsally and slightly caudally into the fossa incudis (described with the Petrosal above) and has a simple, conical shape with a truncated apex. The strong posterior ligament (*lig. incudis posterius*), which fixes the incus to the roof of the fossa incudis, is easily seen in situ in AMNH 240006. The long crus points caudally and slightly ventrally, and it is compressed and rotated as it bends medially to meet the stapes. The tip of the long crus is expanded in the rounded, medially flattened lenticular process (*processus lenticularis*), which matches the head of the stapes. The incudal body has a large facet for the malleus, with the ventral half concave and the rostral half less so. The articular surface is rugose; the ventral part has a triangular shape with the vertex directed caudally, and the caudal part is semicircular with the arch directed dorsally and a concave ventral margin. Ventrolaterally, the incudal body presents a rounded eminence limited ventrally by the border of the facet for the malleus and dorsally by a shallow circular fossa. This fossa is less marked in other specimens examined (e.g., *P. lylei* AMNH 237596).

STAPES: The stapes transmits vibrations from the incus to the fenestra vestibuli of the pars cochlearis of the petrosal in the *syndesmosis tympanostapedia*. The stapes was examined in situ in AMNH 240006 and ex situ in AMNH 274470 (fig. 18; a stapes is figured for *Pteropus edulis* by Doran, 1878: figs. 26, 27). It consists of a base or footplate (*basis stapedis*), two crura or legs—anterior or rostral (*crus rostrale*) and posterior or caudal (*crus caudale*)—a stapedial or intracrural foramen between the legs and base, and a neck and head (*caput stapedis*; fig. 18). The base is elliptical in shape with the major axis rostrocaudally oriented, articulating with the edge of the fenestra vestibuli of the petrosal. The anterior leg is very thin and slightly bowed rostrally, and it reaches the base with little change in diameter. The posterior leg is at least twice as thick as the anterior leg, slightly wider medially, where it is almost as wide as the base, and it is roughly straight save for the rostral margin (facing the stapedial foramen), which is noticeably concave. The two legs connect laterally in a short neck, from which the small muscular process for the attachment of the m. stapedius projects caudally. This muscular process is roughly triangular in shape, and it has a caudal surface placed obliquely with respect to the plane of the head. The head is a flat piece wider than the neck, of round shape in lateral view, that articulates with the lenticular process of incus. The head exhibits a rugose dorsal surface whose caudal margin gently turns medially, being virtually continuous with the caudolateral surface of the muscular process (fig. 18).

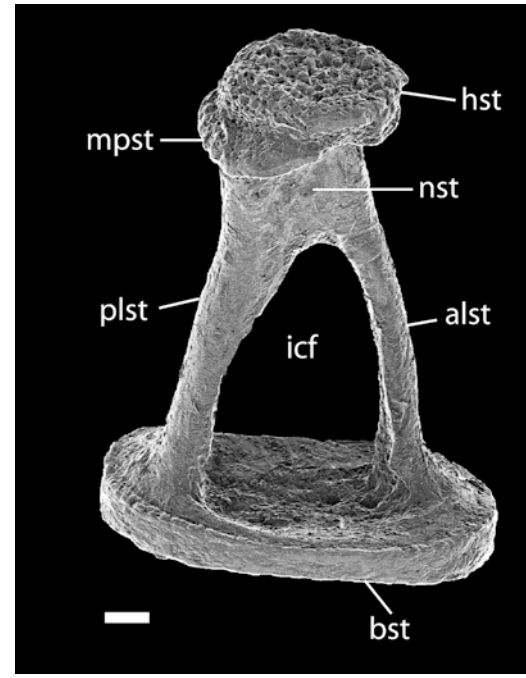

Fig. 18. *Pteropus livingstonii* AMNH 274466, dorsal view of the left stapes. Scale = 0.1 mm. Abbreviations: **alst** anterior leg of stapes; **bst** base of stapes; **hst** head of stapes; **icf** intercrural foramen; **mpst** muscular process of stapes; **nst** neck of stapes; **plst** posterior leg of stapes.

Occipital Complex

The occipital complex (*os occipitale*) is formed by the unpaired basioccipital (*pars basilaris*) and supraoccipital (*squama occipitalis*), and the paired exoccipitals (*pars lateralis*; fig. 5). These four embryological units, each ossified from separate centers, surround the *foramen magnum*, which connects the brain with the spinal cord and associated structures (fig. 5). The bones are fused seamlessly in CM 87972 except for traces of a suture between the basioccipital and exoccipitals in the medial margin of the jugular foramen (see fig. 5 and below). For that reason, precise relationships among these bones will be discussed based on *Pteropus capistratus* AMNH 194276, a younger specimen in which all sutures are present, in the Skull Development section.

Basioccipital: This bone has a roughly rectangular form and contacts the basisphenoid rostrally (suture described above), the exoccipital caudolaterally, forming the ventral intraoccipital synchondrosis (*synchondrosis intraoccipitalis basilateralis*), and the pars cochlearis of the petrosal, forming the posterior basicochlear commissure laterally (figs. 3, 5), the latter being the petro-occipital joint of the dog (Evans, 1993; *synchondrosis petro-occipitalis*). The lateral margin of the basioccipital forms the medial margin of the basicochlear fissure (the petro-occipital fissure of the dog) rostrally and the jugular foramen (*foramen jugulare*) caudally, with both openings separated by the relatively narrow posterior basicochlear commissure. The basicochlear fissure is coalesced with the piriform fenestra and the carotid foramen laterally, although the openings are incompletely delimited by processes of the rostrolateral angle of the basisphenoid and the petrosal (fig. 10). The medial margin of the basicochlear fissure occupies roughly the anterior third of the lateral margin of the basioccipital. The posterior basicochlear commissure is a rather irregular bridge of bone that loosely connects the basioccipital and the pars cochlearis of the petrosal. The basioccipital component of the posterior basicochlear commissure is roughly straight, slightly divergent, and essentially featureless (cf. the dog, in which a muscular tubercle is present in this area). The commissure is approximately as long as the basicochlear fissure. Just past the posterior basicochlear commissure caudally, the basioccipital penetrates slightly into the opening of the jugular foramen on the right side, whereas it is excluded from the foramen by the exoccipital on the left side. In this area is the trace of the ventral intraoccipital synchondrosis, < 1 mm in length and directed posteromedially, deeply incised only in the immediacy of the jugular foramen. The caudal margin of the basioccipital participates in the ventral margin of the foramen magnum at the concave intercondyloid notch (*incisura intercondyloidea*). The surface of the basioccipital is ventrally curved, with the curvature accentuated toward the caudolateral angle. The surface is marked medially by a low crest that extends posterolaterally and that is equivalent to the pharyngeal tubercle of the dog (*tuberculum pharyngeum*). This ill-defined tubercle divides the basioccipital into two parts; rostrolateral to this crest are the shallow, faint marks of the paired, rounded basioccipital pits, which are sites of attachment of the *m. longus capitis* and the *m. rectus capitis ventralis* (figs. 34, 35).

Exoccipital: The paired exoccipitals are located posterolateral to the basioccipital on the ventral side of the cranium and lateral to the foramen magnum on the occipital side of the cranium (fig. 5). The ventral portion has a deeply concave lateral margin that corresponds to the medial margin of the large jugular foramen. Caudomedial to the jugular foramen is the round hypoglossal foramen (*canalis nervus hypoglossum* of the NAV and *foramen hypoglossi* of the dog). The hypoglossal foramen opens ventrolaterally and, based on *Pteropus capistratus* AMNH 194276, it lies entirely within the exoccipital. Caudal to the jugular foramen is the paracondylar process (*processus paracondylaris*), a ventral projection from which the *m. digastricus* originates. The process is broad at its base, tapering to a hooklike, rostrally directed point. Lateral to the paracondylar process is the convex suture with the mastoid exposure of the petrosal, the occipitomastoid suture. Medial to the paracondylar process is the relatively deep ventral condyloid fossa (*fossa condylaris ventralis*).

Lateral to the foramen magnum and medial to the condyloid fossa are the prominent occipital condyles (*condyli occipitales*), the cranial components of the atlanto-occipital joints (*articulatio atlanto-occipitalis*). The condyles are elliptical, taller than wide, and obliquely placed such that their dorsal ends are widely divergent and well outside the dorsolateral margin of the foramen magnum. By contrast, the ventral ends are placed on the arch of the margin of the foramen magnum. The epiphyseal cartilage (*cartilago epiphysealis*) is present as a whitish cap covering most of the surface of the condyle. The outline of the foramen magnum dorsal to the condyles is somewhat triangular with the dorsal vertex rounded; based on *Pteropus capistratus* AMNH 194276, only the dorsolateral portion of this outline lies within the exoccipital, the dorsalmost portion being within the supraoccipital (fig. 43A, but see Skull Development). Two minute nutrient foramina are located symmetrically on each side of each condyle. A third one is ventral to the lateral nutrient foramen of the left side. Laterally, in the tripartite joint between the petrosal, exoccipital, and supraoccipital, is the small, receding mastoid foramen, which opens caudomediodorsally. On the right side, the petrosal is excluded from the opening. The exoccipital is fused without a trace with the supraoccipital in CM 87972; based on *P. capistratus* AMNH 194276, the dorsal intraoccipital synchondrosis (*synchondrosis intraoccipitalis squamolateralis*) is a relatively acute arch that rises between the mastoid foramen and a point in the dorsal two-thirds of the supracondylar outline of the foramen magnum (see fig. 43A). This area corresponds to the dorsal condyloid fossa of the dog (*fossa condylaris dorsalis*), but in CM 87972 it is only minimally depressed.

SUPRAOCCIPITAL: This bone occupies the dorsal part of the occiput, participating in the dorsal margin of the foramen magnum, and bears the incipient lamboid or nuchal crest (*crista nuchae*). The supraoccipital contacts the exoccipitals ventromedially, the mastoid exposure of the petrosal ventrolaterally, the parietal dorsolaterally, and the interparietal dorsomedially (all sutures described above; fig. 5). The nuchal crest is modestly marked as two low arches that meet at the midsagittal line. The crest as a whole divides the supraoccipital into roughly equal dorsal and ventral parts. The dorsal surface is engraved with short incisions that may have been numerous nutrient foramina and their short accompanying sulci. On each side, the nuchal crest is continued laterally into the mastoid exposure of the petrosal. The supraoccipital is domed along the midsagittal line. The round and low external occipital protuberance (*protuberantia occipitalis externa*) is located between the occipitointerparietal suture and the nuchal crest. It is continued ventrally by a narrower, shallow crest, the external occipital crest (*crista occipitalis externa*), a smooth median ridge that inconspicuously reaches the foramen magnum.

MANDIBLE

The mandible (*mandibula*) or dentary bone is paired, bears the lower dentition, and forms a lever that allows for mechanical processing of food in the mouth. Each mandible is formed by a horizontal, tooth-bearing body (*corpus mandibulae*) and a caudal ramus (*ramus mandibulae*; figs. 6, 7). The left and right mandibles diverge caudally at ca. 30 degrees, forming between them the intermandibular space (*spatium mandibulae*, *regio intermandibularis*) where the tongue lies. The mandibles are fused anteriorly without a trace of a suture at the mandibular symphysis (*symphysis mandibulae*).

The body of the mandible (fig. 6) is a relatively thick, bony bar that presents an alveolar surface dorsally (*margo alveolaris*), two vertical surfaces—lingual (*facies lingualis*) and buccal (*facies buccalis*)—a mental surface (*facies labialis*), and a ventral border (*margo ventralis*). The alveolar surface contains the alveoli for two incisors (i1, i2), a canine (c), three premolars (p1, p3, p4), and three molars (m1–3). There are two small diastemata, one between the left i1 and the right i1, and the other between p1 and p3. There are no other marked interdental spaces, but there is a narrow retromolar space between m3 and the ramus. In lateral view, the alveolar line shows a deep emargination that houses the large lower canine. The alveolar line is flat (straight) from the

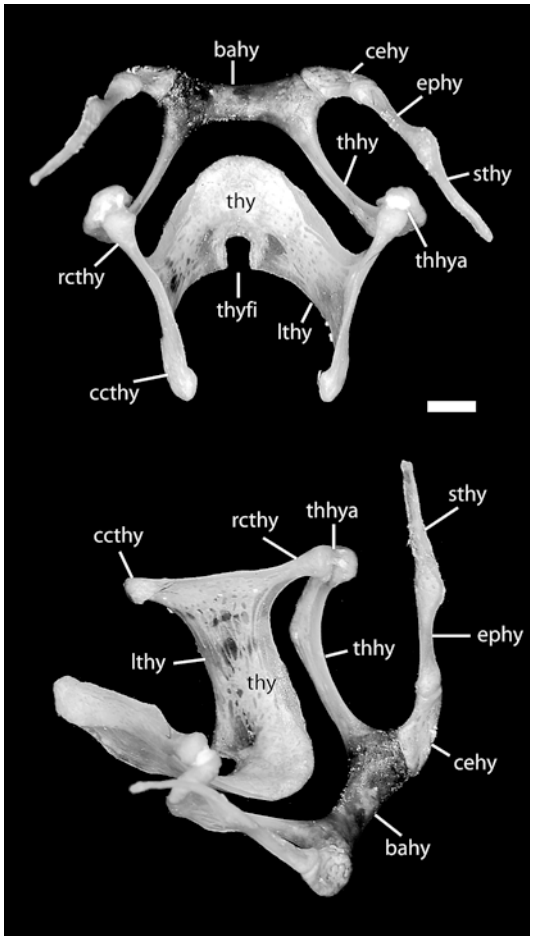

Fig. 19. *Pteropus tonganus* USNM 546610, dorsal (Above) and oblique rostrodorsolateral (Below) views of the hyoid apparatus and the attached thyroid cartilage. Scale = 1 mm. Abbreviations: **bahy** basihyoid; **ccthy** caudal cornu of thyroid; **cehy** ceratohyoid; **ephy** epihyoid; **lthy** lamina of thyroid; **rcthy** rostral cornu of thyroid; **sthy** stylohyoid; **thhy** thyrohyoid; **thhya** thyrohyoid articulation; **thy** thyroid cartilage; **thyfi** thyroid fissure.

canine to the level of p1, after which it takes the shape of a progressively attenuated sinusoid whose peaks occur between the roots of the cheek teeth and whose valleys correspond to the interdental spaces (*septa interalveolaria*). The oscillation of the alveolar line is flattened behind m1, from which it continues smoothly into the dorsal border of the ramus, outlining an uninterrupted ascending profile. The buccal surface of the body is formed by semitranslucent bone through which the roots of p3 and p4 are clearly visible, but the surface itself is smooth (no juga are present). The most noteworthy feature of the buccal surface is the posterior mental foramen (*foramen mentale*, the homologue of the middle mental foramen of the dog; see Foramina Contents and Homology below). This dorsally directed foramen is located directly ventral to p1. The lingual surface of the body is smooth. The thickness of the body decreases gradually toward the rounded ventral border, which is roughly straight in lateral view.

The mandibular symphysis, in the *pars incisiva* of the body, is the median synchondrosis (*synchondrosis intermandibularis* + *sutura intermandibularis*) that connects the left and right mandibular bodies and extends from the anteriormost edge of the mandible to the middle of p3 (fig. 7) with a marked slope in lateral view (fig. 6). The symphyseal region has a rostral and a caudal surface, a dorsal border that bears the alveoli of the incisors (*arcus alveolaris*), and a ventral border. The rostral or mental surface is slightly convex; in anterior view, the alveolar border has a minute notch between the inner lower incisors. The deep emargination for the canines is also visible laterally in anterior view. The mental surface decreases in width ventrally, accompanying the converging canine roots that reach the bottom of the mandibular body (fig. 8). The mental surface bears the anterior mental foramina (fig. 8), which are smaller than the posterior foramina and are located immediately ventral to the i1–i2 embrasure. The anterior mental foramina open somewhat laterally and dorsally. The caudal symphyseal surface is narrowly concave and smooth, with some four small nutrient foramina alongside the intermandibular contact. In the caudal surface, the alveolar line (*arcus alveolaris*) is continuous and the alveoli for the canine and the incisors are coalescent; that is, the bony wall that divides the space between the teeth is incomplete in the middle. The caudoventral margin of the symphyseal region serves for the attachment of the *m. genioglossus*, which draws the hyoid apparatus rostrally when contracted (Griffiths, 1982). In that area, a central knob, visible also in lateral view, is

flanked by two pits caudoventral to the canine roots. Three irregularly distributed, minute nutrient foramina are present in the caudoventral margin.

The ramus is a thin plate of bone that comprises roughly the caudal third of the mandible (fig. 6). It has two processes—the coronoid process (*processus coronoideus*) and the mandibular condyle or articular process (*processus condylaris*). The angle of the mandible (*angulus mandibulae*) lacks a true, salient angular process (*processus angularis*). The coronoid process is directed dorsally and slightly outwardly. Its dorsal border is a continuation of the alveolar line, which rises at a ca. 45 degree angle, starting from a short distance behind m3. The maximum height of the coronoid process is roughly equivalent to the height of the canine. The m. temporalis inserts on the anterodorsal border of the coronoid process. From the curved dorsalmost area, the posterior border of the coronoid terminates in a caudal point and a pronounced mandibular (or lunar) notch (*incisura mandibulae*).

The ventral border of the mandibular notch connects posteriorly with the mandibular condyle, a transverse bar located at the level of the alveolar line (or slightly above the alveolar line in CM 87973). The outline of the convex articular surface is oval and faces dorsocaudally. The surface itself is porous and shows the scar of a ligament attachment (the lateral ligament, *lig. lateralis*). The angle is comparatively inconspicuous, forming the rounded caudoventral border of the ramus. Based on *Pteropus tonganus* (Storch, 1968), its posterior border serves for the insertion of the *pars superficialis* of the *m. massetericus*. The angle lies anterior to the mandibular condyle, which then appears to protrude from the posterior border of the ramus. The thin ventral border of the ramus is only slightly below the level of the ventral border of the mandibular body. The lateral surface of the ramus has a smooth and shallow masseteric fossa (*fossa masseterica*), which is limited anterodorsally by the coronoid crest (*crista coronoidea*, the anterodorsal border of the coronoid process) and ventrally by a low condyloid crest (*crista condyloidea*). The condyloid crest runs horizontally from the posterior end of m3 to the mandibular condyle below the level of the alveolar line. The masseteric fossa as a whole serves for the attachment of the m. massetericus and *m. zygomaticomandibularis*. Based on *Rousettus aegyptiacus* (Storch, 1968), the m. zygomaticomandibularis inserts on the condyloid crest. Based on *R. aegyptiacus* and *P. tonganus* (Storch, 1968), the m. massetericus (both its *pars superficialis et profunda*) inserts on the inconspicuous masseteric line, the crest that accompanies the outline of the angular process. The smooth medial surface of the ramus is divided into two areas (which correspond to the areas on the lateral surface) by a low crest that is the medial counterpart of the lateral condylar crest. Immediately ventral to the crest in the middle of the ramus is the posteriorly directed mandibular foramen. A large sulcus emanates from the foramen caudally. The mandibular canal (*canalis mandibulae*) can be seen through the relatively transparent bone from the mandibular foramen to the level of the p3–p4 embrasure, running nearly parallel and close to the ventral border of the mandibular body. The *m. temporalis* (*pars profunda* and *superficialis*) and *m. pterygoideus medialis* and *lateralis* insert on the medial side of the ramus (Storch, 1968). Based on the fetus, the m. pterygoideus lateralis inserts onto the medial aspect of the mandibular condyle immediately below the articular surface (fig. 32). On CM 87973, this attachment area is not clearly delimited from the surrounding bone, although there is some rugosity just below the lip of the articular surface. The insertion of the m. pterygoideus medialis is on the mandibular angle, again with no clear delimitation of the attachment region visible on the bone of the mandible. It should be noted that the inferior alveolar nerve and vessels reach the mandibular foramen by traveling between the m. pterygoideus medialis and m. pterygoideus lateralis (fig. 32).

POSTERIOR BRANCHIAL SKELETON

Hyoid Apparatus

The tongue and the larynx are suspended from the skull by the hyoid apparatus (*apparatus hyoideus*), a derivative of the second and partially the third pharyngeal

arches (*arcus pharyngeus secundus et tertius*; Nomina Embriologica Veterinaria, 1994 [hereafter NEV]). In general aspect (fig. 19), the hyoid apparatus is formed by a short transverse bar from which two long, hornlike structures arise bilaterally, one roughly dorsocaudolateral in position, whose proximal end attaches to skull in the ear region (the anterior cornu or hyoid arch), and one caudolateral, which articulates with the laryngeal cartilages (the posterior cornu, formed by a single element, the thyrohyoid, which is derived from the third branchial arch). Specifically, the hyoid apparatus is composed of six elements: the single basihyoid (*basihyoideum*) and the paired thyrohyoid (*thyrohyoideum*), ceratohyoid (*ceratohyoideum*), epihyoid (*epihyoideum*), stylohyoid (*stylohyoideum*), and tympanohyoid (*tympanohyoideum*). In Megachiroptera, the basihyoid is fused to the thyrohyoids, and the stylohyoid is not ossified proximally so it does not contact the tympanohyoid (tympanohyal); the remaining elements are all ossified and are connected by minute synovial joints (Sprague, 1943). These joints may fuse in adults of some forms, except the joint between the basi- and ceratohyoid, which generally remains a synovium in megachiropterans (Sprague, 1943).

Based on *Rousettus* (Jurgens, 1963), the basihyoid and thyrohyoids are continuous already in the embryo. The basihyoid component of this unit is an ossification of the basihyoid cartilage (*cartilago basihyoidea*, a composite originated in the *pars ventralis* of both the second and third branchial arches). It is a transverse bar that widens laterally toward the articulation with the ceratohyoid (see fig. 19 and below). The basihyoid is roughly cylindrical in shape, slightly bowed, and depressed dorsoventrally. The basihyoid contacts the ceratohyoid through an elliptical synchondrosis located in the rostrolateral angle of the basihyoid. The thyrohyoid (also termed *cornu branchiale* [Jurgens, 1963] and *cornu majus* [NAV]) is an ossification of the thyrohyoid cartilage (*cartilago thyrohyoidea*) of the pars ventralis of the third branchial arch (first branchial arch in Sprague's [1943] terminology). The thyrohyoids project caudolaterally from the basihyoid as slender elements twice as long as the transverse dimension of the basihyoid. In dorsal view, the thyrohyoids significantly diverge caudally; in lateral view, they form a pronounced inverted arch with almost perfect curvature. Each thyrohyoid is laterally compressed, and its caudal half forms a flange that is slightly deflected laterally. The rounded distal end of the thyrohyoid is the hyoid component of the thyrohyoid articulation (*articulatio thyrohyoidea*). In USNM 566608, a cap of cartilage is present in the proximal end (i.e., the end opposite to the basihyoid).

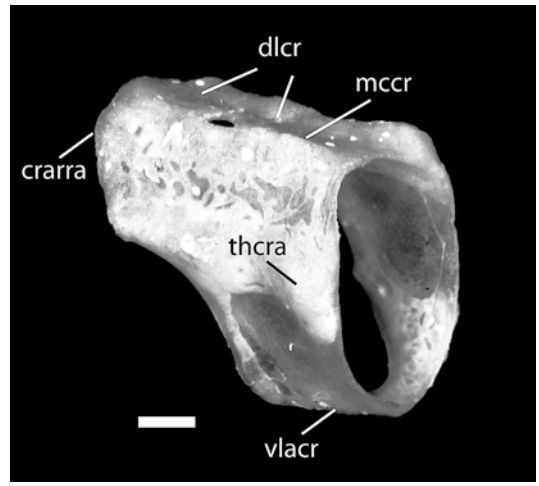

Fig. 20. *Pteropus tonganus* USNM 546610, oblique caudodorsolateral view of the cricoid cartilage. Scale = 1 mm. Abbreviations: **crarra** cricoarytenoid articulation; **dlcr** dorsal lamina of cricoid; **mccr** median crest of cricoid; **thcra** thyrocricoid articulation; **vlacr** ventrolateral arc of cricoid.

The ceratohyoid (also termed *cornu minus* in the NAV) is an ossification of the ceratohyoid cartilage (*cartilago ceratohyoidea*) of the pars ventralis of the second branchial arch (hyoid arch of Sprague [1943] and Jurgens [1963]). It is a short and flat piece that links the basihyoid with the proximal elements that suspend the hyoid apparatus from the skull (fig. 19). The ceratohyoid exhibits an apparent bending, because the major axes of its two elliptical synchondroses in the opposite ends of the bone are oriented differently: the distal synchondrosis (connecting with the basihyoid) faces medially, whereas the proximal

synchondrosis (connecting with the epihyoid) faces caudodorsally. The ventrolateral angle is free, wide, and rounded. There exists a fundamental difference with respect to the ceratohyoid of the dog, as illustrated by Evans (1993: figs. 4–40, 4–41). In the dog, the proximal end of the ceratohyoid is directed almost cranially and meets the epihyoid at a right angle. In *Pteropus*, the ceratohyoid is aligned with the epihyoid and stylohyoid in the dorsocaudolateral direction.

The epihyoid is an ossification of the epihyoid cartilage (*cartilago epihyoidea*) of the pars dorsalis of the second branchial arch (Reichert's cartilage). It is a simple, slender rod that contacts the ceratohyoid distally and the stylohyoid proximally (fig. 19). Its section is roughly circular, although a slight ventral ridge is present. The epihyoid exhibits an apparent torsion, because the oval-shaped synchondroses are oriented differently: the major axis of the distal synchondrosis is horizontal, whereas its counterpart in the proximal synchondrosis is vertical.

The stylohyoid is an ossification of the stylohyoid cartilage (*cartilago stylohyoidea*) of the pars dorsalis of the second branchial arch. It is incompletely ossified in Megachiroptera, as is also the case in our specimens. The stylohyoid is a laterally compressed, short bar that shows an unreduced synchondrosis in its distal end, and a free proximal end (fig. 19). Thus, the bony contact with the tympanohyoid is lost, as in all megachiropterans—the discreto-cornuate condition of Sprague (1963), as opposed to the integrocornuate condition found in Microchiroptera (and many other mammals), in which all elements of the anterior cornu are ossified and the stylohyoid articulates with the tympanohyoid. In *Rousettus*, the tympanostyloid ligament connects the tympanohyoid and the stylohyoid (Jurgens, 1963; Sprague, 1943), but such a ligament was not found in *Pteropus* (Sprague, 1943). The structure and location of the tympanohyoid have been described in the tympanic view of the petrosal, because this element remains attached (and may be fused) to the crista parotica in many specimens. The tympanohyoid forms a joint with the petrosal (*articulatio temporohyoidea*), which serves to suspend the hyoid apparatus and larynx from the skull in forms in which the proximal anterior cornu is completely ossified (e.g., microchiropterans).

In our limited sample, there is no obvious difference between species and sexes in the structure and relative size of elements in the hyoid apparatus of *Pteropus tonganus* (USNM 566608, subadult female, and USNM 566610, subadult male) and *Pteropus dasymallus* (FMNH 14052, adult female, and FMNH 140650, adult male). The hyoid apparatus is structurally similar but larger and markedly more robust in *Pteropus giganteus* (FMNH 57661, adult female). An additional difference found in *P. giganteus* is the presence of a tubercle in the ventralmost point of the arch of the thyrohyoid, probably an attachment point of at least the *m. thyrohyoideus*.

Larynx

The four component elements of the larynx are the single epiglottic cartilage (*cartilago epiglottica*, missing in our specimens), thyroid cartilage (*cartilago thyroidea*), and cricoid cartilage (*cartilago cricoidea*) and the paired arytenoid cartilage (*cartilago arytenoidea*). These cartilages belong to the *partes ventrales* of the last three branchial arches (*arcus pharyngeus quartus, quintus, et sextus*; NEV). The basihyoid + thyrohyoid, and the thyroid and cricoid cartilages form a telescopic arrangement of movable pieces, each of which fits within the space of the next and therefore reduces the diameter of the laryngeal orifice caudally (see Jurgens, 1963: fig. 13). In USNM 566608, the inner distance between the caudal ends of the left and right thyrohyoids is 7.4 mm; the inner distance between the left and right caudal cornua (see below) of the thyroid cartilage is 3.7 mm; and finally the minor (horizontal) axis of the inner ring of the cricoid cartilage is 2.9 mm. The thyroid and cricoid elements, as well as the tracheal rings, are ossified in adult *Pteropus* (Sprague, 1943).

The thyroid is a trough-shaped structure that fits within the space between the thyrohyoids and articulates with them cranially (fig. 19). The thyroid is formed by right and left laminae (*lamina dextra et sinistra*) united ventrally (fig. 19). Dorsally, the

lamina projects the rostral and caudal cornua (*cornu rostralis et caudalis*). The thin rostral cornu is the thyroid component of the thyrohyoid articulation, and it is noticeably expanded toward the joint (cranially). An ample rostral thyroid notch (*incisura thyroidea rostralis*) excavates ventral to the cornu at the expense of the cranial edge of the lamina. The caudal cornu is comparatively shorter and less expanded distally. A correspondingly less pronounced caudal thyroid notch (*incisura thyroidea caudalis*) is present in the caudal margin of the lamina. The end of the caudal cornu is the thyroid component of the cricothyroid articulation (*articulatio cricothyroidea*). In dorsal view, the dorsal margin of the laminae diverges cranially to meet the thyrohyoids. In lateral view, the laminae slightly reduce their width ventrally. The middle part where the laminae meet is projected cranially and approximately follows the curvature of the caudomedial margin of the basihyoid + thyrohyoid (in its postmortem position, the thyroid and the basihyoid + thyrohyoids are separated by approximately 1 mm). In the dog, the cranioventral and caudoventral margins of the thyroid exhibit a laryngeal prominence (*prominentia laryngea*) and a thyroid fissure (*fissura thyroidea*), respectively. In our *Pteropus* specimens, the former is absent, but a conspicuous thyroid fissure is present (fig. 19). Both the medial and lateral surfaces of the laminae are smooth.

The cricoid is a complete ring that fits within the space between the thyroid laminae; it is formed by a dorsal lamina (*lamina cartilaginis cricoideae*) and a ventrolateral arch (*arcus cartilaginis cricoideae*; fig. 20). The lamina is about 5 mm long, with caudal and lateral margins chiefly straight and parallel, and a triangular cranial margin. On the side of this triangle is the indistinct facet of the cricoid component of the cricoarytenoid articulation (*articulatio cricoarytenoidea*). The dorsal surface of the lamina is divided by an irregular median crest (*crista mediana*), and the sides are inclined ventrolaterally as a two-sided roof. The cricoid component of the cricothyroid articulation is a marked tubercle in the caudolateral angle of the lamina. Immediately cranial to it, the lateral margin of the lamina is inflected medially and then continues cranially in the lateral crest, which neatly separates the lamina from the arch. The latter is ventrally no wider than 1 mm. In lateral view, the caudal margin of the arch is roughly vertical, so the cranial edge of the arch is comparatively much longer than the caudal margin, and reaches the cranial edge of the lamina describing a gentle sigmoid line. The cranial margin of the arch is slightly enlarged as a lip. The arch is significantly thinner and becomes translucent in its lateral surface. The caudal margin of the arch connects via ligaments to the first tracheal ring.

The paired arytenoid cartilage is a small element confined to the articular area of the craniolateral facet of the cricoid lamina, in the craniodorsal region of the cricoid. The arytenoid cartilage of *Pteropus* is greatly simplified in comparison with the cartilage of the dog. In *Pteropus*, it exhibits three delicate processes that emerge from a poorly defined body and are oriented in different directions. The process located dorsally is the longest and thinnest, and is craniocaudally compressed, and its dorsal end forms the first (dorsomedial) of two points of contact of the arytenoid cartilage with the cricoid. The other two processes are similar in shape, much shorter than the dorsal, each tapering to a round point. The ventrocaudal process is the second contact with the cricoid. The cranioventral process is free. The whole arytenoid cartilage is curved such that it follows the outline of the laryngeal orifice.

INTERNAL SURFACES OF THE SKULL

Nasal Surface

The *facies interna* of the nasal is the roof of the nasal meatuses. It is a featureless surface, slightly concave, with subparallel margins that are slightly curved ventrally. The ventral view of the nasal generally follows the external shape of the bone; that is, it has a straight medial border and a gently bowed lateral border. The caudal portion of the bone, which is not entirely visible externally because it is overlapped dorsally by the maxilla in the nasomaxillary suture, overlaps in turn the frontal in the frontonasal suture,

expanding laterally into a triangular wedge of very thin bone.

Additionally, the isolated nasal preserves the internal surfaces of two squamous sutures, the nasoincisive and nasomaxillary sutures, and one thin plane suture, the internasal suture. The first two sutures are coalesced anteriorly in the nasal. The surface of overlap forms a lateral shelf on the nasal separated from the externally visible medial part by a sharp longitudinal line, corresponding to the external outline of the two sutures. The internal surface of the internasal suture forms a low, slightly rugose ridge—the septal process (*processus septalis*)—of constant size throughout the anterior four-fifths of the nasal length. There is no nasoethmoidal crest or fossa, because the nasal does not contact the ethmoid.

Premaxillary Surface

The internal surface of the premaxilla is gently concave and generally smooth. The caudal edge of the premaxilla corresponds to the premaxillary part of the maxilloincisive suture. The maxilla overlaps the premaxilla in the ventral half of this suture, and the opposite is true for the dorsal part. In the ventral part, the suture exhibits a low ridge caudally and a shallow groove laterally. The surface of the groove is rugose and is penetrated by two alveolar foramina that connect directly with the large and conical alveoli of the two upper incisors (see alveolar canal below). The foramina are close together in the dorsal portion of the groove, with the dorsal foramen larger than the ventral foramen. The former supplies the alveolus of I1 and the latter the alveolus of I2. The openings of the alveoli are subequal in size, circular in outline, and separated by a thin but firm wall of bone. The depth of the alveoli can be determined from external examination because the bone is very thin. The alveolus of I1 extends half the length of the entire premaxilla, whereas the alveolus of I2 does not surpass a third of that length. A pair of very subtle juga is observable in association with the alveoli on the internal surface of the premaxilla. Ventrally on the internal surface, a small depression is present in the space between the two alveoli. The internal surface of the intermaxillary suture is roughly rectangular, higher than wide, presenting a slightly rugose surface.

The dorsal part of the maxilloincisive suture is suggested, in the premaxilla, by a change in coloration of bone in the overlap area (but see the maxillary counterpart below). In the nasoincisive suture, the nasal is laterally overlapped by the premaxilla, but the extension of this overlap is very limited; it shows as a very subtle thinning of the dorsal margin of the premaxilla.

Maxillary Surfaces

In *Pteropus livingstonii* AMNH 274466, the ventral nasal concha is firmly attached to the medial surface of the maxilla, precluding examination of some structures in medial view. The ventral nasal concha was missing from *P. livingstonii* AMNH 274515, thus exposing the medial surface of the maxilla. Both specimens were used for the description of this region (fig. 21A, B).

The *facies nasalis* of the maxilla is essentially a medial concave surface with one transverse shelf, the palatine process. The latter meets the medial surface of the maxillary body, a medially inclined wall to which the ventral nasal concha attaches medially through a long conchal crest (*crista conchalis*). The internal surfaces of the right and left maxillae contain the nasal meatuses, and the ventral nasal concha divides the nasal meatus into three distinct spaces. These divisions are the common nasal meatus (*meatus nasi communis*), medial to the conchal lamina, the dorsal nasal meatus (*meatus nasi dorsalis*), dorsal to the conchal crest (further separated by the rostral process of the ethmoturbinal from another space ventral to it, the middle nasal meatus or *meatus nasi medius*), and the ventral nasal meatus (*meatus nasi ventralis*), ventral to the conchal crest. The most conspicuous features of the facies nasalis (see details below) include the nasolacrimal canal, the alveolar canal, the internal jugum of the canine, and the wide dorsal lamina that is part of the squamous sutures with the nasal, lacrimal, and frontal.

In the midsagittal plane, two sutures are present: the plane intermaxillary suture and, dorsal to it, the vomeromaxillary suture

(*sutura vomeromaxillaris*). The latter runs along the entire length of the intermaxillary suture, decreasing its dorsal development caudally. The dorsal surface of the palatine process is horizontal, generally smooth, and meets the maxillary body laterally in a gently concave surface that rolls to meet the conchal crest dorsally. A tiny foramen is present bilaterally in this surface at the level of the posterior root of P4, 1 mm lateral to the midsagittal plane. The concave caudal edge of the palatine surface is notched for the opening of the major palatine foramen.

The conchal crest extends from the rostral edge of the maxilla to approximately the level of the anterior root of P4. In medial view, the crest is gently convex dorsally and protrudes medially ca. 1 mm. The alveolar canal (incisivomaxillary canal of the dog, *canalis maxilloincisivus*) runs immediately dorsal to the crest in the substance of the maxilla. This canal supplies the alveoli of the premolars, the canine, and finally the incisors (unlike the dog, the alveolar canal also supplies the root of P4 in *Pteropus*). It opens caudally in a small, round foramen located medial to the maxillary foramen, just above the anterior (dorsally open) root of M1 (fig. 12). In our sample, the alveoli of the two roots of P3 and the single root of the canine are perforated by multiple alveolar foramina, whereas the alveoli of each of the two roots of P4, M1, and M2 open through a single foramen. The course of the alveolar canal is visible externally in several specimens of *P. lylei*, particularly AMNH 237595 (see fig. 39). In this specimen, the alveolar canal follows a curved rostrodorsal path, caudally convex, from the anterior M1 root medial to the infraorbital canal to near the canine root. This latter point is horizontally at the level of the lacrimal foramen and vertically at the level of the anterior root of P3.

One very conspicuous feature of the *facies nasalis* is the nasolacrimal canal (*canalis lacrimalis*). Preceded caudally by a wide *sulcus lacrimalis*, the nasolacrimal canal opens caudally at the level of the posterior root of P3, and slightly ventral to the middle of the facies nasalis dorsal to the conchal crest (fig. 21B). The opening itself is rather irregular and leads to an oblique intramaxillary course that crosses the conchal crest. The nasolacrimal canal opens in the ventral nasal meatus at the level of the P1–P3 embrasure. The course of the nasolacrimal canal is marked as a subtle relief in the facies nasalis. More conspicuous, the internal canine jugum is visible on the facies nasalis both dorsal and ventral to the conchal crest.

The dorsal margin of the maxilla is dominated by the wide nasomaxillary suture (fig. 21). The thin lamina by which the maxilla overlaps the lateral margin of the nasal increases its dorsal extension caudally to form the frontal process of the maxilla (*processus frontalis*), the maxillary component of the frontomaxillary suture. This process, which in the intact skulls lies between the caudolateral angle of the nasal and the lacrimal, is truncated caudally and leads ventrally to the wide, concave notch into which the lacrimal fits. Following this notch to its caudal end and immediately dorsal to the infraorbital canal is a triangular platform on which the lacrimal rests. Just medial and ventral to this platform for the lacrimal, as well as medial to the infraorbital and alveolar canals, is a thin and irregular sheet of bone that is the maxillary part of the ethmoidomaxillary suture (*sutura ethmoidomaxillaris*).

The rostral margin of the maxilla is entirely occupied by the maxilloincisive suture. The premaxilla fits in the deeply incised maxillary margin and is overlapped by the maxilla both medially and laterally. The rostral opening of the alveolar canal is in the middle of the suture and appears as a faint, ventrally directed sulcus. This canal divides within the substance of the maxilloincisive suture, appearing as a double canal (the division leading to each of the two incisor alveoli) on the premaxillary surface of the suture. The caudal edge of the facies nasalis is deeply concave, forming the perpendicular portion of the palatomaxillary suture.

The ventral nasal concha is an elongated vertical lamina of porous bone attached laterally to the conchal crest (fig. 21A; see also fig. 4). The shape of the concha is complex, but it can be described basically as a lamina from which four short folds arise. One fold is in the dorsal edge, as it scrolls laterally and then ventrally. The fold of the ventral edge is double, with one lamina

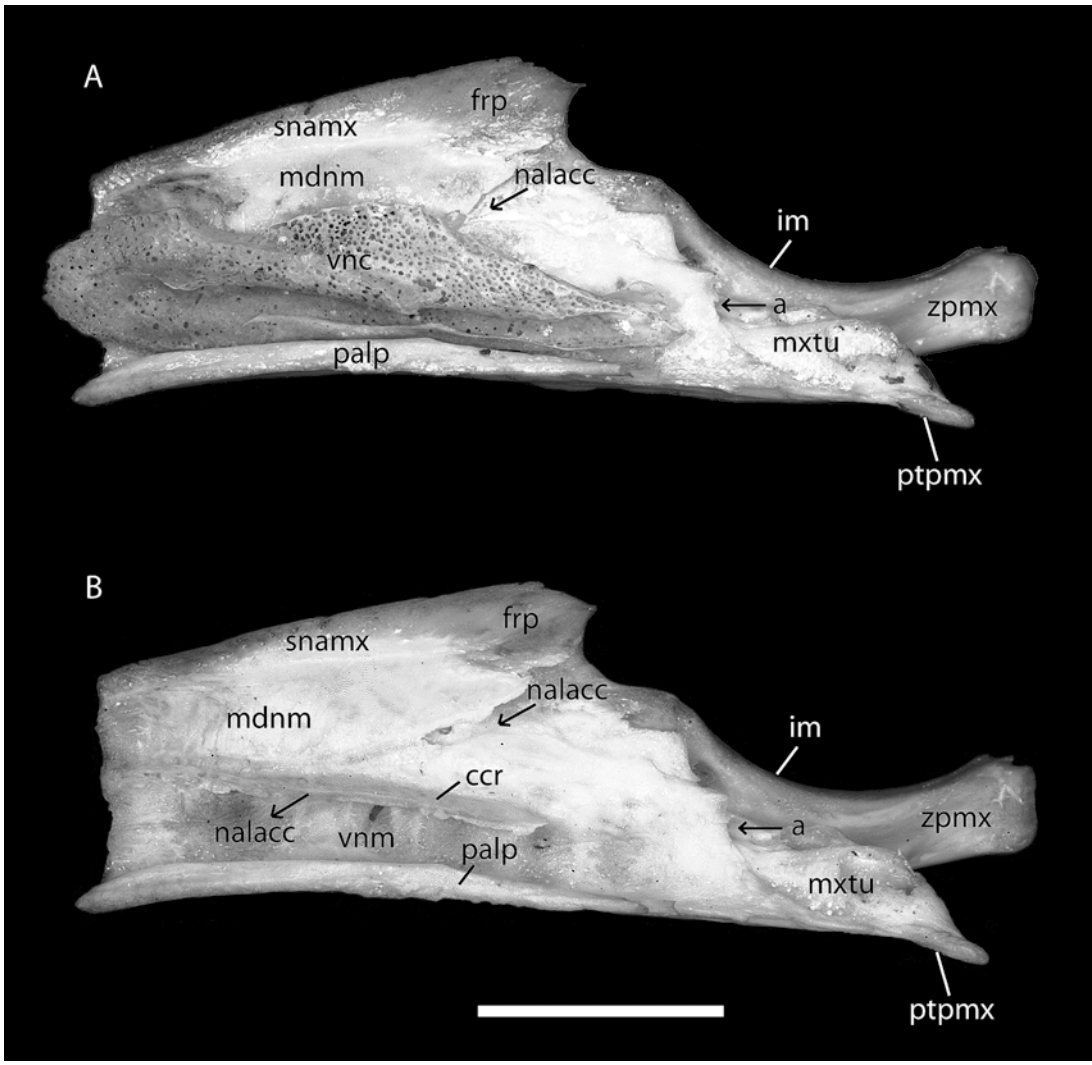

Fig. 21. *Pteropus livingstonii*, medial view of the internal surface (facies interna) of the disarticulated right maxilla of AMNH 274466 with the ventral nasal concha (**vnc**) in place (**A**), and the disarticulated right maxilla of AMNH 274515 with the ventral nasal concha removed (**B**). Arrow labeled **a** indicates the caudal opening of the infraorbital canal (not visible). Arrows labeled **nalacc** indicate the caudal and rostral openings of the intramaxillary course of the nasolacrimal canal. Abbreviations: **ccr** conchal crest of maxilla; **frp** frontal process of maxilla; **im** infraorbital margin; **M2** second upper molar; **mdnm** middle dorsal nasal meatus; **mxtu** maxillary tuberosity; **nalacc** nasolacrimal canal; **palp** palatine process of maxilla; **ptpmx** pterygoid process of maxilla; **snamx** sutura nasomaxillaris; **vnc** ventral nasal concha; **vnm** ventral nasal meatus; **zpmx** zygomatic process of maxilla.

projecting laterally and dorsally, and another lamina projecting medially and then dorsally. The last fold arises from the middle of the concha on the medial side, and scrolls ventrally, leaving a deep excavation in the ventral part of the concha. In medial view, the concha is cigar-shaped. The rostral edge is triangular, with a vertex pointing rostrally. The ventral edge is slightly convex, and it folds laterally and dorsally in the caudal two-thirds of the conchal length. The dorsal edge presents a conspicuous concavity in the

rostral third. From the rostral edge of this concavity, a groove arises and crosses the medial surface obliquely in a caudoventral direction to the middle of the concha. The surface dorsal and caudal to this groove is flat and more lateral than the surface rostral and ventral to this groove. In this dorsal recess fits the rostral process of the ethmoturbinal, which lies caudal, medial, and slightly dorsal to the ventral nasal concha. After the mentioned concavity, the dorsal margin of the ventral nasal concha is convex, then it descends gently throughout the caudal extension of the concha to meet the caudal end of the bone at the level of the ventral margin. A deep, longitudinal groove excavates the medial surface of the concha between the scroll of the ventral margin and the midline, approximately at the level of the lateral attachment to the conchal crest. The dorsal edge of that groove forms the medial midline fold, whose border is altered by a continuation of the oblique groove for the dorsal concha in the form of a ventral tip. The caudal end of the ventral nasal concha exhibits a distinct caudolateral flange. The lateral view of the ventral nasal concha is not available to direct examination, but it can be inferred from the presence of the conchal crest and the development of the dorsal and ventral folds.

Palatine Surface

In the isolated palatine bone, the surfaces of the nasopharyngeal meatus (*facies nasalis*) and the large, squamous frontopalatine suture in the perpendicular process are the most salient internal features (fig. 22). The left and right portions of the nasopharyngeal meatus, each contained in an individual palatine bone, are each oval in outline with the medial side open and communicating with the corresponding portion in the other palatine. Medially and ventrally, the nasopharyngeal meatus is bounded by the nasal crest, which decreases in height rostrally. The articular surface of the nasal crest, or interpalatine suture, is very rugose. Medially and dorsally, the meatus is bounded by the thin sphenoethmoid lamina (*lamina sphenoethmoidalis*). Anteriorly, this lamina forms a medial flange partially roofing the meatus, decreasing its width rostrally. The meatus itself is a smooth tube that gradually funnels caudally into the choanae. Near the rostral end of the palatine is the opening of the sphenopalatine foramen. The crescent-shaped space between the sphenopalatine foramen and the rostral edge of the palatine is the palatine contribution to the maxillary recess (*recessus maxillaris*). The recess is limited ventrally by the ethmoidal crest (*crista ethmoidalis*), a low, rostrally concave ridge connecting the sphenopalatine foramen with the rostroventral angle of the nasopharyngeal meatus. One (left side) or two (right side) extra, smaller openings of the sphenopalatine foramen are present caudal to the main foramen in AMNH 274466 (all of them open to the lateral side of the perpendicular lamina; cf. CM 87972, 87973). Dorsal to the sphenoethmoid lamina, and oriented at a right angle to it, is the palatine contribution to the frontopalatine suture. Through this thin lamina, the palatine overlaps the pars orbitalis of the frontal bone in the frontopalatine suture laterally and also contacts the ethmoid medially in the palatoethmoidal suture (*sutura palatoethmoidalis*). Consequently, the frontal and ethmoid fit in the space between the sphenoethmoid lamina and the dorsal portion of the perpendicular lamina, unlike the dog, in which the contact is with the vomer and not with the ethmoid. This difference results from the reduced wings of the vomer in *Pteropus* (see below).

The rostral end of the palatine, not visible externally, is truncated and formed by the very thin bone of the squamous palatomaxillary suture (fig. 22). Here the palatine is overlapped widely by the maxilla laterally. The rostral external surface of the isolated palatine shows a deep wedge accommodating two connected parts of the maxilla: the caudal part of the palatine process of the maxilla medial to the maxillary tuberosity, and the pterygoid process of the maxilla. Just medial to this area, on the ventral side, is the exposed course of the palatine canal, which opens through the major palatine foramen in the palatine side of the palatomaxillary suture.

The caudal sphenoidal process (*processus sphenoidalis*) contributes to the ectopterygoid process (fig. 10). The sphenoidal process

shows two deep concavities where the other two components of the ectopterygoid process fit: dorsolaterally is a larger, teardrop-shaped surface for the articulation of the alisphenoid contribution to the ectopterygoid process, and ventromedially is a smaller surface for the articulation of the pterygoid. The two surfaces are separated caudally by a thin and sharp lamina of bone.

Fronto-Ethmoidal Surfaces

The frontal, ethmoid, and vomer are solidly fused in the disarticulated specimens of *Pteropus livingstonii* available for examination (figs. 23, 24A, B). Based on AMNH 274466, two distinct internal surfaces can be distinguished. One surface is dorsocaudal, comprising the inner table of the frontal (*facies interna*) and the cribriform plate of the ethmoid (*lamina cribrosa*; fig. 23). The other surface (fig. 24) is ventrolateral and rostral, comprising the ventral surface of the vomer, the rostroventral and partially lateral surfaces of the ethmoid (pleurethmoid of Jurgens, 1963), and the rostral process of the ethmoturbinal (anterior tip of ethmoturbinal of Jurgens, 1963).

The facies interna of the frontal roofs the rostral cranial fossa (*fossa cranii rostralis*) and provides the dorsal and lateral (orbital) walls of the ethmoidal fossae (*fossae ethmoidales*), the space immediately posterodorsal to the cribriform plate (fig. 23). The facies interna of the frontal is a cup-shaped surface. A faint trace of cerebral juga corresponds to the bilateral mark left by the longitudinal fissure of the brain, which is reproduced in the facies interna as two rostrally divergent curved lines, separated caudally by 1 mm and rostrally by ca. 4 mm. The circular border of the postorbital area of the frontal bone is rather irregular. In dorsal view, the extent of the parietal overlap, through its wedge-shaped frontal process of the parietal, becomes evident in the disarticulated skull. The exposed forehead is limited to the median rectangular space marked bilaterally by a groove parallel to the sagittal plane at the level of the postorbital foramen. The caudal margin shows a frontoparietal suture that is part plane and part squamous. In the mid-sagittal line, a wedge-shaped medial process of the caudal margin of the frontal fits into a complementary recess of the rostral border of the parietal (the plane segment of the frontoparietal suture). Lateral to this suture, the frontal slightly overlaps the parietal via a bilateral wedge-shaped process of its caudal border (the squamous segment of the frontoparietal suture).

Rostral to the rostral cranial fossa are the bilateral ethmoidal fossae, each containing an olfactory bulb (*bulbus olfactorius*). In caudal view (fig. 23), the fossae form an ample space, twice as high as wide, with rounded corners and slightly narrower ventrally. This space is ill-defined as two chambers, corresponding to each ethmoidal fossa, with the division marked by a crest in the dorsal wall (contributed by the frontal) and by a low *crista galli* in the rostral wall, the cribriform plate of the ethmoid (*lamina cribrosa*). The thin and low crista galli is the dorsalmost part of the perpendicular lamina of the ethmoid (*lamina perpendicularis*), which forms the osseous nasal septum (*septum nasi osseum*). The cribriform plate is inclined so that the dorsal edge is rostral with respect to the ventral edge. The plate exhibits numerous perforations, the cribriform foramina (*foramina laminae cribrosae*), for the passage of bundles of the olfactory nerves (*nn. olfactorii*). The cribriform foramina are organized into tracts whose positions are, based on a partially damaged specimen of *Pteropus livingstonii* (AMNH 274515), related to the attachment of turbinates on the rostral side of the cribriform plate. In *P. livingstonii* AMNH 274466, the cribriform foramina are grouped into two columns, medial and lateral, within each ethmoidal fossa (fig. 23). The medial column consists of four irregular groups. The dorsal group is the largest and consists of one principal perforation with a bilaterally variable number of very small perforations, especially in the walls of the main foramen as they sink into the ethmoidal labyrinth (*labyrinthus ethmoidalis*). The same pattern is found in the other main foramina of the medial column, which are more closely associated among themselves. In the dorsolateral angle of the ethmoidal fossa is a group of two (right side) to four (left side) main foramina surrounded by some smaller perforations. Immediately

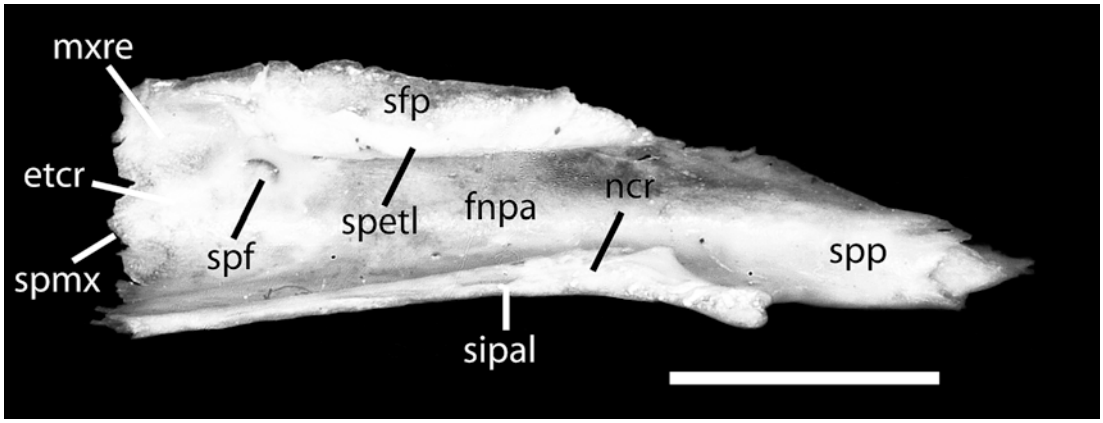

Fig. 22. *Pteropus livingstonii* AMNH 274466, medial view of the internal surface of the palatine. Scale = 5 mm. Abbreviations: **etcr** ethmoidal crest of palatine; **fnpa** facies nasalis of palatine; **mxre** maxillary recess; **ncr** nasal crest of palatine; **sfp** sutura frontopalatina; **sipal** sutura interpalatina; **spetl** sphenoethmoid lamina; **spf** sphenopalatine foramen; **spmx** sutura palatomaxillaris; **spp** sphenoidal process of palatine.

ventral to these is the lateral series of cribriform foramina. These are grouped into five clusters of one or two larger foramina accompanied by smaller perforations, located close to the lateral edge of the cribriform plate. The left and right ventralmost groups of foramina are placed closer to the crista galli. The bone between the medial and lateral columns of foramina, as wide as one of those columns, is perforated occasionally and irregularly by small foramina, but it is essentially solid. The lateral walls of the ethmoidal fossae are smooth, presenting a wide ethmoidal notch (the ethmoidal foramen in the articulated skull, with its caudal concavity closed by the orbitosphenoid). Finally, the dorsal aspect of the ethmoidal fossae is biconcave, formed by two elongated domes separated by the low frontal crest (*crista frontalis*). The morphology of the cribriform plate of *P. livingstonii* (this study, fig. 23) is very similar in every respect to the morphology reported by Bhatnagar and Kallen (1974) for *Pteropus giganteus* (see their plate 1, fig. 8, p. 85).

The ventral surface of the frontoethmoidal complex includes the vomer (medially and rostrally), the ventral surface of the ethmoid (*lamina basalis*, caudolaterally), and the ventral surface of the rostral process of the ethmoturbinal (laterally and rostrally; fig. 24B). In the disarticulated skull, the vomer is fully exposed in ventral view. As long as half the skull length, the vomer extends from the incisive fissure to the sphenoidal sinus. Both ends (the incisive and sphenoidal incisures) are visible externally and, therefore, are described above (see Vomer). Ventrally, the vomer exhibits a paired wing (*ala vomeris*) in the caudal third of its length (only partially visible externally), each separated medially by a longitudinal crest (*crista vomeris*). The wings are very narrow, ca. 1 mm wide throughout their length. The suture with the ethmoid (*sutura vomeroethmoidalis*) is almost straight and barely visible. These alae vomeris are continuous caudally with the bifid ends of the sphenoidal incisure. Due to their narrow width, the alae form only the medial part of the roof of the nasopharyngeal meatus immediately rostral to the choanae. The lateral part of the roof is contributed by the ventral surface of the ethmoid (the pleurethmoid of Jurgens, 1963). The ventral surface of the ethmoid is smooth and thin, and has a roughly rhomboidal shape, with the vomer in the midline, and four borders (two caudolateral and two rostrolateral). The truncated caudal edge of the ethmoid forms the rostral edge of the sphenoidal sinus, which in ventral view appears as a paired notch lateral to the caudal edge of the vomer. Through the rostral opening of the sphenoidal sinus, the nasal septum is visible. In close

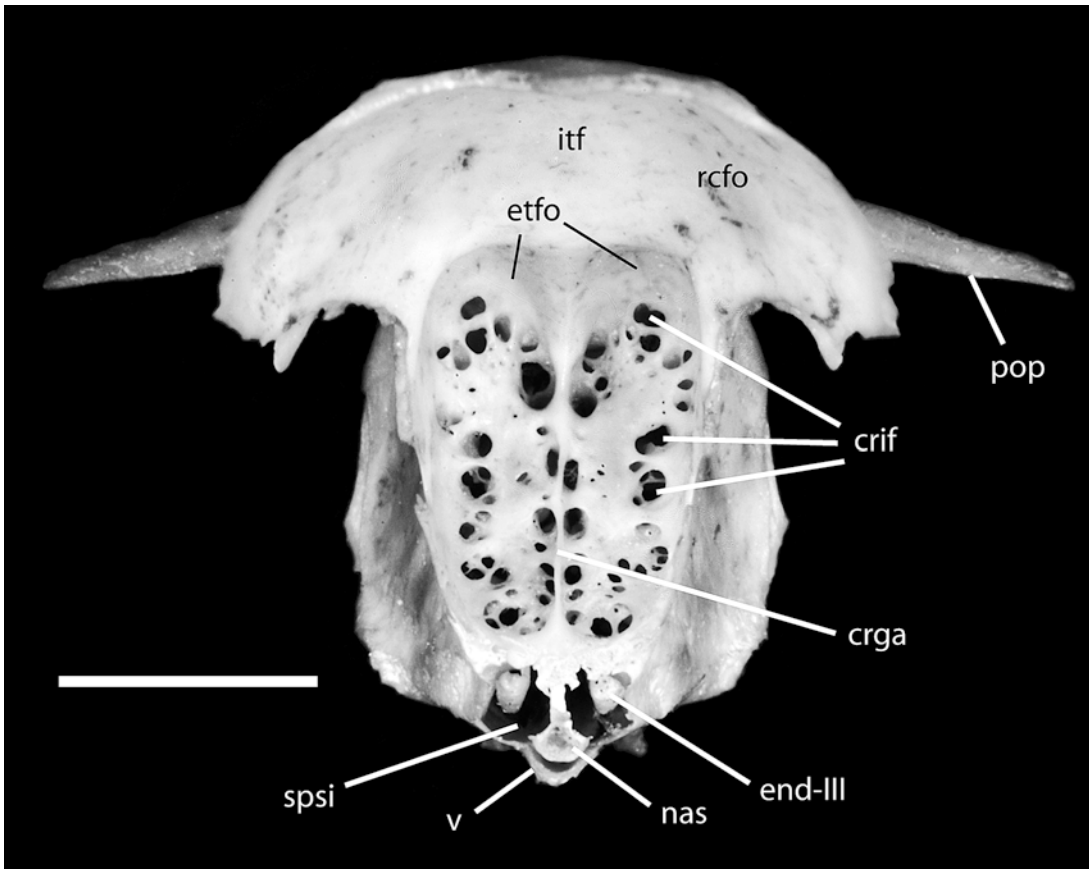

Fig. 23. *Pteropus livingstonii* AMNH 274466, caudal view of the frontoethmoidal complex showing the cribriform plate. Scale = 5 mm. Abbreviations: **crga** crista galli; **crif** cribriform foramina; **end-III** endoturbinate III; **etfo** ethmoidal fossa; **itf** inner table of frontal; **nas** nasal septum (mesethmoid); **pop** postorbital process; **rcfo** rostral cranial fossa; **spsi** sphenoidal sinus; **v** vomer.

examination, traces of the suture between the nasal septum (perpendicular plate, *lamina perpendicularis*) and the cribriform plate are visible. The caudal view of the sphenoidal sinus, on the sides of the nasal septum, shows two rostrocaudally elongated scrolls attached dorsally to the ethmoid, with its ventral border folding laterally (fig. 23). Based on *Rousettus* (Jurgens, 1963), these are endoturbinates (or primary ethmoturbinals; *endoturbinalia*), specifically endoturbinate III. The *labyrinthus ethmoidalis* of *Rousettus* exhibits one ectoturbinate and three endoturbinates, all of which are bilaminar, and a well-developed *crista semicircularis* that arises from the *tectum nasi* close to the nasal septum (Jurgens, 1963). Based on a partially damaged specimen of *Pteropus livingstonii* (AMNH 274515), we were able to preliminarily confirm a similar composition and configuration of ethmoidal elements in *Pteropus*, but a detailed anatomical description of the labyrinth requires further study.

In the caudolateral border is the frontoethmoidal suture, in which the dorsolateral component contributed by the frontal and the medioventral component contributed by the ethmoid meet at an almost right angle. The frontoethmoidal suture is incomplete in sealing the caudolateral border, leaving a cleft that is larger on the right side in AMNH 274466. The rostrolateral border of the ethmoid exhibits a ventral process from the lateral lamina of the ethmoid and the fused base of the rostral process of the ethmoturbinal medially (fig. 24).

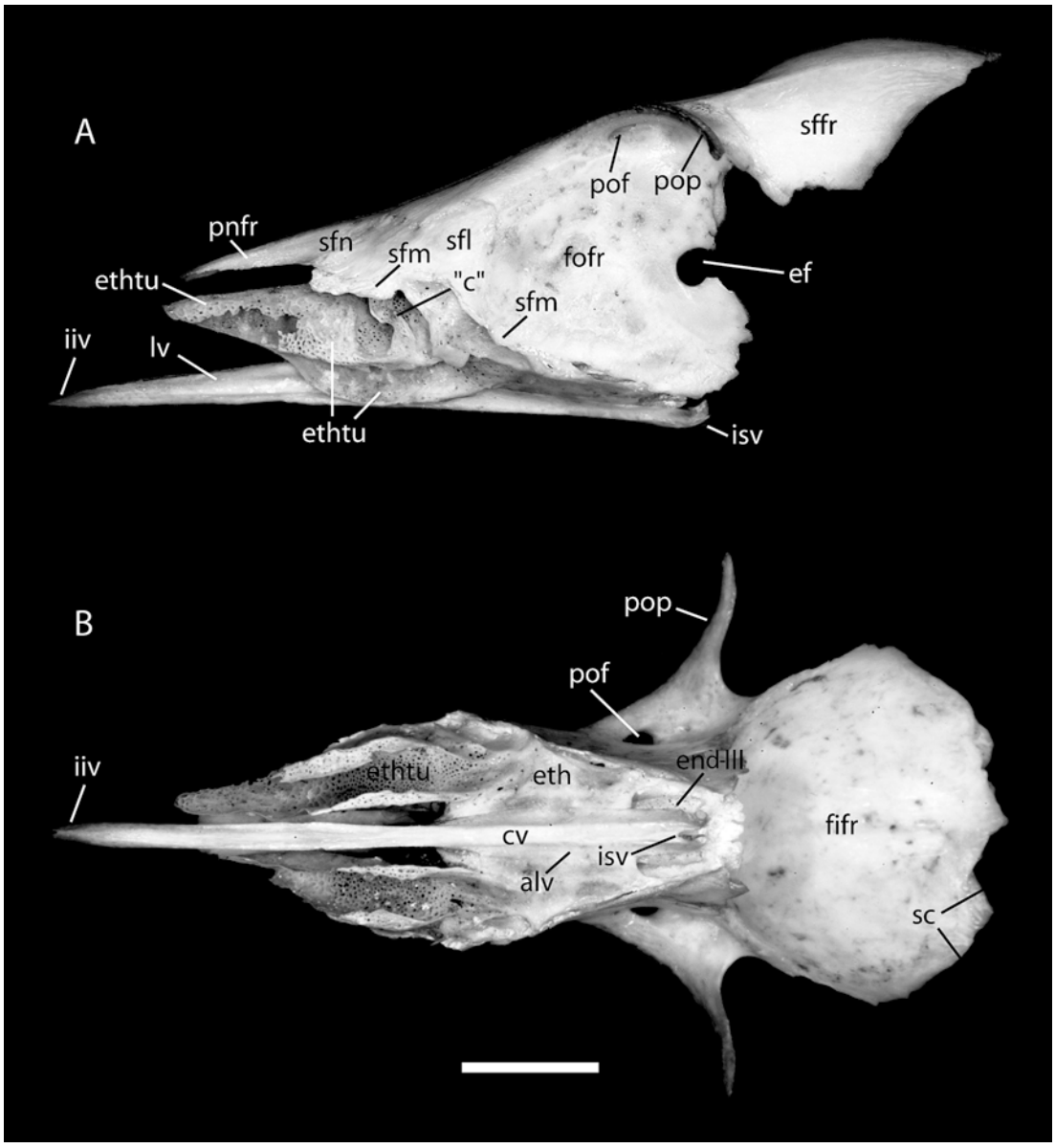

Fig. 24. *Pteropus livingstonii* AMNH 274466, frontoethmoidal complex in lateral view (**A**) and ventral view (**B**). Scale = 5 mm. Abbreviations: **alv** ala vomeris; **"c"** column of bone on lateral side of ethmoturbinal; **cv** crest of vomer; **ef** ethmoidal foramen; **ent-III** endoturbinate III; **eth** ethmoid; **ethtu** ethmoturbinal; **fifr** facies interna of frontal; **fofr** facies orbitalis of frontal; **iiv** incisura incisiva of vomer; **isv** incisura sphenoidalis of vomer; **lv** lamina of vomer; **pnfr** pars nasalis of frontal; **pof** postorbital foramen; **pop** postorbital process; **sc** sutura coronalis; **sffr** squama frontalis of frontal; **sfl** sutura frontolacrimalis; **sfm** sutura frontomaxillaris; **sfn** sutura frontonasalis.

The rostral process of the ethmoturbinal attaches to the rostroventral side of the ethmoid and projects rostrally in the form of a ventrally open tube, presenting a medial and a lateral wall joined dorsally, and defining internal and external surfaces (fig. 24A, B). The rostral process of the ethmoturbinal decreases in height and width

rostrally, acquiring a roughly conical shape. The dorsal surface is domed. The medial wall is roughly vertical and is deeper than the lateral wall. The lateral wall folds its ventral margin medially. Caudally, the lateral wall exhibits a deep incisure that is separated from another, more caudal incisure by a thin, vertical, zigzag column of bone (probably part of the ectoturbinate, based on *Rousettus*; Jurgens, 1963). The caudalmost incisure is separated from the ethmoid by an oblique ridge that is expanded ventrally as a short flange. The space between this ridge and the frontoethmoidal suture caudally has two deep, oblique grooves. In the caudal part of this area is the articulation with the lacrimal in the lacrimoethmoidal suture (*sutura lacrimoethmoidalis* of the dog, probably equivalent to the *sutura lacrimoconchalis* of the NAV). Ventral and caudal to this part, and adjacent to the frontoethmoidal suture, is the ethmoidal component of the ethmoidomaxillary suture. All the surfaces involved are formed by noticeably porous bone. The caudal portion of the ventral nasal concha fits inside the hollowed cone of the rostral process of the ethmoturbinal, and the cleft between both conchae is the middle nasal meatus.

Presphenoid Surface

In the dorsal surface of the presphenoid-orbitosphenoid complex (fig. 25A), the most salient features are the large alae orbitales (orbitosphenoid), the long corpus (presphenoid), the yoke (*jugum sphenoidale*), and the optic canals (*canales optici*). The presphenoid body has two shallow optic grooves, each leading to their respective optic canals, separated by a medial, low, and rounded midsagittal crest, and demarcated laterally by a low ridge at the union of the alae with the corpus caudal to the optic canals. The alae are fused seamlessly to the corpus. Lateral to the corpus is the paired, spine-shaped, very small rostral clinoid process (*processus clinoideus rostralis*). Laterally, the alae connect smoothly to the body and, bridging over the optic canals, connect themselves again dorsal to the corpus. The outline of each optic canal is somewhat oval, with the dorsal orbitosphenoidal crest (*crista orbitosphenoidalis*) forming the flattened dorsal margin. The yoke, the rostral union of the left and right alae, is dorsally gently concave. The alae are very wide and emerge from almost the entire side of the long corpus. The alae first spread widely laterally, more so caudally, and then they gently curve dorsally, keeping a roughly uniform width until reaching the rounded dorsal margin. The caudal alar margin shows a distinct notch representing the rostral margin of the sphenorbital fissure, caudal and lateral to the optic canals. The elevated, roughly vertical part of the alae is oriented obliquely with respect to the midsagittal plane, converging rostrally. The anterior interalar space, where the caudal frontoethmoidal complex fits, is U-shaped in caudal view. Externally, the alae show the wide overlap of the orbitosphenoid's portion of the squamous sphenoparietal suture along the posterior third of the external surface. The corpus itself has truncated anterior and posterior ends. The anterior end shows the very small, paired cavity that the presphenoid contributes to the sphenoidal sinus (*apertura sinus sphenoidalis*). Ventral and slightly caudal to the sphenoidal sinuses, there is a third median cavity that probably houses a rod of cartilage (lost) connecting the presphenoid with the vomer and nasal septum rostrally. The caudal end has a mushroom-shaped section and is also in contact with a rod of cartilage (lost in most macerated specimens, but present, for instance, in *Pteropus giganteus* ROM 75747 and *Dobsonia pannietensis* AMNH 159099) linking the presphenoid and basisphenoid.

Basisphenoid Surface

The dorsal aspect of the basisphenoid-alisphenoid exhibits two large temporal alae (the alisphenoid component) united by a truncated pyramidal corpus (the basisphenoid component; fig. 25B). On each side of the truncated rostral end of the corpus is the short, spinelike pterygoid process (of the basisphenoid). The outline of the rostral end is dorsally convex, with two lateral sides converging in the ventral midline, with all angles rounded. The dorsal surface of the corpus has a large central depression, the *sella turcica*, with its hypophyseal fossa (*fossa*

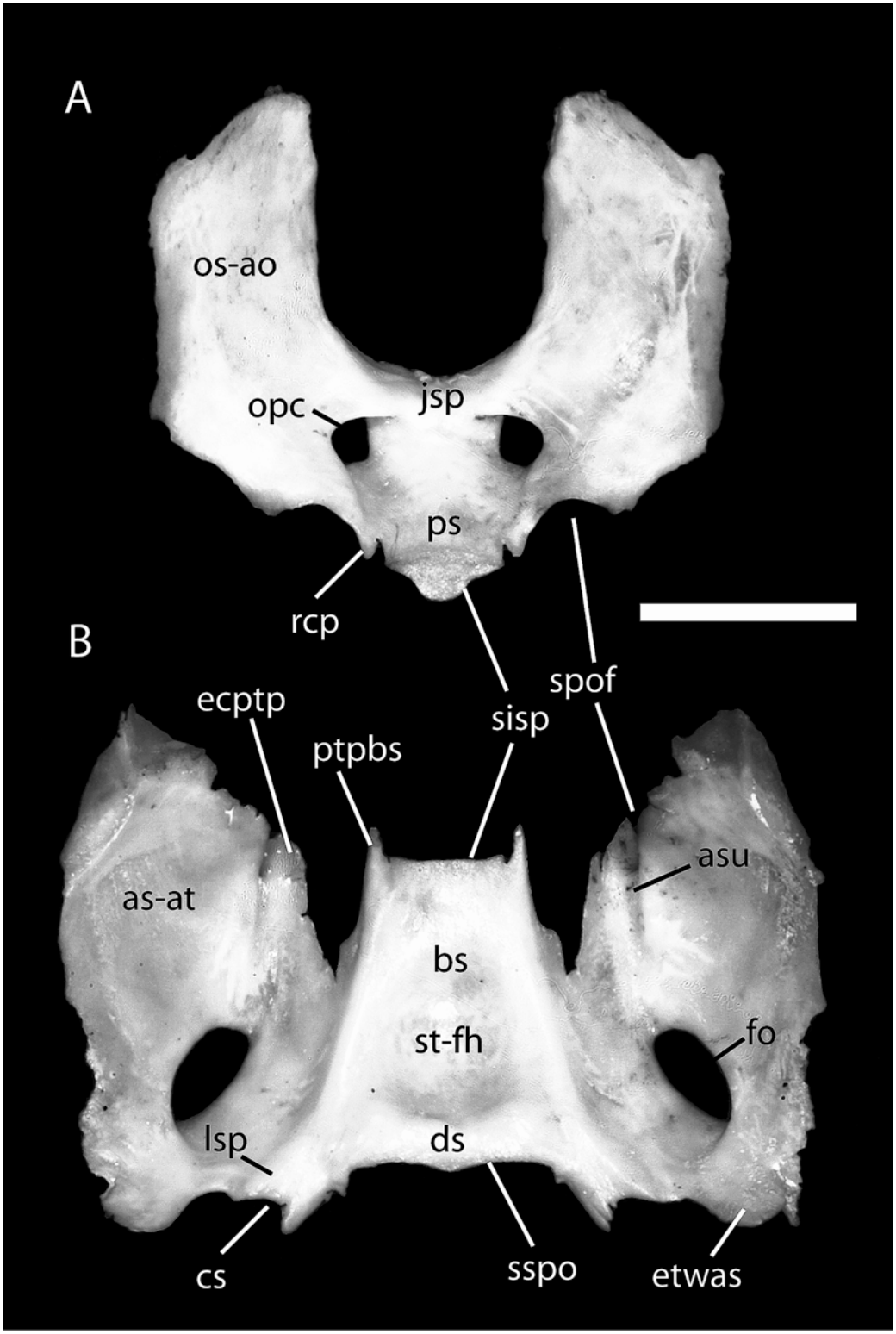
A
os-ao
opc
jsp
ps
rcp
B
ecptp
ptpbs
sisp
spof
asu
as-at
bs
st-fh
fo
lsp
ds
cs
sspo
etwas

hypophysialis) flooring the *hypophysis* in life. The fossa is oval in shape, longer than wide, with its surface very smooth, bounded bilaterally by low, rounded ridges, and caudally by a thicker ridge, which represents a weak *dorsum sellae*. Caudally, the corpus presents a rather flat, lip-shaped articular surface for the cartilage of the spheno-occipital synchondrosis (lost). Lateral to this synchondrosis is the shallow carotid sulcus (*sulcus caroticus*), which transmits the contents of the carotid foramen to the sella turcica. The medial border of the carotid sulcus projects caudally as a short spine. Immediately lateral to the sulcus is a low ridge that coincides topographically with the *lingula sphenoidalis* of the dog and human.

The dorsal surface of the alae (*facies cerebralis*) is large, roughly triangular in shape, with a rostral vertex and a caudomedial base. The surface is gently concave, presenting principally two notches, medial and lateral, in the rostral edge immediately lateral to the corpus, and a large foramen ovale in the substance of the ala. The lateral notch forms the caudal edge of the sphenorbital fissure, and projects ventrally a footlike pterygoid process that rests on top of the junction of palatine and pterygoid, and is part of the ectopterygoid process. The larger medial notch presents a deep wedge shape; it is floored by the rostromedial process of the pterygoid, and thus it is not visible externally. The large foramen ovale is elliptical in shape and oriented obliquely so the major axes of the left and right foramina converge rostrally. This foramen, the result of the fusion of the foramen ovale and the caudal alar foramen of the dog, is in the center of the basal alar concavity. A fairly well marked sulcus ascends gently from the rostral edge of the foramen to the sphenorbital fissure, presumably transmitting the contents of the absent alar canal. Caudolaterally, the ala forms a lobe, the epitympanic wing of the alisphenoid, which forms the rostral margin of the piriform fenestra. The epitympanic wing projects into the ear region, where it contacts the petrosal along a serrate suture, and also the epitympanic wing of the parietal. The lateral alar border is rather irregular. The lateral side of the epytimpanic wing shows the small (ca. 1 mm wide) squamous sphenosquamosal suture, by which the squamosal overlaps the alisphenoid laterally, seen in ventral view. In dorsal view, this suture shows as a short, inverse alisphenoid-squamosal overlap, immediately rostral to the epitympanic wing of the alisphenoid, where the ventral and medialmost portions of the squamosal, in the medial angle of the glenoid fossa, contact the alisphenoid and form a partly serrated, partly squamous suture. The triangular rostral edge of the ala, in dorsal view, is divided into two portions, each representing a squamous suture. The smaller medial portion corresponds to the unnamed suture by which the alisphenoid overlaps the orbitosphenoid medially. The second suture corresponds to the portion of the sphenoparietal suture by which the alisphenoid overlaps the parietal medially.

Parietal Surface

The left and right parietals, as well as the interparietal, are articulated in AMNH 274466, forming a parietal complex that is treated as a whole here (fig. 26). Deeply concave, the ventral surface of the parietal complex (*facies interna* of the parietal, *lamina interna* of the *cranium*) reproduces the

←

Fig. 25. *Pteropus livingstonii* AMNH 274466, dorsocaudal view of the internal surface of the presphenoid-orbitosphenoid complex (**A**) and dorsal view of the internal surface of the basisphenoid-alisphenoid complex (**B**). Scale = 5 mm. Abbreviations: **ao** alae orbitales of sphenoid (orbitosphenoid); **as** alisphenoid; **asu** alar sulcus of alisphenoid; **at** alae temporales of sphenoid (alisphenoid); **bs** basisphenoid; **cs** carotid sulcus of basisphenoid; **ds** dorsum sellae; **ecptp** ectopterygoid process; **etwas** epitympanic wing of alisphenoid; **fh** fossa hypophysialis; **fo** foramen ovale; **jsp** yoke or jugum sphenoidale; **lsp** lingula sphenoidalis; **opc** optic canal; **os** orbitosphenoid; **ps** presphenoid; **ptpbs** pterygoid process of basisphenoid; **rcp** rostral clinoid process; **sisp** synchondrosis intersphenoidalis; **spof** sphenorbital fissure; **sspo** synchondrosis spheno-occipitalis; **st** sella turcica.

bulbous shape and some external features of the underlying brain. These features are the digital impressions (*impressiones digitatae*), separated by intermediate ridges, which correspond to the cerebral gyri and sulci, respectively.

In AMNH 274466, the plane, linear interparietal suture is clearly visible for most of its length, on both dorsal and ventral surfaces, becoming indistinguishable only ca. 1 mm rostral to the contact with the parietointerparietal suture. The latter is still visible, but it exhibits a higher degree of fusion. Against a light source, it is possible to see that the parietointerparietal suture is largely a plane suture, with small areas of overlap (by the parietal, dorsally) only in the rostral and the lateral margins.

Rostrally, the parietal widely overlaps the frontal in the coronal (= frontoparietal) suture, a large triangular area of thin bone well delimited caudally by a neat line at the level of the rostral edge of the parietal in the median plane. The externally visible area of the sinciput fits in the rectangular space between the two triangular areas of the frontoparietal suture (fig. 1). The caudal edge of that space (i.e., the rostral margin of the parietal in the median plane) has a V-shaped incisure in the sagittal suture.

The ventral margin of the exposed parietal is complex and presents several angles and borders, for which we propose the following nomenclature (fig. 26B). From rostral to caudal, the angles are the frontal (*angulus frontalis*), sphenoidal (*angulus sphenoidalis*), epitympanic (new term), vascular (new term), and mastoid (*angulus mastoideus*); the margins or edges are the frontal (*margo frontalis*, ventral part), squamous (*margo squamosus*), epitympanic (new term), and caudoventral (new term). The frontal angle, as described above, is the rostralmost extension of the parietal and forms the apex of the frontoparietal suture. The ventral part of the frontal margin is straight; it is inclined ventrocaudally until reaching the ventralmost point in the parietal, where it terminates at the sphenoidal angle, which marks the beginning of the sutura squamosa. The sphenoidal angle is located slightly rostral to the midpoint of the parietal complex. The squamous margin arches dorsally, descending again to the ventral tip of the triangular epitympanic wing of the parietal (i.e., the epitympanic angle), at about three-quarters of the parietal length. While the internal surface of the parietal lacks traces of sutures in this area, the external surface (*facies externa*) of the disarticulated parietal shows the wide overlap area of the sutura squamosa. Dorsal to the arched ventral margin, the area of the sutura squamosa extends generously over the lower region of the parietal's dorsal surface, ascending from the sphenoidal angle to a point high above the epitympanic wing. The caudal margin of the epitympanic wing, or epitympanic margin, is roughly vertical and terminates at the caudoventral margin of the parietal at an almost right angle.

In the angle where the epitympanic and caudoventral margins meet, called here the vascular angle, a complex configuration of vascular sulci is present. Two different vessel systems are involved, and they cross each other in this angle. These are the capsuloparietal emissary vein and the posterior division of the ramus superior of the stapedial artery. The capsuloparietal emissary vein drains the blood from the intracranial transverse sinus, partially encapsulated in a short sulcus in the internal surface of the parietal. The petrosal closes the canal for the capsuloparietal emissary vein medially and caudally, which becomes evident with the petrosal in place (e.g., in the broken skulls of *Pteropus neohibernicus* AMNH 152402 and *P. vampyrus* AMNH 198691). The capsuloparietal emissary vein arrives in a space immediately dorsal to the opening of the temporal canal (see below), between the squamosal and the parietal. This space appears as a depression in the external surface in the vascular angle, and is especially evident in caudolateral view in AMNH 274466. Then, the capsuloparietal emissary vein enters directly into the dorsal opening of the temporal canal in the medial side of the squamosal, exiting the skull through the postglenoid foramen (see below). In turn, the ramus superior follows an inverse, dorsally directed course (marked, in the parietal, as a shallow sulcus on the epitympanic margin), reaching the space in the angle between the caudal epitympanic edge and the caudoventral parietal margin. In that space, the posterior division of the ramus

superior crosses the more external side of the space, and a conspicuous sulcus for the vessel, not visible externally, appears. Immediately dorsal, on the right side, the sulcus divides into a smaller, caudal sulcus, leading to the posterior foramen for ramus temporalis, and a larger, rostral sulcus, which continues further dorsally, leading to the anterior foramen for ramus temporalis. Both foramina open in the sutura squamosa, and their course between the squamosal and the parietal is not exposed externally. Both sulci continue 2–3 mm dorsally in the free dorsal surface of the parietal. On the left side, a single, wider sulcus reaches the sutura squamosa, and a corresponding single foramen for ramus temporalis is present.

The internal surface of the parietal reveals the relatively small size of the sulcus for the transverse sinus, as compared with the dog. The transverse sulcus has a strong, vertically directed medial wall that fuses with the skull roof some 5 mm dorsal to the vascular angle. Two nutrient foramina are present bilaterally in the sulcus. This is more clearly visible in articulated specimens without the skull roof, such as *Pteropus neohibernicus* AMNH 152402 and *Pteropus vampyrus* AMNH 198691. A low sulcus for the transverse sinus, gently concave caudally, bridges the vascular angle and the midsagittal line. The left and right sulci meet at the junction of the interparietal and parietointerparietal sutures. The rostral edge of the sulcus is more marked than the caudal edge. Rostral to the sulci, the parietal surface is lightly marked by digital impressions and intermediate ridges. There are two main intermediate ridges of thickened bone. The medial intermediate ridge runs rostrocaudally, separated from the interparietal suture by ca. 5 mm, and extends caudally up to half the distance between the medial rostral edge of the parietal and the ridge of the transverse sulcus. The lateral intermediate ridge is somewhat divergent rostrally, but is still roughly parallel to the medial intermediate ridge and separated by ca. 3 mm from it. Another, barely marked ridge extends between the caudal end of the lateral intermediate ridge and the vascular angle. A somewhat blurred vascular groove for the middle meningeal artery (*sulcus arteriae meningeae mediae*) and veins arises from the ventral border (right side) and may be from the epitympanic angle as well (left side). The ramifications of the meningeal vessels are not consistently marked bilaterally, being more numerous on the right side (some nine inconspicuous branches versus six on the left side).

The caudal part of the ventral surface of the parietal complex comprises most of the interparietal and the two caudolateral lobes of the parietal (fig. 26). The interparietal has a domed ventral surface, surrounded by the parietointerparietal and occipitointerparietal sutures. The left side of the parietointerparietal suture is more deeply marked than the right side. The occipital margin of the interparietal shows three concave suture segments. The two lateral segments are the areas by which the interparietal overlaps the supraoccipital (see below). In turn, the median segment shows a small squamous area on the dorsal surface by which the supraoccipital slightly overlaps the interparietal. The caudolateral lobes of the parietal exhibit two large suture areas. The parietal component of the occipitoparietal suture (which corresponds to the occipital margin of the parietal, *margo occipitalis*) is a flange of poorly consolidated bone presenting numerous notches and longitudinal striations. This wide lamina overlaps the supraoccipital dorsally. The caudoventral margin of the parietal is occupied by an unnamed, plane suture with the petrosal (see Petrosal) that is triangular in shape. In this area, the parietal widely overlaps the pars canalicularis of the petrosal.

Squamosal Surface

The squama of the squamosal laterally overlaps parts of the parietal, the petrosal, and the alisphenoid. The squama covers the parietal rostrodorsally, which projects its epitympanic wing ventrally almost to the level of the anterior margin of the external acoustic meatus. The squama also covers the pars canalicularis of the petrosal and the alisphenoid caudoventrally and rostroventrally, respectively. Consequently, there is a very small brain exposure on the squamosal. In medial view (fig. 27), the outline of the squama is the same as described externally (see Squamosal above).

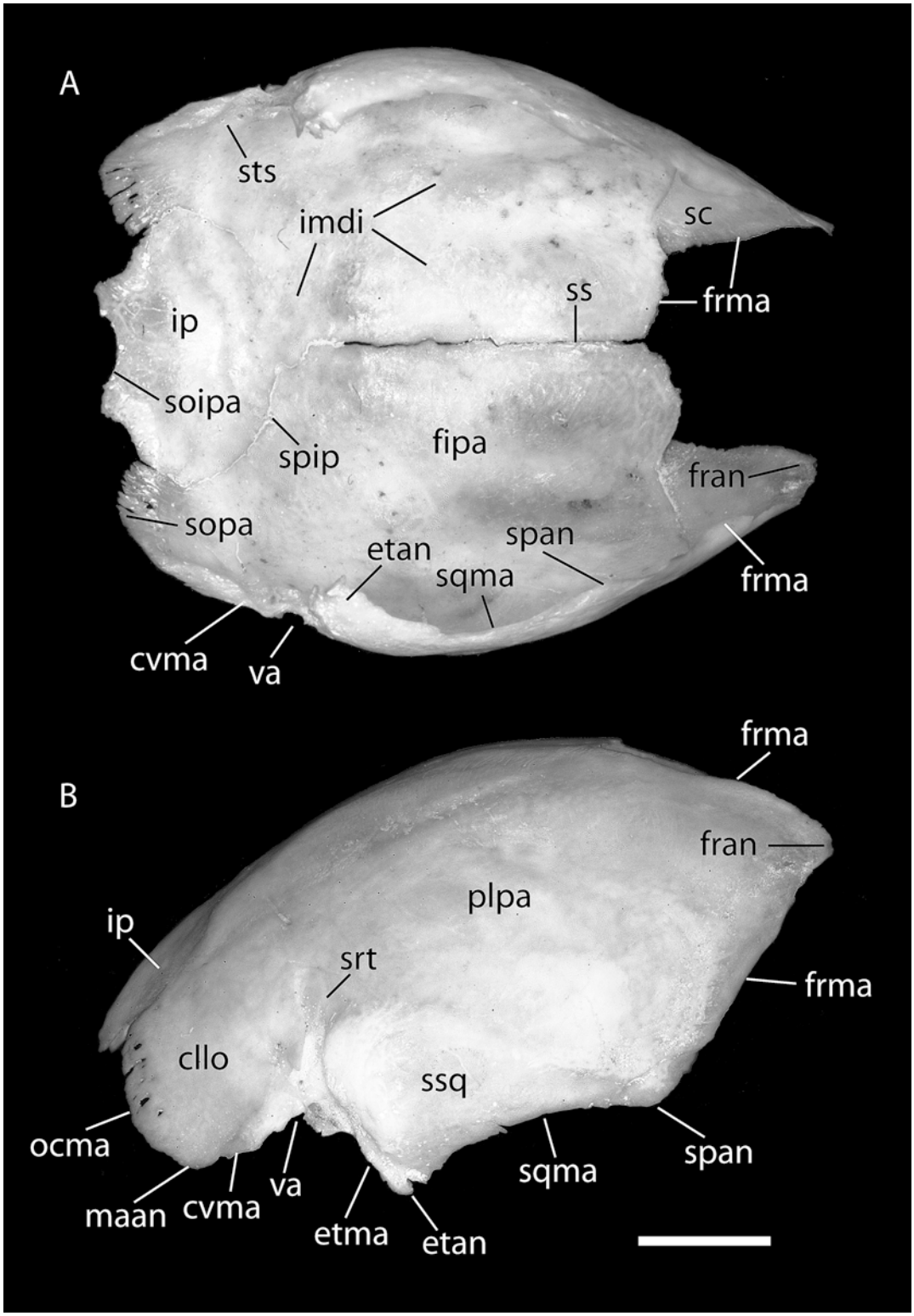
A
sts
imdi
sc
ss
frma
ip
soipa
spip
fipa
fran
sopa
etan
span
sqma
frma
cvma
va
B
frma
fran
plpa
ip
srt
frma
cllo
ssq
ocma
sqma
span
maan
cvma
va
etma
etan

The internal, or medial, surface of the squamosal is concave, with a very prominent feature: the dorsally directed opening of the temporal canal located in the posterior third of the squama. The temporal canal transmits the capsuloparietal emissary vein from the transverse sinus to its exit at the postglenoid foramen (see Parietal above, and Foramina Contents and Homology below). The opening of the temporal canal is surrounded anteriorly, ventrally, and posteriorly by acute ridges, and opens into a space that in turn leads dorsally to a wide sulcus for the posterior division of the ramus superior of the stapedial artery. Three minute nutrient foramina are found around this space. The posterior division of the ramus superior passes medial to the capsuloparietal emissary vein in a dorsal direction, enters the parietal, and divides shortly after, exiting the skull through two or three openings (the foramina for the rami temporales) at the sutura squamosa. Caudoventral to the opening of the temporal canal, a dorsally concave crest delimits the dorsal extension of the squamosal contribution to the *fossa incudis*, a cavity shared with the petrosal. The rostrodorsal semiarch of this crest is continued caudoventrally in the faint mark of the caudal part of articulation with the petrosal. Immediately caudal to this line is the posttympanic process of the squamosal.

Anteriorly, the triangular rostral lamina of the squama shows a distinctive ridge that marks the sphenosquamosal suture. About 1 mm dorsal is the less conspicuous sutura squamosa. The space between the two sutures is the very limited brain exposure on the squamosal (ca. 4 mm long × 1 mm high).

Occipital Surface

In AMNH 274466, the four occipital bones are fused into a single structure without traces of sutures internally or externally except for the ventral intraoccipital synchondrosis (the joint between basioccipital and exoccipital), which is represented bilaterally by no more than a 1-mm notch. As a consequence, the occipital complex is treated here as a whole. Centered on the foramen magnum, the cup-shaped complex of four bones forms a complete ring, with the basioccipital (*pars basilaris* of the occipital complex) protruding ventrally and rostrally as a long rectangular plate, the exoccipitals (*partes laterales*) forming the short but thick lateral sides, and the supraoccipital (*pars squamosa*) appearing as a relatively thin lamina partially roofing the wide space dorsal to the foramen magnum (fig. 28).

Distinctly two-sided, with each side forming a plane gently converging medially and ventrally, the dorsal surface of the basioccipital forms the *sulcus medullae oblongatae*. Rostrally, the concavity of the dorsal surface is accentuated (in the *impressio pontina*), and the surface is subsequently elevated to reach the dorsal border of the lip-shaped joint that is the basioccipital component of the sphenooccipital synchondrosis. In each of the rostrolateral angles, a short, oblique joint marks the lateral continuation of the sphenooccipital synchondrosis immediately medial to the carotid foramen. Caudally there is a gap that corresponds to the basicochlear fissure; immediately caudal to that is the inconspicuous mark of the posterior basicochlear commissure and then a notch representing the remainder of the ventral intraoccipital synchondrosis. Caudally and medially, the basioccipital is marked by the acutely

←

Fig. 26. *Pteropus livingstonii* AMNH 274466, ventral view of the internal surface (facies interna) of the parietals and interparietal (**A**), and lateral view of the isolated parietal complex (**B**). Scale = 5 mm. Abbreviations: **cllo** caudolateral lobe of parietal; **cvma** caudoventral margin of parietal; **etan** epitympanic angle of parietal; **etma** epitympanic margin of parietal; **fipa** facies interna of parietal; **fran** frontal angle of parietal; **frma** frontal margin of parietal; **imdi** impressiones digitatae; **ip** interparietal; **maan** mastoid angle of parietal; **ocma** occipital margin of parietal; **plpa** planum parietale; **sc** sutura coronalis; **soipa** sutura occipitointerparietalis; **sopa** sutura occipitoparietalis; **span** sphenoidal angle of parietal; **spip** sutura parietointerparietalis; **sqma** squamosal margin of parietal; **srt** sulci for rami temporales; **ss** sutura sagittalis; **ssq** sutura squamosa; **sts** sulcus for transverse sinus; **va** vascular angle of parietal.

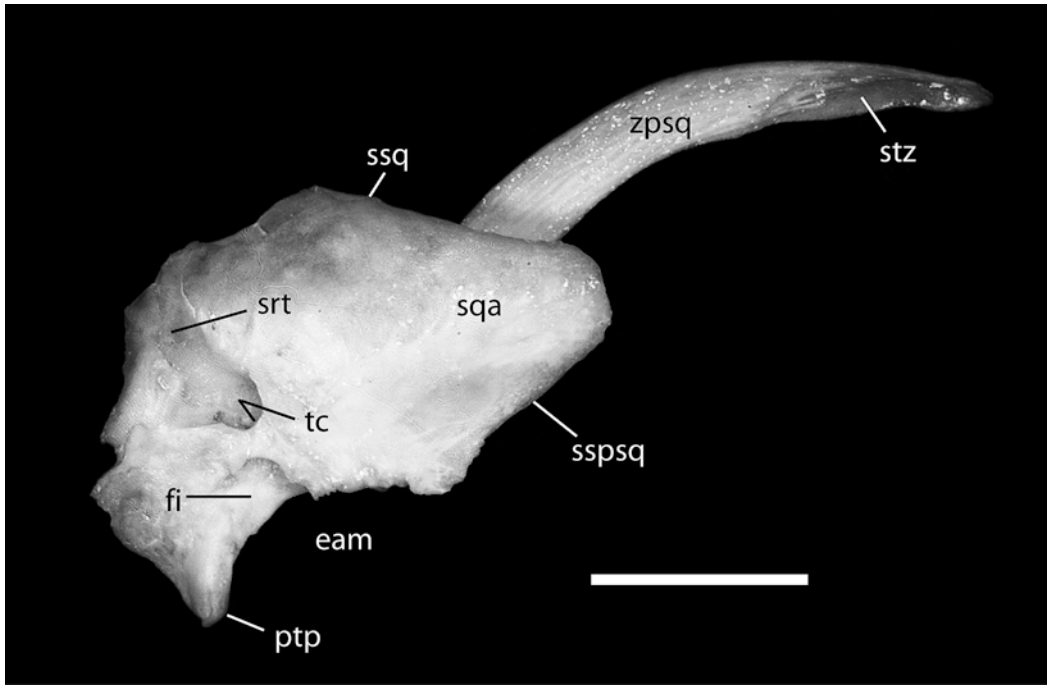

Fig. 27. *Pteropus livingstonii* AMNH 274466, medial view of the internal surface of the squamosal. Scale = 5 mm. Abbreviations: **eam** external acoustic meatus; **fi** fossa incudis (lateral wall); **ptp** posttympanic process of squamosal; **sqa** squama of squamosal; **srt** sulci for rami temporales; **sspsq** sutura sphenosquamosa; **ssq** sutura squamosa; **stz** sutura temporozygomatica; **tc** temporal canal; **zpsq** zygomatic process of squamosal.

concave margin of the foramen magnum, the intercondyloid notch (*incisura intercondyloidea*).

The exoccipital is the shortest component of the occipital complex. Rostrally, it has a dorsoventrally elongated, almost vertical articulation with a convex surface, the exoccipital component of the occipitomastoid suture, or the articulation between the exoccipital and the mastoid exposure of the petrosal (the petrosal component of the suture being deeply concave). This articulation has a notch in its dorsocaudal angle that communicates with the minute mastoid foramen and continues rostrodorsally in a short, almost horizontal suture of ca. 2 mm. This part of the suture is already in the supraoccipital, based on *Pteropus capistratus* AMNH 194276. Ventral to the suture, horizontally oriented, is the wide gap of the concave medial margin of the jugular foramen. This margin shows a distinct sulcus that corresponds to the sulcus for the inferior petrosal sinus (*sinus petrosus ventralis*) in the dog. Internally, the exoccipital has a smooth, convex surface that funnels into the foramen magnum, whose lateral margin is widely concave. Midway between the suture with the petrosal and the foramen magnum is the rounded hypoglossal foramen.

The supraoccipital is a wide, concave lamina of bone overlying the cerebellum. The lateral angle, as described above, is occupied by a notch connected to the mastoid foramen (the foramen being delimited ventrally and internally by the mastoid exposure of the petrosal). The supraoccipital has two sections of different thickness around the foramen magnum, the division roughly coincident with the external nuchal crest. The ventral portion is formed by bone that increases its thickness toward the foramen magnum. The dorsal margin of the foramen magnum is, like its ventral counterpart, acutely concave. The dorsal part of the supraoccipital has a central vermiform im-

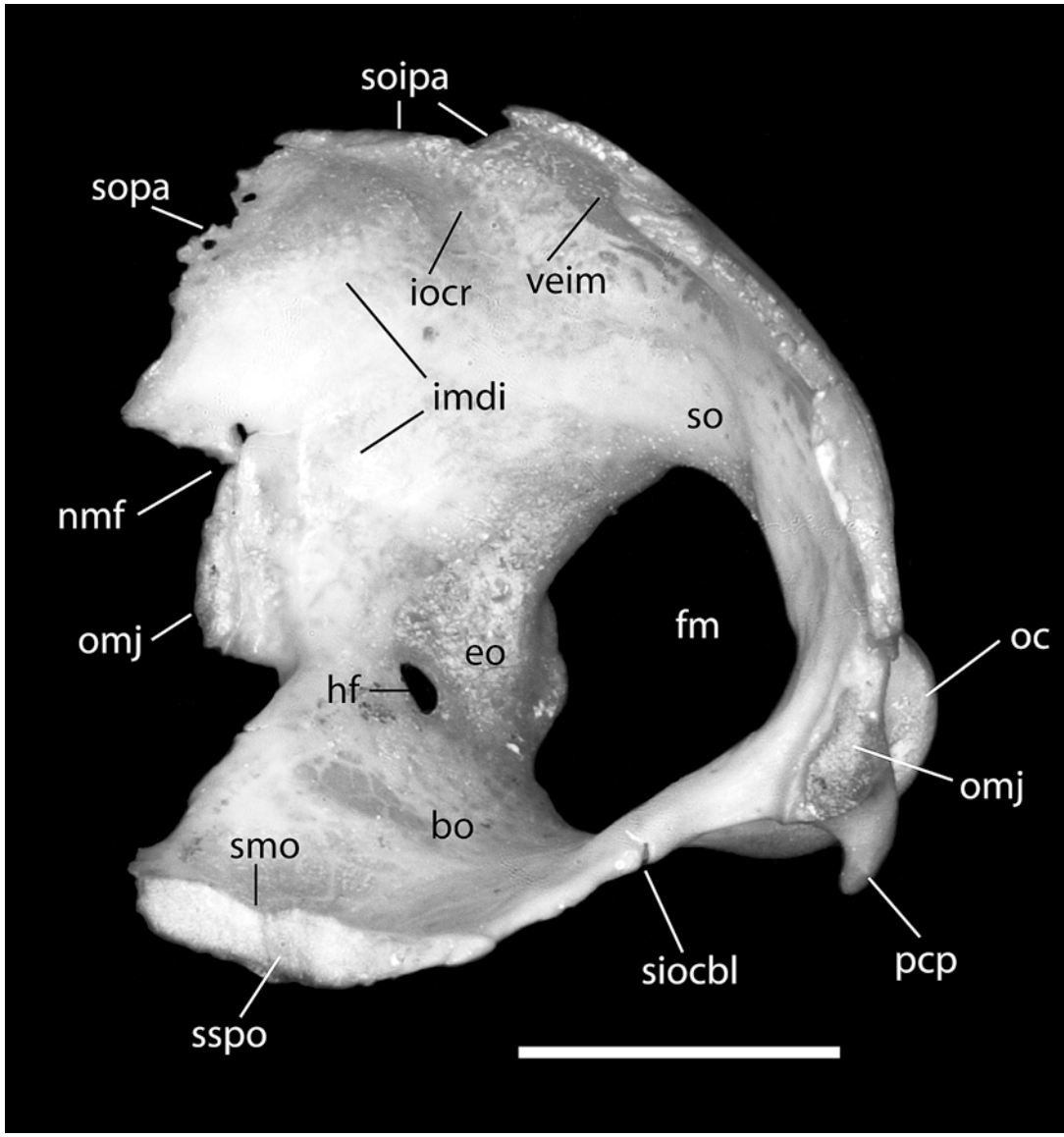

Fig. 28. *Pteropus livingstonii* AMNH 274466, oblique rostrolateral view of the occipital complex. Scale = 5 mm. Abbreviations: **bo** basioccipital; **eo** exoccipital; **fm** foramen magnum; **hf** hypoglossal foramen; **imdi** impressiones digitatae; **iocr** internal occipital crest; **nmf** notch for mastoid foramen; **oc** occipital condyle; **omj** occipito-mastoid joint; **pcp** paracondylar process; **siocbl** synchondrosis intraoccipitalis basilateralis; **smo** sulcus medullae oblongatae; **so** supraoccipital; **soipa** sutura occipitointerparietalis; **sopa** sutura occipitoparietalis; **sspo** synchondrosis spheno-occipitalis; **veim** vermiform impression.

pression (*impressio vermialis*) that is delimited bilaterally by the internal occipital crest (*crista occipitalis interna*). Lateral to the internal occipital crests are the depressions of the *impresiones digitatae*, which accommodate gyri of the brain. The dorsal border of the supraoccipital is formed by the occipitointerparietal and occipitoparietal sutures. In the median part of the supraoccipital is the squamous occipitointerparietal suture by which the interparietal and the supraoccipital interlock. There are two deep

notches on the sides of the vermiform impression. These notches are the areas where the supraoccipital is overlapped dorsally by the interparietal. The middle portion, immediately dorsal to the vermiform impression, is the small rounded area where the supraoccipital slightly overlaps the interparietal. This suture is better seen from the dorsal side of the isolated occipital complex. It has a very irregular dorsal edge, and an irregular area of overlap of up to ca. 2 mm across the entire dorsal margin of the supraoccipital.

FORAMINA CONTENTS AND HOMOLOGY

ACCESSORY PALATINE FORAMINA: In the dog (Evans, 1993), the accessory palatine nerve (*nervus palatinus accessorius*) arises from the major palatine nerve (off the pterygopalatine nerve of V_2) and supplies the caudal part of the hard palate. In the *Pteropus* fetus, the accessory palatine nerves (those supplying the palate between the major and minor palatine nerves) and accompanying arteries reach the palate via small apertures in the lateral aspect of the horizontal process of the palatine. On the right side there are three such foramina, and on the left there are five. Only the anteriormost one on the left arises directly from the palatine canal (see below); the remainder originate posterior to the fully bone-enclosed portion of the palatine canal. *P. lylei* CM 87972 has five small accessory palatine foramina per side in the lateral aspect of the palatine, medial to the molars, situated between the major and minor palatine foramina; the anterior three foramina are dependents of the palatine canal (fig. 9).

ALAR CANAL: See foramen ovale and sphenorbital fissure.

ALVEOLAR CANALS: In the dog (Evans, 1993), alveolar canals carry branches of the infraorbital nerve (of V_2), artery, and vein to the individual roots of the upper teeth and open by numerous alveolar foramina at the apex of each alveolus (*apex radici dentis*). Within the maxilla posterior to the maxillary foramen is an alveolar canal that transmits the caudal superior alveolar nerves to the caudal cheek teeth. Within the infraorbital canal are alveolar canals that transmit middle and rostral superior alveolar nerves; the latter enter the alveolar (= incisivomaxillary) canals to be distributed to the upper canine and incisors. In the *Pteropus* fetus, the middle and rostral superior alveolar nerves and accompanying blood vessels pass through an alveolar canal in the maxilla (fig. 30) posterior to the maxillary foramen at the level of the last premolar and in the premaxilla (fig. 29). The top of the first molar is separated from the pterygopalatine fossa by membrane (the second molar has not yet formed), and the caudal superior alveolar nerves penetrate that membrane to reach that tooth. In *P. lylei* CM 87972, the alveolar canal for the middle and rostral superior alveolar nerves is within the infraorbital canal on the left side and posterior to the maxillary foramen on the right (fig. 12). It is likely that the caudal superior alveolar nerves reach the first and second molars via their open roots, which are visible in the floor of the orbit.

BASICOCHLEAR FISSURE: The basicochlear fissure (basicapsular fenestra) is a gap in the chondrocranium between the auditory capsule laterally and the parachordal plate (central stem) medially (De Beer, 1937), bounded by anterior and posterior basicochlear (basicapsular) commissures, if present (MacPhee, 1981). In some adult mammals, the fissure is not completely obliterated, resulting in the basicranial exposure of part of the inferior petrosal sinus (McDowell, 1958). In the *Pteropus* fetus (figs. 34, 35), the basicochlear fissure is bordered laterally by the pars cochlearis of the petrosal, medially by the basioccipital, and posteriorly by the cartilaginous posterior basicochlear commissure. Anteriorly, the basicochlear fissure is continuous with the carotid foramen, because the anterior basicochlear commissure is lacking. The occupant of the basicochlear fissure is the inferior petrosal sinus, which connects the cavernous sinus to the internal jugular vein. The inferior petrosal sinus exhibits considerable left-right asymmetry. During its course in the right basicochlear fissure, the inferior petrosal sinus principally sits within the cranial cavity but bulges into and out of the fissure and receives some small veins from below. Its principal foramen of

exit is the jugular foramen, which it reaches by passing dorsal to the posterior basicochlear commissure. On the left side, there is a significant drainage of the inferior petrosal sinus out of the posterior part of the basicochlear fissure into the internal jugular system, in addition to that out the jugular foramen. In *P. lylei* CM 87972, the basicochlear fissure is between the pars cochlearis of the petrosal laterally and the basioccipital medially and anteriorly (fig. 3). On the specimen's right side, the rostral entotympanic borders the basicochlear fissure anterolaterally, but on the left side this ossification is missing and the basicochlear fissure is continuous with the carotid foramen. *P. lylei* CM 87973 differs in that the basisphenoid contributes to the anterior border of the basicochlear fissure, and not the basioccipital as in CM 87972.

In the dog (Evans, 1993), the ventral petrosal sinus (= inferior petrosal sinus) runs through the petro-occipital or petrobasilar canal, between the petrous temporal and basioccipital. The caudal opening of the petro-occipital canal is anterior to the jugular foramen in the petro-occipital fissure (= basicochlear fissure of *Pteropus*).

CAROTID FORAMEN: In the dog (Evans, 1993), the course of the internal carotid artery across the basicranium is within a perbullar canal (sensu Wible, 1986). There are three foramina associated with the artery's course: one at its entrance into the carotid canal, a second at its exit from the canal, and a third at its entrance into the cranial cavity. As discussed by Wible and Gaudin (2004), the associated nomenclature employed by Evans (1993) is confusing and contradictory. Following Wible and Gaudin, we reserve the term carotid foramen for the foramen of entrance into the cranial cavity. In the *Pteropus* fetus (fig. 33), the carotid foramen lies between the anterior pole of the pars cochlearis of the petrosal posteriorly and the cartilaginous central stem and sphenoid anteriorly (the basisphenoid and alisphenoids are represented by one ossification center). The carotid foramen lacks medial and lateral borders (which would be the anterior basicochlear and alicochlear commissures, respectively) and is continuous with the basicochlear fissure medially and the piriform fenestra laterally. Passing through the carotid foramen is the internal carotid artery and accompanying nerve and vein. To reach the carotid foramen, the artery, nerve, and vein follow a short perbullar pathway, through the fibrous membrane of the tympanic cavity (sensu MacPhee, 1981; fig. 34), bordered by the caudal entotympanic posterolaterally and the rostral entotympanic anteromedially. In *P. lylei* CM 87972, the carotid foramen on the right side is enclosed between the rostral entotympanic anteriorly and the anterior pole of the promontorium posteriorly (fig. 10). The rostral entotympanic is missing on the specimen's left side, and the carotid foramen's anterior border is formed by the basioccipital medially and the basi-/alisphenoid laterally. Additionally, as in the fetus, the left carotid foramen is confluent with the basicochlear fissure and the piriform fenestra. On both sides, a shallow carotid sulcus runs somewhat obliquely on the anterior pole of the promontorium to the carotid foramen from posteriorly and slightly medially. CM 87973 differs in that the anterior border of the carotid foramen is formed by the basi-/alisphenoid laterally and the rostral entotympanic medially.

CAUDAL PALATINE FORAMEN: See palatine canal.

CAVUM SUPRACOCHLEARE: See hiatus Fallopii.

COCHLEAR CANALICULUS: In the dog (Evans, 1993), the perilymphatic duct enters the petrous temporal (petrosal) via the external opening of the cochlear canaliculus in the rostral edge of the jugular foramen. In the *Pteropus* fetus, the perilymphatic duct enters the posteromedial aspect of the pars cochlearis of the petrosal in the anterolateral aspect of the deep jugular foramen. The external opening of the cochlear canaliculus is posteroventral to the posterior basicochlear commissure, the bar of cartilage connecting the cochlear capsule to the central stem. Accompanying the perilymphatic duct into the petrosal is a vein that drains into the internal jugular. In *P. lylei* CM 87972, the cochlear canaliculus is not visible in direct ventral view, because it lies above the plane of the jugular foramen. As in the fetus, it lies in the anterolateral aspect of the jugular foramen. The placement of the cochlear

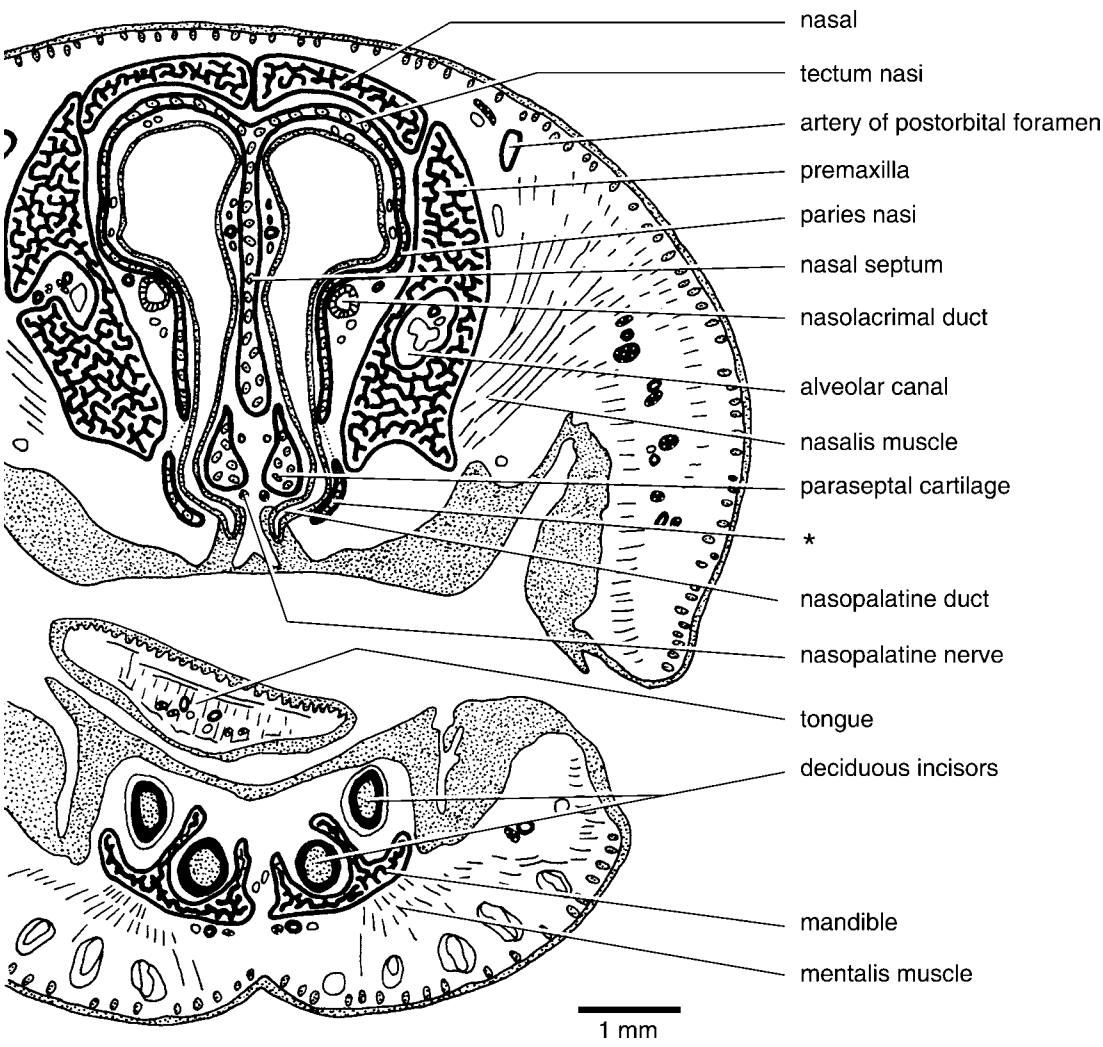

Fig. 29. *Pteropus* sp. DUCEC 831, schematic representation of part of slide 7-1, a frontal section through the rostrum near the opening of the nasopalatine duct into the oral cavity at the front of the incisive fissure. The asterisk (*) represents a paired bar of cartilage connecting the lamina transversalis anterior in front to the palatine cartilage behind.

canaliculus in the isolated petrosal of *P. livingstonii* AMNH 274466 is shown in figure 14. Hinchcliffe and Pye (1969) described the cochlear aqueduct of *Pteropus giganteus* as "duct type" with length greater than diameter, as compared to the "foramen type" of neglible length in the microchiropterans they studied.

ETHMOIDAL FORAMEN: The dog (Evans, 1993) has two ethmoidal foramina (sometimes confluent): a smaller one in the suture between the frontal and orbitosphenoid and a larger dorsocaudal one in the frontal. The ethmoidal nerve of V_1 penetrates the rostral ethmoidal foramen en route to the cribriform plate and nasal cavity; the external ethmoidal artery, a branch of the external ophthalmic, occupies the caudal ethmoidal foramen. In the *Pteropus* fetus, the single ethmoidal foramen is between the frontal and ala orbitalis (the chondrocranial precursor of the orbitosphenoid bone) and transmits the ethmoidal nerve and external ethmoidal artery. In *P. lylei* CM 87972, the single,

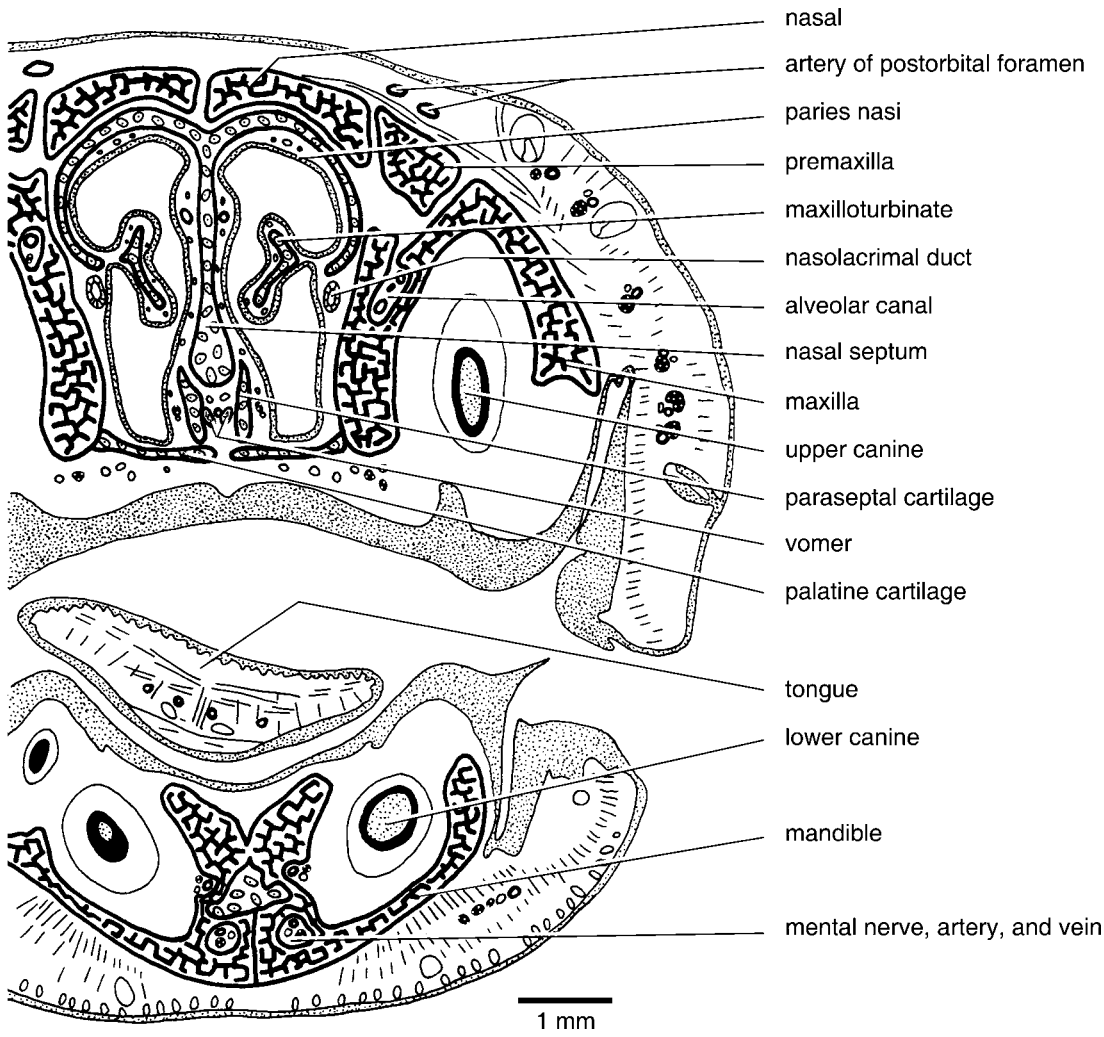

Fig. 30. *Pteropus* sp. DUCEC 831, schematic representation of part of slide 10-1, a frontal section through the rostrum at the back of the incisive fissure. The paired palatine cartilage closes off the posterior part of the incisive fissure. On the left side, the deciduous lower canine (unlabeled) lies lateral to the permanent canine.

subcircular ethmoidal foramen lies in the frontal, anterodorsal to the optic canal, about halfway between the orbital floor and the postorbital process (fig. 11). *P. lylei* CM 87973 differs in that the posterior border of the foramen is formed by the orbitosphenoid, and the foramen is considerably larger (larger than the optic canal).

FORAMEN OVALE: In the dog (Evans, 1993), the foramen ovale for the mandibular nerve (V_3) and a small emissary vein is in the base of the temporal wing of the basisphenoid (alisphenoid); in the posterolateral border of the foramen ovale, a small notch or even a separate foramen spinosum for the middle meningeal artery may be present. Anteromedial to the foramen ovale is the caudal alar foramen, which transmits the maxillary artery (*arteria maxillaris*) and vein (*vena maxillaris*) into the alar canal (= alisphenoid canal of Gregory, 1910). In the *Pteropus* fetus, the foramen for the mandibular nerve is within the basi-/alisphenoid, although the pterygoid approaches its ante-

romedial border and the squamosal approaches its posterolateral border. Three major structures are transmitted (fig. 32): anteriorly the maxillary artery or ramus infraorbitalis (sensu Wible, 1987), centrally an emissary vein of the cavernous sinus, and posteriorly the mandibular nerve (V_3). Consequently, the foramen ovale of *Pteropus* represents the foramen ovale + the caudal alar foramen of the dog (= alisphenoid canal). Positioned below the posterior edge of the foramen ovale in the fetus is the otic ganglion (*ganglion oticum*) off of V_3 (fig. 33). A well-developed middle meningeal artery like that in the dog is lacking; after the maxillary artery enters the foramen ovale it sends off two small meningeal branches to the cavum epiptericum, an extradural space housing the trigeminal ganglion (*ganglion trigeminale*) and associated structures (Gaupp, 1902, 1905). In *P. lylei* CM 87972, the elongate foramen ovale is within the alisphenoid, although the pterygoid approaches its medial border and the squamosal approaches its posterolateral border (figs. 3, 5, 10).

FORAMEN ROTUNDUM: See sphenorbital fissure.

FORAMINA FOR FRONTAL DIPLOIC VEIN: *Pteropus lylei* CM 87972 has several small foramina immediately ventral to the postorbital process of the frontal (fig. 11). Based on the fetus (fig. 31), the three foramina (two on the right side) in the adult that are in close association with the postorbital foramen (see below) transmit diploic veins; the more posterior foramen transmits a small artery and vein into the substance of the frontal. The artery is derived from the large orbital artery, the external ophthalmic artery of the NAV (*arteria ophthalmica externa*), which also supplies the ethmoidal (*arteria ethmoidalis*), lacrimal (*a. lacrimalis*), and frontal arteries and the artery of the postorbital foramen. The diploic veins represent the frontal diploic veins (*venae diploicae frontales*), which have been described in various therians (see Thewissen, 1989; Evans, 1993; Wible, 2003; Wible and Gaudin, 2004).

FORAMINA FOR RAMI TEMPORALES: Following Wible and Gaudin (2004), we use the term foramina for rami temporales for openings in the squamosal dorsal to the suprameatal bridge transmitting rami temporales of the stapedial artery and accompanying veins to the m. temporalis. This term is equivalent to subsquamosal foramina of Wible et al. (2004). The dog has no foramina for rami temporales, and the vascular supply to the m. temporalis follows an entirely extracranial course via the external carotid system (Evans, 1993). In the *Pteropus* fetus, there are two foramina for rami temporales per side between the parietal and squamosal transmitting arteries and veins. The arteries are derived from the posterior division of the ramus superior (fig. 35), and the veins connect to the capsuloparietal emissary vein anteriorly and the vena diploëtica magna posteriorly in the posttemporal canal. The more anterior foramen for ramus temporalis lies above the entrance of the capsuloparietal emissary vein into the squamosal bone endocranially (see postglenoid foramen), and the posterior one lies above the anterior end of the posttemporal canal. In *P. lylei* CM 87972, the dorsally directed foramina for rami temporales are between the parietal and the squamosal, dorsal to the external acoustic meatus, with short sulci carrying the contents onto the parietal (fig. 2). There are two small openings on the left side and a single, larger opening on the right. CM 87973 has two foramina on the right and three on the left.

GLASERIAN FISSURE: According to Klaauw (1931: 164), during ontogeny, the Glaserian fissure (*fissura Glaseri*) forms first in the anterior wall of the presumptive auditory bulla as an aperture for Meckel's cartilage. Meckel's cartilage subsequently disappears and "later on we find the chorda tympani nerve in it and often the ramus inferior of the stapedial artery". As the elements forming the auditory bulla vary among mammals (Klaauw, 1931; Novacek, 1977), so do the elements forming the Glaserian fissure. In the dog (Evans, 1993), the chorda tympani nerve (*chorda tympani*) passes through a small canal in the anterodorsal wall of the auditory bulla and emerges through the petrotympanic fissure by a small opening medial to the postglenoid process. In the *Pteropus* fetus, Meckel's cartilage and the chorda tympani nerve leave the middle ear via a wide gap floored by the

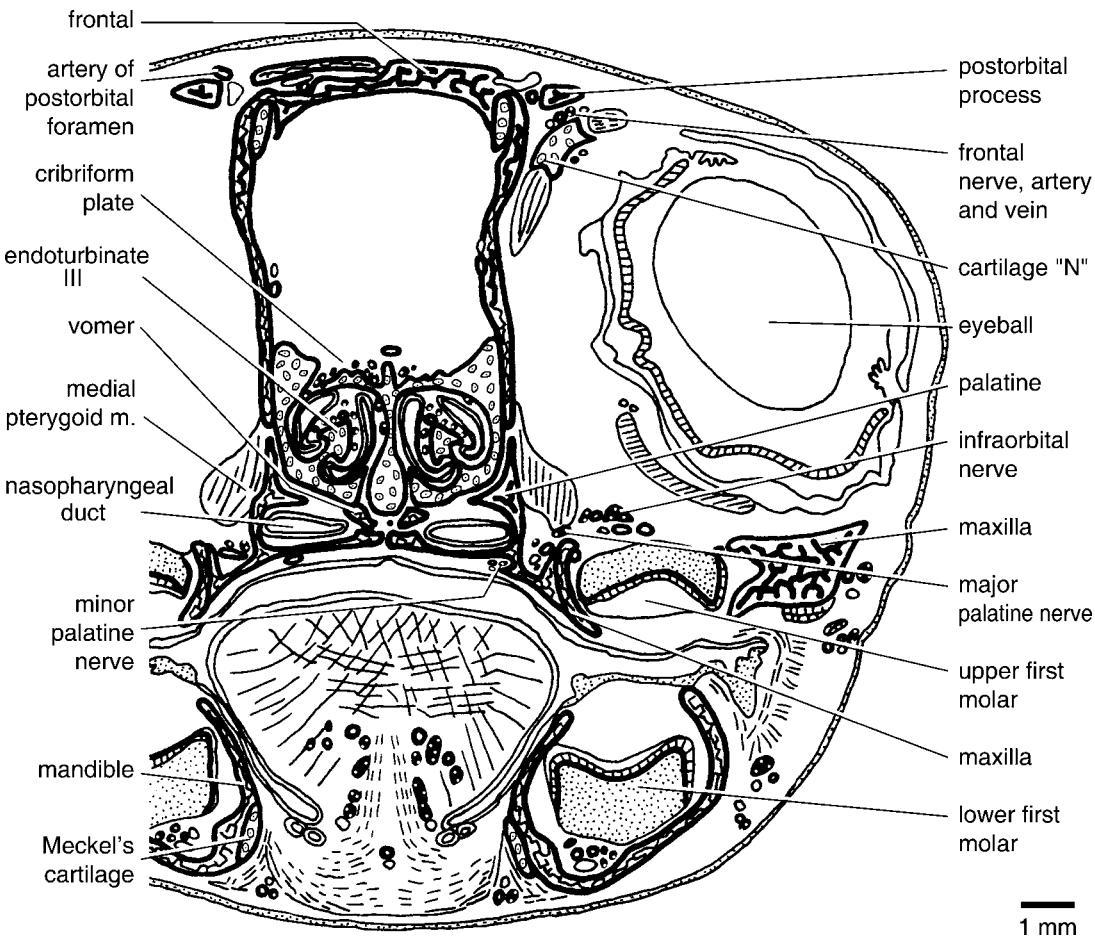

Fig. 31. *Pteropus* sp. DUCEC 831, schematic representation of part of slide 42-1, a frontal section through the orbit at the postorbital process. The artery of the postorbital foramen penetrates the postorbital foramen in the postorbital process, and the frontal nerve, artery, and vein pass anteroventral to the postorbital process. On the left side, a frontal diploic vein (unlabeled) enters a small foramen medial to the postorbital foramen. For cartilage "N", we follow Jurgens (1963: 19), who named it in *Rousettus aegyptiacus* as an enigmatic "discrete convex cartilaginous plate in the orbit . . . it lies medio-dorsally to the anterior part of the sclera with its dorsal edge in the upper eyelid and its ventral part embedded in glands." In *Pteropus* sp., it is closely associated with the m. levator palpebrae superioris.

gonial, roofed by the squamosal, and with open medial and lateral walls (fig. 33). According to Fleischer (1973), the gonial (rostral process of the malleus in part) is fused to the anterior crus of the ectotympanic in adult *Pteropus*, but in *P. lylei* CM 87971–87973, seams still distinguish these elements. In *P. lylei* CM 87971 and 87973, the Glaserian fissure is actually a foramen between the gonial and squamosal, with a distinct groove for the nerve present on the dorsal surface of the gonial.

HIATUS FALLOPII: In the dog (Evans, 1993), the greater petrosal nerve runs forward from the geniculate ganglion (*ganglion geniculi*) of the facial nerve within the petrous temporal (petrosal) in a canal termed the petrosal canal, dorsal to the fossa for the m. tensor tympani. It exits the petrosal canal at a small aperture near the distal end of the petrosquamous suture. For the opening transmitting the greater petrosal nerve from the petrosal, we employ the term hiatus Fallopii (McDowell, 1958); for the space

housing the geniculate ganglion, we employ the term cavum supracochleare (Voit, 1909). In the *Pteropus* fetus, a bone-enclosed hiatus Fallopii is lacking, as is a bone-enclosed cavum supracochleare. The geniculate ganglion sits in a depression on the top of the pars cochlearis, and the greater petrosal nerve runs forward also on top of the pars cochlearis, accompanied by a vein that drains into the cavernous sinus (fig. 35). In *P. lylei* CM 87972, the hiatus Fallopii is hidden from view. However, in *P. livingstonii* AMNH 274477, which has isolated petrosals, the hiatus Fallopii is represented by a well-developed, balloon-shaped opening best viewed in lateral view (fig. 15). Forming the roof of this aperture is the ossified prefacial commissure (suprafacial commissure of Jurgens, 1963). The hiatus Fallopii appears to be larger than the structures that it transmits; one can see into the cavum supracochleare and view both the primary and secondary facial foramina from the hiatus. Reconstructing the isolated petrosal onto the skull, it is apparent that the hiatus Fallopii opens above the plane of the piriform fenestra. Therefore, the greater petrosal nerve exits the piriform fenestra to join the internal carotid (deep petrosal) nerve (*nervus caroticus interna*) beneath the carotid foramen.

HYPOGLOSSAL FORAMEN: In the dog (Evans, 1993), the hypoglossal foramen, the external opening of the hypoglossal canal (*canalis nervum hypoglossum*), is in the exoccipital bone, posterolateral to the jugular foramen; it transmits the hypoglossal nerve and vein. In the *Pteropus* fetus, the hypoglossal foramen is nearly entirely within the exoccipital ossification; the anteromedial border is formed by the cartilage in the chondrocranium's central stem that separates the exoccipital and basioccipital ossifications. Transmitted are the hypoglossal nerve (*nervus hypoglossus*) and vein (*vena canalis hypoglossi*) and a caudal meningeal branch (*arteria meningea caudalis*) of the occipital artery (*arteria occipitalis*). Sutures delimiting the exoccipital and basioccipital are not fully preserved in *P. lylei* CM 87972 (see fig. 5). However, the sutures are preserved in *Pteropus temminckii* AMNH 194276, and the hypoglossal foramen is entirely within the exoccipital.

INCISIVE FISSURE: The dog (Evans, 1993) has paired palatine fissures (= incisive foramina of this report) largely in the incisive bone (= premaxilla of this report) but with the posterior border formed by the maxilla. The occupants are the nasopalatine duct (*ductus incisivus*) connecting the vomeronasal organ (*organum vomeronasale*) to the oral and nasal cavities (*cavum oris* and *cavum nasi*, respectively), the rostral septal branches (*rami septi rostrales*) of the major palatine artery of V_2 (*arteria palatina major*), and the septal branch of the caudal nasal nerve of V_1 (*nervus nasopalatinus*). In contrast, *Pteropus lylei* has one large gap between the premaxillae and maxillae in the anterior hard palate, which we call here the incisive fissure (figs. 3, 9). In the *Pteropus* fetus, the incisive fissure is not as large as it appears in macerated adult skulls, because it is floored posteriorly by paired palatine cartilages that abut each other on the midline, dorsomedially by the anterior paraseptal cartilages, and laterally by the premaxillae (figs. 29, 30). These cartilages correspond to, but are much larger than, the cartilago palatini described by Jurgens (1963); each palatine cartilage is continuous anteriorly with the lamina transversalis anterior (fig. 29). The major occupants of the gap anterior to these cartilages are the paired nasopalatine ducts (fig. 29), which connect the oral and nasal cavities; the vomeronasal organ is lacking. In addition, there are several paired nasal cartilages that extend into the incisive fissure from above: the nasopalatine duct cartilage, which covers the anterior surface of the nasopalatine duct, and the ventral part of the lamina transversalis anterior, which is interposed between the nasopalatine duct cartilage and the paraseptal cartilage. Also anteromedial to the exits of the nasopalatine ducts are the septal branches of the paired caudal nasal nerves of V_2, also called the nasopalatine nerves (fig. 29). No major vessels are transmitted. However, there is a tiny midline gap between the maxillae and palatine cartilages that transmits an artery from the palate into the nasal cavity. This artery runs forward under the nasal septum and divides into right and left arteries to the tip of the snout.

INFRAORBITAL CANAL, INFRAORBITAL FORAMEN, AND MAXILLARY FORAMEN: In

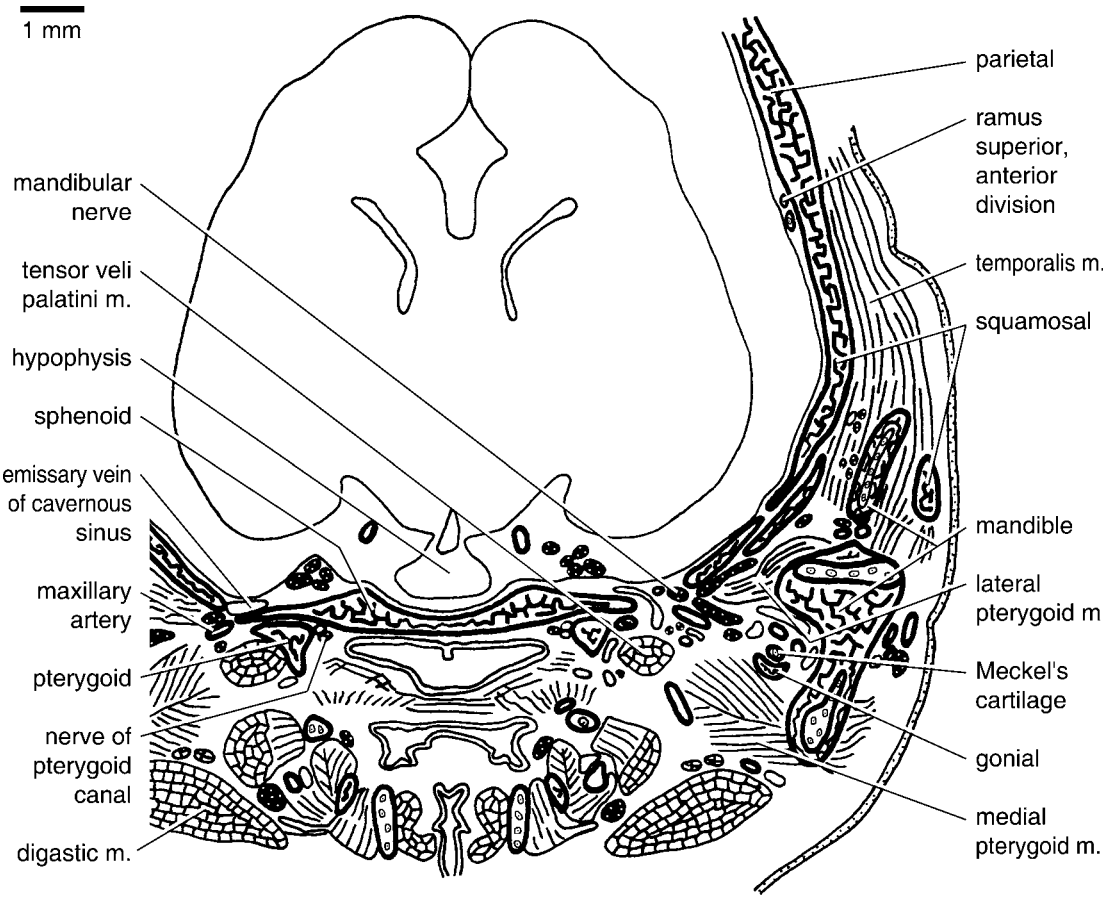

Fig. 32. *Pteropus* sp. DUCEC 831, schematic representation of part of slide 63-1, a frontal section through the temporal fossa at the foramen ovale and fossa hypophysialis. The basisphenoid (housing the fossa hypophysialis) and alisphenoids (housing the foramen ovale) are a single ossification. In sections rostral to this one, the nerve of the pterygoid canal enters the pterygoid canal between the pterygoid and sphenoid. The inferior alveolar nerves and vessels (unlabeled) lie between the mandible and Meckel's cartilage.

the dog (Evans, 1993), the infraorbital canal carries the infraorbital nerve of V_2 (*nervus infraorbitalis*), artery (*arteria infraorbitalis*), and vein (*vena infraorbitalis*) from the orbit to the snout. The anterior opening of each infraorbital canal on the snout, the infraorbital foramen, is within the maxilla, and the posterior opening in the orbit, the maxillary foramen, is between the maxilla, lacrimal, and jugal. The infraorbital canal is roughly the same length as the enlarged upper carnassial tooth (*dens sectorius*), the ultimate upper premolar. In *Pteropus lylei* CM 87972, the infraorbital canal is entirely within the maxilla, dorsal to the M1 (figs. 2, 12). Its anterior opening on the face, the infraorbital foramen, and its posterior opening in the orbit, the maxillary foramen, are nearly contiguous because the infraorbital canal is very short. The orbital process of the lacrimal approaches but does not quite contribute to the dorsal margin of the maxillary foramen. Based on the *Pteropus* fetus, the infraorbital canal transmits the infraorbital nerve, artery, and vein (visible within the orbit in fig. 31).

INTERNAL ACOUSTIC MEATUS: For the internal acoustic meatus, we rely on the

anatomy of the horse (Sisson, 1910), for which greater detail is provided than for the dog. In the horse, the internal acoustic meatus is a short canal on the endocranial surface of the petrous temporal (petrosal) that transmits the facial and vestibulocochlear nerves (*nervus facialis* and *nervus vestibulocochlearis*, respectively) and the internal auditory artery (*arteria labyrinthi*) off the basilar artery (*arteria basilaris*). It is divided by a transverse crest into dorsal and ventral depressions, the foramen acusticum superius and inferius, respectively. In the anterior part of the foramen acusticum superius is the *area nervus facialis*, the cranial opening of the facial canal, and in the posterior part is the dorsal vestibular area perforated by foramina transmitting nerves to the utricle and the *ampullae* of the anterior and lateral semicircular canals. In the foramen acusticum inferius is the *area cochleae*, a central foramen with a spiral tract of minute foramina (*tractus spiralis foraminosus*) for fascicles of the cochlear nerve (*nervus cochlearis*). Posterior to this are small openings transmitting nerves to the saccule and a foramen singulare for the nerve to the ampullae of the posterior semicircular canal. As described by Evans (1993), the internal acoustic meatus of the dog conforms to this pattern, although the details of nervous passages are not as thoroughly described. Rather than a canal, however, the internal acoustic meatus of the dog is an irregularly elliptical depression, and the opening into the depression is the external acoustic porus (*porus acusticus externus*). The internal acoustic meatus in the isolated petrosals of *Pteropus livingstonii* AMNH 274477 conforms to the pattern of that in the dog (fig. 14). The meatus is figure eight–shaped, with the dorsal depression smaller than the ventral one. Visible within the dorsal depression is the aperture by which the facial nerve reaches the cavum supracochleare and the small dorsal vestibular area. Visible within the anterior part of the ventral depression are two central foramina perforated by tiny apertures for the cochlear nerves. Posterior to this are small openings, but we were unable to distinguish one as the foramen singulare. In the *Pteropus* fetus, the internal acoustic meatus resembles that in the dog and adult with one principal exception: the nerves to the saccule and ampulla of the posterior semicircular canal pass through a single opening. A separate foramen singulare is reported for fetal *Rousettus aegyptiacus* (Jurgens, 1963) but not for fetal *R. leschenaulti* (= *Pteropus seminudus*; Starck, 1943).

JUGULAR FORAMEN: In the dog (Evans, 1993), the jugular foramen is between the petrous temporal (petrosal) and the occipital; based on the disarticulated skull of a puppy (Evans, 1993: fig. 4–45), it appears to be largely or wholly the exoccipital bone that borders the jugular foramen. After exiting through the jugular foramen, its contents—the glossopharyngeal (cranial nerve IX), vagus (X), and accessory nerves (XI; i.e., *nervus glossopharyngeus*, *nervus vagus*, and *nervus accessorius*, respectively) and the sigmoid sinus (*sinus sigmoideus*)—then pass through the petro-occipital and tympano-occipital fissures to reach the skull base. In the *Pteropus* fetus, the borders of the jugular foramen are formed by the petrosal laterally and the exoccipital medially, with the unossified portions of the chondrocranium that connect these bones forming the anterior and posterior borders. Occupying the jugular foramen from front to back are the internal jugular vein, the glossopharyngeal, vagus, and accessory nerves, and a caudal meningeal branch of the occipital artery. In the dog, the sigmoid sinus and inferior petrosal sinus join to form the internal jugular vein below the skull base. In the *Pteropus* fetus, the principal exit of the sigmoid sinus is the foramen magnum, but it does have a connection with the inferior petrosal sinus intracranially, with the internal jugular vein then exiting the jugular foramen. *P. lylei* CM 87972 preserves the part of the suture between the basioccipital and exoccipital near the jugular foramen (figs. 3, 5). It shows that foramen is bordered by the pars cochlearis of the petrosal anteriorly, the pars canalicularis of the petrosal laterally, and the exoccipital medially and posteriorly on the left side. On the right side, the basioccipital has a very narrow medial contribution.

LACRIMAL FENESTRA: The right side of *Pteropus lylei* CM 87973 has a small, oval opening in the suture between the orbital

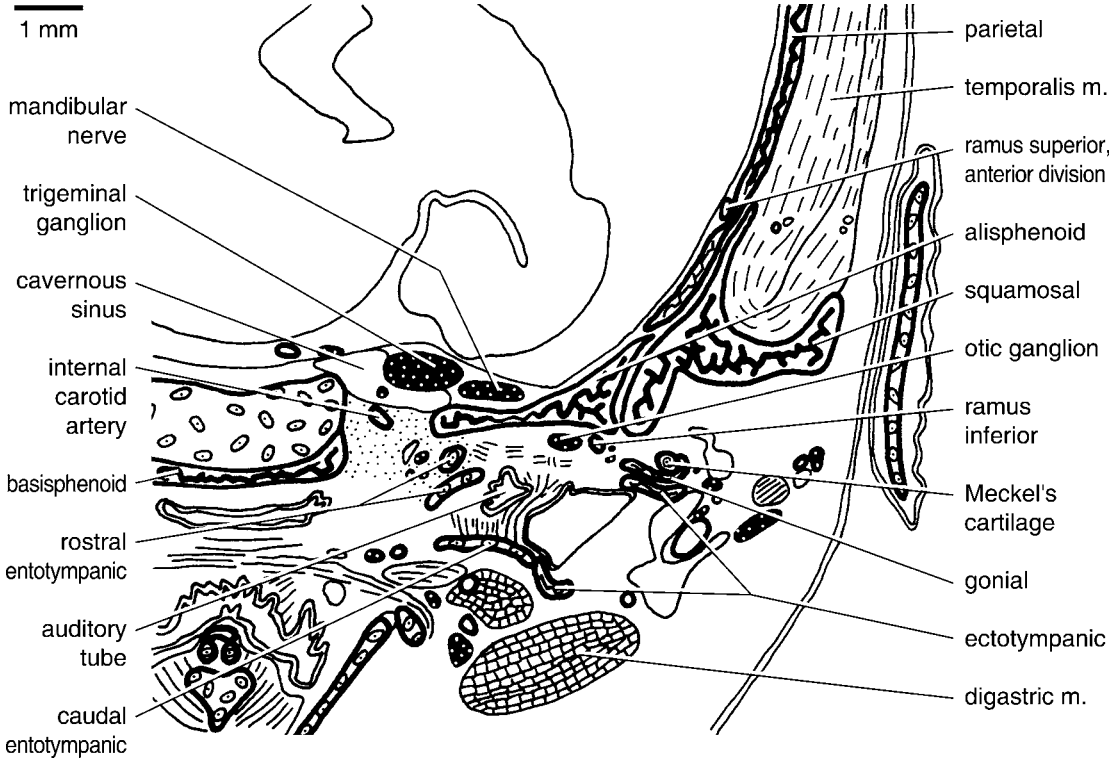

Fig. 33. *Pteropus* sp. DUCEC 831, schematic representation of part of slide 68-2, a frontal section through the basicranium at the carotid foramen, which is continuous laterally with the front of the piriform fenestra and posteriorly with the basicochlear fissure. The chorda tympani nerve (unlabeled) lies in the Glaserian fissure, between the ramus inferior and otic ganglion medially, and Meckel's cartilage, the gonial, and the anterior crus of the ectotympanic laterally.

processes of the lacrimal and frontal, slightly below the level of the lacrimal foramen; the specimen's left side has a shallow pit there, as is present bilaterally in CM 87972 (fig. 12). Based on the *Pteropus* fetus, this accommodates one of the extraocular muscles, the inferior oblique (*musculus obliquus ventralis*), which attaches to the lacrimal and the underlying nasal capsule. A similar arrangement has been reported for the yellow armadillo, with the aperture called the lacrimal fenestra (Wible and Gaudin, 2004).

LACRIMAL FORAMEN: In the dog (Evans, 1993), there is a large opening in the center of the orbital process of the lacrimal called the fossa for the lacrimal sac (*fossa sacci lacrimalis*). The lacrimal sac is formed by the union of the two lacrimal ducts (each one a *canaliculus lacrimalis*), one from each eyelid (*palpebra*), and in turn leads into the lacrimal canal, which transmits the nasolacrimal duct forward to the nasal vestibule (*vestibulum nasi*). Here, we use the term foramen lacrimale from the NAV for the bony aperture that transmits the nasolacrimal duct from the lacrimal fossa to the lacrimal canal. In *Pteropus lylei* CM 87972, the large lacrimal foramen is in the anteroventral aspect of the facial process of the lacrimal, with the maxilla forming its ventral margin (figs. 2, 12). Based on the *Pteropus* fetus, the sole occupant of the lacrimal foramen is the nasolacrimal duct.

MAJOR PALATINE FORAMEN: In the dog (Evans, 1993), the major palatine nerve (*nervus palatinus major*) off the pterygopalatine nerve of V_2 (*nervus pterygopalatinus*) supplies the rostral hard palate, which it reaches via the major palatine foramen at the palatomaxillary suture. In the *Pteropus* fetus,

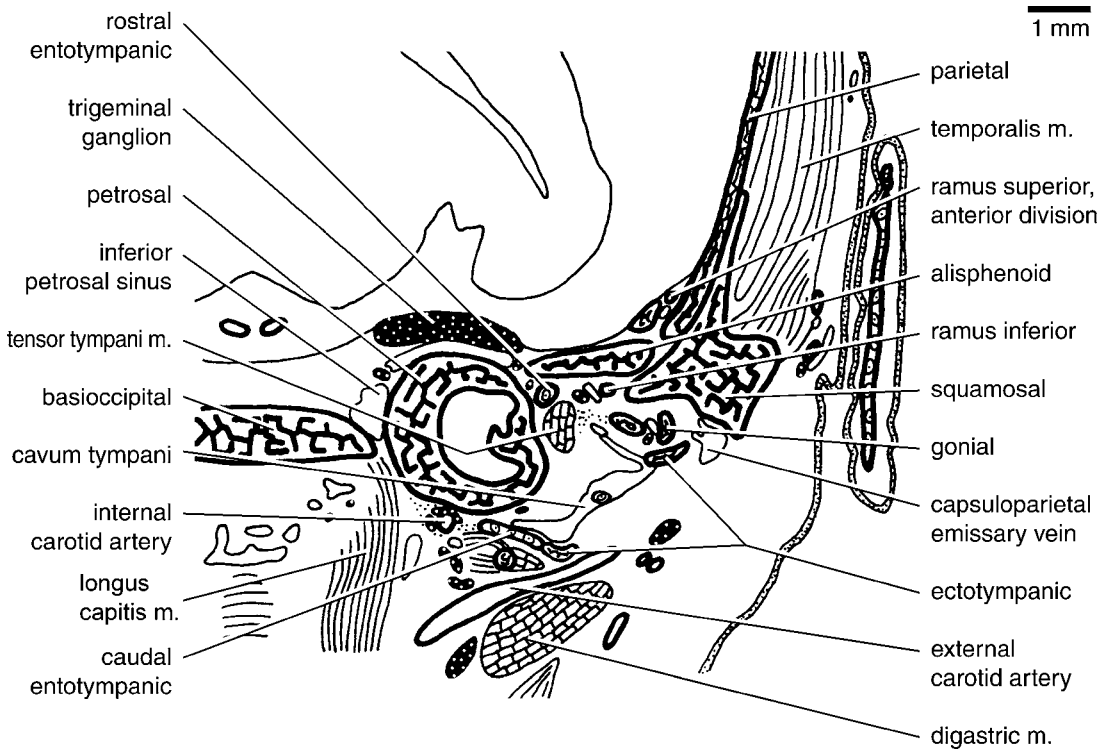

Fig. 34. *Pteropus* sp. DUCEC 831, schematic representation of part of slide 71-2, a frontal section through the basicranium at the postglenoid process. The gap between the petrosal and alisphenoid is the back of the piriform fenestra; the gap between the petrosal and basisphenoid is the front of the basicochlear fissure. The internal carotid artery runs through a mass of connective tissue fibers, the fibrous membrane of the tympanic cavity of MacPhee (1981). The chorda tympani nerve (unlabeled) penetrates a foramen in the gonial. The anterior division of the ramus superior penetrates a foramen in the ventral aspect of the parietal, which represents the epitympanic wing. The capsuloparietal emissary vein lies beneath the postglenoid process; the postglenoid foramen is in sections rostral to this one.

the major palatine nerve and artery (*arteria palatina major*) arise from the pterygopalatine nerve of V_2 within the orbit (fig. 31), run through the caudal palatine foramen into the palatine canal (see below), and exit onto the hard palate along the anterior contact between the palatine and maxilla. The right side of the fetus has two major palatine foramina: a larger anterior one in the transverse palatine suture, as on the left side, and a smaller posterior one wholly within the palatine. In *P. lylei* CM 87972, the major palatine foramen lies in or in front of the anteriormost suture between the palatine and maxilla and has a short palatine sulcus extending forward from it on the maxilla (figs. 3, 9).

MANDIBULAR FORAMEN: In the dog (Evans, 1993), the mandibular foramen is the caudal opening of the mandibular canal for the inferior alveolar nerve (*nervus alveolaris inferior*) and vessels (*arteria alveolaris inferior et vena alveolaris inferior*); it is located on the medial side of the mandibular ramus, roughly in the anterior–posterior center, below the alveolar plane of the mandibular dentition. In *Pteropus lylei* CM 87972, the posteriorly directed mandibular foramen is centrally located on the mandibular ramus. Extending posteriorly and slightly dorsally from the foramen is a deep sulcus, the dorsal border of which is formed by a low crest that nearly reaches to the condyle. In the fetus, the inferior alveolar nerve, artery, and vein

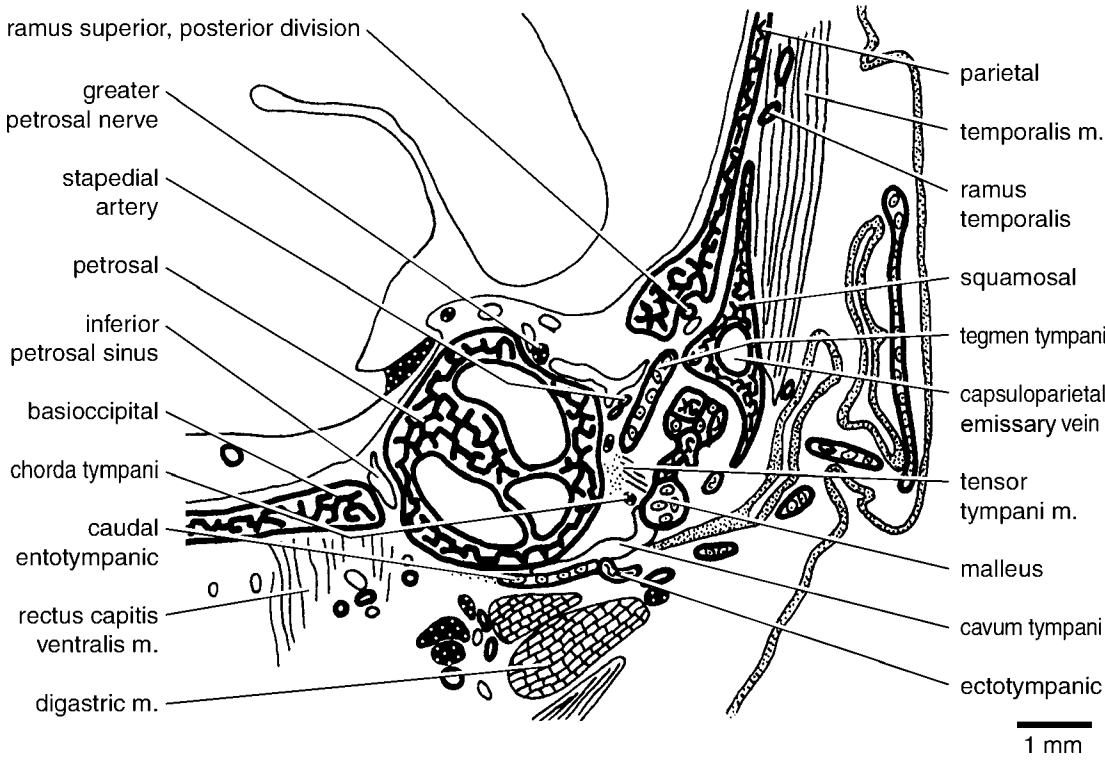

Fig. 35. *Pteropus* sp. DUCEC 831, schematic representation of part of slide 75-1, a frontal section through the basicranium at the epitympanic recess over the mallear-incudal articulation. The inferior petrosal sinus lies in the basicochlear fissure between the petrosal and basioccipital. The posterior division of the ramus superior occupies a sulcus in the ventral aspect of the parietal, which represents the epitympanic wing. The part of the tegmen tympani here is the near vertical component; ventral to it is the tensor tympani muscle's attachment to the malleus, and medial to it is the distal remnant of the stapedial artery, which fails to reach the stapes.

first run in a deep sulcus on the mandibular ramus that is then covered laterally by Meckel's cartilage (fig. 32) and then ultimately enclosed in the mandible.

MASTOID FORAMEN: In the dog (Evans, 1993), the mastoid foramen is on the occiput between the exoccipital, supraoccipital, and mastoid process (= mastoid exposure of the petrosal of this report); it transmits the occipital emissary vein (*vena emissaria occipitalis*), which drains the deep muscles on the cranial part of the neck into the sigmoid sinus. Evans (1993: 608) also reported a caudal meningeal artery off the occipital artery that "goes through the supramastoid foramen and ramifies in the dura of the occipital cranial fossa". The supramastoid foramen is not mentioned elsewhere in the text, and we speculate that it may in fact be the mastoid foramen. In the *Pteropus* fetus, the mastoid foramen is at the junction of the pars canalicularis of the auditory capsule (*capsula otica*), exoccipital, and supraoccipital and transmits the occipital emissary vein to the sigmoid sinus. In *P. lylei* CM 87972, the small mastoid foramen (0.4 mm on the left and smaller on the right) is between the mastoid exposure of the petrosal and the occipital (the ex- and supraoccipital being fused; fig. 5); the left mastoid foramen in CM 87973 is comparable in size, but the right one is twice as large. In *Pterotus capistratus* AMNH 194276, a very small mastoid foramen is present on the left side only at the junction of the exoccipital, supraoccipital, and petrosal.

MAXILLARY FORAMEN: See infraorbital canal.

MENTAL FORAMINA: The dog has several mental foramina per side that transmit the mental nerves (*nervi mentales*), artery (*arteria mentalis*), and vein (*vena mentalis*) from the mandibular canal (Evans, 1993). The largest, the middle mental foramen, is beneath the embrasure between the first two cheek teeth. An anterior one is positioned beneath the central incisor, and one or more small foramina are positioned caudal to the middle mental foramen. *Pteropus lylei* CM 87972 has two mental foramina per side: a larger posterior mental foramen beneath p1 and an anterior mental foramen beneath the embrasure between the first and second incisors (fig. 6). The fetus also has two mental foramina, both of which transmit mental nerve, artery, and vein: a medial one just off the midsagittal line beneath the i1 and a lateral one beneath the first deciduous premolar.

MINOR PALATINE FORAMINA: In the dog (Evans, 1993), the minor palatine nerve (*nervus palatinus minor*) off the pterygopalatine nerve of V_2 supplies the soft palate, and the caudal part of the hard palate is supplied by an accessory palatine nerve off the major palatine nerve, which in turn supplies the rostral hard palate. In the *Pteropus* fetus, the nerves that supply the soft palate also supply the caudal hard palate. We identify these as minor palatine nerves and their foramina in the palate as the minor palatine foramina, following Wible and Rougier (2000). As in the dog, the minor palatine nerves in the *Pteropus* fetus arise from the pterygopalatine nerve off V_2 lateral to the m. pterygoideus medialis and pass through three asymmetrically arranged, small foramina in the posterolateral border of the palatine, accompanied by branches of the minor palatine artery (*arteria palatina minor*) derived from the maxillary artery (*arteria maxillaris*). In *P. lylei* CM 87972, the two posteriormost foramina on the left palatine are directed medially and caudally, respectively, and identified by us as minor palatine foramina; on the right side there are three, two directed medially and one caudally (fig. 9).

OPTIC CANAL: In the dog (Evans, 1993), the optic canal (*canalis opticus*) is in the center of the orbital wing of the presphenoid bone (orbitosphenoid) and transmits the optic nerve (*nervus opticus*), the internal ophthalmic artery (*arteria ophthalmica interna*, = ophthalmic artery of this report) off the Circle of Willis (*circulus arteriosus cerebri*), and the internal ophthalmic vein (*vena ophthalmica interna*). In the *Pteropus* fetus, the optic canal is between the presphenoid and orbitosphenoid ossification centers within the orbital cartilages and transmits the same structures as in the dog. Also as in the dog, within the orbit the ophthalmic artery joins the external ophthalmic artery (= the ramus orbitalis of Wible, 1987). In *P. lylei* CM 87972, the presphenoid and orbitosphenoid are fused seamlessly. As interpreted by us, the floor of the ovoid optic canal is formed by the presphenoid and the remaining borders by the orbitosphenoid (fig. 11).

ORBITOTEMPORAL CANAL: In various extant placentals, the anterior division of the ramus superior of the stapedial artery (and accompanying vein) extends from its endocranial origin above the front of the middle ear to the orbit in a channel called the sinus canal (Gregory, 1910; McDowell, 1958) or the orbitotemporal canal (Rougier et al., 1992; Wible et al., 2004). We prefer the latter term, because it best describes the position of this vascular canal, and it best reflects the broader homology of these structures, having already been applied to a broad spectrum of cynodonts (see Rougier et al., 1992). The orbitotemporal canal and its orbital opening are lacking in the dog (Evans, 1993). In the *Pteropus* fetus, the anterior division of the ramus superior arises over the anterolateral aspect of the middle ear in the extracranial space roofed by the epitympanic wing of the parietal and floored by the squamosal and the tympanic roof. The artery enters the cranial cavity via a foramen in the ventrolateral aspect of the parietal epitympanic wing (fig. 34) and runs anterodorsolaterally along the medial surface of the parietal (fig. 33). It enters a gap between that bone laterally and the back of the ala orbitalis (the cartilaginous precursor of the orbitosphenoid) medially and disappears. The existence of the orbitotemporal canal, such as in the fetus, cannot be studied in the intact *Pteropus* skulls. However, in *P. livingstonii* AMNH 274517, a disarticulated skull, the endocranial surfaces of the squamosals and parietals can be

studied. Ventral to the endocranial aperture by which the capsuloparietal emissary vein enters the squamosal, there is a deep, nearly vertical sulcus for the posterior division of the ramus superior. In the anteroventral margin of this sulcus is a notch that leads into a shallow, longitudinal sulcus for the anterior division of the ramus superior that runs forward on the endocranial surface of the parietal to the level of the anterior extent of the squamosal. This shallow sulcus represents the open channel for the orbitotemporal canal.

PALATINE CANAL: In the dog (Evans, 1993), the course of the major palatine nerve and artery from the pterygopalatine fossa to the palate is via a palatine canal in the horizontal process of the palatine. The posterior opening into the palatine canal is the caudal palatine foramen (Schaller, 1992). In the *Pteropus* fetus, the palatine canal is only fully enclosed within the palatine in the central portion of the nerve's course through that bone. Posteriorly, between the minor palatine foramina and the caudal palatine foramen, the major palatine nerve and artery occupy a deep sulcus that is open dorsally into the pterygopalatine fossa (fig. 31). It is in the ventral floor of this sulcus that all but one of the accessory palatine foramina are found. Anteriorly, just behind the major palatine foramen, there is another sulcus for the major palatine nerve and artery that is open dorsally in the floor of the nasopharyngeal meatus. In *P. lylei* CM 87972, a posterior sulcus is clearly retained in the pterygopalatine fossa and leads to the posterior opening into the palatine canal, opposite the anterior root of the last molar, M2 (fig. 12). The existence of an anterior sulcus as in the fetus cannot be confirmed or denied in the adult without CT scans of the specimen.

PIRIFORM FENESTRA: The piriform fenestra is the large gap present in all fetal mammals and in a few adults anterior to the auditory capsule, usually between that element, the sphenoid (basi- and alisphenoid), and the squamosal (MacPhee, 1981). These elements are in close contact in the adult dog (Evans, 1993), and, therefore, the piriform fenestra is absent. In the *Pteropus* fetus, the piriform fenestra is between the anterior pole of the promontorium and the basi-/alisphenoid and is continuous medially with the carotid foramen (there being no alicochlear commissure). Flooring the piriform fenestra is the rostral entotympanic. Running across the piriform fenestra dorsal to this cartilage is the greater petrosal nerve, which joins the internal carotid (deep petrosal) nerve beneath the carotid foramen. Entering the cavum epiptericum via the piriform fenestra are a nerve connecting the greater petrosal nerve and the mandibular nerve and a vein draining from the auditory capsule to the cavernous sinus. In *P. lylei* CM 87972, the piriform fenestra is an obliquely oriented, roughly cigar-shaped opening between the anterior pole of the promontorium and the alisphenoid (figs. 3, 5, 10); the epitympanic wing of the parietal approximates but does not contribute to the posterolateral border. The piriform fenestra is continuous medially with the carotid foramen; these apertures are separated by a narrow petrosal-alisphenoid contact in CM 87973.

POSTGLENOID FORAMEN: In the dog (Evans, 1993), the retroarticular foramen (= postglenoid foramen) lies in the squamous part of the temporal bone (= squamosal), behind the retroarticular process (= postglenoid process). It transmits the retroarticular vein (= postglenoid vein or capsuloparietal emissary vein of Gelderen, 1924), a major distributary of the transverse sinus (*sinus transversus*). In the *Pteropus* fetus, over the back of the auditory capsule the transverse sinus divides into a posteroventrally directed sigmoid sinus and an anteriorly directed sinus. The latter soon divides into the dorsal petrosal sinus and the capsuloparietal emissary vein. The capsuloparietal emissary vein continues forward into a space at first between the dorsolateral aspect of the pars canalicularis of the auditory capsule and the parietal, but then bordered by the squamosal bone as well; passing through the anterior part of this space is the ramus superior of the stapedial artery. Over the epitympanic recess, the capsuloparietal emissary vein enters the squamosal bone (fig. 35). Anterolateral to the epitympanic recess (*recessus epitympanicus*), the vein leaves the squamosal via the postglenoid foramen in company with a tiny artery off the posterior auricular artery (*arteria auricularis caudalis*).

In *P. lylei* CM 87972, the postglenoid foramen is in the squamosal, although the anterior crus of the ectotympanic approaches its posteromedial margin (figs. 3, 5, 11). On the right side of *P. lylei* CM 87973, the alisphenoid approaches the anteromedial margin as well.

POSTORBITAL FORAMEN: The name postorbital (or frontal) foramen for the large opening in the anterior root of the postorbital process of the frontal bone has been regularly used in the megachiropteran literature since the nineteenth century (see references in Andersen, 1912). Prior to our study, we anticipated that the occupants of the postorbital foramen in *Pteropus* were the frontal nerve of V_1 (*nervus frontalis*) and accompanying vessels, which occupy analogous positions in other placentals (e.g., the rabbit, Bensley, 1931; the dog, Evans, 1993). If true, the postorbital foramen of *Pteropus* would be analogous to the supraorbital foramen of human anatomy, as Andersen (1912) proposed. However, in the fetus (fig. 31), the frontal nerve and accompanying vessels leave the orbit anterior to the postorbital process and move laterally onto the side of the snout. Instead, the postorbital foramen transmits a tiny branch of the frontal nerve and a large artery and vein. The large artery runs anteriorly along the frontal bone and then along the nasomaxillary suture to ramify in the tip of the snout (figs. 29, 30). Within the orbit, the large artery and vein ultimately join the vessels accompanying the frontal nerve (fig. 31). We are uncertain what to name this large artery, because that accompanying the frontal nerve is best called the postorbital (supraorbital) artery. Because this vessel with its long rostral course is to our knowledge unique, we have chosen to call it the artery of the postorbital foramen.

POSTTEMPORAL CANAL: In monotremes and some placentals, the posterior division of the ramus superior of the stapedial artery, the arteria diploëtica magna of Hyrtl (1853, 1854), and an accompanying vein travel in a canal between the petrosal and squamosal that opens onto the occiput (Wible, 1987; Wible and Hopson, 1995). For this channel, we employ the term posttemporal canal, which is widely used in the literature of nonmammalian cynodonts (Wible, 1989; Rougier et al., 1992). The posttemporal canal is wholly absent in the dog. The *Pteropus* fetus has a short segment of the posttemporal canal, but it is a blind canal with no egress on the occiput. It begins anteriorly beneath the posterior foramen for ramus temporalis where the tiny continuation of the posterior division of the ramus superior or arteria diploëtica magna and a sizable vein enter a canal between the squamosal, parietal, and pars canalicularis of the auditory capsule, just above the fossa incudis. Behind the posterior extent of the squamosal, the canal continues posteriorly a short distance between the parietal and the gyrus of the anterior (superior) semicircular canal. The artery disappears, whereas the vein runs endocranially over the pars canalicularis into the transverse sinus. Regarding the existence of the posttemporal canal in adult *Pteropus*, we were not able to identify any grooves indicating this canal on the isolated petrosals, squamosals, and parietals studied with *P. livingstonii* AMNH 274477 and 274517.

PTERYGOID CANAL: In the dog (Evans, 1993), an extremely small pterygoid groove on the basisphenoid runs anteriorly into a minute pterygoid canal. The caudal opening of the pterygoid canal is in the suture between the basisphenoid and pterygoid, and the rostral opening is in the caudal part of the pterygopalatine fossa, between the pterygoid and pterygoid process of the sphenoid (the ventral projection of the sphenoid that abuts the pterygoid bone). Transmitted are the nerves of the pterygoid canal (*nervus canalis pterygoidei*) and occasionally a small artery of the pterygoid canal off the maxillary artery. In the *Pteropus* fetus, the greater petrosal nerve (*nervus petrosus major*) and internal carotid (deep petrosal) nerve form the nerve of the pterygoid canal beneath the carotid foramen. The nerve of the pterygoid canal runs forward between the basi-/alisphenoid and the tiny tubal cartilage, and then enters the cavum epiptericum via a foramen between the basi-/alisphenoid and the underlying pterygoid (fig. 32). Within the cavum epiptericum, the nerve enters the pterygopalatine ganglion off V_2. During its course within the cavum, the nerve is accompanied by a tiny artery off the maxil-

lary artery. In *P. lylei* CM 87973, the nerve of the pterygoid canal runs in a tiny, oblique canal between the basisphenoid and rostral entotympanic immediately anterior to the carotid foramen. It then crosses the ventrolateral surface of the basisphenoid without any bony impression and enters a small foramen in the suture between the basisphenoid and pterygoid. The foramen opens within the braincase, but it can be viewed via the sphenorbital fissure. The placement of the caudal opening of the pterygoid canal in *P. lylei* CM 87972 is indicated in figure 10.

SECONDARY FACIAL FORAMEN: In the dog (Evans, 1993), the course of the facial nerve through the petrous temporal (petrosal) between the internal acoustic meatus endocranially and the stylomastoid foramen on the skull base is entirely within a bony facial canal. In *Pteropus livingstonii* AMNH 274477, the course of the facial nerve through the middle ear is within a sulcus that is walled laterally by the crista parotica (De Beer, 1937) and ends posteriorly at the stylomastoid notch. To reach this sulcus, the facial nerve passes from the internal acoustic meatus endocranially to the cavum supracochleare within the petrosal to the middle ear, the cavum supracochleare (Voit, 1909) being the space housing the geniculate ganglion. Following Wible (1990), we identify the foramen of entrance into the cavum supracochleare from the internal acoustic meatus as the primary facial foramen, and the foramen of entrance into the middle ear from the cavum supracochleare as the secondary facial foramen. The secondary facial foramen in *P. livingstonii* AMNH 274477 is fully enclosed in bone and lies anterolateral to the fenestra vestibuli (fig. 13). In the *Pteropus* fetus, the secondary facial foramen is not yet fully enclosed in bone and/or cartilage and is represented by a notch in the anterolateral aspect of the pars cochlearis of the petrosal.

SPHENOPALATINE FORAMEN: In the dog (Evans, 1993), the caudal nasal nerve (*nervus nasalis caudalis*) off the pterygopalatine nerve of V_2 and sphenopalatine artery (*arteria sphenopalatina*) and vein (*vena sphenopalatina*) leave the pterygopalatine fossa and enter the nasal cavity via the sphenopalatine foramen (*foramen sphenopalatinum*) in the palatine bone, which lies just dorsal to the caudal palatine foramen. The *Pteropus* fetus has two foramina in the palatine dorsolateral to the palatine canal that transmit caudal nasal nerves and sphenopalatine arteries into the nasopharyngeal meatus and nasal cavity. The larger, anteroventral foramen sends nerves and vessels forward into the ventrolateral aspect of the nasal cavity, and the smaller, posterodorsal foramen sends nerves and vessels forward along the ventromedial aspect of the nasal cavity, lateral to the vomer. The latter nerves and vessels reach their foramen in the palatine via a course through the origin of the m. pterygoideus medialis, whereas the former run ventral to that muscle. *P. lylei* CM 87973 has two openings in the palatine that probably correspond to the two sphenopalatine foramina occurring in the fetus, whereas CM 87972 has only one (fig. 12). These foramina lie anterior and dorsal to the caudal palatine foramen.

SPHENORBITAL FISSURE: In the dog (Evans, 1993), the orbital fissure (*fissura orbitalis*) lies lateral to the body of the sphenoid in the suture between the orbital and temporal wings (orbito- and alisphenoid). It transmits the oculomotor (cranial nerve III), trochlear (IV), ophthalmic (V_1), and abducens nerves (VI; i.e., *nervus oculomotorius*, *nervus trochlearis*, *nervus ophthalmica*, and *nervus abducens*, respectively), the anastomotic artery (*arteria anastomotica*) connecting the maxillary and internal carotid arteries, and the ophthalmic venous plexus (*plexus ophthalmicus*). The maxillary nerve (cranial nerve V_2, *nervus maxillaris*) has a foramen of exit separate from the ophthalmic nerve: the foramen rotundum into the substance of the alar canal (alisphenoid canal of Gregory, 1910) and then into the orbit via the rostral alar foramen. The other principal occupant of the alar canal, the maxillary artery, has a course wholly outside the cranial cavity. It enters the caudal opening of the alar canal on the basicranium, in the base of the temporal wing of the basisphenoid (alisphenoid), anterior to the foramen ovale, and enters the orbit with the maxillary nerve. Within the orbit, the maxillary artery supplies the external ophthalmic artery. Between the orbital fissure and the rostral alar foramen, a small *foramen alare parvum* may

be present, transmitting the zygomatic nerve from the alar canal to the orbit.

In the *Pteropus* fetus, there is a single foramen of exit for the various structures passing through the orbital fissure, foramen rotundum, and alar canal of the dog. This aperture, which we term the sphenorbital fissure (*fissura sphenorbitalis*) as in Gregory (1910) but also including the foramen rotundum, is between the alisphenoid, orbitosphenoid, the cartilaginous central stem between the pre- and basisphenoid ossifications, pterygoid, and palatine. It transmits two distinct bundles of structures within their respective connective tissue sheaths from the cavum epiptericum to the back of the orbit. Superiorly are the oculomotor, trochlear, ophthalmic (V_1), and abducens nerves, the external ophthalmic artery or ramus orbitalis (sensu Wible, 1987), and the ophthalmic venous plexus. Inferiorly are the maxillary nerve (V_2), the maxillary artery or ramus infraorbitalis (sensu Wible, 1987), and accompanying veins. The maxillary artery enters the cavum epiptericum via the foramen ovale, and during its intracranial course sends off the external ophthalmic artery. The *Pteropus* fetus is further distinguished from the dog by the position of the pterygopalatine ganglion on the maxillary nerve; in the dog it lies within the orbit, well anterior to the rostral opening of the alar canal, but in the bat it is within the cavum epiptericum.

In *Pteropus lylei* CM 87972, the large sphenorbital fissure is between the alisphenoid, orbitosphenoid, and pterygoid, with the palatine nearly contributing to its floor (fig. 11). On the right side of CM 87972 and bilaterally in CM 87973, the alisphenoid forming the lateral wall of the sphenorbital fissure has a distinct medial process that partially divides that opening into superior and inferior halves. This partial division reflects the situation in the fetus, with its distinct superior and inferior bundles.

In summary, *Pteropus* has a single opening (sphenorbital fissure) that serves the function of the orbital fissure, foramen rotundum, rostral alar foramen, and foramen alare parvum of the dog. Additionally, two structures present in the orbit in the dog are present in the cavum epiptericum of *Pteropus*: the external ophthalmic artery and the pterygopalatine ganglion (*ganglion pterygopalatinum*).

STYLOMASTOID FORAMEN: In the dog (Evans, 1993), the stylomastoid foramen (*foramen stylomastoideum*) is the opening that transmits the facial nerve from the middle ear to the posterolateral surface of the auditory bulla. It is in the posterolateral aspect of the auditory bulla entirely within the petrous temporal (petrosal) and is also occupied by the stylomastoid artery (*arteria stylomastoidea*, sometimes double) off the posterior (caudal) auricular artery. In the *Pteropus* fetus, the facial nerve leaves the middle ear via a gap between the cartilaginous tympanohyoid laterally and ventrally and the m. stapedius medially. Also transmitted is a small artery to the m. stapedius from the posterior auricular artery. In *P. lylei* CM 87973 and *P. livingstonii* AMNH 274477, the exit of the facial nerve is the stylomastoid notch (fig. 13). Flooring the notch is the ossified tympanohyoid, and forming the lateral wall is the crest that represents the posterior continuation of the crista parotica (De Beer, 1937), the lateral section of the caudal tympanic process of the petrosal (MacPhee, 1981).

STAPEDIAL ARTERY: In extant placentals, three major paired arteries supply blood to the adult head: the internal carotid (*arteria carotis interna*) and the vertebral artery (*arteria vertebralis*) supply the brain, and the external carotid (*arteria carotis externa*) supplies extracranial soft tissues (Tandler, 1899, 1901). During development, another major paired artery, the stapedial artery (*arteria stapedia*) off the internal carotid, forms and sends branches that accompany the three divisions of the trigeminal nerve (Tandler, 1902; Wible, 1984, 1987). However, over the course of development in many placentals, including megachiropterans, the stapedial artery involutes, and most or all of its end branches are annexed to the external carotid system (Tandler, 1899, 1901; Bugge, 1974, 1978, 1979; Wible, 1984, 1987). When present, the placental stapedial artery often runs on the back of the promontorium of the petrosal in a groove directed at the fenestra vestibuli (Wible, 1987) and invariably passes through the intracrural foramen of the stapes

(Novacek and Wyss, 1986; Wible, 1987). Beyond the stapes, in the embryonic pattern, the stapedial artery has two major branches: the ramus superior and ramus inferior (Tandler, 1902; Wible, 1984, 1987). The bulk of the course of the ramus superior is within the cranial cavity, where it divides into an anterior division that enters the orbit to supply the ramus supraorbitalis accompanying the branches of the ophthalmic nerve and a posterior division that supplies temporal rami into the temporal fossa and an arteria diploëtica magna that reaches the occiput. In contrast, the bulk of the course of the ramus inferior is extracranial; its principal end branches are the ramus infraorbitalis and ramus mandibularis, which accompany branches of the maxillary and mandibular nerves, respectively.

To date, the cranial arterial pattern has been studied in only three adult megachiropterans: *Pteropus vampyrus* (= *P. edulis*) (Tandler, 1899) and *Rousettus aegyptiacus* and *Rousettus* sp. (= *Cynonycteris aegyptiaca* and *Cynonycteris* sp.) (Grosser, 1901). In all three, the main stem of the stapedial artery is lacking and the end branches of the stapedial artery are annexed to the external carotid system via the maxillary artery. The ramus inferior arises from the maxillary artery behind the foramen ovale, runs posteriorly into the middle ear, and supplies the main stem of the ramus superior. The ramus superior ends endocranially and does not reach the orbit; Grosser (1901) reported temporal rami of the ramus superior, but Tandler (1899) did not. Beyond the origin of the ramus inferior, the maxillary artery (= ramus infraorbitalis) follows an unusual course through the cranial cavity, entering with the mandibular nerve and exiting with the maxillary nerve.

The *Pteropus* fetus studied here shows essentially the same pattern (see also reconstructions in Wible, 1992: figs. 1, 2). However, our study of serial sections provides significantly more detail than the accounts by Tandler (1899) and Grosser (1901). In the fetus, the ramus inferior of the stapedial artery arises from the maxillary artery posteroventral to the foramen ovale. It runs posteriorly beneath the alisphenoid lateral to the otic ganglion (fig. 33), which extends into the front of the middle ear. At the back of the alisphenoid, the ramus inferior moves into a fissure between the epitympanic wing of the parietal dorsally and the squamosal ventrolaterally; this fissure is open ventromedially, dorsal to the plane of the tympanic roof, as defined by the tegmen tympani. Within this fissure, the ramus inferior is joined by an artery that runs dorsally into the cranial cavity through a foramen in the ventromedial aspect of the parietal (fig. 34). This artery, the anterior division of the ramus superior, runs anterodorsally along the endocranial surface of the parietal (fig. 33) and ends between the parietal and the back of the cartilaginous ala orbitalis, the precursor of the orbitosphenoid. The artery formed at the junction of the ramus inferior and anterior division of the ramus superior continues posteriorly in a deep sulcus in the ventral surface of the parietal; ventrolateral to this sulcus is the squamosal and ventromedial is a space above the tegmen tympani and rostral entotympanic, which is occupied medially by the lesser petrosal nerve (*nervus petrosus minus*). After a short course, this artery divides into a smaller stapedial artery that moves posteromedially toward the middle ear and a larger posterior division of the ramus superior that moves posterodorsolaterally, still within a deep sulcus in the parietal that is floored ventrolaterally by the squamosal (fig. 35). The stapedial artery runs in the gap between the tegmen tympani and the pars cochlearis of the petrosal and disappears beneath the secondary facial foramen, far from its embryonic origin from the internal carotid artery. The posterior division of the ramus superior runs dorsal to the capsuloparietal emissary vein as it enters the squamosal and provides the first of two rami temporales, which run dorsolaterally between the parietal and squamosal into the m. temporalis. After the origin of the first ramus temporalis, the posterior division continues posteriorly between the parietal medially and squamosal laterally. The second ramus temporalis is sent off over the fossa incudis, and the small posterior division continues as the arteria diploëtica magna a short distance into the posttemporal canal between the parietal, squamosal, and pars canalicularis of the auditory capsule.

VASCULAR FORAMEN OF THE LACRIMAL: In addition to the lacrimal foramen, CM 87972 (and the other specimens of *Pteropus lylei* examined in this study) has a small foramen in the orbital process of the lacrimal (between the lacrimal and maxilla on the right side) that leads into a canal opening in the posterior floor of the lacrimal foramen (fig. 12), termed here the vascular foramen of the lacrimal. In CM 87973, this foramen is double on the left side. Based on the *Pteropus* fetus, this foramen transmits an artery and vein into the lacrimal canal; these vessels originate from the infraorbital vessels prior to their entrance into the maxillary foramen.

DENTITION

The dental formula in *Pteropus lylei* is I2/2, C1/1, P3/3, M2/3. Homologies of incisor and premolar teeth in bats have been the source of debate for the last century (e.g., Miller, 1907; Andersen, 1912; Handley, 1959; Slaughter, 1970; Thenius, 1989). We follow Andersen (1912) in adopting the following nomenclature for the teeth in *Pteropus*: in the upper dentition, the incisors are assumed to represent I1 and I2, the premolars P1, P3, and P4, and the molars M1 and M2. Similarly, the lower dentition is assumed to include i1, i2, p1, p3, p4, m1, m2, and m3. The dental nomenclature used here includes the following terms: upper and lower tooth rows (*arcus dentalis superior et inferior*), permanent teeth (*dentes permanentes*), deciduous teeth (*dentis decidui*), incisor teeth (*dentes incisivi*), canine teeth (*dentes canini*), premolar teeth (*dentes praemolares*), molar teeth (*dentes molares*), crown (*corona dentis*), shaft (= neck; *collum dentis*), root (*radix dentis*), cusp or cuspule (*cuspis dentis*), *cingulum*, tip of tooth or cusp (*apex cuspidis*), occlusal surface (*facies occlusalis*), lateral (= vestibular, = buccal, = labial) surface (*facies vestibularis*, *facies labialis*), and medial (= lingual) surface (*facies lingualis*). Homology of cusps with respect to a typical tribosphenic molar is discussed in Comparisons: Dentition.

PERMANENT DENTITION

None of the individuals examined for this study exhibited anomalies in dental formulae other than those that can be attributed to age and tooth wear. Anomalies in dental formulae appear to be rare in *Pteropus*; Andersen (1912) examined over 600 skulls of *Pteropus* but found aberrations in dental formulae in only 10 individuals (less than 2%). All of the anomalies noted by Andersen (1912) were found in individuals referred to *Pteropus giganteus*, *P. vampyrus*, or *P. scapulatus*, including: (1) presence of a well-developed i3 on both sides in one individual; (2) presence of a supernumerary p2 in the broad diastema between p1 and p3 on one side in one individual; (3) presence of a supernumerary premolar between p3 and p4 on both sides in one individual; (4) absence of m3 (and its alveolus) on both sides in five individuals and on one side in another; (5) absence of m2 on one side in one individual (which also lacked m3); (6) presence of a m4 on one side in one individual; and (7) presence of M3 on both sides in one individual.

UPPER INCISORS: The upper incisors of *Pteropus lylei* are blunt and somewhat spatulate, with the crown distinct from the shaft (fig. 4). Neither I1 nor I2 has a posterobasal cingulum. Adjacent upper incisors are separated by small diastemata, and do not contact one another at either crown or alveolus. The crowns of opposing right and left I1 converge ventromedially but these teeth never approach contact with one another, even in young animals with unworn teeth (fig. 4). I2 is separated from the upper canine by a large diastema. I1 and I2 are subequal in height, but I1 projects further ventrally as a result of the more ventral position of its alveolus on the premaxilla. The crown of I1 is broader than the crown of I2. The relative proportions of these teeth vary with tooth wear, but the width of I1 never exceeds 1.25 times the width of I2. The crown of I1 is slightly asymmetrical, achieving its greatest height and breadth medial to the long axis of the tooth. This asymmetry is most obvious in unworn teeth and may become somewhat obscured when tooth wear reduces crown height. Faint traces of two cusps are visible on the tip of the crown of I1 in some unworn dentitions (e.g., AMNH 237598), with the medial cusp the larger of the two. Only one cusp is ever visible on I2.

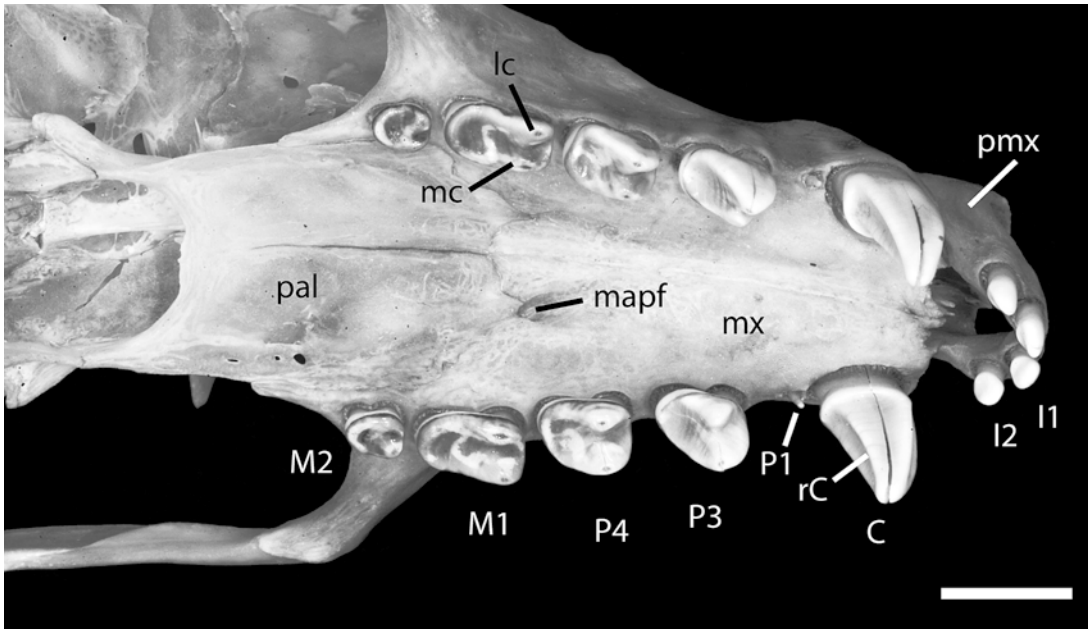

Fig. 36. *Pteropus lylei* AMNH 237595, ventrolateral view of the permanent upper dentition and hard palate. Scale = 5 mm. Abbreviations: **C** upper canine; **I1** first upper incisor; **I2** second upper incisor; **lc** lateral cusp of cheek teeth; **M1** first upper molar; **M2** second upper molar; **mapf** major palatine foramen; **mc** medial cusp of cheek teeth; **mx** maxilla; **P1** first upper premolar; **P3** third upper premolar; **P4** fourth upper premolar; **pal** palatine; **pmx** premaxilla; **rc** posteromedial ridge of upper canine.

This cusp is centrally located and gives I2 a somewhat more pointed appearance than I1.

In old individuals, the crowns of both I1 and I2 may wear completely away, leaving these teeth as flat-topped pegs. Wear is usually greatest on I1 because this tooth projects further ventrally than I2, and erosion of the crown of I1 may be complete before the crown of I2 is completely ablated. In one extremely old individual (AMNH 217045; fig. 38B), both right and left I1 have been broken off at their bases, but the root and alveolus of each tooth remains clearly distinct (unlike those of missing molar teeth, which are grown over with bone). I2 in this individual remains on both sides as a peglike stub.

UPPER CANINE: The upper canine of *Pteropus lylei* is long, slender, and gently recurved (fig. 4, 36). The right and left canines are slightly divergent, such that the tip of each tooth lies directly ventral to the outer edge of its alveolus in relatively unworn dentitions. The length (= crown height) of the canine is approximately equal to the height of the nasal process of the premaxilla, and canine length is greater than the height of the rostrum above the canine alveolus in young animals with unworn teeth. The tip of the canine tapers to a relatively sharp point when unworn, but rapidly wears to a blunt point in older individuals. A narrow basal cingulum forms a continuous rim around the posterior and medial base of the canine. In some individuals with unworn teeth (e.g., AMNH 237598), the edge of the cingulum is marked by traces of several small cuspules. The anterior face of the crown of the canine is marked by a deep and broad vertical groove that runs from the base of the crown to nearly the tip of the tooth (fig. 4). Breadth of the groove is greatest near the base, and the groove narrows and becomes more shallow as it approaches the tip of the tooth. The posteromedial surface of the tooth is marked by a keel-like ridge that runs from the base of the tooth (just inside the basal cingulum) to almost the tip of the tooth (fig. 36). This ridge forms the medial

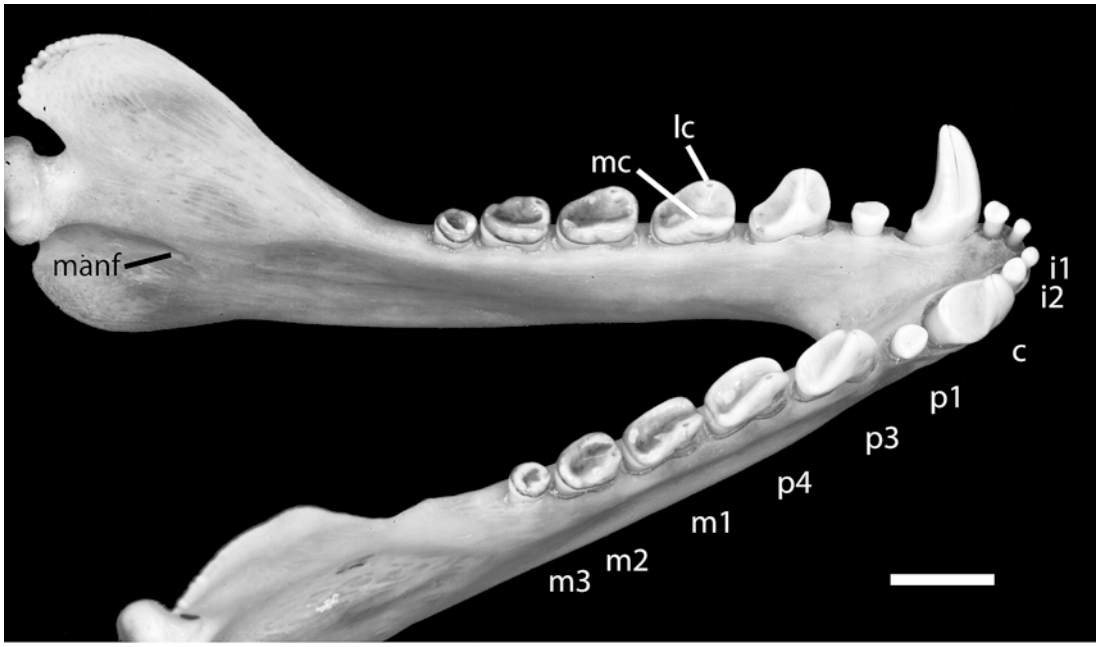

Fig. 37. *Pteropus lylei* AMNH 237595, dorsocaudolateral view of the mandible showing permanent lower dentition. Scale = 5 mm. Abbreviations: **c** canine; **i1** first lower incisor; **i2** second lower incisor; **lc** lateral cusp of cheek teeth; **m1** first lower molar; **m2** second lower molar; **m3** third lower molar; **manf** mandibular foramen; **mc** medial cusp of cheek teeth; **p1** first lower premolar; **p3** third lower premolar; **p4** fourth lower premolar.

boundary of the posterior face of the tooth, which is broadly concave and runs roughly parallel to the groove on the anterior face of the tooth. The lateral face of the tooth is gently convex, and the medial surface is flat. The canine is roughly rectangular in cross section throughout most of its length, with the two long edges corresponding to the medial and lateral faces of the tooth, and the shorter edges corresponding to the anterior and posterior faces.

Wear on the canine apparently continues throughout life, often beginning before tooth wear is apparent elsewhere in the dentition. Young adults generally exhibit at least some wear on the tip of the canine. As wear progresses, the basal cingulum becomes obscured, and a large wear facet forms down the posteromedial face of the tooth, obscuring the keel-like ridge. Wear reaches its extreme in very old individuals, in which the canine has been worn down to a flat-topped, mushroom-shaped peg (fig. 38B). The canines in most museum specimens have a single large vertical crack running from the tip to the base of the crown, but these cracks are apparently postmortem artifacts of the preparation process.

Upper Premolars: The upper premolar dentition of *Pteropus lylei* consists of three teeth: a tiny P1, and a large P3 and P4. The P1 is not deciduous but is often absent on one or both sides in older adults. P1 is a tiny, styliform tooth with an undifferentiated crown that tapers to a blunt point (fig. 36). P1 has a single root, and its alveolus typically lies just posterior to the alveolus for the canine. In some young individuals, the P1 alveolus is partially confluent with the canine alveolus, but these alveoli are separate in most adults. Skull growth appears to affect the relative position of the P1, as the size of the diastema between the canine and P1 alveoli tends to be greater in older, larger animals. In one of the oldest individuals in our sample (AMNH 30217), the remnant of the empty alveolus for P1 lies midway between the canine and P3 on both sides of

the skull. Comparisons among skulls reveal that the distance between P1 and P3 varies little with age, suggesting that differential growth occurs in the skull in the region between the canine and P1. Because P1 is so small, the functional cheek tooth row consists of four teeth: the two posterior premolars (P3 and P4) and the two molars (M1 and M2). These teeth are always separated from the canine by a large diastema, and are separated from each other by very small diastemata that prevent adjacent tooth crowns from touching one another.

The posterior upper premolars (P3 and P4) are large, double-rooted teeth with crown lengths slightly shorter than M1 (fig. 36). As in other *Pteropus* species, crown height decreases from anterior to posterior along the cheek tooth row (P3–M2), so P3 is the largest of the cheek teeth in lateral view. Both P3 and P4 have a large lateral cusp and a smaller medial cusp. The cusps on each tooth consist of longitudinal ridges that are incompletely separated at their bases by a median groove (fig. 36). The median groove terminates posteriorly in a small basin bounded by a weakly developed posterobasal ledge, which forms a narrow rim around the back of the tooth. Traces of small cuspules can occasionally be seen along the posterobasal rim.

The crown of P3 is slightly higher than it is long. The anterior edge of the tooth is convex and the posterior edge is concave, so the tooth appears slightly recurved in lateral view. The main bulk of the tooth is centered over the anterior root, with the tips of both cusps offset anteriorly from the midpoint of the tooth. The occlusal outline of P3 is oval to subrectangular. The large lateral cusp is roughly triangular in cross section, with a medial ridge that connects it to the lower medial cusp across the median groove. The anteroposterior length of the medial cusp is somewhat smaller than that of the lateral cusp. The posterobasal rim is very low on P3 (fig. 36).

Crown height of P4 is markedly less than that of P3, and both cusps on P4 have lower, more rounded tips than their counterparts on P3 (fig. 36). The posterior edge of the lateral cusp of P4 is either straight or very slightly convex, so the tooth does not appear recurved in lateral view. P4 is always subrectangular in occlusal view, and is somewhat broader posteriorly than P3. The posterobasal rim is also higher on P4 than on P3, giving the posterior portion of P4 a molariform appearance. Indeed, overall morphology of P4 is intermediate between that of P3 and M1.

Wear on the large premolars (P3 and P4) typically occurs on the ventromedial aspect of the cusps. Although the lateral cusps are higher than the medial cusps, the degree of wear is typically similar on both cusps, suggesting that abrasion occurs on both cusps simultaneously during feeding. Wear may progress until the entire surface of the crown is worn away (e.g., AMNH 30217; fig. 38A), and some very old individuals may lose the cheek teeth altogether (e.g., AMNH 217045; fig. 38B). In older individuals, the plane of tooth wear is obvious across the entire cheek tooth dentition. The wear plane is oriented such that wear is greatest posteriorly and medially on both individual teeth and on the dentition as a whole.

UPPER MOLARS: The upper molar dentition of *Pteropus lylei* consists of two double-rooted teeth: a large M1 and a small M2. The M1 has the longest crown length of any tooth in the upper dentition, and it is only slightly narrower than P4. The M2 is much smaller, less than half the length of M1 and markedly narrower than all of the other cheek teeth except P1 (fig. 36).

The M1 is subrectangular in occlusal outline, with the posterior end of the tooth more rounded in outline than the anterior end (fig. 3). Like the premolars, the crown of M1 is marked by a median groove that is flanked by two ridges, each of which rises to form a cusp near the anterior limit of the tooth. The lateral cusp is slightly higher than the medial cusp. The cusps are rounded and not recurved. Posteriorly, each cusp is continuous with a posterobasal rim that runs around the back of the tooth. In some individuals, traces of a distinct posterolateral cusp can be seen. The basin is broad and is continuous with the median groove that separates the medial and lateral cusps.

The M2 is small and oval in occlusal outline (fig. 3). Only one cusp is well developed: a bulbous cusp on the anterolat-

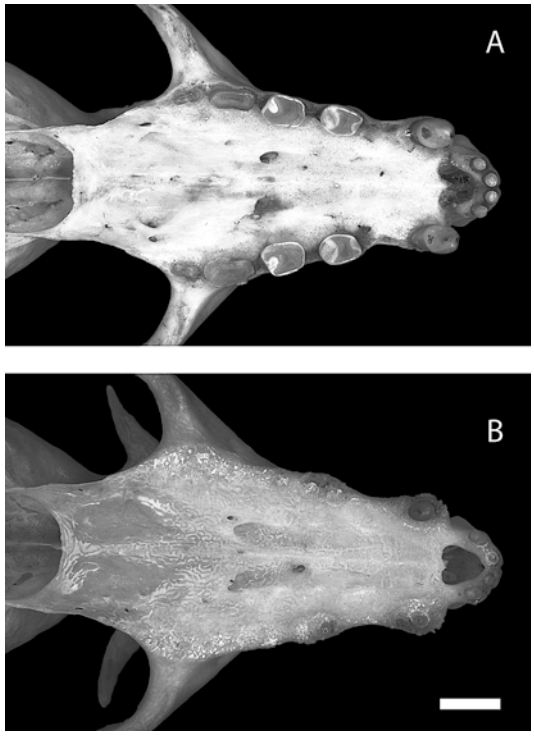

Fig. 38. *Pteropus lylei*, tooth wear of upper dentition in AMNH 30217 (**A**) and AMNH 217045 (**B**). Scale = 5 mm.

eral edge of the tooth. The base of this cusp intrudes into an otherwise oval central basin (fig. 36). The basin is bounded laterally, posteriorly, and medially by a raised rim that is not continuous with the anterolateral cusp. This raised rim is separated from the cusp by shallow notches anteriorly and laterally. In some individuals with unworn teeth (e.g., AMNH 237598), a tiny cusp is developed on the posterolateral corner of the rim. None of the cusps or ridges on M2 are very high, so the crown of the tooth appears relatively flat in lateral view. The occlusal surface of M2 lies in roughly the same plane as the posterior half of M1.

As noted above under the discussion of premolars, wear on the cheek teeth occurs along an oblique plane that is oriented such that wear is greatest posteriorly and medially on both individual teeth and on the dentition as a whole. Accordingly, M2 typically exhibits greater wear than M1, and M1 exhibits greater wear than the premolars. Wear may progress until the entire surface of the crown of each molar tooth is worn away (e.g., AMNH 30217; fig. 38A), and some very old individuals may lose these teeth altogether (e.g., AMNH 217045; fig. 38B). As the upper cheek teeth are worn down to nubs, it seems likely that they are lost progressively beginning at the back of the tooth row, where wear is greatest. This seems confirmed by examination of AMNH 217045, which lacks P3–M2 on both sides (fig. 38B). In this individual, the alveoli of the molar teeth are completely overgrown with spongy bone. The P4 alveoli are largely overgrown, and those of P3 are still visible, with the broken anterior root of P3 still present on one side.

Lower Incisors: The lower incisors of *Pteropus lylei* are markedly smaller than the upper incisors. The i2 is roughly twice the size of i1 in crown breadth, crown height, and cross-sectional area, but the height of the tip of i1 above the alveolar line is only slightly less than that of i2 due to differences in root length and the relative placement of the alveoli (fig. 8). Right and left i1 are separated by a median diastema, and these teeth are somewhat divergent (i.e., the shaft of each tooth is directed dorsally and slightly laterally). The i1, i2, and canine on each side of the jaw are placed close together (with no obvious diastemata), but adjacent tooth crowns do not contact one another.

Both i1 and i2 have a circular cross section when seen in occlusal (dorsal) view (fig. 7). The i1 is a peglike tooth that has a crown only slightly differentiated from the root. In relatively unworn dentitions, traces of a single cusp can be seen centered on the crown. In contrast, i2 shows clear evidence of two cusps in younger animals. These cusps are oriented side by side, parallel to the anterior face of the tooth. Crown development is much more pronounced in i2 than in i1, with the crown of i2 clearly distinct from the shaft of the root.

Wear begins very early on the incisors, and distinct wear facets can be seen on both i1 and i2 even in relatively young adults. Wear occurs on the anterodorsal surface of each tooth. In older individuals, a distinct wear plane forms across the entire lower incisor dentition; this plane runs obliquely from

posterodorsal to anteroventral, so that the flat wear facet on each tooth is directed anterodorsally. As wear progresses, the crowns of the incisors are worn away to leave these teeth as flat-topped pegs. In very old individuals, some or all of the lower incisors may be lost and their alveoli filled with spongy bone (e.g., AMNH 217045, which lacks both left lower incisors).

LOWER CANINE: The lower canines of *Pteropus lylei* are somewhat shorter, more slender, more strongly recurved, and more divergent than the upper canines (figs. 8, 37). Unlike the upper canines, which are approximately the same size in both sexes, there is considerable sexual dimorphism in the lower canines, which are markedly longer in males than in females. In females with minimal tooth wear, the height of the canine is approximately equal to the depth of the ramus of the mandible; in males, canine height exceeds depth of the ramus. The tip of the canine tapers to a relatively sharp point when unworn, but wears to a blunt point in older individuals. A poorly developed basal cingulum forms a continuous rim around the posterior and medial base of the canine. In some individuals with unworn teeth (e.g., AMNH 237598), the edge of the cingulum may be marked by traces of several small cuspules.

The anterior (fig. 8) and lateral (fig. 6) faces of the lower canine typically form a smoothly curving convex surface around the tooth. There is no anterior groove on the lower canine. However, in some individuals (e.g., AMNH 240005), the anterior and lateral surfaces are each relatively flat, meeting at a poorly developed ridge that runs from the tooth base to the tip along the anteromedial aspect of the tooth. The posteromedial surface of the tooth is marked by a keel-like ridge that runs from the base of the tooth (just inside the basal cingulum) to almost the tip of the tooth (fig. 37). This ridge forms the medial boundary of the posterior face of the tooth (which is flat or slightly concave), and the posterior boundary of the medial face of the tooth (which is flat). The lateral face of the tooth is gently convex, and the medial surface is flat.

Wear on the lower canine appears to proceed at a slower rate than wear on the upper canine. Most adults show some wear at the tip of the tooth, but large wear facets are uncommon until very late in the life of the animal. When a wear facet does form, it wraps around the posterior and medial surfaces of the tooth, eventually extending around the anterior face of the tooth to leave only the lateral surface of the enamel intact (e.g., AMNH 30217). The canine remains pointed even as the tooth wears away, becoming more conical as the wear facet develops. Wear reaches its extreme in very old individuals, in which the canine has been worn down to a flat-topped peg (e.g., AMNH 217045).

LOWER PREMOLARS: The lower premolar dentition of *Pteropus lylei* consists of three teeth: a small p1, and a large p3 and p4 (figs. 6, 7, 37). Although relatively small, p1 is much larger than P1, and it is also not deciduous like the latter. The p1 is single rooted and is approximately twice the size of i2. The crown is oval and relatively flat, with a very shallow central depression. In young animals, the lateral edge may be slightly higher than the medial edge of p1, and traces of two cusps may be seen along the lateral border of the tooth. The p1 is separated from the lower canine by a small diastema (somewhat less than the diameter of the crown of p1), and from the crown of p3 by a diastema that is the same size or somewhat larger. Wear on p1 is not evident until late in life, when wear on the anterior dentition reduces the distance between the upper and lower jaws during occlusion, bringing the posteromedial surface of the upper canine into contact with the lateral surface of p1. This occlusal contact produces a distinct wear facet on p1 in older adults (e.g., AMNH 30217). Like the other cheek teeth, p1 eventually wears down to become a flat-topped peg in very old animals (e.g., AMNH 217045).

The posterior lower premolars (p3 and p4) are large, double-rooted teeth with crown lengths approximately equal to that of m1. The morphology of these teeth is very similar to that of their upper counterparts (cf. figs. 36 and 37). As in the upper dentition, crown height decreases from anterior to posterior along the cheek tooth row (p3 to m3), so p3 is the largest of the cheek teeth in lateral view

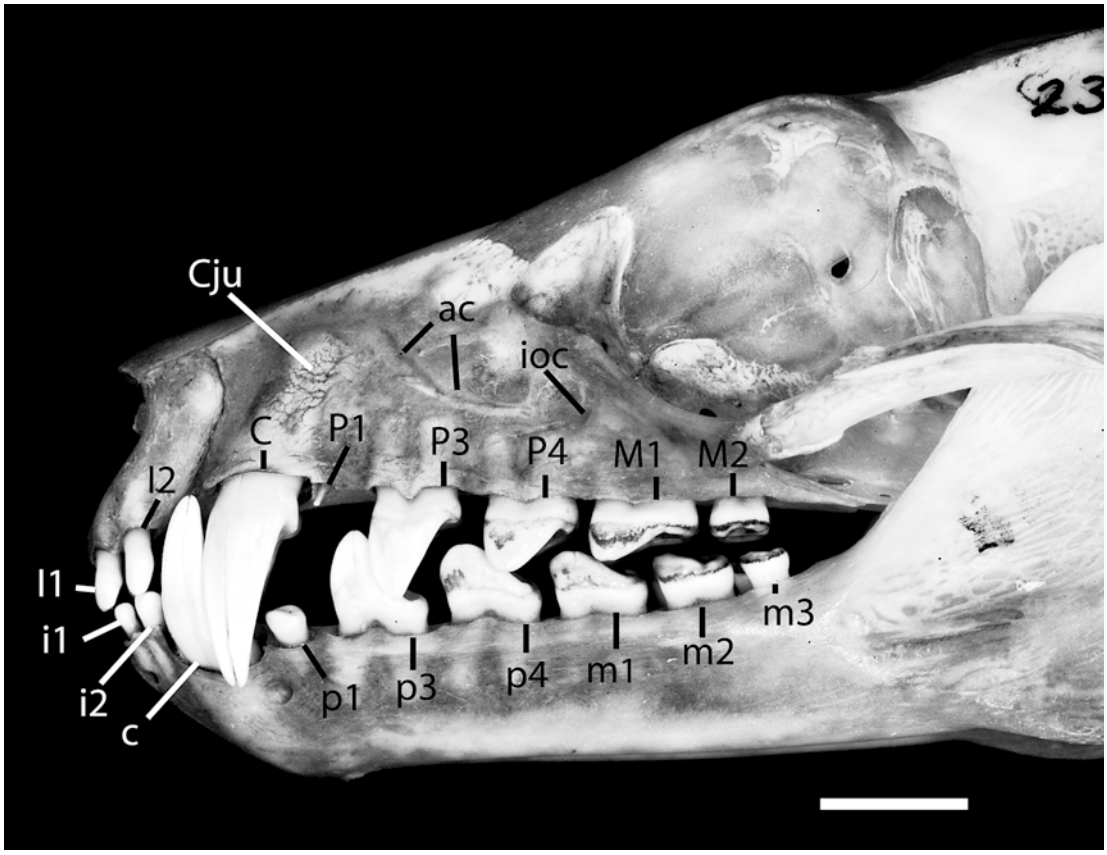

Fig. 39. *Pteropus lylei* AMNH 237595, lateral view of the rostrum and occluding mandible showing pattern of occlusion in the permanent dentition. Scale = 5 mm. Abbreviations: **ac** alveolar canal; **C** upper canine; **c** lower canine; **Cju** upper canine jugum; **I1** first upper incisor; **i1** first lower incisor; **I2** second upper incisor; **i2** second lower incisor; **ioc** infraorbital canal; **M1** first upper molar; **m1** first lower molar; **M2** second upper molar; **m2** second lower molar; **m3** third lower molar; **P1** first upper premolar; **p1** first lower premolar; **P3** third upper premolar; **p3** third lower premolar; **P4** fourth upper premolar; **p4** fourth lower premolar.

(fig. 37). Both p3 and p4 have a large lateral cusp and a smaller medial cusp. The crown of p3 is slightly higher than it is long, and the main bulk of the tooth is centered over the anterior root, with the tip of the lateral cusp offset anteriorly from the midpoint of the tooth. The anterior edge of the tooth is convex and the posterior edge is concave, so the tooth appears recurved in lateral view. The occlusal outline of p3 is subrectangular (fig. 7). The large lateral cusp is roughly triangular in cross section, with a medial ridge that connects it to the lower medial cusp (fig. 37). There is no median groove on p3, just a small notch that separates the two cusps. The degree of differentiation of the medial cusp is variable; in many individuals, it is clearly present and distinct from the lateral cusp (e.g., AMNH 237598), whereas in other specimens the medial cusp is barely visible (e.g., AMNH 237599). Posteriorly, a smooth, slightly concave surface runs from the medial ridge to the back of the tooth, and there is no posterior basin. The posterobasal rim is very low, and traces of small cuspules can occasionally be seen along its edge.

The morphology of p4 is nearly identical to that of P4 (cf. figs. 36 and 37). The crown height of p4 is markedly less than that of p3, and the lateral cusp on p4 has a lower, more

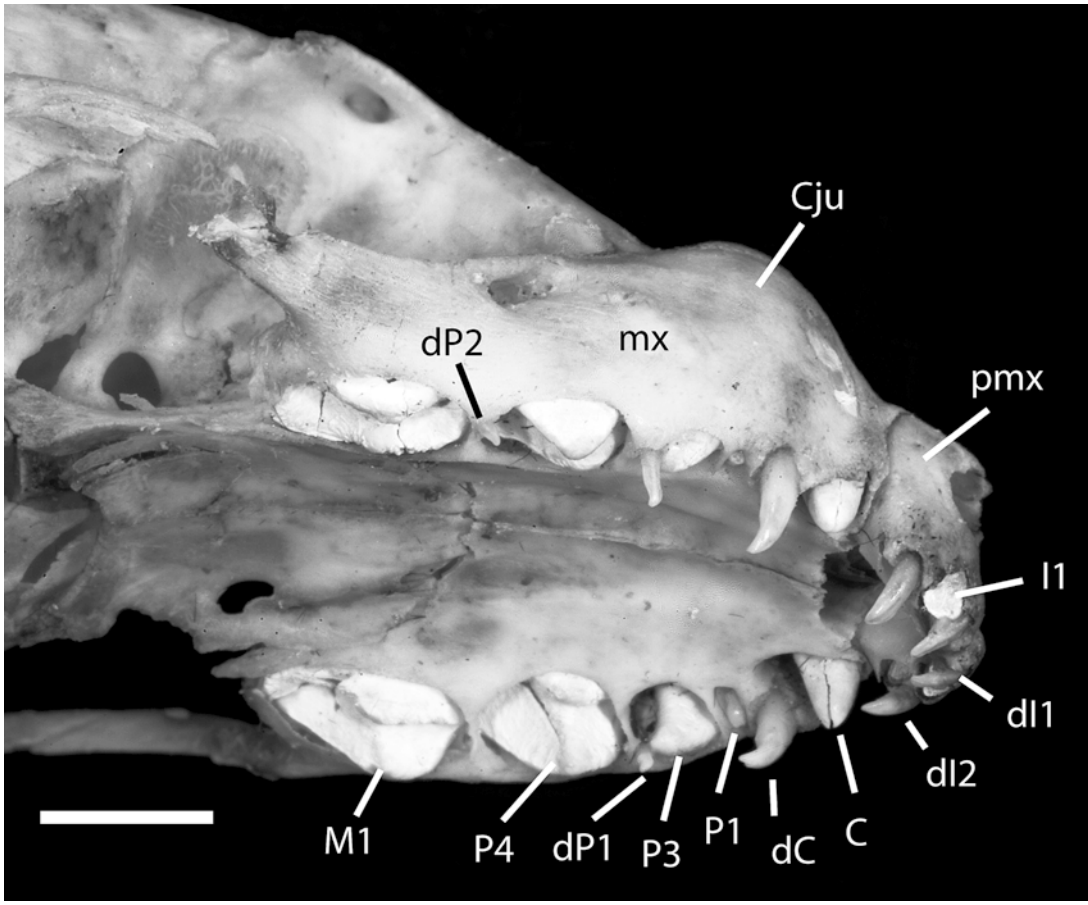

Fig. 40. *Pteropus hypomelanus luteus* AMNH 159084, ventrolateral view of the upper deciduous dentition. Scale = 5 mm. Abbreviations: **C** permanent upper canine; **Cju** upper canine jugum; **dC** deciduous upper canine; **dI1** deciduous first upper incisor; **dI2** deciduous second upper incisor; **dP1** deciduous first upper premolar; **dP2** deciduous second upper premolar; **I1** permanent first upper incisor; **M1** permanent first upper molar; **mx** maxilla; **P1** permanent first upper premolar; **P3** permanent third upper premolar; **P4** permanent fourth upper premolar; **pmx** premaxilla.

rounded tip than its counterpart on p3. The posterior edge of the lateral cusp of p4 is either straight or somewhat convex, so the tooth does not appear recurved in lateral view. The p4 is always subrectangular in occlusal view, and is approximately the same width as p3. The cusps on p4 consist of longitudinal ridges that are incompletely separated at their bases by a median groove. The median groove terminates posteriorly in a small basin bounded by a weakly developed posterobasal ledge, which forms a narrow rim around the back of the tooth. Traces of small cuspules can sometimes be seen along the posterobasal rim.

Wear of p3 and p4 is typically confined to the tips of the cusps until old age, with much greater wear occurring on the lateral cusp than on the medial cusp. In old individuals (e.g., AMNH 30217), a large wear facet may develop on the posterolateral aspect of the main cusp on p3 where it comes in contact with P3. A smaller wear facet may also develop on the anterior side of the main cusp on p4 where it contacts the posterior portion of the lateral cusp of P3 during chewing. Contact between upper and lower premolars is precluded in younger adults by prior occlusion of the anterior dentition. No contact seems to occur between p4 and P4

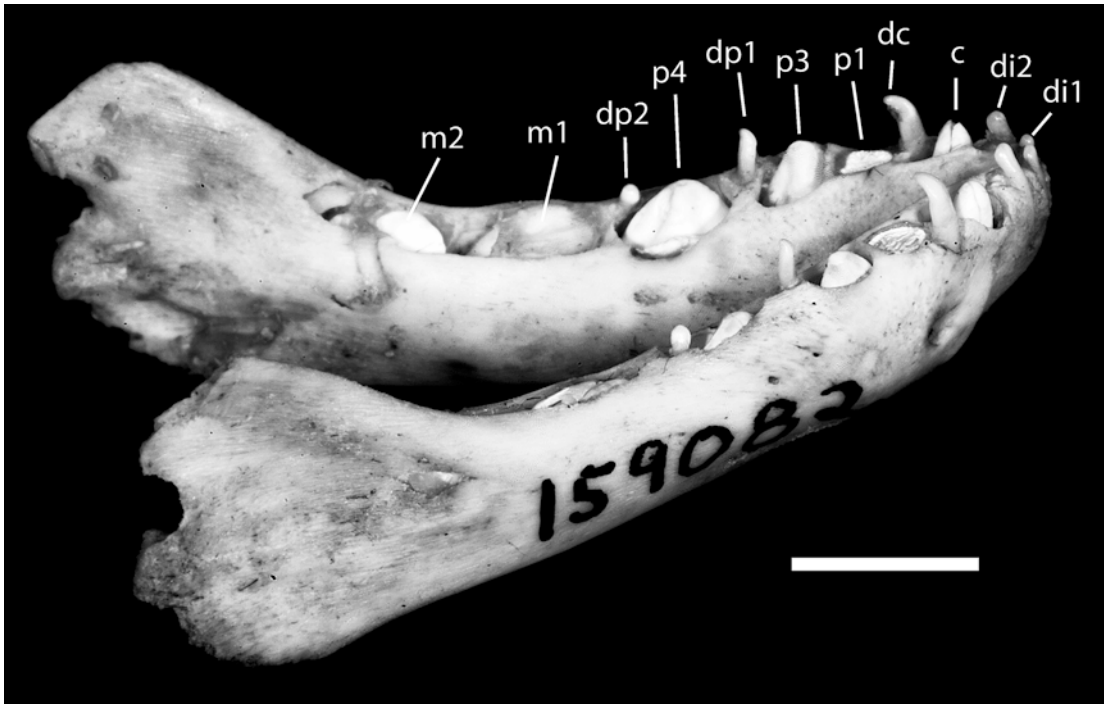

Fig. 41. *Pteropus hypomelanus luteus* AMNH 159082, dorsocaudolateral view of the mandible showing the deciduous lower dentition. Scale = 5 mm. Abbreviations: **c** permanent lower canine; **dc** deciduous lower canine; **di1** deciduous first lower incisor; **di2** deciduous second lower incisor; **dp1** deciduous first lower premolar; **dp2** deciduous second lower premolar; **m1** permanent first lower molar; **m2** permanent second lower molar; **p1** permanent first lower premolar; **p3** permanent third lower premolar; **p4** permanent fourth lower premolar.

at any age. Wear on the cheek teeth may progress until the entire surface of the crown is worn away (e.g., p4 in AMNH 30217), and some very old individuals may lose the cheek teeth altogether (e.g., AMNH 217045). In older individuals, a continuous, slightly convex plane of tooth wear occurs across p4–m3. The wear plane is oriented such that wear is greatest posteriorly, so teeth in the back of the cheek tooth dentition show greater wear than those in the front.

LOWER MOLARS: The lower molar dentition of *Pteropus lylei* consists of three teeth: a large m1 and m2, and a small m3 (figs. 6, 7, 37). Crown lengths of m1 and m2 are similar, and both teeth are double rooted and subrectangular in occlusal outline. The m3 is much smaller, with a crown that is almost circular in occlusal view. The m3 is approximately the same size as p1 and is single rooted, although the roots may be partially divided inside the jaw. The m1 and m2 lie in line with the posterior premolars; in contrast, m3 is slightly offset toward the medial side of the ramus of the mandible.

The morphology of m1 is very similar to that of its upper counterpart (cf. figs. 36 and 37). The crown of m1 is marked by a median groove that is flanked by two ridges, each of which rises to form a cusp near the anterior limit of the tooth (fig. 37). The lateral cusp is slightly higher than the medial cusp, and both are rounded and not recurved. The medial cusp in some young adults (e.g., AMNH 237598) can be seen to be composed of two adjacent cusps that are distinct only at their tips. However, only a single, somewhat elongate medial cusp is distinct on m1 in most individuals. Posteriorly, each cusp is continuous with a posterobasal rim that runs around the back of the tooth. The basin defined by this rim is continuous with the

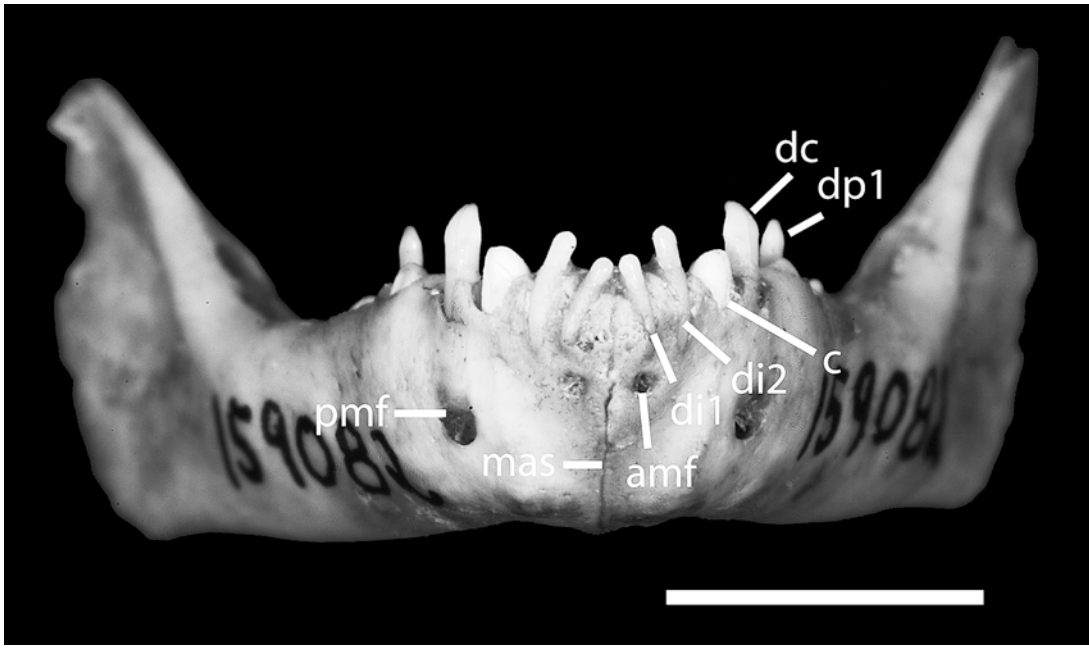

Fig. 42. *Pteropus hypomelanus luteus* AMNH 159082, rostral view of the mandible showing the deciduous dentition. Scale = 5 mm. Abbreviation: **amf** anterior mental foramen; **c** permanent lower canine; **dc** deciduous lower canine; **di1** deciduous first lower incisor; **di2** deciduous second lower incisor; **dp1** deciduous first lower premolar; **mas** mandibular symphysis; **pmf** posterior mental foramen.

median groove that separates the medial and lateral cusps. Because the posterobasal rim is very weakly developed across the back end of the tooth, the basin appears open posteriorly in most individuals.

The m2 is somewhat smaller than m1 in both length and height, but is approximately the same width (fig. 37). Only the lateral cusp is developed, and it is low and rounded. The medial groove is broad and shallow, forming a central basin that runs from the anteromedial portion of the tooth (medial to the cusp) to the posterior of the tooth. A raised rim with no distinct cusps surrounds the central basin anteriorly, medially, and posteriorly, and terminates at a notch on the lateral edge of the tooth just posterior to the cusp. The medial portion of the ridge is roughly horizontal.

The m3 is small and nearly round in occlusal outline (fig. 7). It is approximately the same size as p1. Only one cusp is developed on m3: a bulbous cusp on the anterolateral edge of the tooth (fig. 37). The center of the occlusal surface of the tooth is marked by a slight depression, but there is no clear definition of a rim. The crown of the tooth appears relatively flat in lateral view.

No contact seems to occur between the upper and lower molars at any age. Nevertheless, wear on the molar teeth may progress until the entire surface of the crown of each tooth is worn away (e.g., AMNH 30217), and some very old individuals may lose most of the lower molars (e.g., AMNH 217045, which retains only the roots of the left m2 and one root of the right m1). In older individuals, a continuous, slightly convex plane of tooth wear occurs across p4–m3. The wear plane is oriented such that wear is greatest posteriorly, so teeth in the back of the cheek tooth dentition show greater wear than those in the front.

OCCLUSION: As in other members of *Pteropus*, in *P. lylei* occlusion is controlled by the anterior dentition (see fig. 39). When the mandible is centered and the mouth closed, the only teeth in direct contact are either the upper and lower canines or the upper and lower incisors, depending upon the

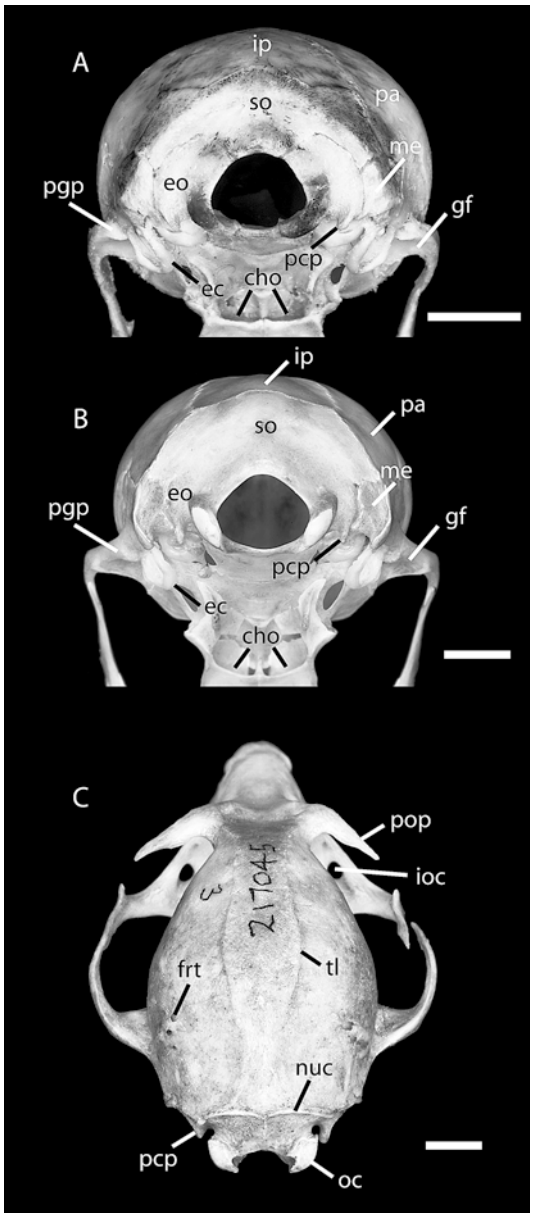

Fig. 43. Caudal view of the occiput of the pup of *Pteropus capistratus* AMNH 194276 (**A**) and the young adult of *Pteropus lylei* CM 87972 (**B**), and caudodorsal view of the skull of *P. lylei* AMNH 217045 (**C**). Scales = 5 mm. Abbreviations: **cho** choanae; **ec** ectotympanic; **eo** exoccipital; **frt** foramina for rami temporales; **gf** glenoid fossa; **ioc** infraorbital canal; **ip** interparietal; **me** mastoid exposure of petrosal; **nuc** nuchal crest; **oc** occipital condyle; **pa** parietal; **pcp** paracondylar process; **pgp** postglenoid process; **pop** postorbital process; **so** supraoccipital; **tl** temporal line.

position of the mandible. When the mandible is thrust forward, the incisors occlude; when it is retracted, the canines occlude. When the mouth is closed, the crowns of the lower incisors fit in behind those of the upper incisors, and the lower canine fits in front of the upper canine. The lower first premolar (p1) opposes the posteromedial ridge on the upper canine but does not occlude with it in younger adults due to prior occlusion of the canines and incisors. However, as wear reduces crown height of the anterior teeth in older adults, p1 approaches the upper canine and subsequently begins to occlude with the posteromedial ridge.

The upper and lower cheek teeth are generally not in contact when the jaw is centered and at rest. The main cusps of the lower teeth fit in front of and slightly medial to their counterparts in the upper dentition, alternating like the teeth on a pair of pinking shears (fig. 39). Accordingly, the main cusp of p3 fits into the diastema between P1 and P3. The main cusp of p4 fits into the posterior basin on P3, just anterior to the cusps on P4 and posterior to the cusps on P3. Subsequent teeth maintain this pattern, although reduction in cusp height on the rear teeth (M2, m2, and m3) reduces the degree to which opposing teeth interlock. The M2, which has a relatively flat crown, lies in opposition to the anterior half of the crown of m3 and the posterior half of the crown of m2. The m3 is the most posterior tooth in the dentition when the jaws are closed. Although all cheek teeth exhibit considerable wear in older adults, there is no evidence that upper and lower molars ever contact one another. However, some contact does occur between P3 and p3, and P3 and p4, in old adults when wear is advanced in the anterior dentition.

Deciduous Dentition

We examined the deciduous dentition in juvenile skulls of four specimens of *Pteropus hypomelanus luteus* (AMNH 159082–159085). The upper deciduous dentition consists of two incisors, a canine, and two deciduous premolars (Leche, 1876–1877; fig. 40). All are simple spicules. The deciduous incisors and canine are markedly recurved and are always implanted so that

the tips are directed posteriorly (fig. 40). The deciduous premolars are slightly recurved at the tip, but their orientation is irregular. The anterior deciduous premolars are usually oriented vertically (e.g., AMNH 159083) but may project somewhat anteriorly (e.g., AMNH 159082). The posterior deciduous premolars are very small and may project in any direction, especially when displaced by eruption of the anterior molar (fig. 40).

The adult replacements for the deciduous dentition are typically visible in even the youngest pups (fig. 40). I1 and I2 erupt with their crowns directly lingual to dI1 and dI2. The permanent canine erupts anterior and lingual to the deciduous canine. The deciduous premolars are located more posteriorly and appear to be associated with the spaces between erupting permanent teeth. The anterior deciduous premolar lies between the erupting P3 and P4, and the posterior deciduous premolar lies between the erupting P4 and M1. There is no deciduous tooth associated with P1 in any of the specimens we examined, as is the rule in many mammals (e.g., the dog; Evans, 1993).

The lower deciduous dentition resembles the upper dentition in comprising two incisors, a canine, and two premolars (fig. 41). However, the morphology of these teeth differs somewhat from their upper counterparts. The deciduous lower incisors are both peglike and blunt, and are not recurved (figs. 41, 42). The medial incisor (di1) is markedly smaller than the lateral tooth (di2) in both length and breadth (fig. 42). The lower deciduous canine resembles the upper dC, and is a relatively large, recurved tooth. The first of the two deciduous premolars is similarly recurved, but the second deciduous premolar is more peglike and blunt in form. They also differ in their orientation: the anterior deciduous premolar projects dorsally and somewhat anteriorly (although its tip is recurved and thus points slightly posteriorly); in contrast, the posterior deciduous premolar lies almost horizontally in our specimens, with the crown pointed anteriorly.

Like their upper counterparts, the deciduous lower teeth occupy consistent positions with respect to their erupting replacements (fig. 41). The permanent incisor teeth erupt with their crowns directly lingual to di1 and di2. The permanent canine erupts anterior and lingual to the deciduous canine. The anterior deciduous premolar lies between the erupting p3 and p4, and the posterior deciduous premolar lies dorsal to the posterolabial corner of the erupting p4. As in the upper dentition, there is no deciduous tooth associated with p1 in any of the specimens we examined.

SKULL DEVELOPMENT

Shape Change

AMNH 194276, a pup of *Pteropus capistratus*, is the youngest osteological specimen of *Pteropus* that we examined (see fig. 43A). As compared with adults of *Pteropus* of the *hypomelanus* type, the most striking features of this specimen are the very short rostrum and the large, rounded braincase. The orbit is also very large, but this is typical of the *temminckii* species group and is not general for *Pteropus*. The large jugum of the canine occupies almost all of the space of the *facies fascialis* of the maxilla in AMNH 194276. In contrast, the jugum of the canine has a definite rostral position in the adult. Therefore, during growth, the maxilla is apparently displaced rostrally and gains bone between the canine and the zygomatic process, presumably as the upper cheek teeth are added to the tooth row in a rostrocaudal order. This process of maxillary elongation is accompanied by simultaneous elongation of the nasals, which, judging from the relative position of the canine juga, occurs chiefly in the caudal half of the nasals. Likewise, the nasopharyngeal meatus and the palate experience noticeable elongations during development.

At the same time that the rostrum is undergoing elongation, the frontal bones are remodeled such that a postorbital constriction (nonexistent in AMNH 194276) becomes apparent, clearly delineated by the temporal lines (*linea temporalis*; fig. 43C). Relative development of these features varies greatly within *Pteropus*; as in larger species the postorbital constriction is well marked (sometimes narrower than the interorbital constriction), and the temporal lines are so

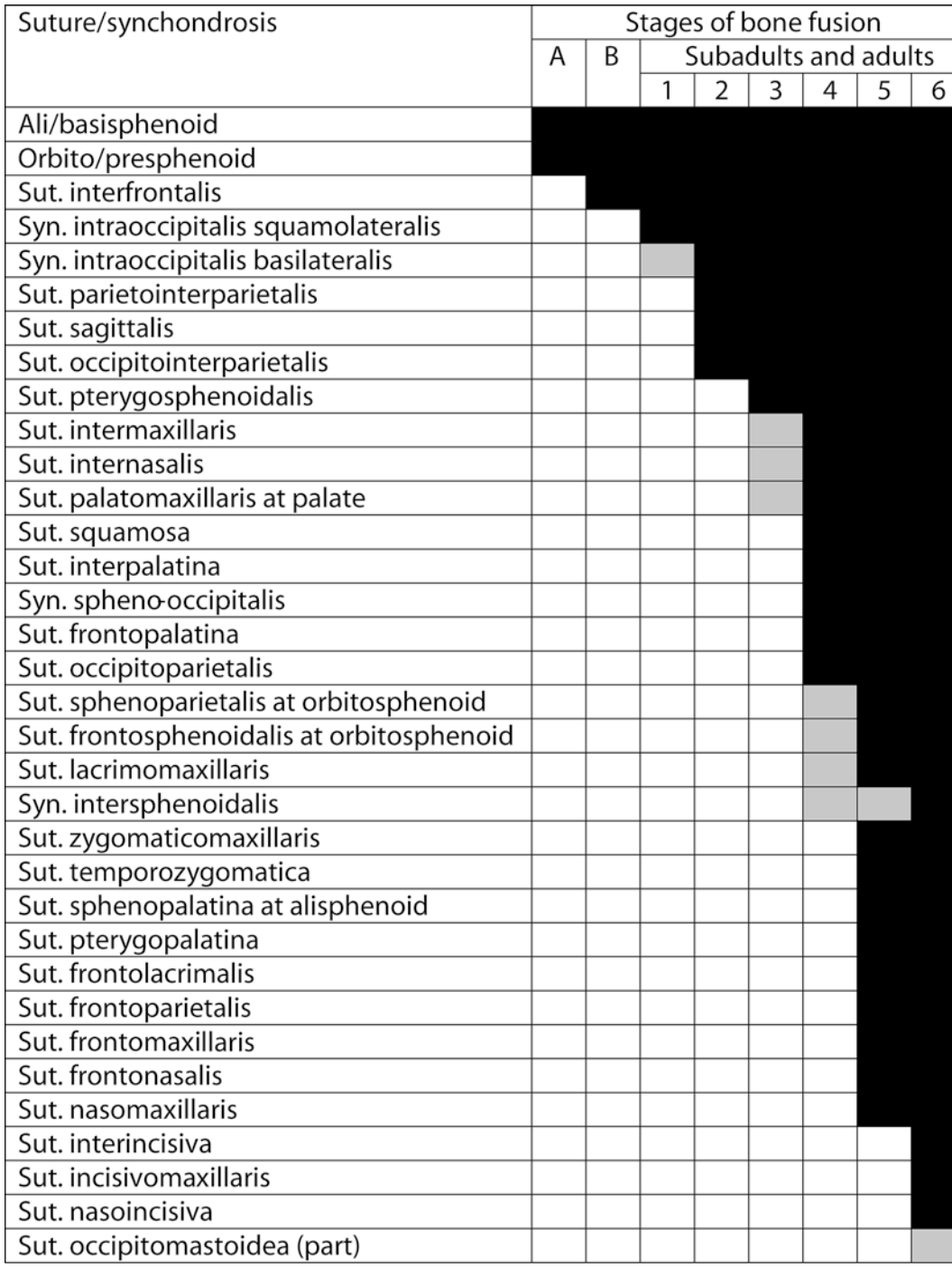

Fig. 44. Sequence of bone fusion in the AMNH and CM series of *Pteropus*. Columns indicate the stage of bone fusion from 1 to 6, defined on the basis of a combination of tooth wear and selected osteological traits (see text). Rows list sutures and synchondroses that are lost by fusion of their contributing bones, in successive order with respect to the age stages. From left to right, the first black cell for each suture or

well developed that they form a ridge over the postorbital processes and join immediately caudal to the processes into a sagittal crest (*crista sagittalis*). In AMNH 194276, the posterior zygomatic root lies close to the braincase and is oriented rostrally (fig. 43A). In adults, the posterior zygomatic root becomes stronger and more sharply angled, arising laterally from the braincase and forming a triangular shelf that overlies the glenoid fossa (fig. 43B, C).

The occipital region elongates caudally during skull development in *Pteropus*. In AMNH 194276, the ventral rim of the foramen magnum lies only slightly caudal to a relatively small jugular foramen, and anterior to the paracondylar processes. In adults, the ventral rim of the foramen magnum is displaced caudally so that it lies posterior to the paracondylar processes, the jugular foramen is much larger in its rostrocaudal dimension, and the margin of the occiput is located farther caudal from the petrosal. Modifications in the occiput may account for the apparent decrease in the deflection of the rostrum seen during development in many megachiropterans. Bergmans (1989) noted that young specimens of many megachiropteran species (e.g., *Nanonycteris veldkampi*) show a greater degree of rostrum deflection than adults. This also holds for *Pteropus*: in most adult *Pteropus* specimens, if the alveolar line is projected caudally, it intersects the occiput at the supraoccipital (see above). In younger animals, such as AMNH 194276, the projected alveolar line intersects the occiput more dorsally, at the occipitointerparietal suture, indicating a more pronounced rostrum deflection than seen in adults. Changes in cranial deflection presumably occur during development by addition of bone in the central-stem synchondroses, which elongates the basicranium and may rotate it dorsally a few degrees.

Sequence of Bone Fusion

We investigated the sequence of bone fusion in *Pteropus* using a series of specimens ranging from a fetus to old adults. The two youngest specimens in our series were a fetus (*Pteropus* sp.; DUCEC 831) and a newborn pup (*Pteropus capistratus*; AMNH 194276) with milk teeth but no permanent teeth erupted. The remainder of our sample consisted of subadult and adult *P. lylei*, which we arranged into six composite age stages based on degree of tooth eruption, tooth wear, tooth loss, and fusion of cranial elements. Stage 1 was defined as including subadults with no tooth wear and M2 not fully erupted (examples included CM 87972, 87973, and AMNH 240005). Stage 2 was defined as including individuals with M2 fully erupted but with minimal tooth wear throughout the dentition (e.g., AMNH 237598). Stage 3 was defined on the basis of tooth wear (all cheek tooth cusps showing signs of wear but ridges and cusps still distinguishable) and degree of fusion of selected cranial elements (e.g., palatal elements partially fused; e.g., AMNH 237594, 237595, and 237599). Stage 4 was characterized by the same degree of tooth wear as in stage 3 (all cheek tooth cusps showing signs of wear) but with additional cranial fusions suggesting more advanced age (e.g., joints of the basicranium and orbit fused; e.g, AMNH 237593). Stage 5 was recognized on the basis of advanced tooth wear throughout the dentition, with no ridges or cusps distinguishable on any molar teeth (e.g., AMNH 30217). Stage 6 was defined by advanced tooth wear and tooth loss (all cheek teeth lost and canines worn to their roots; e.g., AMNH 217045). On the basis of these categories, we examined the sequence of bone fusion in our *Pteropus* sample. A graphic interpretation of this sequence is shown in figures 44–48.

A distinct pattern of fusion of cranial elements emerges from analysis of specimens

---

←
synchondrosis indicates the stage in which the suture/synchondrosis is lost. Gray cells indicate the beginning of a fusion process in one stage that will be completed in later stages. Abbreviations: **A** prenatal stage; **B** newborn stage; **Sut** suture; **Syn** synchondrosis.

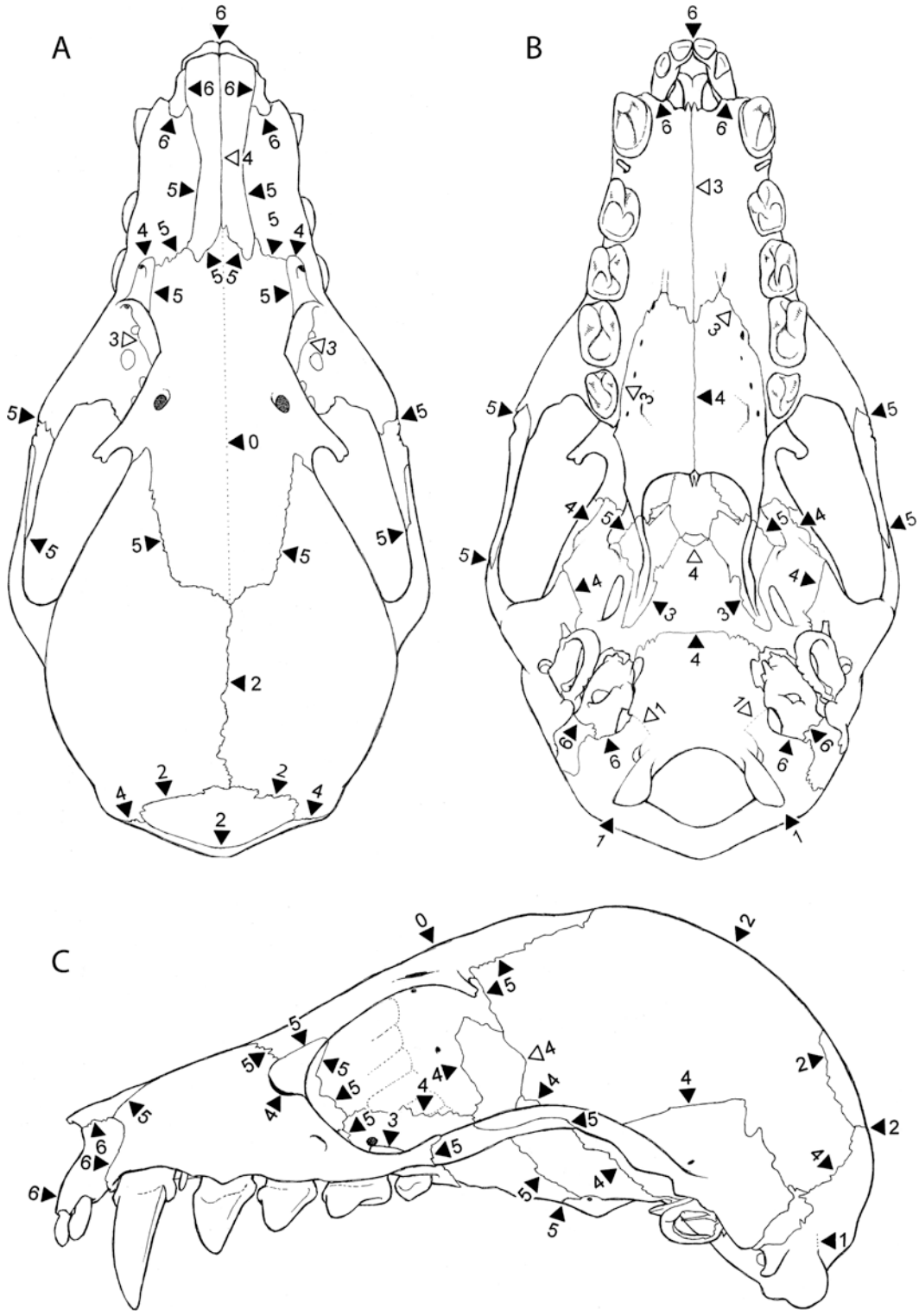
A
B
C

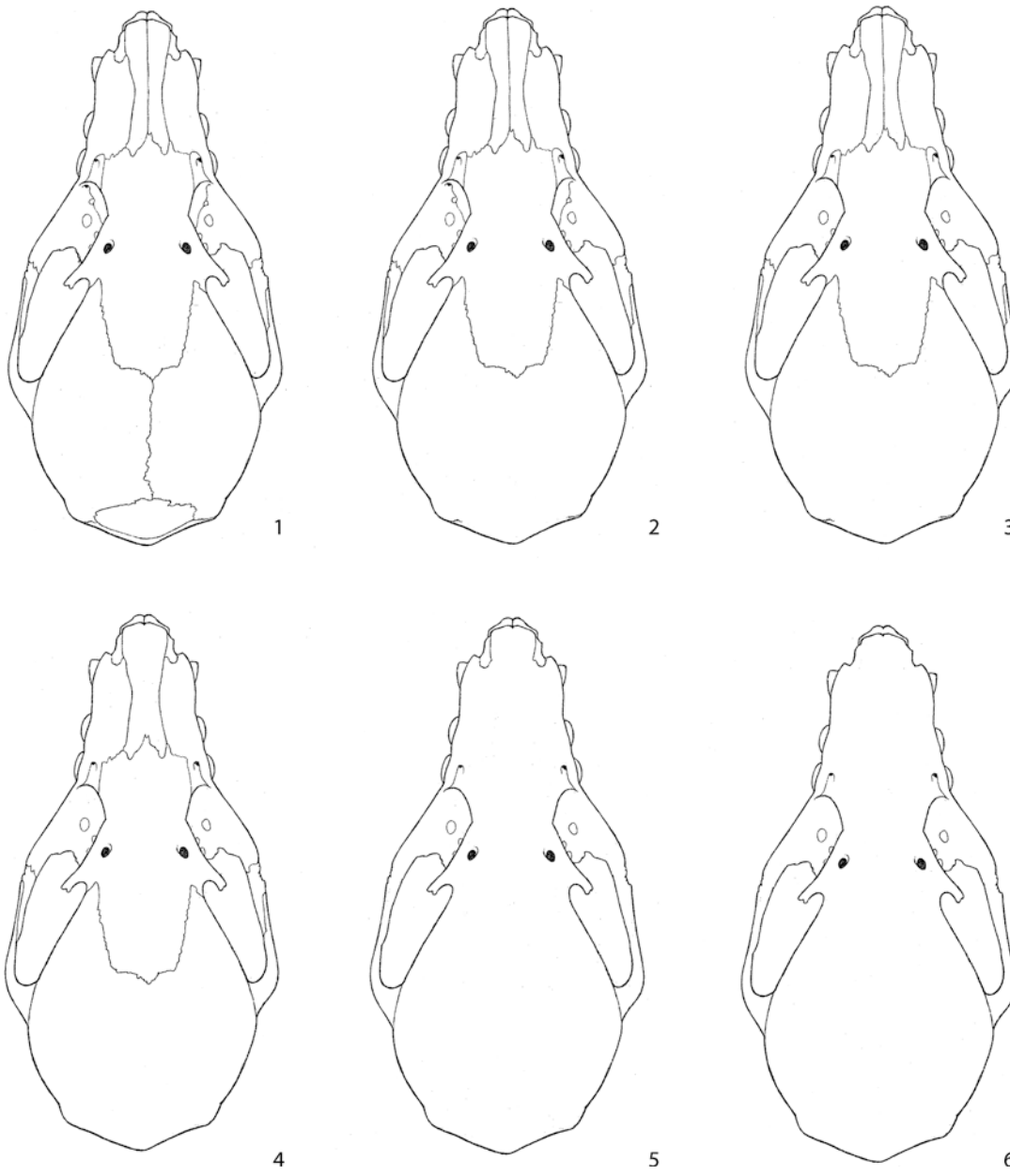

Fig. 46. Schematic dorsal views of the skull of *Pteropus lylei* based on CM 92972, showing the sequence of bone fusion. Each skull is representative of one ontogenetic stage from young subadults to old adults. The figure shows the successive loss of sutures from age stage **1** to **6** (see text and figs. 44 and 45A).

←

Fig. 45. Schematic dorsal (**A**), ventral (**B**), and lateral (**C**) views of the skull of *Pteropus lylei* based on CM 92972, emphasizing sutures and synchondroses. Numbers represent the age stage of subadults (see text and fig. 44) at which a given suture or synchondrosis is lost completely (indicated by black arrowheads) or incompletely (indicated by open arrowheads).

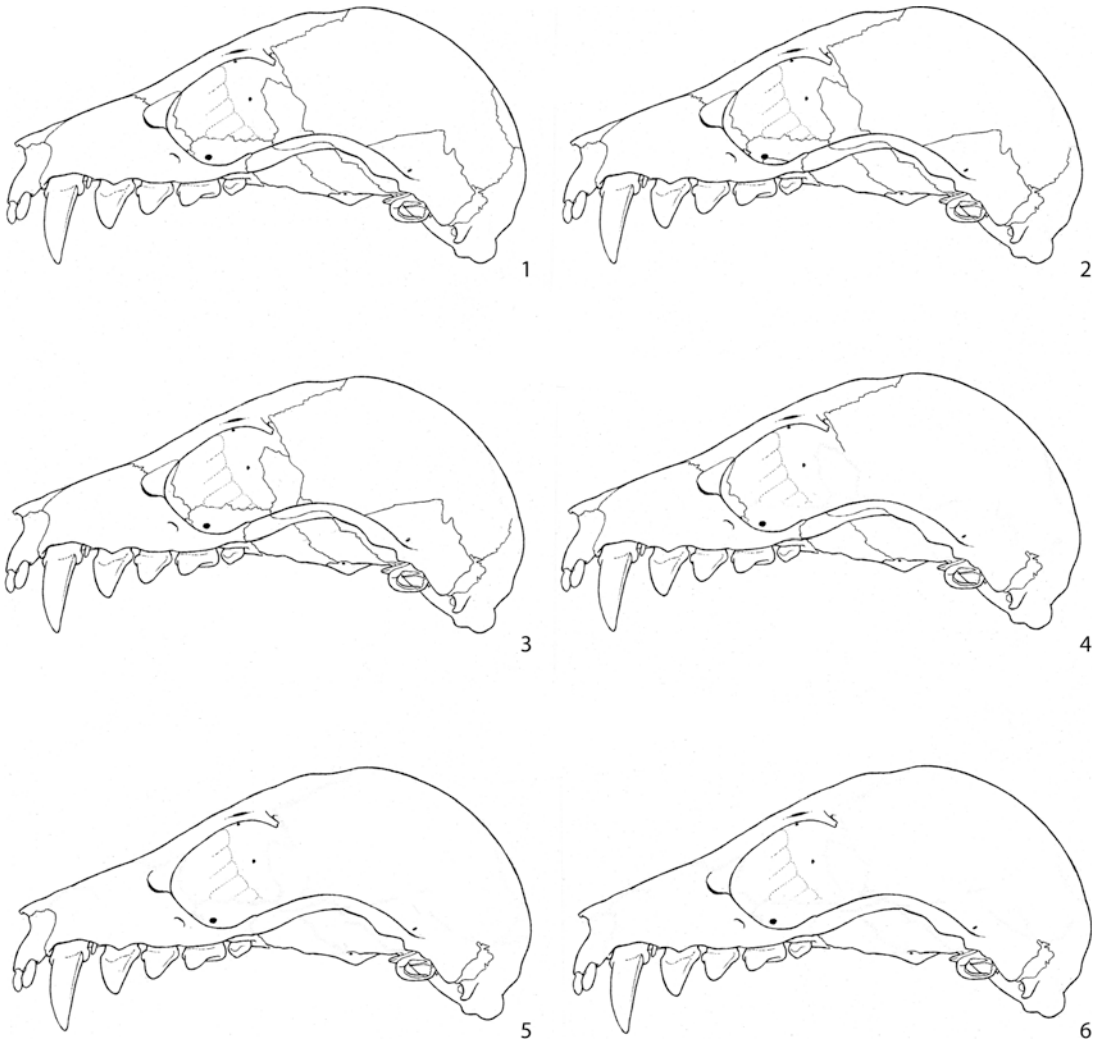

Fig. 47. Schematic lateral views of the skull of *Pteropus lylei* based on CM 92972, showing the sequence of bone fusion. Each skull is representative of one ontogenetic stage from young subadults to old adults. The figure shows the successive loss of sutures and synchondroses from age stage **1** to **6** (see text and figs. 44 and 45C).

representing the eight age categories defined above. In the fetus, the alisphenoid and the basisphenoid form a single ossification, but the frontals are not completely fused to one another: the rostral and caudal ends of the interfrontal suture disappear shortly after birth (based on *Pteropus hypomelanus* AMNH 159082–159085). A rare example of a pteropodid specimen showing a complete interfrontal suture is *Dobsonia pannietensis* AMNH 108486 (fig. 49). Next, in subadult stage 1, the occipital region is consolidated in a single unit (figs. 45B, C, 48 part 1). This is followed in stage 2 by the fusion of the dorsal and caudal components of the braincase (figs. 45A, 46 part 2). Next, in stage 3, the hard palate and pterygoids start to fuse across the midline (figs. 45B, 48 part 3). Stage 4 includes a major series of fusions that affect several regions of the skull, namely the central stem, the caudal hard palate, and the lateral braincase and orbit (figs. 45B, C, 47, 48 part 4). This is followed in stage 5 by the frontal, jugal, and palate fusing with the

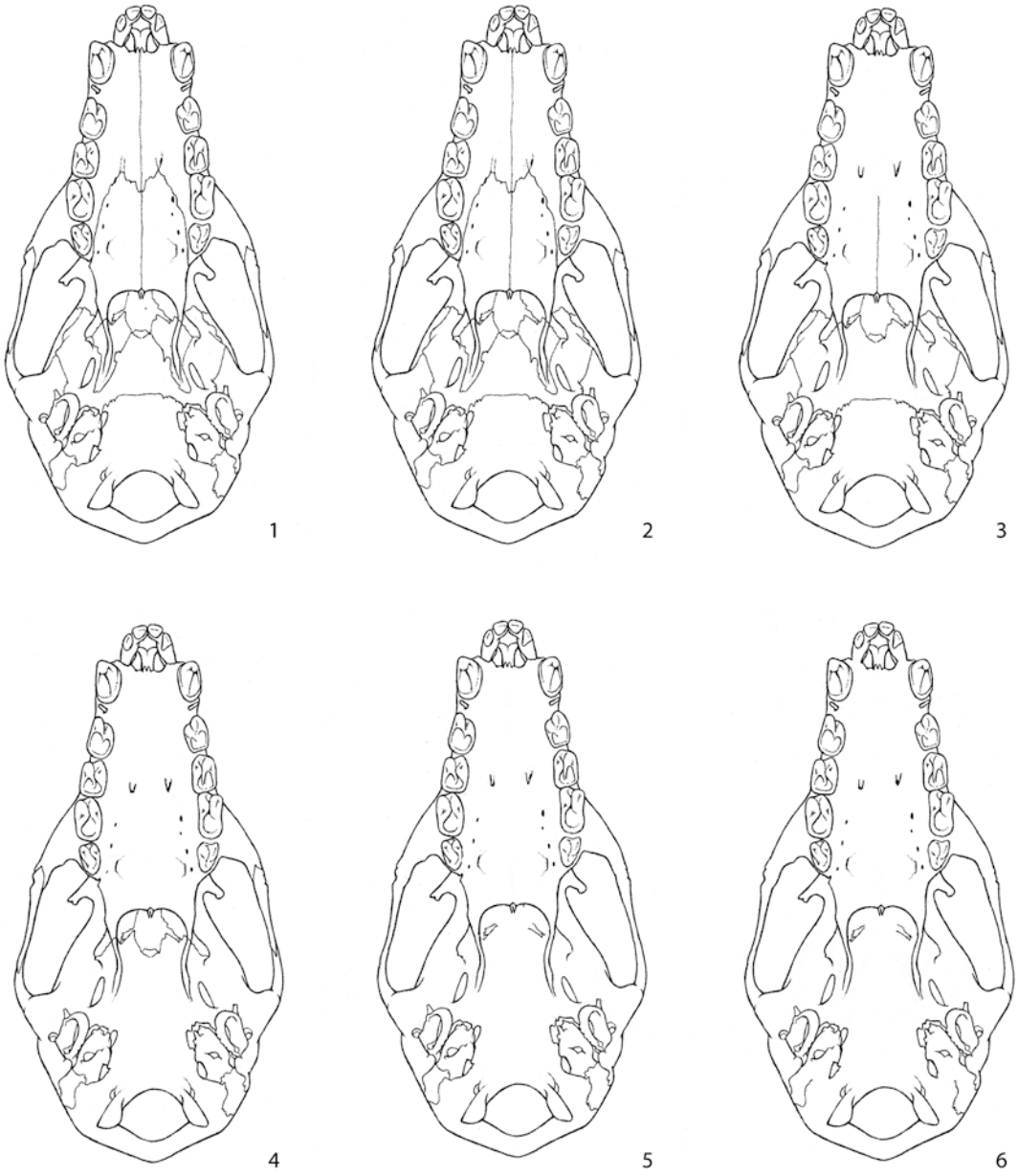

Fig. 48. Schematic ventral views of the skull of *Pteropus lylei* based on CM 92972, showing the sequence of bone fusion. Each skull is representative of one ontogenetic stage from young subadults to old adults. The figure shows the successive loss of sutures and synchondroses from age stage **1** to **6** (see text and figs. 44 and 45B).

remainder of their neighboring bones, as well as disappearance of the conspicuous naso-maxillary suture (figs. 45, 46–48 part 5). By this stage, only the maxilla and the petrosal remain unfused to surrounding bones. Next, in stage 6, the three sutures involving each premaxilla disappear, as well as one part of the occipitomastoid suture (figs. 45, 46–48 part 6). Specifically, the occipitomastoid joint is fused between the jugular foramen and the mastoid exposure, rostrolateral to the paracondylar process. This is the only part of

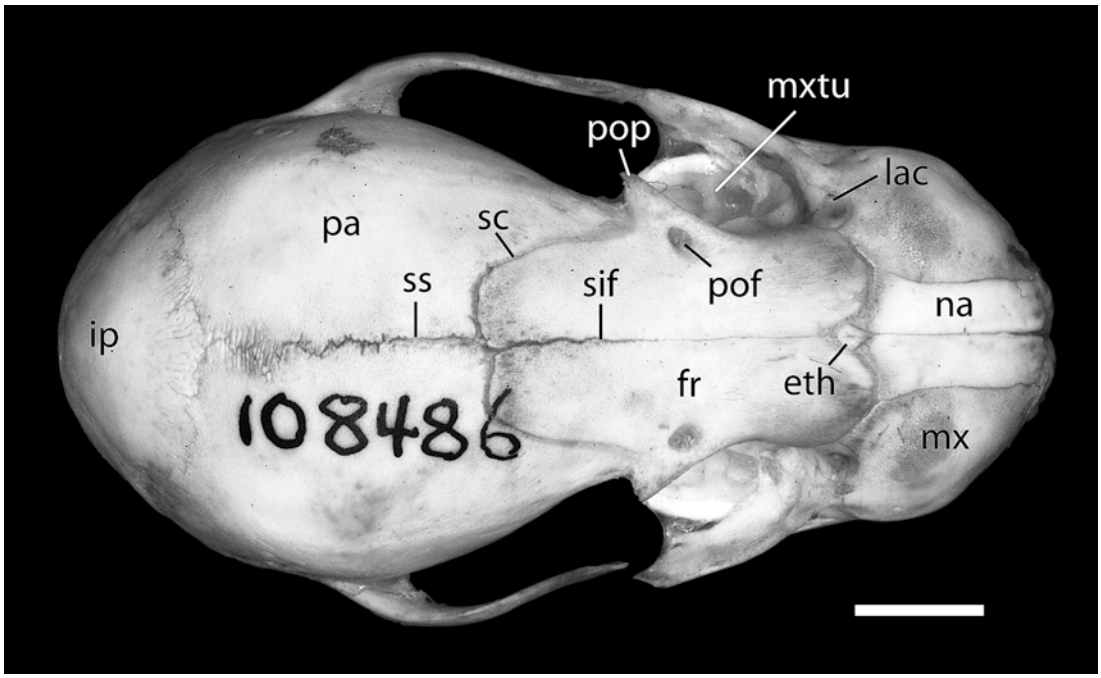

Fig. 49. *Dobsonia pannietensis* AMNH 108486, dorsal view. Scale = 1 mm. Abbreviations: **eth** ethmoid; **fr** frontal; **ip** interparietal; **lac** lacrimal; **mx** maxilla; **mxtu** maxillary tuberosity; **na** nasal; **pa** parietal; **pof** postorbital foramen; **pop** postorbital process; **sc** sutura coronalis; **sif** sutura interfrontalis; **ss** sutura sagittalis.

a petrosal joint to be fused, at least in external view.

Although we do not have an absolute time scale to contrast with, our observations indicate that bone fusion continues to occur throughout life in an orderly fashion. Specimens exhibiting the degree of tooth wear of AMNH 30217 and 217045 (stages 5 and 6) are extremely rare in *Pteropus*; the most typical stage of bone fusion in adult *P. lylei* is represented by AMNH 237593 (stage 4), in which a number of joints or parts of joints are still clearly distinguishable (e.g., those involving the premaxilla, petrosal, lacrimal, pterygoid, jugal, and parietal, and some of their neighboring bones).

A functional interpretation can be deduced from the sequence of bone fusion, taking into account the types of joints involved (primarily plane or squamous sutures, and synchondroses) as well as the sequence of fusions. The first bone fusion visible in the pup, the interfrontal, is a plane suture. We also know from *Pteropus livingstonii* AMNH 274466 and 274467 that the frontals are fused to the ethmoid in the young. This frontoethmoid complex can be interpreted functionally as a solidly fused centerpiece that connects the rostrum and the cranium through widely overlapping surfaces—squamous sutures that will fuse much later. Because the overlap zone is so wide (see fig. 26), these squamous sutures may presumably be both very resistant to stress and resilient to bending forces (Evans, 1993). In addition, the zygomatic arches are rooted posteriorly to the braincase via another widely overlapping surface (the sutura squamosa), whereas the anterior root is simply a stout process of the maxilla. As a very general and simplified rule, the basic connecting parts that hold the skull together tend to fuse early, whereas wide squamous sutures tend to fuse in later stages. One large plane suture that fuses late is the interpalatine. This seemingly weak line is buttressed dorsally by the vomer and the

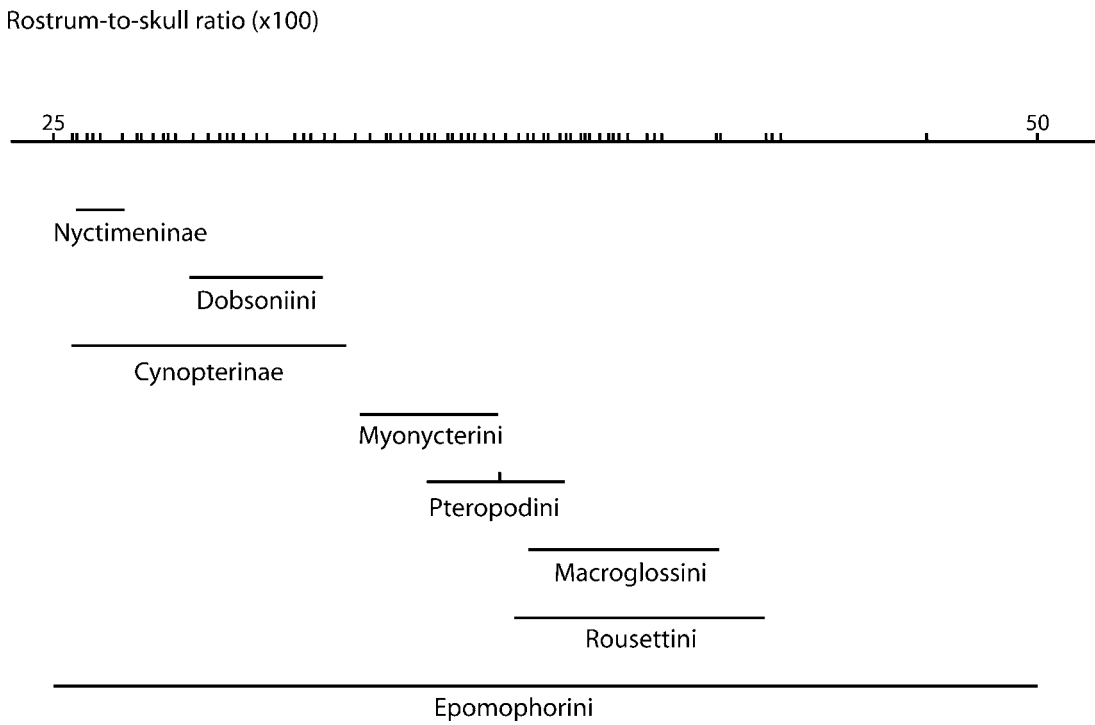

Fig. 50. Rostral proportions in Pteropodidae, based on 70 species representing all the currently recognized genera. The horizontal axis is the ratio of rostrum length, measured between the rostral ends of the nasals and orbit (at the lacrimal), to skull length, measured from the rostral end of the nasals to the caudalmost portion of the supraoccipital. In Pteropodidae, this index (× 100) varies between 25 (rostrum shortest, roughly ¼ the total length of the skull) and 50 (rostrum longest, roughly ½ the total length of the skull). A horizontal line represents the observed range for a selected megachiropteran group (tribes and subfamilies; after Bergmans, 1997). The marks in the axis represent the observed ratios of all species measured. The mark in Pteropodini represents the position of *Pteropus lylei*. Note that the Epomophorini span the entire range observed in Pteropodidae.

osseous and cartilaginous nasal septum, and laterally by the maxillary tuberosity, which has a medial fixation (sensu Cobb, 1943).

COMPARISONS

Skull Shape in Adult Megachiropterans

Three major structural aspects of skull morphology vary across megachiropteran species: the relative length of the rostrum (producing a continuum from short-faced to long-faced morphologies), the relative orientation of the two fundamental cranial axes, rostral and basicranial (deflection of the rostrum), and the development of structures associated with the strength of mastication (e.g., size and orientation of the coronoid process and configuration of the temporal lines on the skull). These features were discussed by Andersen (1912) and continue to play a role in modern systematic treatments.

Pteropus is a long-faced genus in the context of Pteropodidae as a whole. In *P. lylei*, palatal length accounts for approximately 50% of the length of the skull (figs. 1–3). Andersen (1912) calculated the rostrum length/skull length ratios for a number of species and divided them into discrete categories for the purpose of composing a key. Springer et al. (1995) and Romagnoli and Springer (2000) used these data in their phylogenetic analyses, recognizing three

character states: state 0 for rostrum "short, ¼ to ⅕ of skull", state 1 for rostrum "medium, ⅓ to 2/7 of skull", and state 2 for rostrum "long, ⅖ to ½ of skull". We measured a sample of 70 species from all currently recognized megachiropteran genera and found a virtually continuous distribution for the rostrum/skull length ratio, with no gaps allowing for splitting these data into discrete, nonoverlapping character states (fig. 50). As observed by Andersen (1912), epomophorines occupy the entire range of ratios, including genera with the shortest (*Casinycteris*) and the longest (*Hypsignathus*) rostra. Macroglossines sensu Andersen (1912; i.e., the six genera of nectar-feeding megachiropterans), pteropodines, and rousettines tend to exhibit longer-than-average rostra, whereas cynopterines, nyctimenines, and dobsonines have shorter-than-average rostra. Myonycterines sensu stricto (*Myonycteris* + *Lissonycteris*) occupy an intermediate position on this continuum. As clearly shown in *P. lylei* (see above), the length of the rostrum tends to increase ontogenetically.

Like rostral length, deflection of the rostrum also changes during ontogeny, and the state of this character may be affected by putative neoteny (e.g., in *Nanonycteris*; Bergmans, 1989). However, our examinations of series of individuals suggest that adults typically reach a characteristic degree of rostral deflection that is consistent across specimens of a given species. As discussed, the degree of rostral deflection can be defined with reference to the basicranial axis; if the latter is held horizontal, the alveolar line, representing the facial axis, may cross the occiput at different points: specifically, either below the basioccipital, at the foramen magnum, at the supraoccipital, or at the interparietal (character states used by Giannini and Simmons, 2005). Pteropodine megabats exhibit two of these conditions: a moderate-to-low rostrum deflection (alveolar line intersects the occiput at the foramen magnum; seen, for instance, in *Pteropus tonganus* and *P. dasymallus*, as well as in two species of *Acerodon*) and a moderate-to-high rostrum deflection (alveolar line intersects the occiput at the supraoccipital; seen, for instance, in *Pteropus admiralitatum*, *P. giganteus*, *P. hypomelanus*, and *P. scapulatus*, as well as in *Eidolon*, *Neopteryx*, *Pteralopex*, and *Stylocteniu*m). As in its close relative *Pteropus giganteus*, in *P. lylei* the alveolar line crosses the occiput at the level of the supraoccipital.

As discussed at length by Andersen (1912), there seems to exist a structural correlation among several traits related to mastication in *Pteropus* and related genera (probably in all Pteropodidae). Briefly, the size and vertical orientation of the coronoid process appears related to the configuration of the temporal lines on the skull. These traits, in turn, correlate to the strength of the dentition. Andersen (1912) identified two extremes of a likely continuous variation. Species characterized by an almost vertical and very wide coronoid process, and strongly marked temporal lines that join immediately caudal to the orbits (sometimes forming a sagittal crest), are also characterized by strong dentition (i.e., elements of large size, sometimes with additional cuspidation). An example is *Pteropus anetianus*, which also exhibits the short rostrum typical of forms with "heavy" dentition (sensu Andersen, 1912). At the other end of the spectrum, Andersen (1912) identified species with excessively weak dentition, a trait accompanied by a sloping (dorsocaudally oriented) and thin coronoid process and weak temporal lines that never join behind the orbits or form a sagittal crest. *Pteropus scapulatus* is an example of this type; these forms tend to be pollinators (Andersen, 1912). *P. lylei* belongs to an intermediate category, the *hypomelanus* type of Andersen (1912), which is characterized by an intermediate condition in the expression and development of the dentition, coronoid, and associated traits of the masticatory apparatus.

Interspecific Suture Variation

Several of the *suturae capitis* listed in the NAV are absent in the *Pteropus* examined. The vomeroincisive suture (*sutura vomeroincisiva*) is missing as a consequence of the lack of ossification of the palatine process of the premaxilla, to which the incisive incisure of the vomer articulates in most mammals, including yangochiropteran bats. The ethmoidonasal suture (*sutura ethmoidonasalis*) is

missing because the frontal has taken over the whole caudal contact area of the nasal, precluding a nasal-ethmoid contact. The reduction of the jugal bone—a possible synapomorphy of bats (Wible and Novacek, 1988; Simmons, 1994)—accounts for the lack of a lacrimozygomatic suture (*sutura lacrimozygomatica*). In bats, the jugal is a small element in the middle of the zygomatic arch, so the anterior root of the zygoma is entirely within the maxilla. Therefore, the lacrimal is isolated from contact with the jugal by the zygomatic process of the maxilla. As in the dog, and most placental mammals, the nasal does not contact the lacrimal, the two bones being, in *Pteropus*, separated by the wide frontomaxillary contact, so the nasolacrimal suture (*sutura nasolacrimalis*) is absent. The frontal and the squamosal are widely separated by the parietal and orbitosphenoid, so the squamosofrontal suture (*sutura squamosofrontalis*) is absent. Finally, the sphenomaxillary suture (*sutura sphenomaxillaris*) is also absent.

The frontozygomatic suture (*sutura frontozygomatica*) is present in some megachiropterans, specifically those species of *Acerodon*, *Pteralopex*, and *Pteropus* that possess a complete orbital ring produced by ossification of the orbital ligament. The postorbital process of the frontal contacts the zygomatic arch in these taxa, but the contact occurs between the frontal and the zygomatic process of the maxilla, not the jugal, which is greatly reduced in all bats (Wible and Novacek, 1988; Simmons, 1994).

Some sutures have systematic importance (Andersen, 1912). Such is the case of the three sutures involving the megachiropteran premaxilla. First, the nature of the interincisive suture varies widely among megachiropterans. The left and right premaxillae may be separated and not contact one another (e.g., *Boneia*), or they may be sutured (e.g., *Rousettus*) or fused (e.g., *Nyctimene*). Similarly, the maxilloincisive suture may be sutured (the most common condition in megachiropterans) or fused (e.g., *Pteralopex*, *Styloctenium*, *Neopteryx*). The shape of the pathway of the suture may also vary. Some pteropodines exhibit a ''squared off'' maxilloincisive suture, whereas in most megabats this suture is gently curved. The nasoincisive suture varies in relative length within Megachiroptera. It is a long suture in many of the nectar-feeding bats (e.g., *Macroglossus*, *Melonycteris*, *Notopteris*) and exhibits relative reduction in other taxa: it is of moderate length in most megachiropterans, it is reduced to a point nasal-premaxilla contact in some others (e.g., many cynopterines and dobsonines), and the nasal-premaxilla contact is lost in a few forms (e.g., nyctimenines).

Internal Surfaces of the Skull

Descriptions of the internal surfaces of the skull are almost entirely lacking for bats and are infrequent for mammals in general. One exception is the cribriform plate, described and figured for representatives of most bat families by Bhatnagar and Kallen (1974). The cribriform plate of *Pteropus livingstonii* (this study) is very similar to that of *Pteropus giganteus*, *Rousettus leschenaulti*, and *Cynopterus sphinx* (Bhatnagar and Kallen, 1974), although the cribiform plate of the latter taxon is relatively wider. These four megachiropterans differ from all microchiropterans examined by Bhatnagar and Kallen (1974) in that the entire cribriform plate is perforated by cribriform foramina, whereas microchiropterans exhibit a cribriform plate with wide nonperforate areas.

For other structures, we compared our observations of internal surfaces in *Pteropus livingstonii* with the descriptions available for the dog (Evans, 1993). *Pteropus* shows a number of striking differences, detailed as follows.

The nasal bone of *Pteropus* lacks a nasoethmoidal crest and fossa. This appears to be related to the fact that the nasal does not contact the ethmoid as it does in the dog. The frontal process of the nasal overlies only the rostral surfaces of the frontal bone in *Pteropus*.

As discussed above when dealing with the external surfaces, the premaxilla lacks a caudal projection of the nasal process, and the palatine processes are missing altogether. These structural differences from the dog also are reflected on the internal surface of the premaxilla. Regarding the maxillary internal surface, the most significant difference with respect to the dog is the relative

simplicity of the ventral nasal concha, which in *Pteropus* lacks the rich covering of delicate bony scrolls present in the dog. In the palatine, the chief differences from the dog are the limited dorsal extension of the perpendicular lamina in *Pteropus* and the noticeable caudal extension of the horizontal lamina, forming a long postdental palate inclusive of the minor palatine foramen (a notch in the dog).

The internal surfaces of the frontoethmoidal complex include the frontal, cribriform plate of the ethmoid, ethmoturbinal, and vomer. Differences between *Pteropus* and the dog include the following. First, the inner table of the frontal (*facies interna*) is not affected by the frontal sinus, as the sinus in *Pteropus* is located more rostrally in the interorbital area. Note, however, that in other megachiropterans, chiefly in cynopterines, nyctimenines, and dobsoniines, the frontal sinus reaches the postorbital area, as in the dog. The inner table of the frontal also is shaped differently in *Pteropus*; it does not show the strong, wedge-shaped internal frontal crest between the ethmoidal fossae dorsally. Second, the remarkable dorsal extension of the orbitosphenoid in *Pteropus* leaves a wide notch on the lateral side of the frontal, thus neatly separating the postorbital part of the *squama frontalis* from the *pars orbitalis*. Third, ventrally, the *ala vomeris* is extremely narrow in *Pteropus*, so the floor of the nasal capsule chiefly is exposed ventrally. In the dog, the *ala vomeris* is significantly wider.

The presphenoid and orbitosphenoids of *Pteropus* differ notably from those of the dog. Considering the body first, in *Pteropus* a differentiated rostrum (*rostrum sphenoidale* of the dog) is absent; the optic canals are more rostral in position, so the corpus is elongated caudally; and the sphenoidal sinuses are very small. The alae in *Pteropus* possess a very large vertical component that contributes significantly to the orbit wall, reaching two-thirds of the orbit height, an arrangement that stands in striking contrast to the limited orbital exposure of the orbitosphenoid in the dog. The main difference can be thought of as a combination of two modifications: an enlargement of the alae and a rostral displacement of the yoke.

The basisphenoid and alisphenoid of *Pteropus* also differ significantly from those of the dog, especially in dorsal view. In *Pteropus*, there is no trace of alar canal and hence no differentiated foramen rotundum, its contents instead being transmitted directly to the sphenorbital fissure. The sella turcica is also different in being significantly elongated and in lacking a distinct caudal clinoid process (*processus clinoideus caudalis*) and dorsum sellae. The sizable pterygoid processes present in the dog are minute in *Pteropus*. Caudally, *Pteropus* exhibits a very distinct epitympanic wing of the alisphenoid, which is absent or inconspicuous in the dog.

The internal surface of the parietal complex in *Pteropus* differs from that of the dog in several important aspects. First, *Pteropus* wholly lacks the tentorial process (*processus tentoricus*). Second, due to the fact that in the dog the vascular supply to the m. temporalis is entirely extracranial, all structures (sulci and foramina) directly associated with the intracranial course of the ramus superior and rami temporales in *Pteropus* are correspondingly absent in the dog. Third, the development and conspicuousness of the sulcus for the transverse sinus is much less marked in *Pteropus*. Fourth, the interparietal in the dog is a wedge-shaped bone fitting a narrow interparietal space and is more intimately associated with the supraoccipital than with the parietals. The interparietal in *Pteropus* is a subcircular, domed plate more intimately associated with the parietal than with the supraoccipital. Additionally, the interparietal of *Pteropus* lacks a foramen for the dorsal sagittal sinus (*foramen sinus sagittalis dorsalis*). Finally, the degree of parietal overlap of the frontal is much more pronounced in *Pteropus* than in the dog, and the parietal overlaps the supraoccipital.

Comparisons between the internal surface of the squamosal in *Pteropus* and the dog are difficult because in the dog the squamosal is solidly integrated in the temporal complex. One difference that should be noted, however, is the absence in the dog of the sulcus that leads the ramus superior outside the braincase through the foramina for the rami temporales. This sulcus is absent because the ramus superior and the rami temporales are entirely lacking in the dog. Also, in

Pteropus, the transverse sulcus is less marked, and even less so in the parietal with respect to the squamosal (see above).

Major differences exist between *Pteropus* and the dog in the internal surfaces of the occipital complex. These include the absence in *Pteropus* of an occipital contribution to the sulcus for the venous transverse sinus (also reduced in the parietal) and the absence of the condyloid canal (*canalis condylaris*). Another difference occurs in the shape of the foramen magnum, which is rhomboidal in *Pteropus* but is dorsally constricted in the dog by the presence of the paired nuchal tubercles (*tuberculum nuchale*) in most adult individuals.

Foramina

Species of *Pteropus* including *P. lylei* show neither the full set of foramina present in Megachiroptera as a group, nor the same degree of development in all the foramina whose presence is shared with other forms. Here we point out the differences and generalities that arise from comparing *P. lylei* with other *Pteropus* species, as well as with other pteropodine and nonpteropodine megachiropterans.

Basicochlear Fissure, Piriform Fenestra, and Jugular Foramen: *Pteropus lylei* lacks an alicochlear commissure and has a robust basicochlear commissure. As a consequence, the basicochlear fissure is connected to the piriform fenestra rostrolaterally, and is widely separated from the jugular foramen caudally. Three modifications with respect to this pattern in other pteropodids are worth mentioning. First, the alicochlear commissure may be present, so the piriform fenestra is well separated from the basicochlear fissure (e.g., in *Nyctimene*). Second, the basicochlear commissure may be greatly reduced, so both the basicochlear fissure and the jugular foramen are enlarged (e.g., in *Cynopterus*). Third, in species of *Pteralopex* and large *Pteropus* and *Acerodon*, the basicochlear fissure may be concealed in ventral view by a comparatively strong muscular tubercle (*tuberculum musculare*) of the basioccipital (not developed in *P. lylei*) and a similarly enlarged medial ridge on the promontorium (present in adult *P. lylei*).

Foramen Ovale: *Pteropus lylei* exhibits a large opening in the alisphenoid that corresponds to the foramen ovale + the caudal alar foramen of the dog. Confluence of these foramina is observed in many *Pteropus* species (including *P. livingstonii* and *P. temminckii*), but the two openings are separated in other species (e.g., *P. admiralitatum*, *P. tonganus*) and still other taxa show varying degrees of separation in different individuals (e.g., *P. hypomelanus*, *P. giganteus*). When not fully separated, the foramina are found in a distinct elongate, shallow pit. Other pteropodines (except *Neopteryx*) show two well-separated openings. The foramen ovale and caudal alar foramen are similarly separate in *Rousettus*, *Eonycteris*, *Boneia*, *Stenonycteris*, *Eidolon*, *Lissonycteris*, *Myonycteris*, *Aproteles*, *Dobsonia*, most epomophorines (except *Epomophorus gambianus* and *Nanonycteris*), some cynopterines (*Balionycteris*, *Chironax*, *Sphaerias*, *Pentethor*, *Thoopterus*, and *Alionycteris*), and one macroglossine (*Melonycteris woodfordi*). In contrast, these foramina are confluent in the remainder of cynopterines (*Cynopterus*, *Megaerops*, *Ptenochirus*, *Aethalops*, *Dyacopterus*, and *Haplonycteris*), macroglossines, and nyctimenines (*Nyctimene* and *Paranyctimene*).

Foramen in the Postpalatine Torus: In all species of *Pteropus*, the foramen in the postpalatine torus is absent. In contrast, such a foramen is present in many other genera, including *Rousettus* and *Eidolon*. Based on *Monodelphis* (Wible, 2003), the foramen in the postpalatine torus likely transmits contents from the minor palatine foramina to the soft palate (Wible, 2003).

Foramen for the Ramus Supraorbitalis: *Pteropus* lacks a foramen for the ramus supraorbitalis of the ramus superior in the sphenoparietal suture (the cranio-orbital foramen of Wible, 1987, or the anterior opening of the orbitotemporal canal of Wible and Gaudin, 2004). This foramen is present in many other megachiropterans, irrespective of skull size (e.g., in the large *Eidolon* and the small *Otopteropus*). In many of these taxa (e.g., in *Rousettus*), the orbitotemporal canal is externally visible. The intracranial course

of the ramus supraorbitalis of the ramus superior extends from the foramen in the sphenoparietal suture to a rather ill-defined area in the suprameatal bridge. As pointed out above, in *Pteropus* (e.g., in specimens of our sample of *P. livingstonii*) the orbitotemporal canal can be observed in the medial surface of the parietal in disarticulated skulls.

FORAMINA FOR RAMI TEMPORALES: Whereas *Pteropus* presents the typical multiple openings per side of the foramina for the rami temporales in the sutura squamosa, some megachiropterans have lost these foramina entirely. This is the case in all epomophorines except *Casinycteris* and *Scotonycteris*, some cynopterines (e.g., *Chironax* and *Otopteropus*), and all macroglossines sensu Andersen (1912). This loss implies that the vascular supply for the m. temporalis from the stapedial artery system is absent, probably having been replaced by an extracranial supply from the external carotid system, as in the dog.

INFRAORBITAL FORAMEN: Most megachiropterans, including species of *Pteropus*, exhibit a short infraorbital canal that opens very close to the orbital rim. Two genera, *Notopteris* and *Melonycteris* (forming the *Notopteris* section of Andersen, 1912), have an infraorbital foramen located more anteriorly, at a greater relative distance from the orbital rim. As a consequence, the infraorbital canal has a longer intramaxillary course.

LACRIMAL FORAMEN: In *Pteropus*, the lacrimal foramen is large and conspicuous, representing the typical condition in megachiropterans. By contrast, in *Nyctimene* the lacrimal foramen is comparatively very small, as in many microchiropterans, in which the lacrimal foramen is greatly reduced or absent.

MAJOR PALATINE FORAMEN: In *Pteropus lylei* and several other species of *Pteropus*, the major palatine foramen is located in the transverse palatine suture roughly at the level of the P4–M1 embrasure. In other species of *Pteropus* (e.g., *P. scapulatus*), the foramen is located more rostrally, at the level of P4. This condition is also seen in other pteropodines and *Eidolon.* The major palatine foramen is even more rostrally located in certain species of *Pteralopex* (e.g., *P. atrata* and *P. anceps*), in which the major palatine foramen is located at the level of P3, lying entirely within the palatine process of the maxilla. By contrast, many epomophorines and cynopterines have the major palatine foramen situated caudal to the level of M1, in which case the foramen lies entirely within the horizontal process of the palatine bone.

MASTOID FORAMEN: In Pteropodidae, this foramen exhibits three different sizes. The species of *Pteropus* we examined, as well as some other megachiropterans (e.g., *Nyctimene*), show a remarkably small mastoid foramen. By contrast, some epomophorine pteropodids have a very large mastoid foramen (e.g., *Hypsignathus*, *Epomophorus*). The remainder of our sample presents an intermediate condition.

MINOR PALATINE FORAMEN: In *Pteropus lylei*, the minor palatine foramen opens in the substance of the horizontal process of the palatine. This is also the case in the majority of megachiropterans. The most significant modification found in megachiropterans is in the pteropodine *Neopteryx frosti*. In this species, a large notch opens on the lateral margin of the postdental palate in place of the foramen. This resembles the condition seen in the dog, in which the minor palatine nerve and vessels penetrate the ventral side of the palate through an unnamed notch in the caudal part of the maxillary bone. In *Neopteryx*, however, the notch is entirely within the horizontal process of the palatine. Less extraordinary modifications are found in species of *Nyctimene* (e.g., *N. major*) and *Pteropus* (e.g., *P. hypomelanus*). In these forms, the postdental palate is constricted laterally to produce the "pandurate" (hourglass-shaped) condition described by Andersen (1912) for *Nyctimene*. In these palates, the minor palatine foramen can be very close to the lateral margin of the postdental palate, and in some individuals (e.g., *P. hypomelanus* AMNH 159043) just a tiny splint of bone prevents the foramen from being a notch.

OPTIC CANAL: Limited variation exists regarding the shape of the optic canal. In a number of species of pteropodines (e.g., *Pteropus niger*, *Pteropus voeltzkowi*, *Acerodon jubatus*, *Pteralopex acrodonta*), the optic canal protrudes rostrodorsolaterally as a short tube, with a distinct depression formed rostroventral to that tube in the

orbitosphenoid. In all other megachiropterans, including *P. lylei*, the optic canal consists of only a simple foramen and there is no development of a tubelike structure.

POSTORBITAL FORAMEN: This foramen is conspicuous and consistently present in all species of *Pteropus* and many other megachiropterans. In *Dyacopterus*, *Pteralopex* (e.g., *Pteralopex atrata* BMNH 89.4.3.3), and *Harpyionycteris*, the postorbital foramen is reduced in size and may be absent on one or both sides in some individuals. Finally, in *Dobsonia minor*, many cynopterines (all but *Cynopterus*, *Megaerops*, *Ptenochirus*, and *Dyacopterus*), and all nyctimenines, the postorbital foramen is entirely lacking in all individuals.

SPHENORBITAL FISSURE AND ALAR CANAL: *Pteropus* is typical among megachiropterans in that a single opening—the sphenorbital fissure—transmits all of the structures that pass through the orbital fissure, foramen rotundum, and alar canal (*canalis alaris*) of the dog. However, two species in the related genus *Pteralopex* exhibit a typical alar canal (based on *Pteralopex anceps* BMNH 8.11.16.7 and *Pteralopex acrodonta* BMNH 77.3097). In these taxa, the caudal alar foramen is widely separated from the foramen ovale posteriorly, and the rostral alar foramen is separated anteriorly from the sphenorbital fissure by a bony wall of the alisphenoid. In contrast, the other two species of *Pteralopex* examined by us (*Pteralopex flanneryi* USNM 277112, 276973-4, and *Pteralopex atrata* BMNH 88.1.5.9, 89.4.3.3, 34.4.2.31, 89.4.3.1) show the typical megachiropteran condition, as described above. In the dog, the foramen rotundum is clearly differentiated and opens in the dorsal side of the alar canal. It is not possible to determine whether the foramen rotundum is differentiated or not in intact skulls of *P. anceps* and *P. acrodonta*. Other foramina were not examined in detail in a sufficiently complete sample of megachiropterans.

SUMMARY: From the available comparisons, we conclude that *Pteropus* seems typical among megachiropterans in the presence and development of most foramina, while showing significant variations in some areas. Some foramina present in most megabats are absent in *Pteropus*, including the foramen in the postpalatine torus and the anterior opening of the orbitotemporal canal. One foramen (the mastoid foramen) is reduced in relative size in *Pteropus* in comparison to the condition seen in other megabats. Still other foramina have been modified by coalescence: foramen ovale + caudal alar foramen (in some species like *P. lylei*), and the piriform fenestra + basicochlear fissure + carotid foramen. In addition, *Pteropus* and megachiropterans as a group exhibit the following noteworthy conditions: an incisive fissure instead of paired incisive foramina, resulting from the lack of ossification of the palatine process of the premaxilla; a sphenorbital fissure that includes the contents of the orbital fissure, rostral alar canal, and foramen rotundum; a well-defined postorbital foramen carrying an apparently unique artery; a shortened infraorbital canal with the correspondingly retracted position of the infraorbital foramen (except *Macroglossus*, *Melonycteris*, and *Notopteris*); a minor palatine foramen in the substance of the postdental palate (horizontal process of the palatine); and lack of the posttemporal foramen.

DENTITION

The most complete dental formula known in bats is I2/3, C1/1, P3/3, M3/3 $\times$ 2 = 38, which is seen in echolocating bats such as *Myotis*. Megachiropterans have reduced dental formulae, the most complete (I2/2, C1/1, P3/3, M2/3 $\times$ 2 = 34) being present as a rule in *Pteropus* but also in other genera such as *Rousettus* and *Eidolon*. *P. lylei* is no exception, and the morphology of its dentition is also typical of both the genus and the *hypomelanus* type. Significant variations in dental formulae and tooth morphology exist among megachiropterans, most of which were discussed in detail by Andersen (1912). Seven genera and many species were discovered after the publication of Andersen's monographic treatment, but no particularly different tooth morphologies occur in the genera described after 1912. We direct the reader to Andersen (1912) for a complete analysis of dental variation in Megachiroptera. Important additional discussion is

found in Hill and Beckon (1978), and in the remarkable series of papers by Win Bergmans (Bergmans, 1976, 1977, 1980, 1988, 1989, 1990, 1994, 1997, 2001; Bergmans and Rozendaal, 1988).

The homology of specific dental structures (such as cusps, basins, and ridges) with respect to a typical tribosphenic molar is uncertain. Miller (1907), on the basis of comparisons with frugivorous phyllostomid microchiropterans, assumed that the megachiropteran upper premolars and molars each bear a protocone (medial cusp and ridge) and a paracone (lateral cusp and ridge), whereas the lower molars bear a metaconid (medial cusp and ridge) and a protoconid (lateral cusp and ridge). Andersen (1912) arrived at a similar conclusion based on comparisons with *Talpa europaea*, a mole with dilambdodont molars. Andersen (1912) postulated that the lateral ridge of the upper molars of megabats corresponded to a paracone + metacone, and the medial ridge corresponded to the protocone + hypocone; in the lower molars, the lateral ridge corresponded to a protoconid + hypoconid, and the medial ridge to paraconid + metaconid + entoconid. Both Miller (1907) and Andersen (1912) agreed that megachiropterans lack a stylar shelf; that is, the lateralmost cusps of a chiropteran tribosphenic molar (parastyle, mesostyle, and metastyle) are entirely absent.

Although most megachiropterans have simplified cheek teeth characterized by medial and lateral ridges, several taxa exhibit multicuspidate cheek teeth, most notably *Harpyionycteris* and *Pteralopex*. Miller (1907) and Andersen (1912) believed that additional cusps were the product of secondary divisions of the basic megachiropteran lateral and medial ridges. However, other authors, including Slaughter (1970; see also Thenius, 1989) homologized all individual cusps with normal tribosphenic elements, stating that an upper molar of *Harpyionycteris* exhibits a paracone, protocone, metacone, hypocone, and metastyle, and that the lower molar supports a protoconid, metaconid, hypoconid, entoconid, and two stylids (the proto- and metastylid). Peterson and Fenton (1970) dismissed the cusp homologies of Slaughter (1970) on the basis of inconsistent variation they observed in series of specimens of *Harpyionycteris*. In turn, Hill and Beckon (1978), on the basis of an extensive comparative study of the dentition in *Pteralopex*, favored Andersen's (1912) view that the multicuspidate condition of *Pteralopex* was probably derived from more typical pteropodine molars, such as those of the *pselaphon* species group within *Pteropus*. We concur with Hill and Beckon (1978) in concluding that support for detailed homology statements linking multiple cusps of molariform teeth in megachiropterans like *Pteralopex* with the cusps of the microchiropteran dentition is lacking or contradictory. While the loss of the stylar shelf seems a safe assumption, there is little or no support for identification of megachiropteran cusps with typical tribosphenic elements. Certainly, the most conservative approach to this unresolved problem would be to recognize that the two main ridges and accompanying cusps of the megachiropteran cheek tooth may derive from nonstylar, large tribosphenic cusps, but the specific homology of contributing cusps remains unknown.

DIRECTIONS FOR FUTURE RESEARCH

In this work, we provide a detailed description of external and internal surfaces of the skull of *Pteropus*, a study of the dentition and foramina contents, and propose a standard nomenclature for bat skull structures. We also provide a series of comparisons that address homology of structures, cranial ontogeny, and the level of generality of our findings within Pteropodidae as a whole. The next obvious step would be to provide comparisons with other bats, but such analyses are far beyond the scope of the current study. Echolocating bats, representing either a single clade Microchiroptera (Simmons, 1998; Simmons and Geisler, 1998, 2002) or two lineages (with yinochiropteran bats forming a clade with megachiropterans; Teeling et al., 2000, 2005), are enormously diverse in terms of skull morphology (for images of skulls of most bat genera, see Koopman, 1994). Indeed, it is largely on the basis of craniodental variation that 18 families of echolocating bats are now

recognized (Simmons, 1998, 2005). It is our intention to follow the current contribution with a similar study of skull morphology in microbats, including detailed considerations of the cranial modifications associated with evolution of echolocation.

Another area that has received inadequate attention is the morphology of the postcranial skeleton of bats. At least one broad survey of skeletal variation has been published (Walton and Walton, 1970), as well as focused studies of limb girdles (e.g., Walton and Walton, 1968; Strickler, 1978), but no truly comprehensive description has been completed that addresses anatomical nomenclature of all postcranial structures. Some skeletal features have been given different names by different authors, whereas other structures remain unnamed, and homology of some structures has yet to be fully resolved (e.g., see character descriptions in Simmons and Geisler, 1998). As with the skull, we hope to provide a solid basis of description and nomenclature for future comparative functional analyses, systematic studies, and phylogenetic analyses involving bat postcranial morphology.

ACKNOWLEDGMENTS

We are thankful to Patricia Wynne and Gina Scanlon for the illustrations. Paula Jenkins (Natural History Museum, London), Mark Engstrom and Burton Lim (Royal Ontario Museum), and Bruce Patterson and Larry Heaney (Field Museum, Chicago) permitted access to specimens in their care. Mariko Kageyama kindly assisted with photography, and Roberto Keller and Angela Klaus assisted with SEM images. We offer special thanks to Ana C. Quinteros Orio. Funding for this report was provided by the National Science Foundation (grant DEB-0129127 to JRW and grant DEB-9873663 to NBS) and Coleman and Vernay postdoctoral fellowships at the AMNH to NPG.

REFERENCES

Andersen, K. 1912. Catalogue of the Chiroptera in the collection of the British Museum Volume I: Megachiroptera. London: Trustees British Museum (Natural History).

Bensley, B.A. 1931. Practical anatomy of the rabbit. Philadelphia: P. Blakison's Son & Co.

Bergmans, W. 1976. A revision of the African genus *Myonycteris* Matschie, 1899 (Mammalia, Megachiroptera). Beaufortia 24(24): 189–216.

Bergmans, W. 1977. Notes on new material of *Rousettus madagascariensis* Grandidier, 1929 (Mammalia, Megachiroptera). Mammalia 41(1): 67–74.

Bergmans, W. 1980. A new fruit bat of the genus *Myonycteris* Matschie, 1899, from Eastern Kenya and Tanzania (Mammalia, Megachiroptera). Zoologische Mededelingen 55(14): 171–181.

Bergmans, W. 1988. Taxonomy and biogeography of African fruit bats (Mammalia, Megachiroptera). 1. General introduction; material and methods; results: the genus *Epomophorus* Bennett, 1836. Beaufortia 38(5): 75–146.

Bergmans, W. 1989. Taxonomy and biogeography of African fruit bats (Mammalia, Megachiroptera). 2. The genera *Micropteropus* Matschie, 1899, *Epomops* Gray, 1870, *Hypsignathus* H. Allen, 1861, *Nanonycteris* Matschie, 1899, and *Plerotes* Andersen, 1910. Beaufortia 39(4): 89–153.

Bergmans, W. 1990. Taxonomy and biogeography of African fruit bats (Mammalia, Megachiroptera). 3. The genera *Scotonycteris* Matschie, 1894, *Casinycteris* Thomas, 1910, *Pteropus* Brisson, 1762, and *Eidolon* Rafinesque, 1815. Beaufortia 40(7): 111–177.

Bergmans, W. 1994. Taxonomy and biogeography of African fruit bats (Mammalia, Megachiroptera). 4. The genus *Rousettus* Gray, 1821. Beaufortia 44(4): 79–126.

Bergmans, W. 1997. Taxonomy and biogeography of African fruit bats (Mammalia, Megachiroptera). 5. The genera *Lissonycteris* Andersen, 1912, *Myonycteris* Matschie, 1899, and *Megaloglossus* Pagenstecher, 1885; general remarks and conclusions; annex: key to all species. Beaufortia 47(2): 11–90.

Bergmans, W. 2001. Notes on the distribution and taxonomy of Australasian bats. I. Pteropodinae and Nyctimenina (Mammalia, Megachiroptera, Pteropodidae). Beaufortia 51(8): 119–152.

Bergmans, W., and F.G. Rozendaal. 1988. Notes on collections of fruit bats from Sulawesi and some off-lying islands (Mammalia, Megachiroptera). Zoologische Verhandelingen 248: 1–74.

Bhatnagar, K.P., and F.C. Kallen. 1974. Cribriform plate of ethmoid, olfactory bulb and olfactory acuity in forty species of bats. Journal of Morphology 142: 71–90.

Bugge, J. 1974. The cephalic arterial system in insectivores, primates, rodents and lagomorphs,

with special reference to the systematic classification. Acta Anatomica 87(suppl. 62): 1–159.

Bugge, J. 1978. The cephalic arterial system in carnivores, with special reference to systematic classification. Acta Anatomica 101: 45–61.

Bugge, J. 1979. Cephalic arterial pattern in New World edentates and Old World pangolins with special reference to their phylogenetic relationships and taxonomy. Acta Anatomica 105: 37–46.

Campbell, P., C.J. Schneider, A.M. Adnan, A. Zubaid, and T.H. Kunz. 2004. Phylogeny and phylogeography of Old World fruit bats in the *Cynopterus brachyotis* complex. Molecular Phylogenetics and Evolution 33(3): 764–781.

Cobb, W.M. 1943. The cranio-facial union and the maxillary tuber in mammals. American Journal of Anatomy 72: 39–111.

De Beer, G.R. 1937. The development of the vertebrate skull. Oxford: Clarendon Press.

Doran, A.H.G. 1878. Morphology of mammalian ossicula auditûs. Transactions of the Linnean Society of London, Second Series, Zoology 1: 391–497.

Dumont, E.R. 1999. The effect of food hardness on feeding behavior in frugivorous bats (family Phyllostomidae): an experimental study. Journal of Zoology 248: 219–229.

Dumont, E.R. 2003. Bats and fruit: an ecomorphological approach. *In* T.H. Kunz and B. Fenton (editors), Bat ecology. Chicago: The University of Chicago Press.

Evans, H.E. 1993. Miller's anatomy of the dog, 3rd ed. Philadelphia: W.B. Saunders.

Fleischer, G. 1973. Studien am Skelett des Gehörorgans der Säugetiere, einschließlich des Menschen. Säugetierkunde Mitteilungen 53: 131–239.

Gaupp, E. 1902. Über die Ala temporalis des Säugetierschädels und die Regio orbitalis einiger anderer Wirbeltierschädels. Anatomische Hefte 19: 155–230.

Gaupp, E. 1905. Neue Deutungen auf dem Gebiete der Lehre vom Säugetierschädel. Anatomischer Anzeiger 27: 273–310.

Gaupp, E. 1908. Zur Entwicklungsgeschichte und vergleichenden Morphologie des Schädels von *Echidna aculeata* var. *typica*. Semon's Zoologishe Forschungsreisen in Australien. Denkschriften der Medicinisch-Naturwissenschaftliche Gesellschaft zu Jena 6: 539–788.

Gelderen, C. van. 1924. Die Morphologie der Sinus durae matris. Zweiter Teil. Die vergleichende Ontogenie der neurokraniellen Venen der Vögel und Säugetiere. Zeitschrift für Anatomie und Entwickelungsgeschichte 74: 432–508.

Giannini, N.P., and N.B. Simmons. 2005. Conflict and congruence in a combined DNA-morphology analysis of megachiropteran bat relationships (Mammalia: Chiroptera: Pteropodidae). Cladistics 21: 1–27.

Gray, A.A. 1907. The labyrinth of animals, including mammals, birds, reptiles and amphibians. London: J. & A. Churchill.

Gregory, W.K. 1910. The orders of mammals. Bulletin of the American Museum of Natural History 27: 1–524.

Griffiths, T.A. 1982. Systematics of the New World nectar-feeding bats (Mammalia, Phyllostomidae), based on the morphology of the hyoid and lingual regions. American Museum Novitates 2742: 1–45.

Grosser, O. 1901. Zur Anatomie und Entwickelungsgeschichte des Gefässsystems der Chiropteren. Anatomische Hefte 17: 203–424.

Gunnell, G.F., and N.B. Simmons. In press. Fossil evidence and the origin of bats. Journal of Mammalian Evolution.

Handley, C.O., Jr. 1959. A revision of American bats of the genera *Euderma* and *Plecotus*. Proceedings of the United States National Museum 110: 95–246.

Henson, O.W. 1961. Some morphological and functional aspects of certain structures in the middle ear in bats and insectivores. University of Kansas Science Bulletin 42: 151–255.

Henson, O.W. 1970. The ear and audition. *In* W.A. Wimsatt (editor), Biology of bats 2:181–263. New York: Academic Press.

Hiatt, J.L., and L.P. Gartner. 1987. Textbook of head and neck anatomy, 2nd ed. Baltimore: Williams & Wilkins.

Hill, J.E., and W.N. Beckon. 1978. A new species of *Pteralopex* Thomas, 1888 (Chiroptera: Pteropodidae) from the Fiji Islands. Bulletin of the British Museum of Natural History (Zoology) 34(2): 65–82.

Hinchcliffe, R., and A. Pye. 1969. Variations in the middle ear of the Mammalia. Journal of Zoology 157: 277–288.

Hyrtl, J. 1853. Beiträge zur vergleichenden Angiologie. IV. Das arterielle Gefäss-system der Monotremen. Denkschriften Akademie der Wissenschaft, Wien, mathematisch-naturwissenschaftliche Klasse 5: 1–20.

Hyrtl, J. 1854. Beiträge zur vergleichenden Angiologie. V. Das arterielle Gefäss-system der Edentata. Denkschriften Akademie der Wissenschaft, Wien, mathematisch-naturwissenschaftliche Klasse 6: 21–65.

Jurgens, J.D. 1963. Contributions to the descriptive and comparative anatomy of the cranium of the Cape fruit-bat *Rousettus aegyptiacus*. Annale van die Universiteit van Stellenbosch, series A 38(1): 3–37.

Kämper, R., and U. Schmidt. 1977. Die Morphologie der Nasenhöhle bei einigen neotropischen Chiropteren. Zoomorphologie 87: 3–19.

Klaauw, C.J. van der. 1922. Ueber die Entwickelung des Entotympanicums. Tijdschrift Nederlandsche Dierkundige Vereeniging 18: 135–174.

Klaauw, C.J. van der. 1931. The auditory bulla in some fossil mammals. Bulletin of the American Museum of Natural History 62: 1–352.

Koopman, K.F. 1993. Order Chiroptera. *In* D.E. Wilson and D.M. Reeder (editors), Mammal species of the world, a taxonomic and geographic reference, 2nd ed.: 137–241. Washington, DC: Smithsonian Institution.

Koopman, K.F. 1994. Chiroptera systematics Handbook of Zoology [vol. 8, part 60], Mammalia, New York: Walter de Gruyter.

Leche, W. 1876–1877. Zur Kenntniss des Milchgebisses und der Zahnhomologien bei Chiroptera. II. Theil. Lunds Universitets Ars-Skrift. Tom XIII: 1–37.

MacIntyre, G.T. 1972. The trisulcate petrosal pattern of mammals. *In* T. Dobzhansky, M.K. Hecht, and W.C. Steere (editors), Evolutionary biology. New York: Appleton-Century-Crofts, 6: 51–70.

MacPhee, R.D.E. 1981. Auditory region of primates and eutherian insectivores. Contributions to Primatology 18: 1–282.

Marshall, L.G., and C. de Muizon. 1995. Part II. The skull. *In* L.G. Marshall, C. de Muizon, and D. Sigogneau-Rusell (editors), *Pucadelphys andinus* (Marsupialia, Mammalia) from the early Paleocene of Bolivia. Mémoires du Muséum National d'Histoire Naturelle 165: 21–90.

Maryanto, I., and M. Yani. 2003. A new species of *Rousettus* (Chiroptera: Pteropodidae) from Lore Lindu, Central Sulawesi. Mammal Study 28(2): 111–120.

Mayer, F., and O. von Helversen. 2001. Cryptic diversity in European bats. Proceedings of the Royal Society of London B 268: 1825–1832.

McDowell, S.B., Jr. 1958. The Greater Antillean insectivores. Bulletin of the American Museum of Natural History 115: 113–214.

Miller, G.S., Jr. 1907. The families and genera of bats. Bulletin of the United States National Museum 57: 1–282.

Nicolay, C.W., and E.R. Dumont. 2000. An experimental analysis of feeding behavior in a nectarivorous bat, *Syconycteris australis*. Mammalia 64(2): 155–161.

Nomina Anatomica Veterinaria. 1994. 4th ed. Zürich and New York: World Association of Veterinary Anatomists.

Nomina Embriologica Veterinaria. 1994. Zürich and New York: World Association of Veterinary Anatomists.

Novacek, M.J. 1977. Aspects of the problem of variation, origin and evolution of the eutherian auditory bulla. Mammal Review 7: 131–149.

Novacek, M.J. 1980. Cranioskeletal features in tupaiids and selected Eutheria as phylogenetic evidence. *In* W.P. Luckett (editor), Comparative biology and evolutionary relationships of tree shrews. New York: Plenum Press, 35–93.

Novacek, M.J. 1985a. Evidence for echolocation in the oldest known bats. Nature 315: 140–141.

Novacek, M.J. 1985b. Comparative morphology of the bat auditory region. Fortschritte der Zoologie 30: 149–151.

Novacek, M.J. 1986. The skull of leptictid insectivorans and the classification of eutherian mammals. Bulletin of the American Museum of Natural History 183: 1–112.

Novacek, M.J. 1987. Auditory features and affinities of the Eocene bats *Icaronycteris* and *Plaeochiropteryx* (Microchiroptera, *incertae sedis*). American Museum Novitates 2877: 1–18.

Novacek, M.J. 1991. Aspects of the morphology of the cochlea in microchiropteran bats: an investigation of character transformation. Bulletin of the American Museum of Natural History 206: 84–100.

Novacek, M.J., and A. Wyss. 1986. Origin and transformation of the mammalian stapes. *In* K.M. Flanagan and J.A. Lillegraven (editors), Vertebrates, phylogeny, and philosophy. Contributions to Geology, University of Wyoming, Special Paper 3: 35–53.

Peterson, R.L., and B.M. Fenton. 1970. Variation in the bats of the genus *Harpyionycteris*, with the description of a new race. Royal Ontario Museum Life Science Contribution 17: 1–15.

Romagnoli, M.L., and M.S. Springer. 2000. Evolutionary relationships among Old World fruitbats (Megachiroptera: Pteropodidae) based on 12S rRNA, tRNA valine and 16S rRNA gene sequences. Journal of Mammalian Evolution 7: 259–284.

Rougier, G.W., J.R. Wible, and J.A. Hopson. 1992. Reconstruction of the cranial vessels in the Early Cretaceous mammal *Vincelestes neuquenianus*: implications for the evolution of the mammalian cranial vascular system. Journal of Vertebrate Paleontology 12: 188–216.

Ruedi, M., and F. Mayer. 2001. Molecular systematics of bats of the genus *Myotis* (Vespertilionidae) suggests deterministic ecomorphological convergences. Molecular Phylogenetics and Evolution 21(3): 436–448.

Schaller, O. 1992. Illustrated veterinary anatomical nomenclature. Stuttgart: Ferdinand Enke Verlag.

Segall, W. 1970. Morphological parallelisms of the bulla and auditory ossicles in some insecti-

vores and marsupials. Fieldiana Zoology 51: 169–205.

Simmons, N.B. 1994. The case for chiropteran monophyly. American Museum Novitates 3103: 1–54.

Simmons, N.B. 1998. A reappraisal of interfamilial relationships of bats. *In* T.H. Kunz and P.A. Racey (editors), Bat: phylogeny, morphology, echolocation, and conservation biology: 1–47. Washington, DC: Smithsonian Institution Press.

Simmons, N.B. 2005. Order Chiroptera. *In* D.E. Wilson and D.M. Reeder (editors), Mammal species of the world: a taxonomic and geographic reference, 3rd ed. Washington, DC: Smithsonian Institution Press.

Simmons, N.B., and J.H. Geisler. 1998. Phylogenetic relationships of *Icaronycteris*, *Archaeonycteris*, *Hassianycteris*, and *Palaeochiropteryx* to extant bat lineages, with comments on the evolution of echolocation and foraging strategies in Microchiroptera. Bulletin of the American Museum of Natural History 235: 1–182.

Simmons, N.B., and J.H. Geisler. 2002. Sensitivity analysis of different methods of coding taxonomic polymorphism: an example from higher-level bat phylogeny. Cladistics 18(6): 571–584.

Sisson, S. 1910. A text-book of veterinary anatomy. Philadelphia: W.B. Saunders.

Slaughter, B.H. 1970. Evolutionary trends in chiropteran dentitions. *In* B.H. Slaughter and D.W. Walton (editors), About bats. Fondren Science Series: 11:51–83. Dallas: Southern Methodist University Press.

Sprague, J.M. 1943. The hyoid region of placental mammals with especial reference to the bats. American Journal of Anatomy 72: 385–472.

Springer, M.S., L.J. Hollar, and J.A. Kirsch. 1995. Phylogeny, molecules versus morphology and rates of character evolution among fruit bats (Chiroptera: Megachiroptera). Australian Journal of Zoology 43: 557–582.

Starck, D. 1943. Beitrag zur Kenntnis der Morphologie und Entwicklungsgeschichte des Chiropterencraniums. Das Chondrocranium von *Pteropus seminudus*. Zeitschrift für Anatomie und Entwicklungsgeschichte 112: 588–633.

Storch, G. 1968. Funktionsmorphologische Untersuchungenan der Kaumuskulatur und an korrelierten Schädelstrukturem der Chiropteren. Abhandlungen der Senckenbergischen Naturforschenden Gesellschaft 517: 1–92.

Stricker, T.L. 1978. Functional osteology and myology of the shoulder in the Chiroptera. Contributions to Vertebrate Evolution 4: 1–198.

Tandler, J. 1899. Zur vergleichenden Anatomie der Kopfarterien bei den Mammalia. Denkschriften Akademie der Wissenschaften, Wien, Mathematisch-Naturwissenschaftliche Klasse 67: 677–784.

Tandler, J. 1901. Zur vergleichenden Anatomie der Kopfarterien bei den Mammalia. Anatomische Hefte 18: 327–368.

Tandler, J. 1902. Zur Entwickelungsgeschichte der Kopfarterien bei den Mammalia. Gegenbaurs Morphologisches Jahrbuch 30: 275–373.

Teeling, E.C., M. Scally, D. Kao, M. Romagnoli, M.S. Springer, and M.J. Stanhope. 2000. Molecular evidence regarding the origin of echolocation and flight in bats. Nature 403(6766): 188–192.

Teeling, E.C., M.S. Springer, O. Madsen, P. Bates, S.J. O'Brien, and W.J. Murphy. 2005. A molecular phylogeny for bats illuminates biogeography and the fossil record. Science 307: 580–584.

Thenius, E. 1989. Zähne und Gebiß der Saugëtiere. *In* J. Niethammer, H. Schliemann, and D. Starck (editors), Handbook of zoology, vol. VIII, Mammalia, part 56. Berlin: Walter de Gruyter.

Thewissen, J.G.M. 1989. Mammalian frontal diploic vein and the human foramen caecum. Anatomical Record 223: 242–244.

Voit, M. 1909. Das Primordialcranium des Kaninchens unter Berücksichtigung der Deckknochen. Anatomische Hefte 38: 425–616.

Walton, D.W., and G.M. Walton. 1968. Comparative osteology of the pelvic and pectoral girdles of the Phyllostomatidae (Chiroptera: Mammalia). Journal of the Graduate Research Center, Southern Methodist University 37: 1–35.

Walton, D.W., and G.M. Walton. 1970. Postcranial osteology of bats. *In* B.H. Slaughter and W.D. Walton (editors), About bats. Fondren Science Series 11: 93–126. Dallas: Southern Methodist University Press.

Wassif, K. 1948. Studies on the structure of the auditory ossicles and tympanic bone in Egyptian Insectivora, Chiroptera and Rodentia. Bulletin of the Faculty of Science, Fouad I University 27: 177–213.

Wible, J.R. 1984. The ontogeny and phylogeny of the mammalian cranial arterial pattern. Ph.D. dissertation, Duke University: Durham, NC. 705 pp.

Wible, J.R. 1986. Transformations in the extracranial course of the internal carotid artery in mammalian phylogeny. Journal of Vertebrate Paleontology 6: 313–325.

Wible, J.R. 1987. The eutherian stapedial artery: character analysis and implications for superordinal relationships. Zoological Journal of the Linnean Society 91: 107–135.

Wible, J.R. 1989. Vessels on the side wall of the braincase in cynodonts and primitive mammals. Fortschritte der Zoologie 35: 406–408.

Wible, J.R. 1990. Late Cretaceous marsupial petrosal bones from North America and a cladistic analysis of the petrosal in therian mammals. Journal of Vertebrate Paleontology 10: 183–205.

Wible, J.R. 1992. Further examination of the basicranial anatomy of the Megachiroptera: a reply to A.J. King. Acta Anatomica 143: 309–316.

Wible, J.R. 2003. On the cranial osteology of the short-tailed opossum *Monodelphis brevicaudata* (Didelphidae, Marsupialia). Annals of Carnegie Museum 72: 137–202.

Wible, J.R., and D.L. Davis. 2000. Ontogeny of the chiropteran basicranium, with reference to the Indian false vampire bat *Megaderma lyra*. *In* R.A. Adams and S.C. Pedersen (editors), Ontogeny, functional ecology and evolution of bats: 214–246. New York: Cambridge University Press.

Wible, J.R., and T.J. Gaudin. 2004. On the cranial osteology of the yellow armadillo *Euphractus sexcinctus* (Dasypodidae, Xenarthra, Placentalia). Annals of Carnegie Museum 73: 117–196.

Wible, J.R., and J.A. Hopson. 1993. Basicranial evidence for early mammal phylogeny. *In* F.S. Szalay, M.J. Novacek, and M.C. McKenna (editors), Mammal phylogeny: mesozoic differentiation, multituberculates, monotremes, early therians, and marsupials: 45–62. New York: Springer Verlag.

Wible, J.R., and J.A. Hopson. 1995. Homologies of the prootic canal in mammals and nonmammalian cynodonts. Journal of Vertebrate Paleontology 15: 331–356.

Wible, J.R., and J.R. Martin. 1993. Ontogeny of the tympanic floor and roof in archontans. *In* R.D.E. MacPhee (editor), Primates and their relatives in phylogenetic perspective: 111–148. New York: Plenum Press.

Wible, J.R., and M.J. Novacek. 1988. Cranial evidence for the monophyletic origin of bats. American Museum Novitates 2911: 1–19.

Wible, J.R., M.J. Novacek, and G.W. Rougier. 2004. New data on the skull and dentition in the Mongolian Late Cretaceous eutherian mammal *Zalambdalestes*. Bulletin of the American Museum of Natural History 281: 1–144.

Wible, J.R., and G.R. Rougier. 2000. Cranial anatomy of *Krytobaatar dashzevegi* (Mammalia, Multituberculata), and its bearing on the evolution of mammalian characters. Bulletin of the American Museum of Natural History 247: 1–124.

APPENDIX 1

List of Anatomical Terms

Terms used in the text are listed alphabetically, along with references and/or Nomina Anatomica Veterinaria (NAV) and Nomina Embryologica Veterinaria (NEV) equivalents. Single asterisks (*) indicate structures discussed in the text but absent in *Pteropus lylei* (e.g., Alar canal). Double asterisks (**) indicate structures discussed in the text whose development in *P. lylei* is minimal or negligible, or structures of uncertain homology (e.g., Dorsum sellae).

Abducens nerve (= cranial nerve VI)—Nervus abducens (NAV)
Accessory nerve (= cranial nerve XI)—Nervus accessorius (NAV)
Accessory palatine artery (Evans, 1993)
Accessory palatine foramen (Wible and Rougier, 2000) = Minor palatine foramen (Evans, 1993)
Accessory palatine nerve—Nervus palatinus accessorius (NAV)
Ala hypochiasmatica (De Beer, 1937)
Alae of vomer—Alae vomeris (NAV)
Ala orbitalis (= orbitosphenoid) (NAV)
Ala temporalis (= alisphenoid) (NAV)
Alar canal (= alisphenoid canal)*—Canalis alaris (NAV)
Alicochlear commissure* (De Beer, 1937)—Processus cochlearis ossis sphenoidalis (Henson, 1970)
Alisphenoid—Os basisphenoidale, ala temporalis (NAV)
Alveolar canal—Canalis alveolaris (NAV)
Alveolar foramina—Foramina alveolaria (NAV)
Alveolar line or border—Margo alveolaris (NAV)
Alveolar nerve—Nervus alveolaris (NAV)
Alveolar process or surface of maxilla—Processus alveolaris (NAV)
Alveoli—Alveoli dentales (NAV)
Ampulla—Ampulla ossea (NAV)
Anastomotic artery = Arteria anastomotica (Wible, 1987)
Angle of mandible—Mandibula, angulus mandibulae (NAV)
Angular process**—Processus angularis (NAV)
Anterior basicochlear commissure* (De Beer, 1937)
Anterior cornu (= hyoid arch) (Sprague, 1943)—Cornu minus (NAV)
Anterior crus (= leg) of ectotympanic—Annulus tympani, crus anterior (NAV)
Anterior (= rostral) crus (= leg) of stapes—Stapes, crus rostrale (NAV)
Anterior division of ramus superior (Wible, 1987)
Anterior mental foramen: see Mental foramen
Anterior opening, orbitotemporal canal* (Rougier et al., 1992) = Cranio-orbital foramen (= foramen for ramus supraorbitalis) (Wible, 1987)
Anterior paraseptal cartilages—Cartilago paraseptalis anterior (Jurgens, 1963)
Anterior semicircular canal—Canalis semicircularis anterior (NAV)
Apex of alveolus—Apex radici dentis (NAV)
Apex of skull (Evans, 1993)
Apex partis petrosae (NAV)
Arch of cricoid—Arcus cartilaginis cricoideae (NAV)
Arcus alveolaris (NAV)
Area cochleae (NAV)
Area nervus facialis (NAV)
Arteria diploëtica magna (Hyrtl, 1853, 1854; Wible, 1987)
Artery of postorbital foramen (this study)
Artery of pterygoid canal (Evans, 1993)
Articular (Goodrich, 1930)
Articulatio temporohyoidea (NAV)
Arytenoid cartilage—Cartilago arytenoidea (NAV)
Atlanto-occipital joint—Articulatio atlanto-occipitalis (NAV)
Auditory capsule—Capsula otica (NEV)
Auditory region—Auris (NAV)
Auditory tube—Tuba auditiva (NAV)
Basicochlear fissure (= basicapsular fenestra; = petro-occipital fissure) (De Beer, 1937)—Fissura petro-occipitalis (Evans, 1993)
Basicranial axis (Andersen, 1912)
Basicranium—Basis cranii interna et externa (NAV)
Basihyoid—Basihyoideum (NAV)
Basihyoid cartilage—Cartilago basihyoidea (NAV)
Basilar artery—Arteria basilaris (NAV)

Basioccipital—Os occipitale, pars basilaris (NAV)
Basioccipital pit (this study)
Basipharyngeal canal (Evans, 1993)
Basisphenoid—Os basisphenoidale, corpus (NAV)
Body of mandible—Corpus mandibulae (NAV)
Body of maxilla—Os maxillare, corpus maxillae (NAV)
Body of premaxilla—Corpus ossis incisivi (NAV)
Brain—Encephalon (NAV)
Braincase—Calvaria (NAV)
Buccal (= vestibular; lateral) surface of mandible—Mandibula, facies buccalis (NAV)
Canines—Dentes canini (NAV)
Capsuloparietal emissary vein (Gelderen, 1924)
Carnassial tooth* (Evans, 1993)—Dens sectorius (NAV)
Carotid foramen (Wible and Gaudin, 2004)—Canalis caroticus (NAV)
Carotid sulcus—Sulcus caroticus (NAV)
Cartilage "N" (Jurgens, 1963)
Caudal alar foramen*—Foramen alare caudale (NAV)
Caudal clinoid process*—Os basisphenoidalis, processus clinoideus caudalis (NAV)
Caudal cornu of thyroid—Cartilago thyroidea, cornu caudale (NAV)
Caudal entotympanic—Caudales entotympanicum (Klaauw, 1922)
Caudal meningeal artery—Arteria meningea caudalis (NAV)
Caudal nasal nerve—Nervus nasalis caudalis (NAV)
Caudal palatine foramen (Evans, 1993)—Foramen palatinum caudale (NAV)
Caudal process of pterygoid (this study)
Caudal thyroid notch—Incisura thyroidea caudalis (NAV)
Caudal tympanic process of petrosal (MacPhee, 1981)
Caudolateral angle of parietal (this study)
Caudoventral margin of parietal (this study)
Cavernous sinus—Sinus cavernosus (NAV)
Cavum epiptericum (Gaupp, 1902, 1905; De Beer, 1937)
Cavum supracochleare (= genu of facial canal) (Voit, 1909; De Beer, 1937)—Geniculum canalis facialis (NAV)
Cavum tympani (NAV)
Central stem (= parachordal plate) (De Beer, 1937)
Ceratohyoid—Ceratohyoideum (NAV)
Ceratohyoid cartilage—Cartilago ceratohyoidea (NAV)
Cerebellum (NAV)
Cerebral juga—Juga cerebralia (Evans, 1993)
Choanae (NAV)
Chorda tympani nerve—Chorda tympani (NAV)
Cingulum of teeth—Dentes, cingulum (NAV)
Circle of Willis (= arterial circle of brain)—Circulus arteriosus cerebri (NAV)
Cochlear area of petrosal—Area cochleae (NAV)
Cochlear canaliculus—Apertura externa canaliculus cochleae (NAV) = Aqueductus cochleae (Evans, 1993)
Cochlear duct—Ductus cochlearis (NAV)
Cochlear fossula (MacPhee, 1981)
Cochlear nerve—Nervus cochlearis (NAV)
Common nasal meatus—Meatus nasi communis (NAV)
Conchal crest—Crista conchalis (NAV)
Condyloid canal*—Canalis condylaris (NAV)
Condyloid crest of mandible—Mandibula, crista condyloidea (NAV)
Condyloid fossa—Fossa condylaris ventralis (NAV)
Coronal (= frontoparietal) suture—Sutura coronalis (NAV) = Sutura frontoparietalis (Evans, 1993)
Coronoid crest—Crista coronoidea (Evans, 1993)
Coronoid process—Processus coronoideus (NAV)
Cranio-orbital foramen (= foramen for ramus supraorbitalis)* (Wible, 1987)
Cranioventral process of arytenoid (this study)
Cranium (NAV)
Crest of vomer—Crista vomeris (NAV)
Cribriform foramina—Foramina laminae cribrosae (NAV)
Cribriform plate of ethmoid—Os ethmoidale, lamina cribrosa (NAV)
Cricoarytenoid articulation—Articulation cricoarytenoidea (NAV)
Cricoid cartilage—Cartilago cricoidea (NAV)

Cricothyroid articulation—Articulatio cricothyroidea (NAV)
Crista galli of ethmoid—Os ethmoidale, crista galli (NAV)
Crista parotica of petrosal (De Beer, 1937)
Crista semicircularis (Jurgens, 1963)
Crown of teeth—Dentes, corona dentis (NAV)
Crus breve of incus—Incus, crus breve (NAV)
Crus commune of semicircular canals (Wible, 1990)—Crus osseum commune (Henson, 1970)
Cusp of teeth—Dentes, cuspis dentis (NAV)
Deciduous teeth—Dentes decidui (NAV)
Deep petrosal nerve—Nervus petrosus profundis (NAV)
Diastema (NAV)
Digastric muscle—Musculus digastricus (NAV)
Digital impressions—Cranium, lamina interna, impressiones digitatae (NAV)
Dorsal condyloid fossa—Fossa condylaris dorsalis (Evans, 1993)
Dorsal intraoccipital synchondrosis—Synchondrosis intraoccipitalis squamolateralis (NAV)
Dorsal lamina of cricoid—Lamina cartilaginis cricoideae (NAV)
Dorsal nasal meatus—Meatus nasi dorsalis (NAV)
Dorsal process of arytenoid (this study)
Dorsal surface of basisphenoid—Os basisphenoidalis, facies cerebralis (NAV)
Dorsal surface of palate—Os palatinum, facies nasalis (NAV)
Dorsal vestibular area of petrosal—Area vestibularis superior (NAV)
Dorsum sellae** (NAV)
Ectopterygoid process (Novacek, 1986)
Ectotympanic—Annulus tympanicus (NAV)
Embrasure—Septa interalveolaria (NAV)
Emissary vein of cavernous sinus (Evans, 1993)
Encephalic surface of petrosal—Os temporale, pars petrosa, facies encephalica (Evans, 1993)
Endolymphatic duct—Ductus endolymphaticus (NAV)
Endoturbinates—Endoturbinalia (NAV)
Entoconid (Miller, 1907)
Entotympanic—Entotympanicum (Klaauw, 1922) = Os temporale, pars endotympanica (NAV)
Epiglottic cartilage—Cartilago epiglottica (NAV)
Epihyoid—Epihyoideum (NAV)
Epihyoid cartilage—Cartilago epihyoidea (NAV)
Epiphyseal cartilage—Cartilago epiphysialis (NAV)
Epitympanic angle of parietal (this study)
Epitympanic margin of parietal (this study)
Epitympanic recess—Recessus epitympanicus (NAV)
Epitympanic wing of alisphenoid (MacPhee, 1981)
Epitympanic wing of parietal (this study)
Ethmoid—Os ethmoidale (NAV)
Ethmoidal artery—Arteria ethmoidalis (NAV)
Ethmoidal crest of palatine—Crista ethmoidalis (NAV)
Ethmoidal foramen/notch—Foramen ethmoidale (NAV)
Ethmoidal fossae—Fossae ethmoidales (NAV)
Ethmoidal nerve—Nervus ethmoidalis (NAV)
Ethmoidomaxillary suture—Sutura ethmoidamaxillaris (NAV)
Ethmoidonasal suture*—Sutura ethmoidonasalis (NAV)
Ethmoturbinal—Ethmoturbinale (NAV)
Exoccipital—Os occipitale, pars lateralis (NAV)
External acoustic meatus—Meatus acusticus externus (NAV)
External acoustic porus—Porus acusticus externus (NAV)
External carotid artery—Arteria carotis externa (NAV)
External nasal aperture—Apertura nasi ossea (NAV)
External occipital protuberance—Protuberantia occipitalis externa (NAV)
External occipital crest—Crista occipitalis externa (NAV)
External ophthalmic (= orbital) artery (= ramus orbitalis)—Arteria ophthalmica externa (NAV)
External surface of parietal—Os parietale, facies externa (NAV)
Eyeball—Bulbus oculi (NAV)

Eyelids—Palpebrae (NAV)
Facial canal—Canalis facialis (NAV)
Facial nerve (= cranial nerve VII)—Nervus facialis (NAV)
Facial nerve area—Area nervus facialis (NAV)
Facial sulcus (MacPhee, 1981)
Facial surface of lacrimal—Os lacrimale, facies facialis (NAV)
Fenestra cochleae (NAV)
Fenestra vestibuli (NAV)
Fifth pharyngeal arch—Arcus pharyngeus quintus (NEV)
Footplate (= base) of stapes—Stapes, basis stapedis (NAV)
Foramen acusticum inferius = Ventral vestibular area (Evans, 1993)
Foramen acusticum superius = Facial canal + dorsal vestibular area (Evans, 1993)
Foramen alare parvum* (NAV)
Foramen for chorda tympani nerve (Jurgens, 1963)
Foramen for dorsal sagittal sinus*—Foramen sinus sagittalis dorsalis (NAV)
Foramina for frontal diploic vein (Thewissen, 1989)
Foramen for ramus temporalis (= subsquamosal foramen) (Wible and Gaudin, 2004; Wible et al., 2004)
Foramen in the postpalatine torus* (Wible, 2003)
Foramen for zygomatic nerve* (Evans, 1993)
Foramen magnum (NAV)
Foramen ovale (NAV)
Foramen rotundum* (NAV)
Foramen singulare* (NAV)
Foramen spinosum* (NAV)
Forehead—Frons (NAV)
Fossa cerebellaris of petrosal—Fossa cerebellaris, pars petrosa (NAV)
Fossa for lacrimal sac—Fossa sacci lacrimalis (NAV)
Fossa for stapedius muscle (MacPhee, 1981)—Fossa m. stapedius (Evans, 1993)
Fossa for tensor tympani muscle (MacPhee, 1981)—Fossa m. tensor tympani (Evans, 1993)
Fossa incudis (MacPhee, 1981)
Fossa infratemporalis (NAV)
Fossa temporalis (NAV)
Fourth pharyngeal arch—Arcus pharyngeus quartus (NEV)
Frontal—Os frontale (NAV)
Frontal angle of parietal—Os parietale, angulus frontalis (NAV)
Frontal crest—Os frontale, facies interna, crista frontalis (NAV)
Frontal diploic vein—Vena diploica frontalis (NAV)
Frontal margin of parietal—Os parietale, margo frontalis (NAV)
Frontal nerve—Nervus frontalis (NAV)
Frontal process of jugal—Os zygomaticum, processus frontalis (NAV)
Frontal process of maxilla—Os maxillare, processus frontalis (NAV)
Frontal process of nasal—Os nasale, processus frontalis (NAV)
Frontal region—Regio frontalis (NAV)
Frontal sinus—Sinus frontalis (NAV)
Frontoethmoidal suture—Sutura frontoethmoidalis (NAV)
Frontolacrimal suture—Sutura frontolacrimalis (NAV)
Frontomaxillary suture—Sutura frontomaxillaris (NAV)
Frontonasal suture—Sutura frontonasalis (NAV)
Frontopalatine suture—Sutura frontopalatina (NAV)
Frontozygomatic suture*—Sutura frontozygomatica (NAV)
Geniculate ganglion—Ganglion geniculi (NAV)
Gonial (= prearticular) (Gaupp, 1908; De Beer, 1937)
Glaserian fissure—Fissura Glaseri (Klaauw, 1931) = Fissura petrotympanica (NAV)
Glenoid fossa (= retroarticular fossa)—Fossa mandibularis (NAV)
Glossopharyngeal nerve (= cranial nerve IX)—Nervus glossopharyngeus (NAV)
Greater petrosal nerve—Nervus petrosus major (NAV)
Groove for middle meningeal artery—Sulcus arteriae meningeae mediae (Evans, 1993)
Gyri of brain—Cerebrum, gyri cerebri (NAV)
Hamulus—Hamulus pterygoideus (NAV)
Hard palate—Palatum osseum (NAV)
Head of malleus—Caput mallei (NAV)
Head of stapes—Caput stapedis (NAV)
Hiatus Fallopii (McDowell, 1958) = Petrosal canal (Evans, 1993)
Horizontal part of vomer (Evans, 1993)

Horizontal process of palatine—Os palatinum, lamina horizontalis (NAV)
Hyoid apparatus—Apparatus hyoideus (NAV)
Hypocone** (Miller, 1907)
Hypoconid** (Miller, 1907)
Hypoglossal canal* (Evans, 1993)
Hypoglossal foramen—Canalis n. hypoglossum (NAV) = Foramen hypoglossi (Evans, 1993)
Hypoglossal nerve—Nervus hypoglossus (NAV)
Hypoglossal vein—Vena canalis hypoglossi (Evans, 1993)
Hypophyseal fossa—Fossa hypophysealis (NAV)
Hypophysis (NAV)
Incisive fissure (this study)—Fissura palatina (NAV)
Incisive foramen (= palatine fissure)—Fissura palatina (NAV)
Incisive incisure of vomer—Vomer, incisura incisiva (NAV)
Incisivomaxillary canal (= alveolar canal)—Canalis maxilloincisivus (Evans, 1993)
Incisors—Dentes incisivi (NAV)
Incudal body—Corpus incudis (NAV)
Incudomalleolar joint—Articulation incudomallearis (NAV)
Incudostapedial joint—Articulation incudostapedia (NAV)
Incus (NAV)
Inferior alveolar artery—Arteria alveolaris inferior (NAV)
Inferior alveolar nerve—Nervus alveolaris inferior (NAV)
Inferior alveolar vein—Vena alveolaris inferior (NAV)
Inferior (= ventral) petrosal sinus—Sinus petrosus ventralis (NAV)
Infraorbital artery—Arteria infraorbitalis (NAV)
Infraorbital canal—Canalis infraorbitalis (NAV)
Infraorbital foramen—Foramen infraorbitale (NAV)
Infraorbital margin—Margo infraorbitalis (NAV)
Infraorbital nerve—Nervus infraorbitalis (NAV)
Infraorbital vein—Vena infraorbitalis (NAV)
Infratemporal crest—Crista infratemporalis (NAV)
Infratemporal fossa—Fossa infratemporalis (NAV)
Inner lamella of malleus (= rostral process of malleus, part) (Jurgens, 1963)
Inner table of frontal—Os frontale, facies interna (NAV)
Intercondyloid (= odontoid) notch—Incisura intercondyloidea (Evans, 1993)
Interdental palate (Andersen, 1912)
Interfrontal suture—Sutura interfrontalis (NAV)
Interincisive suture—Sutura interincisiva (NAV)
Intermandibular space—Spatium mandibulae (NAV)
Intermaxillary suture—Sutura intermaxillaris (Evans, 1993) = [Rostral part of] sutura palatina mediana (NAV)
Internal acoustic meatus—Meatus acusticus internus (NAV)
Internal auditory artery (= labyrinthine artery)—Arteria labyrinthi (NAV)
Internal carotid artery—Arteria carotis interna (NAV)
Internal carotid (= deep petrosal) nerve—Nervus caroticus interna (NAV)
Internal jugular vein—Vena jugularis interna (NAV)
Internal occipital crest of supraoccipital—Os occipitale, pars squamosa, crista occipitalis interna (NAV)
Internal surface of maxilla—Os maxillare, facies nasalis (NAV)
Internal surface of nasal—Os nasale, facies interna (NAV)
Internal surface of parietal—Os parietale, facies interna (NAV)
Internasal suture—Sutura internasalis (NAV)
Interorbital area of frontal (Miller, 1907)
Interpalatine suture (this study)—[Caudal part of] sutura palatina mediana (NAV)
Interparietal—Os interparietalis (NAV)
Intersphenoidal synchondrosis—Synchondrosis intersphenoidalis (NAV)
Intracrural (= stapedial) foramen—Stapes, foramen intracrurale (Fleischer, 1973)
Jugal—Os zygomaticum (NAV)
Jugular foramen—Foramen jugulare (NAV)
Jugular incisure—Incisura jugularis (NAV)
Juga—Juga alveolaria (NAV)
Labyrinthus ethmoidalis (NAV)
Lacrimal—Os lacrimale (NAV)

Lacrimal artery—Arteria lacrimalis (NAV)
Lacrimal canal—Canalis lacrimalis (NAV)
Lacrimal duct—Canaliculus lacrimalis (NAV)
Lacrimal fenestra (Wible and Gaudin, 2004)
Lacrimal foramen—Foramen lacrimale (NAV)
Lacrimal sac—Saccus lacrimalis (NAV)
Lacrimoethmoidal suture—Sutura lacrimoethmoidalis (Evans, 1993)
Lacrimomaxillary suture—Sutura lacrimomaxillaris (NAV)
Lacrimozygomatic suture*—Sutura lacrimozygomatica (NAV)
Lambdoid suture—Sutura lambdoidea (NAV); see Occipitointerparietal and Occipitoparietal sutures
Lamina basalis of ethmoid—Os ethmoidale, lamina basalis (NAV)
Lamina interna of skull—Cranium, lamina interna (NAV)
Lamina transversalis anterior (Jurgens, 1963)
Laminae lateralis of vomer (Evans, 1993)
Laryngeal prominence*—Cartilago thyroidea, prominentia laryngea (Evans, 1993)
Larynx (NAV)
Lateral ligament—Ligamentum lateralis (NAV)
Lateral process of malleus—Malleus, processus lateralis (NAV)
Lateral pterygoid muscle—M. pterygoideus lateralis (NAV)
Lateral ridge of cheekteeth (Andersen, 1912)
Lateral surface of jugal—Os zygomaticum, facies lateralis (NAV)
Lateral surface of petrosal—Os temporale, pars petrosa, facies lateralis (MacIntyre, 1972; Wible, 1990)
Lateral (= vestibular; = buccal; = facial; = labial) surface of teeth—Dentes, facies vestibularis (= facialis) (NAV)
Lateral surface of zygomatic arch—Arcus zygomaticus, facies lateralis (NAV)
Left lamina of thyroid—Cartilago thyroidea, lamina sinistra (NAV)
Lenticular process of incus—Incus, processus lenticularis (NAV)
Lesser petrosal nerve—Nervus petrosus minor (NAV)
Levator palpebrae superioris (NAV)
Lingual surface of mandible—Mandibula, facies lingualis (NAV)
Lingula sphenoidalis**—Os basisphenoidalis, lingula sphenoidalis (Evans, 1993)
Long crus (= leg) of incus—Incus, crus longum (NAV)
Longitudinal fissure of brain—Fissura longitudinalis cerebri (NAV)
Lower tooth row—Arcus dentalis inferior (NAV)
Major palatine artery—Arteria palatina major (NAV)
Major palatine foramen—Foramen palatinum majus (NAV)
Major palatine nerve—Nervus palatinus major (NAV)
Malleus (NAV)
Mandible (= dentary)—Mandibula (NAV)
Mandibular canal—Canalis mandibulae (NAV)
Mandibular condyle (= condylar process)—Processus condylaris (NAV)
Mandibular foramen—Foramen mandibulae (NAV)
Mandibular nerve—Nervus mandibularis (NAV)
Mandibular (= lunar) notch (Evans, 1993)—Incisura mandibulae (NAV)
Mandibular symphysis (Evans, 1993)
Manubrium of malleus—Manubrium mallei (NAV)
Masseter muscle—Musculus masseter (NAV)
Masseteric fossa—Fossa masseterica (NAV)
Masseteric line (Evans, 1993)
Masseteric margin of maxilla—Margo massetericus (Evans, 1993)
Mastoid angle of parietal—Os parietale, angulus mastoideus (NAV)
Mastoid exposure of petrosal—Processus mastoideus (NAV)
Mastoid foramen—Foramen mastoideum (NAV)
Maxilla—Os maxillare (NAV)
Maxillary artery (= ramus infraorbitalis)—Arteria maxillaris (NAV)
Maxillary foramen—Foramen maxillare (NAV)
Maxillary nerve—Nervus maxillaris (NAV)
Maxillary recess—Recessus maxillaris (NAV)
Maxillary tuberosity—Tuber maxillae (NAV)
Maxillary vein—Vena maxillaris (NAV)
Maxilloincisive suture—Sutura maxilloincisiva (NAV)

Maxilloturbinal (= dorsal nasal concha)—Os conchae nasalis ventralis (NAV)
Meckel's cartilage (De Beer, 1937; Jurgens, 1963)—Cartilago mandibularis (NEV)
Medial pterygoid muscle—Musculus pterygoideus medialis (NAV)
Medial (= lingual) surface of teeth—Dentes, facies lingualis (NAV)
Medial surface of zygomatic arch—Arcus zygomaticus, facies medialis (NAV)
Median crest of cricoid—Cartilago cricoidea, crista mediana (NAV)
Median palatine suture—Sutura palatina mediana (NAV)
Median ridge of cheek teeth (Andersen, 1912)
Mental foramen—Foramen mentale (NAV)
Mental artery—Arteria mentalis (NAV)
Mental nerves—Nervi mentales (NAV)
Mental vein—Vena mentalis (NAV)
Mental surface of mandible—Mandibula, facies labialis (NAV)
Mentalis muscle—Musculus mentalis (NAV)
Mesostyle* (Miller, 1907)
Metacone** (Miller, 1907)
Metaconid** (Miller, 1907)
Metastyle* (Miller, 1907)
Metastylid* (Slaughter, 1970)
Middle nasal meatus—Meatus nasi medius (NAV)
Middle ear—Auris media (NAV)
Middle ear ossicles—Ossicula auditus (NAV)
Middle meningeal artery—Arteria meningea media (NAV)
Minor palatine artery—Arteria palatina minor (NAV)
Minor palatine foramen (Wible and Rougier, 2000)—Foramen palatinum caudale (NAV)
Minor palatine nerve—Nervus palatinus minor (NAV)
Molars—Dentes molares (NAV)
Muscular process of malleus*—Malleus, processus muscularis (NAV)
Muscular process of stapes—Stapes, processus muscularis (Henson, 1970)
Muscular tubercle*—Os occipitale, pars basilaris, tuberculum musculare (NAV)
M. digastricus (NAV)
M. genioglossus (NAV)
M. longus capitis (NAV)
M. masseter, pars profunda (NAV)
M. masseter, pars superficialis (NAV)
M. pterygoideus lateralis (NAV)
M. pterygoideus medialis (NAV)
M. rectus capitis ventralis (NAV)
M. stapedius (NAV)
M. sternomastoideus (Evans, 1993) = M. sternocephalicus, pars mastoidea (NAV)
M. temporalis (NAV)
M. tensor tympani (NAV)
M. thyrohyoideus (NAV)
M. zygomaticomandibularis (Storch, 1968)
Nasal—Os nasale (NAV)
Nasal cavity (= Nasal fossa)—Cavum nasi (NAV)
Nasal crest of palatine—Os palatinum, crista nasalis (NAV)
Nasal process of premaxilla—Os incisivum, processus nasalis (NAV)
Nasal septum—Septum nasi osseum (NAV)
Nasal surface of maxilla—Os maxillare, facies nasalis (NAV)
Nasal vestibule—Vestibulum nasi (NAV)
Nasalis muscle = Maxillonasolabial muscle (Evans, 1993)
Nasoethmoidal crest of nasal* (Evans, 1993)
Nasoethmoidal fossa of nasal* (Evans, 1993)
Nasoincisive suture—Sutura nasoincisiva (NAV)
Nasolacrimal canal—Canalis nasolacrimalis (NAV)
Nasolacrimal duct—Ductus nasolacrimalis (NAV)
Nasolacrimal suture*—Sutura nasolacrimalis (NAV)
Nasomaxillary suture—Sutura nasomaxillaris (NAV)
Nasopalatine duct (Cooper and Bhatnagar, 1976)—Ductus incisivus (NAV)
Nasopalatine duct cartilage—Cartilago ductus nasopalatine (Jurgens, 1963)
Nasopharyngeal meatus—Meatus nasopharyngeus (NAV)
Nasopharyngeal surface of pterygoid—Os pterygoideum, facies nasopharyngea (NAV)
Neck of malleus—Malleus, collum mallei (NAV)
Nerve of pterygoid canal—Nervus canalis pterygoidei (NAV)
Nuchal (= lambdoid) crest—Crista nuchae (NAV)
Nuchal tubercle*—Os occipitalis, pars lateralis, tuberculum nuchale (NAV)
Occipital—Os occipitale (NAV)
Occipital artery—Arteria occipitalis (NAV)

Occipital (= caudal) border of parietal—Os parietale, margo occipitalis (NAV)
Occipital condyle—Condylus occipitalis (NAV)
Occipital emissary vein—Vena emissaria occipitalis (NAV)
Occipital margin of parietal—Os parietale, margo occipitalis (NAV)
Occipitointerparietal suture—Sutura occipitointerparietalis (this study) = Sutura lambdoidea (NAV)
Occipitomastoid suture—Sutura occipitomastoidea (NAV)
Occipitoparietal suture—Sutura occipitoparietalis (Evans, 1993) = Sutura lambdoidea (NAV)
Occiput (NAV)
Occlusal surface of teeth—Dentes, facies occlusalis (NAV)
Oculomotor nerve (= cranial nerve III)—Nervus oculomotorius (NAV)
Olfactory bulb—Bulbus olfactorius (NAV)
Olfactory nerve (= cranial nerve I)—Nervi olfactorii (NAV)
Ophthalmic artery—Arteria ophthalmica interna (NAV)
Ophthalmic nerve (= cranial nerve V_1)—Nervus ophthalmica (NAV)
Ophthalmic vein—Vena ophthalmica interna (NAV)
Ophthalmic venous plexus—Plexus ophthalmicus (NAV)
Optic canal/foramen—Canalis opticus (NAV)
Optic grooves (Evans, 1993)
Optic nerve (= cranial nerve II)—Nervus opticus (NAV)
Oral cavity—Cavum oris (NAV)
Orbicular apophysis (Henson, 1961, 1970)
Orbit—Orbita (NAV)
Orbital crest—Crista orbitalis (NAV)
Orbital fissure*—Fissura orbitalis (NAV)
Orbital fossa—Orbita (NAV)
Orbital ligament—Ligamentum orbitale (NAV)
Orbital margin of maxilla—Os maxillare, margo orbitalis (NAV)
Orbital region—Regio orbitalis (NAV)
Orbital surface of frontal—Os frontale, pars orbitalis (NAV)
Orbital surface of jugal—Os zygomaticum, facies orbitalis (NAV)
Orbital surface of lacrimal—Os lacrimale, facies orbitalis (NAV)
Orbitosphenoid—Os presphenoidale, ala orbitalis (NAV)
Orbitosphenoidal crest—Crista orbitosphenoidalis (NAV)
Orbitotemporal canal* (Rougier et al., 1992; Wible et al., 2004) = Sinus canal (Gregory, 1910; McDowell, 1958)
Ossa cranii (NAV)
Ossa faciei (NAV)
Osseus lamina of mallei (Evans, 1993) = Lamina (Henson, 1970)
Osseous nasal aperture—Apertura nasi ossea (NAV)
Osseous nasal septum—Septum nasi osseum (NAV)
Otic ganglion—Ganglion oticum (NAV)
Outer lamella of malleus (= rostral process of malleus, part) (Jurgens, 1963) = Tympanic plate of anterior process (Henson, 1970)
Oval window—Fenestra vestibuli (NAV)
Palatine—Os palatinum (NAV)
Palatine canal—Canalis palatinus (NAV)
Palatine cartilage—Cartilago palatini (Jurgens, 1963)
Palatine process of maxilla—Maxillare, processes palatinus (NAV)
Palatine process of premaxilla*—Os incisivum, processus palatinus (NAV)
Palatine sulcus—Sulcus palatinus (NAV)
Palatine surface of palatine—Os palatinum, facies palatina (NAV)
Palatoethmoidal suture—Sutura palatoethmoidalis (NAV)
Palatolacrimal suture—Sutura palatolacrimalis (NAV)
Palatomaxillary suture—Sutura palatomaxillaris (Evans, 1993) = Sutura palatina transversa (NAV)
Paracondylar process of exoccipital—Processus paracondylaris (NAV)
Paracone** (Miller, 1907)
Paraconid** (Miller, 1907)
Parachordal plate (= central stem) (DeBeer, 1937)
Paraflocculus of cerebellum—Paraflocculus (NAV)
Parastyle* (Miller, 1907)
Paries nasi (Jurgens, 1963)
Parietal—Os parietale (NAV)
Parietal region—Regio parietalis (NAV)

Parietointerparietal suture—Sutura parietointerparietalis (Evans, 1993)
Paroccipital process (Wible and Gaudin, 2004)—Processus mastoideus (Schaller, 1992)
Pars canalicularis of petrosal (Wible, 1990; Wible et al., 1995, 2001)
Pars cochlearis of petrosal (Wible, 1990; Wible et al., 1995, 2001)
Pars incisiva of mandible—Mandibula, pars incisiva (NAV)
Pars orbitalis of frontal—Os frontale, pars orbitalis (NAV)
Perbullar canal* (Wible, 1986)
Perilymphatic duct—Ductus perilymphaticus (NAV)
Permanent teeth—Dentes permanentes (NAV)
Perpendicular lamina of ethmoid—Os ethmoidale, lamina perpendicularis (NAV)
Perpendicular process of palatine—Os palatinum, lamina perpendicularis (NAV)
Petrosal (= petrous temporal)—Os temporale, pars petrosa (NAV)
Petro-occipital (= petrobasilar) canal*—Canalis petrooccipitalis (NAV)
Pharyngeal tubercle of basioccipital—Os basioccipitalis, tuberculum pharyngeum (NAV)
Piriform fenestra (= foramen lacerum) = Pyriform fenestra (McDowell, 1958)—Foramen lacerum (NAV)
Planum parietale (NAV)
Pleurethmoid (Jurgens, 1963)
Palatomaxillary suture—Sutura palatomaxillaris (NAV)
Pontine impression of basioccipital—Os occipitalis, pars basilaris, impressio pontina (NAV)
Porus acusticus internus (NAV)
Postdental palate (Andersen, 1912)
Posterior auricular artery—Arteria auricularis caudalis (NAV)
Posterior basicochlear (= basicapsular) commissure (De Beer, 1937)—Syncondrosis petro-occipitalis (NAV)
Posterior cornu of hyoid (Sprague, 1943)—Cornu majus (NAV) = Cornu branchiale (Jurgens, 1963)
Posterior crus (= leg) of ectotympanic—Annulus tympanicus, crus posterior (NAV)
Posterior (= caudal) crus (= leg) of stapes—Stapes, crus caudale (NAV)
Posterior ligament of incus—Ligamentus incudis posterius (NAV)
Posterior mental foramen: see Mental foramen
Posterior semicircular canal—Canalis semicircularis posterior (NAV)
Posterobasal ledge of cheek teeth (Andersen, 1912)
Postglenoid foramen (= retroarticular foramen)—Foramen retroarticulare (NAV)
Postglenoid process (= retroarticular process)—Processus retroarticulare (NAV)
Postglenoid (= retroarticular; = capsuloparietal emissary) vein—Vena emissaria foraminis retroarticularis (NAV)
Postorbital area of frontal (Andersen, 1912; Miller, 1907)
Postorbital ligament—Ligamentum orbitale (NAV)
Postorbital process—Os frontale, processus zygomaticus (NAV)
Postpalatine torus (Novacek, 1986)
Posttemporal canal* (Wible, 1989; Rougier et al., 1992)
Posttemporal foramen (Notch)* (Rougier et al., 1992)
Posttympanic process (Kielan-Jaworwoska, 1981; Novacek, 1986)—Processus retrotympanicus (NAV)
Prearticular (= gonial) (Goodrich, 1930)
Prefacial (= suprafacial) commissure (De Beer, 1937; Jurgens, 1963)
Premaxilla—Os incisivum (NAV)
Premolars—Dentes praemolares (NAV)
Preorbital area of frontal—Os frontale, pars nasalis (NAV)
Presphenoid—Os presphenoidale, corpus (NAV)
Primary facial foramen (Wible, 1990; Wible and Hopson, 1993)
Promontorium of petrosal (Evans, 1993)
Protocone** (Miller, 1907)
Protoconid** (Miller, 1907)
Protostylid* (Slaughter, 1970)
Pterygoid—Os pterygoideum (NAV)
Pterygoid canal—Canalis pterygoideus (NAV)
Pterygoid process of basisphenoid (Evans, 1993)
Pterygoid process of maxilla—Os maxillare, processus pterygoideus (NAV)

Pterygopalatine fissure (this study)
Pterygopalatine fossa—Fossa pterygopalatina (NAV)
Pterygopalatine ganglion—Ganglion pterygopalatinum (NAV)
Pterygopalatine nerve—Nervus pterygopalatinus (NAV)
Pterygopalatine surface of pterygoid—Os pterygoideum, facies pterygopalatina (NAV)
Pterygopalatine suture—Sutura pterygopalatina (NAV)
Pterygosphenoid suture—Sutura pterygosphenoidalis (NAV)
Ramus inferior of stapedial artery (Wible, 1987)
Ramus infraorbitalis (Wible, 1987)
Ramus mandibularis (Wible, 1987)
Ramus supraorbitalis (Wible, 1987)
Ramus of mandible—Ramus mandibulae (NAV)
Ramus superior of stapedial artery (Wible, 1987)
Ramus temporalis of stapedial artery (Wible, 1987)
Regio dorsalis nasi (NAV)
Regio frontalis (NAV)
Regio intermandibularis (NAV)
Regio maxillaris (NAV)
Regio naris (NAV)
Regio orbitalis (NAV)
Regio parietalis (NAV)
Regio temporalis (NAV)
Regio zygomatica (NAV)
Reichert's cartilage (= second pharyngeal arch) (De Beer, 1937; Jurgens, 1963)
Retromolar space = Retromolar fossa (Hiatt and Gartner, 1987)
Right lamina of thyroid—Thyroid cartilage, lamina dextra (NAV)
Rostral axis (Andersen, 1912)
Rostral alar foramen*—Foramen alare rostrale (NAV)
Rostral (= frontal) border of parietal—Os parietale, margo frontalis (NAV)
Rostral clinoid process—Os presphenoidale, processus clinoideus rostralis (NAV)
Rostral cornu of thyroid—Cartilago thyroidea, cornu rostralis (NAV)
Rostral cranial fossa of frontal—Os frontale, facies interna, fossa cranii rostralis (Evans, 1993)
Rostral entotympanic—Rostrales entotympanicum (Klaauw, 1922)
Rostral process of ethmoturbinal (this study) = "Anterior tip" of ethmoturbinal (Jurgens, 1963)
Rostral (= anterior) process of malleus—Malleus, processus rostralis (NAV) = Processus gracilis (outer lamella; Jurgens, 1963)
Rostral (= facial) process of maxilla—Os maxillare, facies facialis (NAV)
Rostral septal branch of major palatine artery—Rami septi rostrales (Evans, 1993)
Rostral thyroid notch—Incisura thyroidea rostralis (NAV)
Rostromedial process of pterygoid (this study)
Rostrum (NAV)
Rostrum of presphenoid*—Os presphenoidale, rostrum sphenoidale (NAV)
Root of teeth—Dentes, radix dentis (NAV)
Round window—Fenestra cochleae (NAV)
Saccule—Sacculus (NAV)
Sagittal (= dorsal) border of parietal—Os parietale, margo sagittalis (NAV)
Sagittal crest—Crista sagittalis externa (NAV)
Sagittal part of vomer (Evans, 1993)
Sagittal suture—Sutura sagittalis (NAV)
Second pharyngeal arch (= Reichert's cartilage = Hyoid arch (Sprague, 1943)—Arcus pharyngeus secundus (NEV)
Secondary facial foramen (Wible, 1990; Wible and Hopson, 1993)
Secondary tympanic membrane—Membrana tympani secundaria (NAV)
Sella turcica (NAV)
Septal branch of caudal nasal nerve (= Nasopalatine nerve) (Evans, 1993)—Nervus nasopalatinus (NAV)
Septal cartilage—Cartilago septi nasi (NAV)
Septal process of nasal—Os nasale, processus septalis (NAV)
Semicircular canal—Canalis semicircularis (NAV)
Shaft (= neck) of teeth—Dentes, collum dentis (NAV)
Short crus (= leg) of incus—Incus, crus breve (NAV)
Sigmoid sinus—Sinus sigmoideus (NAV)
Sinciput (NAV)
Sixth pharyngeal arch—Arcus pharyngeus sextus (NEV)

Sphenoethmoid lamina of palatine—Os palatinum, lamina sphenoethmoidalis (NAV)
Sphenofrontal suture—Sutura sphenofrontalis (NAV)
Sphenoidal angle of parietal—Os parietale, angulus sphenoidalis (NAV)
Sphenoidal crest—Crista sphenoidalis (NAV)
Sphenoidal incisure of vomer—Incisura sphenoidalis (NAV)
Sphenorbital fissure (Novacek, 1986)—Fissura orbitalis + foramen rotundum + foramen alare rostrale + foramen alare parvum (NAV)
Sphenoidal process of palatine—Os palatinum, processus sphenoidalis (NAV)
Sphenoidal sinus—Sinus sphenoidalis (NAV)
Sphenomaxillary suture*—Sutura sphenomaxillaris (NAV)
Spheno-occipital synchondrosis—Synchondrosis spheno-occipitalis (NAV)
Sphenopalatine artery—Arteria sphenopalatina (NAV)
Sphenopalatine foramen—Foramen sphenopalatinum (NAV)
Sphenopalatine suture—Sutura sphenopalatina (NAV)
Sphenopalatine vein—Vena sphenopalatina (NAV)
Sphenoparietal suture—Sutura sphenoparietalis (NAV)
Sphenosquamosal suture—Sutura sphenosquamosa (NAV)
Spinal cord—Medulla spinalis (NAV)
Spiral tract of minute foramina—Tractus spiralis foraminosus (NAV)
Squama frontalis of frontal (NAV)
Squamosal—Os temporale, pars squamosa (NAV)
Squamosofrontal suture*—Sutura squamosofrontalis (NAV)
Squamosomastoid suture—Sutura squamosomastoidea (NAV)
Squamous border of parietal—Os parietale, margo squamosus (NAV)
Stapedial artery—Arteria stapedia (Tandler, 1899; Wible, 1984, 1987)
Stapedius muscle—Musculus stapedius (NAV)
Stapes (NAV)
Stylar (= labial) shelf (Slaughter, 1970)
Stylid* (Slaughter, 1970)
Styliform process of ectotympanic (Henson, 1970)
Stylohyoid—Stylohyoideum (NAV)
Stylohyoid cartilage—Cartilago stylohyoidea (NAV)
Stylomastoid artery—Arteria sylomastoidea (NAV)
Stylomastoid foramen*—Foramen stylomastoideum (NAV)
Stylomastoid notch—Foramen stylomastoideum (NAV)
Subarcuate fossa—Fossa subarcuata (NAV)
Sulci of brain—Sulci cerebri (NAV)
Sulcus for capsuloparietal emissary vein—Transverse sulcus of temporal bone (Evans, 1993)
Sulcus for inferior petrosal sinus—Sulcus sinus petrosa ventralis (NAV)
Sulcus for venous transverse sinus*—Sulcus sinus transversi (NAV)
Sulcus lacrimalis (NAV)
Sulcus medullae oblongatae (NAV)
Sulcus septi nasi (Evans, 1993)—Sulcus vomeris (septalis) (NAV)
Sulcus tympanicus (NAV)
Suprameatal bridge = Dorsal boundary of external acoustic meatus (Evans, 1993)
Supraoccipital—Os occipitalis, squama occipitalis (NAV)
Supraorbital margin—Margo supraorbitalis (NAV)
Superior petrosal sinus—Sinus petrosus dorsalis (NAV)
Sutura intermandibularis (NAV)
Sutura squamosa (NAV)
Suturae capitis (NAV)
Syndesmosis tympanostapedia (NAV)
Tectum nasi (Jurgens, 1963)
Tegmen tympani (NAV)
Temporal canal (Evans, 1993)
Temporal fossa—Fossa temporalis (NAV)
Temporal line—Linea temporalis (NAV)
Temporal process of jugal—Os zygomaticum, processus temporalis (NAV)
Temporal region—Regio temporalis (NAV)
Temporomandibular joint—Articulatio temporomandibularis (NAV)
Tendon of tensor tympani muscle (Jurgens, 1963)
Tensor tympani muscle—Musculus tensor tympani (NAV)
Tentorial process*—Processus tentoricus (NAV)
Third pharyngeal arch—Arcus pharyngeus tertius (NEV)

Thyrohyoid—Thyrohyoideum (NAV)
Thyrohyoid articulation—Articulatio thyrohyoidea (NAV)
Thyrohyoid cartilage—Cartilago thyrohyoidea (NAV)
Thyroid cartilage—Cartilago thyroidea (NAV)
Thyroid fissure—Fissura thyroidea (NAV)
Tip of dental cusp—Dentes, apex cuspidis (NAV)
Tracheal rings—Cartilagines tracheales (NAV)
Transverse crest of petrosal—Crista transversa (NAV)
Transverse palatine suture—Sutura palatina transversa (NAV)
Transverse sinus—Sinus transversus (NAV)
Tribosphenic molar (Slaughter, 1970)
Trigeminal ganglion—Ganglion trigeminale (NAV)
Trigeminal nerve (= cranial nerve V)—Nervus trigeminus (NAV)
Trochlear nerve (= cranial nerve IV)—Nervus trochlearis (NAV)
Tubal cartilage—Cartilago tubae auditivae (NAV)
Tympanic (= middle ear) cavity—Cavum tympani (NAV)
Tympanic membrane—Membrana tympani (NAV)
Tympanic surface of petrosal—Os temporale, pars petrosa, facies tympanica (Evans, 1993)
Tympanohyoid (= tympanohyal)—Tympanohyoideum (NAV)
Tympanostyloid ligament (Sprague, 1943; Jurgens, 1963)
Upper tooth row—Arcus dentalis superior (NAV)
Utricle—Utriculus (NAV)
Vagus nerve (= cranial nerve X)—Nervus vagus (NAV)
Vascular angle of parietal (this study)
Vascular foramen of lacrimal (this study)
Vena diploëtica magna (Hyrtl, 1853, 1854)
Ventral border of mandible—Mandibula, margo ventralis (NAV)
Ventral condyloid fossa—Fossa condylaris ventralis (NAV)
Ventral intraoccipital synchondrosis (Evans, 1993)—Synchondrosis intraoccipitalis basilateralis (NAV)
Ventral nasal concha (= maxilloturbinate)—Concha nasalis ventralis (NAV)
Ventral nasal meatus—Meatus nasi ventralis (NAV)
Ventral vestibular area of petrosal—Area vestibularis inferior (NAV)
Ventrocaudal process of arytenoid (this study)
Vermiform impression of supraoccipital—Os occipitale, pars squamosa, impressio vermialis (NAV)
Vertebral artery—Arteria vertebralis (NAV)
Vestibular aqueduct—Apertura externa aqueductus vestibuli (NAV)
Vestibular fossula (MacPhee, 1981)
Vestibular nerve—Nervus vestibularis (NAV)
Vestibulocochlear nerve (= cranial nerve VIII)—Nervus vestibulocochlearis (NAV)
Vomer (NAV)
Vomeroethmoidal suture—Sutura vomeroethmoidalis (NAV)
Vomeroincisive suture*—Sutura vomeroincisiva (NAV)
Vomeromaxillary suture—Sutura vomeromaxillaris (NAV)
Vomeronasal organ—Organum vomeronasale (NAV)
Vomeropalatine suture—Sutura vomeropalatina dorsalis (NAV)
Vomerosphenoidal suture—Sutura vomerosphenoidalis (NAV)
Wings of vomer—Alae vomeris (NAV)
Yoke—Jugum sphenoidale (NAV)
Zygoma—Arcus zygomaticus (NAV)
Zygomatic arch—Arcus zygomaticus (NAV)
Zygomatic process of maxilla—Os maxillare, processus zygomaticus (NAV)
Zygomatic process of squamosal—Os temporale, pars squama, processus zygomaticus (NAV)
Zygomaticomaxillary suture—Sutura zygomaticomaxillaris (NAV)

APPENDIX 2

List of Anatomical Abbreviations Used in Figures

ac alveolar canal
alec anterior leg of the ectotympanic
alst anterior leg of stapes
alv ala vomeris
amf anterior mental foramen
an angle of mandible
ao alae orbitales of sphenoid complex
apf accessory palatine foramina
aplin attachment of posterior ligament of incus
app apex parties petrosa
as alisphenoid
asc anterior semicircular canal
asu alar sulcus of alisphenoid
at alae temporales of sphenoid complex
attm attachment of m. tensor tympani
av aqueductus vestibuli
bcc posterior basicochlear commissure
bcf basicochlear fissure
bo basioccipital
bs basisphenoid
bst base of stapes
C upper canine
c lower canine
"c" column of bone on lateral side of ethmoturbinal
cc cochlear canaliculus
ccr conchal crest of maxilla
ccthy caudal cornu of thyroid
cehy ceratohyoid
cf carotid foramen
Cju upper canine jugum
cllo caudolateral lobe of parietal
con mandibular condyle
cor coronoid process of mandible
cp crista parotica
cppt caudal process of pterygoid
crarra cricoarytenoid articulation
crc crus commune
crga crista galli
crif cribriform foramina
cs carotid sulcus of basisphenoid
ct crista transversa of petrosal
ctpp caudal tympanic process of petrosal
cty crista tympanica
cv crest of vomer
cvma caudoventral margin of parietal
dC deciduous upper canine
dc deciduous lower canine
dI1 deciduous first upper incisor
di1 deciduous first lower incisor
dI2 deciduous second upper incisor
di2 deciduous second lower incisor
dlcr dorsal lamina of cricoid
dP1 deciduous first upper premolar
dp1 deciduous first lower premolar
dP2 deciduous second upper premolar
dp2 deciduous second lower premolar
ds dorsum sellae
eam external acoustic meatus
ec ectotympanic
ecptp ectopterygoid process
ef ethmoidal foramen
ein unnamed round eminence of incus
en rostral entotympanic
ent-III endoturbinate III
eo exoccipital
ephy epihyoid
etan epitympanic angle of parietal
etfo ethmoidal fossae
eth ethmoid
ethtu ethmoturbinal
etma epitympanic margin of parietal
etwas epitympanic wing of alisphenoid
fai foramen acusticum inferius
fam incudal facet for head of malleus
fas foramen acusticum superius
fc fenestra cochleae
fcb fossa cerebellaris
fctn foramen for the chorda tympani nerve
fdv foramen for frontal diploic vein
fh fossa hypophysialis
fi fossa incudis
fifr facies interna of frontal
fipa facies interna of parietal
fm foramen magnum
fo foramen ovale
fofr facies orbitalis of frontal
fr frontal
fran frontal angle of parietal
frma frontal margin of parietal
frp frontal process of maxilla
frt foramina for rami temporales
fs facial sulcus of petrosal
fv fenestra vestibuli
gc anterior groove of upper canine
gf glenoid fossa
ham hamulus pterygoideus
hF hiatus Fallopii
hf hypoglossal foramen
hm head of malleus

hppal horizontal process of palatine
hst head of stapes
I1 first upper incisor
i1 first lower incisor
I2 second upper incisor
i2 second lower incisor
iam internal acoustic meatus
icf intercrural foramen of stapes
if incisive fissure
iiv incisura incisiva of vomer
im infraorbital margin
imdi impressiones digitatae
in incus
ioc infraorbital canal
iocr internal occipital crest
iof infraorbital foramen
ip interparietal
isv incisura sphenoidalis of vomer
itf inner table of frontal
ja juga
jf jugular foramen
ji jugular incisure
jsp yoke or jugum sphenoidale
ju jugal
lac lacrimal
lacf lacrimal foramen
lacfe lacrimal fenestra
lc lateral cusp of cheek teeth
lcin long crus of incus
lm lamina of malleus
lp lenticular process of incus
lpm lateral process of malleus
lppt lateral process of pterygoid
lsp lingula sphenoidalis
lthy lamina of thyroid
M1 first upper molar
m1 first lower molar
M2 second upper molar
m2 second lower molar
m3 third lower molar
ma malleus
maan mastoid angle of parietal
mam manubrium of malleus
manf mandibular foramen
mapf major palatine foramen
mas mandibular symphysis
mc medial cusp of cheek teeth
mccr median crest of cricoid
mdnm middle dorsal nasal meatus
me mastoid exposure of petrosal
mf mastoid foramen
mpf minor palatine foramen
mpst muscular process of stapes
ms mental surface
mx maxilla
mxf maxillary foramen
mxtu maxillary tuberosity
na nasal
nas nasal septum
nalacc nasolacrimal canal
nm neck of malleus
nmf notch for mastoid foramen
nspof notch of sphenorbital fissure
nst neck of stapes
nuc nuchal crest
oam orbicular apophysis of malleus
oc occipital condyle
ocma occipital margin of parietal
omj occipito-mastoid joint
opc optic canal
os orbitosphenoid
P1 first upper premolar
p1 first lower premolar
P3 third upper premolar
p3 third lower premolar
P4 fourth upper premolar
p4 fourth lower premolar
pa parietal
pal palatine
palp palatine process of maxilla
pc palatine canal
pcp paracondylar process
pfc prefacial commissure
pgf postglenoid foramen
pgp postglenoid process
pif piriform fenestra
plec posterior leg of ectotympanic
plst posterior leg of stapes
pmf posterior mental foramen
pmx premaxilla
pnfr pars nasalis of frontal
pof postorbital foramen
pop postorbital process
pp paroccipital process of petrosal
pppal perpendicular process of palatine
pr promontorium of petrosal
ps presphenoid
psc posterior semicircular canal
pt pterygoid
ptc pterygoid canal
ptmx pterygoid process of maxilla
ptp posttympanic process of squamosal
ptpbs pterygoid process of basisphenoid
ptpfi pterygopalatine fissure
ptpmx pterygoid process of maxilla
r1M1 anterior root of first upper molar

r2M1 posterior root of first upper molar
rc posteromedial ridge of upper canine
rcfo rostrocranial fossa
rcp rostral clinoid process
rcthy rostral cornu of thyroid
rM2 roots of second upper molar
rmppt rostromedial process of pterygoid
rpm rostral process of malleus
saf subarcuate fossa
sc sutura coronalis
scev sulcus for capsuloparietal emissary vein
scin short crus of incus
sf stapedial fossa
sff secondary facial foramen
sffr squama frontalis of frontal
sfl sutura frontolacrimalis
sfm sutura frontomaxillaris
sfn sutura frontonasalis
sif sutura interfrontalis
simx sutura intermaxillaris
sin sutura internasalis
siocbl synchondrosis intraoccipitalis basilateralis
sipal sutura interpalatina
sisp synchondrosis intersphenoidalis
smi sutura maxilloincisiva
smn stylomastoid notch
smo sulcus medullae oblongatae
snamx sutura nasomaxillaris
snm sutura nasomaxillaris
so supraoccipital
soipa sutura occipitointerparietalis
sopa sutura occipitoparietalis
spamx sutura palatomaxillaris
span sphenoidal angle of parietal
spc sphenoidal crest
spetl sphenoethmoid lamina
spf sphenopalatine foramen
spip sutura parietointerparietalis
spof sphenorbital fissure
spsi sphenoidal sinus
sq squamosal
sqa squama of squamosal
sqma squamosal margin of parietal
srt sulci for rami temporales
ss sutura sagittalis
sspal sutura sphenopalatina
sspar sutura sphenoparietalis
sspo synchondrosis spheno-occipitalis
sspsq sutura sphenosquamosa
ssq sutura squamosa
st sulcus tympanicus
sthy stylohyoid
sts sulcus for transverse sinus
stz sutura temporozygomatica
Sut suture
Syn synchondrosis
szmx sutura zygomaticomaxillaris
tc temporal canal
th tympanohyoid
thcra thyrocricoid articulation
thhy thyrohyoid
thy thyroid cartilage
thyfi thyroid fissure
tl temporal line
tt tegmen tympani
ttf tensor tympani fossa
v vomer
va vascular angle of parietal
veim vermiform impression
vflac vascular foramen of lacrimal
vlacr ventrolateral arc of cricoid
vnc ventral nasal concha
vnm ventral nasal meatus
zpmx zygomatic process of maxilla
zpsq zygomatic process of squamosal